supplemento ai
rendiconti
del Circolo matematico di Palermo

I^{st} summer school quantitative methods for economic agricultural-food and enviromental sciences

Castiglione di Sicilia - Italia, 22nd-24th September 2010

serie II - numero 83 - anno 2011

sede della società: Palermo - Via Archirafi, 34

SUPPLEMENTO

AI

RENDICONTI DEL CIRCOLO MATEMATICO DI PALERMO

DIREZIONE E REDAZIONE
Via Archirafi, 34 - Tel. 091.23891069 - 90123 Palermo (Italia)
E-mail: vetro@math.unipa.it

Tipografia «A.C.» s.n.c. - Via Filippo Marini, 15 - Tel. e Fax 091422758 - 90128 Palermo
e-mail: tipografiaac@tin.it

SUPPLEMENTO

AI

RENDICONTI DEL CIRCOLO MATEMATICO DI PALERMO

DIRETTORE: **P. VETRO**

IST SUMMER SCHOOL
QUANTITATIVE METHODS FOR ECONOMIC AGRICULTURAL-FOOD AND ENVIROMENTAL SCIENCES

Castiglione di Sicilia - Italy, 22nd-24th September 2010

Edited by:
Giuseppe Caristi

SERIE II - NUMERO 83 - ANNO 2011

PALERMO
SEDE DELLA SOCIETÀ
VIA ARCHIRAFI, 34

CONFERENCE DATA

Castiglione di Sicilia, Italy, 22nd - 24th September, 2010

Scientific Committee

M. I. Stoka (Torino - Italia); D. Bosq (Paris - France); G. Caristi (Messina - Italia); A. Duma (Hagen - Germany); A. Florian (Salisburg - Austria); P. Gruber (Wien - Austria); A. Miceli (Messina - Italia); D. Lo Bosco (Reggio Calabria - Italia); G. Restuccia (Messina - Italia); A. Bertirotti (Firenze - Italia)

Host Organizations

University of Messina - Faculty of Economics

Organizing Committee

G. Caristi; D. Barilla; P. Bartolomeo; M. Bisaia; V. Bonanzinga; G. Leonardi; A. Puglisi; A. Romolo; E. La Sorte; L. Sorrenti

Supported by

Sicily Region
Assembly Regional Sicilian
Province of Messina
Municipality of Messina
Alcantara Park
N.G.I. Shipping Company
University of Messina

Contents

Preface pag. 9

Barczak S. – *Grey system theory applied to first price auctions systems* » 11

Barilla D. - Duma A. - Puglisi A. – *The distribution function of a chord in a non-convex poligon* » 23

Bäsel U. – *Geometric probabilities for a cluster of needles and a lattice of parallel planes* » 41

Bosq D. – *Models associated with extended exponential smoothing* » 57

Caristi G. - Stoka M. – *A Buffon type problem for an irregular lattice I* » 65

Caristi G. - Stoka M. – *A Buffon type problem for an irregular lattice II* » 83

Čerin Z. - Gianella G. M. – *On Jones S(E) – triples and S(E)-quadruples in rings* » 95

Corriere F. - Di Vincenzo D. – *L'ottimizzazione degli interventi manutentivi sulle linee ferroviarie con l'utilizzo di un modello markoviano: analisi di un caso studio* » 111

Czernik T. – *First passage phenomena from the new perspective and generalized maximal loss* » 131

Duma A.- Rizzo S. – *La funzione di distribuzione di una corda in un trapezio rettangolo* » 147

Dziwok E. – *The implied forward rate as an indicator of disturbances in polish interbank market* » 161

Esteves E. - Marchisio M. – *Invariant theory of foliations of the projective plane* » 175

Failla G. – *A problem of Buffon type for regular lattices with regular obstacles* » 189

Iskra D. - *Value at risk – Securities of portfolio optimization. A geometric Brownian motion case* » 199

Leonardi G. - Ferrara R. – *Evaluation of global comfort for train passengers* » 209

Pettineo M. – *Laplace problems for regular lattices with asymmetric cell and different obstacles* » 219

Raguso G. - Ancona A. - Chieppa L. - L'Abbate S. - Pepe M. L. - D'Ovidio F. D. – *Exploring breast cancer diagnosis with fractal analysis and classification methods* » 229

Romolo A. – *Un problema di tipo Buffon per un reticolo irregolare* » 237

Sorrenti L. – *Geometric probability of the lenght of a chord for an arbitrary regular polygon* » 249

Węgrzyn T. – *Analysis of the CPPI strategy for index portfolio at the Warsaw stock exchange* 259

Zirilli A.- Alibrandi A. – *Use of alternative link functions in regression models for ordinal response variables: an application to the customer satisfaction measurement in a sample of fitness centers in Messina* » 269

Zirilli A.- Alibrandi A. – *A statistical approach to compare Ang-2 and α-FP serum levels into detecting hepatocellular carcinom* » 279

Preface

The first Summer School "Quantitative Methods for Economic Agricultural-Food and Enviromental Sciences" took place in Castiglione di Sicilia from 22nd-24th September 2010.

This volume collect the Proceedings of the first Summer School, organized by the Research Group on Integral Geometry, Geometrical Probabilities and Convex Bodies, together Faculty of Economics of Messina University.

The conference was sponsored by the following:

- Messina University – Faculty of Economics
- Sicily Region
- Province of Messina
- Municipality of Messina
- Alcantara Park
- N.G.I. Shipping Company

Our grateful acknowledgements.

We want to thank the Scientific Committee of the Journal "Rendiconti del Circolo Matematico di Palermo" for accepting to publish the Proceedings of the Conference in a supplement of the Journal.

Giuseppe Caristi

RENDICONTI DEL CIRCOLO MATEMATICO DI PALERMO
Serie II, Suppl. 83 (2011), pp. 11-22

GREY SYSTEM THEORY APPLIED TO FIRST PRICE AUCTIONS SYSTEMS

Stanisław Barczak
University of Economics in Katowice
Department of Applied Mathematics

1. Introduction

Auction is a market institution with an explicit set of rules determining resource allocation and price on the basis of bid from the market participants.[1]

First question is why the auction markets are so widespread in the whole world? The answer could be very simply but not necessary correct. Thus, we can say that all auctions have a well-defined rules and all the participants are anonymous. Thus, from the point of view of the auction markets are highly transparent. Second problem is what are the best bidding strategies at a particular auction system ? In other words, we know that bids made at auction are mutually competitive. Thus enabling the selection of the best strategy to win the auction depends on a set of information available to the participant in the auction and its awareness of the facility issued a preliminary valuation. Let's see how it was in the long past. In 193 A.D. after the death of the Emperor Pertinax, Pretorians decided to sell by auction the entire Roman Empire. The winning price was 25,000 sesterces for

[1] McAfee, R. P., & McMillan, J., "Auctions and Bidding," Journal of Economic Literature, vol. 25 no. 2, 1987, pp. 699-738.

a man to Guard. The winner was Didius Julianus. As it turns out, this is one of the earliest and most extreme cases, to win the auction at heavily inflated offer. Today it is a so-called 'winner course'. Today, through the auction system are sold any goods such as tobacco, master pieces, fish, fresh flowers, collections, natural resources, services, etc.

From an analytical point of view, the question arises of how to modeling auction markets - the formal markets ? This problem applies to both sellers and buyers. Sellers count on maximum profit and the buyer want the lowest price. There is therefore an obvious conflict of interest of both the actors of the market - the seller and buyer. From a theoretical point of view as well as some practical applications in the form of strategies for players were very well described by the application of The Game Theory. Game theory points to the use of specific strategies reported by participants of tenders in the light of balance. In the case of rational behavior of players such equilibrium is reached. It must be remembered that the player does not always proceed rationally. Often, therefore, comes to the deviations from such behavior which usually means losing the sense to pay a higher price than that which would ensure victory in the bidding – 'winner course'. The article is the proposed econometric method of estimation of future prices/offers received on the basis of previous bids at the auction. The proposed method requires a basic knowledge of the principles of rules of auction markets.

From the standpoint of the buyer, the basic problem in each lot is the forecast of future bid, which may decide the winner. From the standpoint of the theory of econometric forecasts of the number of execution - submitted bids is very small for the auction for one object. Time series of offers is very short. Then there is not the possibility of applying classical methods of time series analysis. In the article proposes use of the gray model GM(1,1) for forecasting the future offers.

2. Auctions and auctions formats

Consider the basic auction systems. Auction markets can be divided into the two following groups: first common auctions and second equivalent auctions. In terms of Game Theory we are talking about open systems and sealed-bid systems (Fig.1).

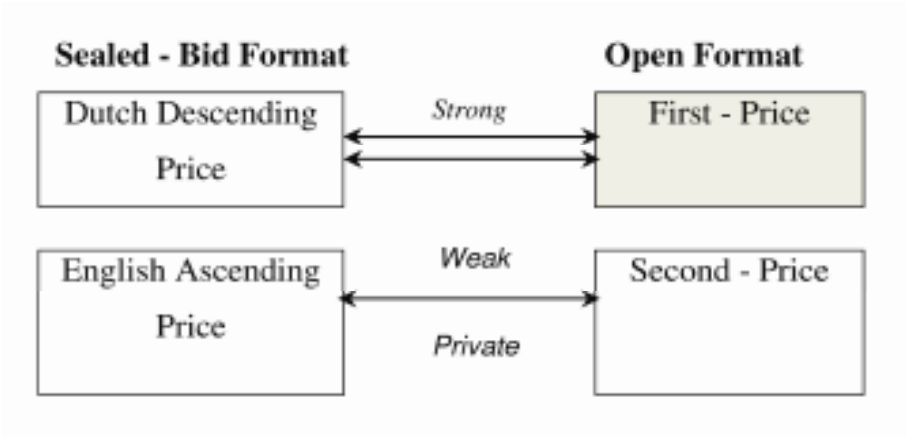

Figure 1. Open and Sealed-Bid Auction Formats
Source: Prepared on the basis: V. Krishna, Auction Theory, Academic Press 2002, p. 5

Figure 1 shows how to derive four basic auction formats. Thus we have two open auction formats: Dutch and English, and two formats sealed-bid auctions: first-price and second-price.

Let consider the first one – open format. Open auctions require that their members were gathered in one place physically or through the web server. Each bidder can observe the bids submitted by other participants and decide to keep the amount of its own bid. Should be noted that the English auction format is the oldest auction system. One of the variants of English auctions is that the auctioneer who begins by calling out a low price and raises it, as long as there are at least two interested bidders. We have to remember that price increment is small. The auction stops when there is only one interested bidder. This bidder wins the object and pays the auctioneer an amount equal to the price which he declares. From the perspective of modeling assumes that bids are increasing continuously. Second one open auction format is Dutch auction. This auction format is the open descending price counterpart of the English auction. In practice, the Dutch auction is not widely used but from the perspective of the auction system is an interesting subject of study. The price is gradually lowered until some participant indicates her interest. The object is sold to this participant at the given price - appropriately low price. Now, consider the second auction format – sealed-bid auctions. The sealed-bid first-price auction is that participants bid from lowest to highest price. Winning the maximum bid. The winner is obliged to pay a price equal to the amount reported by its bid plus transaction costs. Recent primary

auction system is the second price auction. The winner submitting the highest bid wins the object but pays not what he bids but the second highest bid.

Should be noted that in a closed bid auction format shall be submitted in envelopes, and there is no possibility of tracing the course of the auction. Only open systems in the English format allow observation of bids submitted by other participants. From the standpoint of gray systems are the only auction formats that allow you to track the history of deals made - that is, gathering relevant data.

The paper proposed a method of forecasting prices will only open auction formats with particular reference to the English first-price auction. The choice of auction format is dependent on the possibility of direct observation reported bids. This fact is the basis for predicting the amount of bids during the auction.

3. Grey Systems – the basic idea.

The "Grey System Theory" was first proposed by Deng Julong in 1982. Gray systems theory for a long time was not known. The first lecture was published only in 1989 and its author was Deng Julong. The first book released in Europe appeared in 2005. Its authors are Sifeng and Lin. In a general sense of Gray System Theory is applicable wherever the information about the process is very limited. However, the mechanisms governing the processes are partially known. The name was created on the basis of the theory of color names. For example, "black" is used to represent unknown information and "white" is the color used for complete information. Those partially know and partially unknown information is called the "Grey System Theory". The analysis conducted on the theory of gray system has applications wherever the researcher has a mix of familiar and unfamiliar information. Firstly, in terms of theory and econometric time series should be stressed that its application requires the most significant set of information - usually long time series. Often knowledge of the distribution from which the observations come. Secondly, compliance with many theoretical assumptions the model is specified. An alternative theory to the classical theory of time series has become a gray system theory. Its main advantage is the simplification of modeling of processes in discrete time. This simplification is necessary to minimize the collection of information

and minimizing the assumptions about the model itself. This approach is sufficient to describe the process and the construction of accurate forecasts. Grey Systems Theory is in some sense alternative to the theory of time series and the theory of Fuzzy Logic, which also was recognized as the classical theory. Differences in approach to the classical approach of modeling and the theory of gray system are presented in Table 1.

Econometric model	**Minimum number of observations**	**Type of sample**	**Sample length**	**Level of mathematical sophistication**
Simple exponential function	5 - 10	Interval	Short	Basic
Regression Analysis	10 - 20	Trend	Short	Middle
Casual Regression	10	Any type	Long	Advanced
ARMA/ARIMA process	50	Interval	Long	Advanced
Neural Network	Large number	Interval or other	Short	Advanced
Grey Systems	**4**	**Interval**	**Long**	**Basic**

Table 1. Compare the main characteristics of the traditional econometric modeling, and modeling on the basis of gray systems.
Source: Prepared on the basis: Lim D., Anthony P., Chong Mun H., Kah Wai N., Assessing the Accuracy of Grey System Theory against Artificial Neural Network in Predicting Online Auction Closing Price, Proceedings of the International MultiConference of Engineers and Computer Scientists 2008 Vol I IMECS 2008, 19-21 March, 2008, Hong Kong.

The idea of modeling on the basis of Gray System Theory can be summarized as follows[2]:

- qualitative analysis process should be the basis for further modeling,
- qualitative analysis provides the basis for the specification of

[2] Liu S.,Lin Y. Grey information. Theory and practical informations., Sprnger-Verlag, 2006, page:193-194

the quantitative model,

- explanations of the factors, the relationship between these factors, and relationships between agents and the system are the main target of research,
- it must be remembered that a particular factor can dynamically change the status,
- any relationship between factors and between factors and the system is relative,
- modeling process must be continuously reviewed,
- types of data used for modeling are as follows: data of scientific experiments, empirical data, decision-making data,
- the fundamental data for grey modeling are sequence of generations,
- improving the quality of the gray models can take place through various methods of generating gray numbers, reorganization or modification of the data series, the choice of data and model specification,
- the quality of the gray model is examined through an assessment of its fit to reality.

4. Algorithm of GM(1,1) model.

GM(1,1)'s name mean successive first-order Grey Model with one variable. Model

GM(1,1) is often treated as a local predictor This model has wide application in predicting the short time series data. Simple algorithm for estimating grey model parameters are as follows:

Step 1. Empirical data raw vector.

Empirical time series is given as:

$$y^{(0)} = \left[y^{(0)}(1), y^{(0)}(2), \ldots, y^{(0)}(n)\right] \quad \text{for} \quad n \geq 4 \qquad [1]$$

where:

(0) - the superscription represents the original/empirical data series.

Important assumption is that in a number of empirical data in models of gray must be positive. Negative values are prohibited. But it is

possible that negative values appear in the data sequence. Therefore absolute value of the maximum negative data is added to shift all data to be positive. Main objective is to determine the future value of $y^{(0)}(n+p)$ where p determines forecast horizon, $(p \geq 1)$.

Step 2. Transformation of empirical data: pre-processing.

Empirical data transformation involves the application of the algorithm AGO[3]. AGO's advantage of the algorithm is to eliminate the accidental observation. This algorithm can be written as follows[4]:

$$y^{(0)}(k) = AGO \cdot y^{(0)} = \sum_{m=1}^{k} y^{(0)}(m) \qquad k = 1,2,3,...,m \qquad [2]$$

$$y^{(1)}(k) = \left[y^{(1)}(1), y^{(1)}(2), \ldots, y^{(1)}(n)\right] \qquad [3]$$

Step 3. Whitening equation (WE)

$y^{(1)}$ process is modeled by the equation of the WE, which is first-order differential equation.

$$\frac{dy^{(1)}}{dt} + \alpha \cdot y^{(1)} = u \qquad [4]$$

where:

α - development coefficient,

u - grey input.

Next, define a mean operation $z^{(1)}(k)$ as follows:

$$z^{(1)}(k) = \alpha y^{(1)}(k) + (1-\alpha) y^{(1)}(k-1) \qquad \alpha \in [0,1] \qquad [5]$$

Since, sampling time is:

$$\frac{dy^{(1)}}{dt} = y^{(1)}(k) - y^{(1)}(k-1)^{AGO} = y^{(0)}(k) \qquad [6]$$

---

[3] AGO - Accumulated Generating Operations

[4] Dounis A.I.,Tiropanis P., Tseles D.,Nikolaou G., Syrcos G.P., A Comparison of Grey Model and Fuzzy Predictive Model for Time Series, International Journal of Computational Intelligence 2;3 2006, page:177-178

Final form GDE[5] of the model is as follows:

$$y^{(0)}(k)+\alpha z^{(1)}(k)=u \qquad [6]$$

In order to estimate the parameters of the equation method is used Least Squared Error Method. We therefore:

$$Y=B\cdot\Theta \qquad [7]$$

where:

$$Y=\begin{bmatrix} y^{(0)}(2) \\ y^{(0)}(3) \\ \vdots \\ y^{(0)}(n) \end{bmatrix};\quad B=\begin{bmatrix} -z^{(1)}(2) & 1 \\ -z^{(1)}(3) & 1 \\ \vdots & \vdots \\ -z^{(1)}(n) & 1 \end{bmatrix};\quad \Theta=\begin{bmatrix} a \\ u \end{bmatrix}$$

Hence the formula for vector parameters is given as:

$$\Theta=\left(B^T B\right)^{-1}B^T y^N \qquad [8]$$

How easy it is to see the solution of equation WE is the exponential function with the initial condition as:

$$y^{(1)}(0)=y^{(0)}(1) \qquad [9]$$

Therefore, the solution can be represented as:

$$y^{*(1)}(n+p)=\left(y^{(0)}(1)-\frac{u}{\alpha}\right)\cdot e^{-\alpha(n+p-1)}+\frac{u}{\alpha} \qquad n\geq 4 \qquad [10]$$

where:

$n+p$ - forecasting p step size,

$k+1=n+p$ - time instant of the prediction.

Step 4. IAGO[6]

The IAGO on the sequence of $y^{(1)}(k)$ is as follow:

$$y^{*(0)}(n+p)=\left(y^{(0)}(1)-\frac{u}{\alpha}\right)\cdot e^{-\alpha(n+p-1)}\cdot\left(1-e^{\alpha}\right) \qquad [11]$$

---

[5] GDE – Grey Differential Equation

[6] IAGO – the inverse of AGO

The advantage of grey model is that GM model does not require a large number of observations, since there are only one regressor.

5. Application of the model GM (1,1) on the example of English first price auction

Suppose the English format of the first-price auction. Suppose further that we know closing price for the five lots of auction item. Time / date of closing auction does not matter. The main objective is to estimate the level of the closing bid price for the type of object. Such an approach is the historical approach. This allows the choice of strategy on the level of bidding for an item. This approach to modeling the price can be described as "horizontal".

So, vector from the "*hammer price*" [in Euro] is given as:

Step 1.

$$y^{(0)} = [69;79;83;89;93;99]$$

$$n = 6$$

Step 2. AGO transformation

$$y^{(1)} = [69;148;231;320;413;512]$$

Step 3. Least Square Estimation of parameters

$$\begin{bmatrix} \alpha \\ \rho \end{bmatrix} = \begin{bmatrix} a \\ u \end{bmatrix} = \begin{bmatrix} -0.0565 \\ 72,7523 \end{bmatrix}$$

Determine the model, we have:

$$\frac{dy^{(1)}}{dt} - 0,0565y^{(1)} = 72,7523$$

Solve the model for the simulation value of $y^{(1)}$ is:

$$\hat{y}^{(1)} = [69;147,8574;231,2983;319,5891;413,0118;511,8646]$$

Step 4.

Restore the $\hat{y}^{(1)}$-value to find the simulation value of $y^{(0)}$. We have:

$$\hat{y}^{(0)} = [69;78{,}8574;83{,}4409;88{,}2908;93{,}4227;98{,}8528]$$

Step 5.

Verification

$y^{(0)}$	$\hat{y}^{(0)}$	$\varepsilon = y^{(0)} - \hat{y}^{(0)}$	$\frac{y^{(0)} - \hat{y}^{(0)}}{y^{(0)}}$
69	69	0	0
79	78,8574	0,1426	0,0018
83	83,4409	-04409	0.0053
89	88,2908	0,7092	0,0080
93	93,4227	-0,4227	0,0045
99	98,8528	0,1472	0,0015

Table 2. Summary of results
Source: Own work

MAPE error is:

$$MAPE = 0{,}4223[\%]$$

Quality of the model is determined by its adjustment to the empirical data (Fig.1).

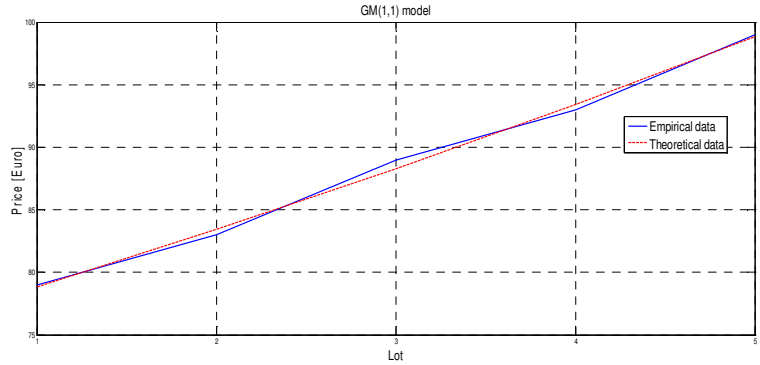

Figure 1. Empirical vs theoretical values.
Source: Own work

R^2 coefficient is equal to 99,64% for this model and F-statistics is equal to 821,2172.

This means that high fit model to empirical data. The high value of statistic F is the statistical significance of the estimated model parameters. Hence, it follows that the specification of the model is correct and its adaptation to the reality it is sufficient for the needs of future bids submitted by bidders. As you can see there are areas of a revaluation, which may mean winning the auction due to the amount of the reported bid. From the viewpoint of stochastic nature of the model, it is difficult to say to the autocorrelation of the random component, given the low number of observations. The residual of model presents Fig 2.

Figure 2. Residuals.
Source: Own work

In short gray models of systems which allow the performance of the drawings. These models do not determine winner prices of action. Winning depends on the bidding process and the budget available to the participant. Each participant in the auction must be aware of their own budgetary constraints and in accordance with the auction to take the game - to act rationally.

6. Conclusion.

In conclusion, the modeling of market prices for the auction to be extremely difficult due to the low number of observed prices and the tightness of the market. Application of classical methods of

econometrics and artificial intelligence methods may lead to a breakthrough in the description of the extremely popular markets.

In future studies will provide a review of models of gray systems based on real auction data. Auction models are gray systems enriched with tools of artificial intelligence and neural networks.

LITERATURE

[1] Dounis A.I.,Tiropanis P., Tseles D.,Nikolaou G., Syrcos G.P., A Comparison of Grey Model and Fuzzy Predictive Model for Time Series, International Journal of Computational Intelligence 2;3, 2006

[2] Krishna V., "Auction Theory", Academic Press, 2002

[3] Lim D., Anthony P., Chong Mun H., Kah Wai N., Assessing the Accuracy of Grey System Theory against Artificial Neural Network in Predicting Online Auction Closing Price, Proceedings of the International MultiConference of Engineers and Computer Scientists 2008 Vol I IMECS 2008, 19-21 March, 2008, Hong Kong

[4] Liu S.,Lin Y. Grey information. Theory and practical informations., Sprnger-Verlag, 2006

[5] McAfee, R. P., & McMillan, J., "Auctions and Bidding," Journal of Economic Literature, vol. 25 no. 2, 1987

RENDICONTI DEL CIRCOLO MATEMATICO DI PALERMO
Serie II, Suppl. 83 (2011), pp. 23-40

The distributions function of a chord in a non-convex polygon

D. Barilla, A. Duma**, A. Puglisi**
Department S.E.A.
*University of Messina
**University of Hagen
e-mail: puglisia*@unime.it*

1 Introduction

In the last three years some results were obtained on the probability, that a line of the lattice $\mathcal{R}_D$ of Buffon composed of parallel lines from a distance D each other intersects a segment of length greater than or equal to s in a convex poligon P, that is small compared to $\mathcal{R}_D$, therefore the diameter $diam(P)$ of P is less than D. This poligon P is a rectangle by M. Pettineo, an equilateral traingle by M. Stoka and A. Duma, a triangle by S. Rizzo and A. Duma, a regular hexagon by V. Conserva and A. Duma, a rectangle trapezium by S. Rizzo and A. Duma and an isosceles trapezium by L. Sorrenti.

A fundamental problem in the papers of Rizzo and Duma and in the paper of Sorrenti is the large number of the cases that must be considered, because between different sides and diagonals of P there are a lot of different situations. The same problem is when we consider a non-convex polygon as in the follow figure:

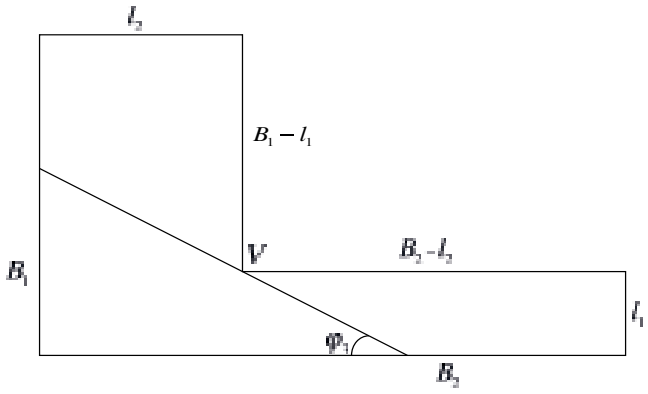

fig.1 - A non convex polygon

In order to compute the announced probability we must to distinguish a large number of different possible relations between the lengthes

$$B_1,\ B_2,\ l_1,\ l_2,\ B_1-l_1,\ B_2-l_2,\ \sqrt{B_1^2+l_2^2},\ \sqrt{B_2^2+l_1^2},\ \sqrt{l_1^2+l_2^2},$$

$$\sqrt{B_1^2-2B_1l_1+l_1^2+l_2^2},\ \sqrt{B_2^2-2B_2l_2+l_2^2+l_1^2},\ \frac{B_2}{B_2-l_2}\sqrt{B_2^2-2B_2l_2+l_2^2+l_1^2},$$

$$\frac{B_1}{B_1-l_1}\sqrt{B_1^2-2B_1l_1+l_1^2+l_2^2}\ \textit{and}\ \beta.$$

β is the smallest segment between the following sides B_1 and B_2, that contain the angle V. This is the reason why we try to find only the particular case

$$B_1 = B_2 =: A, \qquad l_1 = l_2 =: a,$$

therefore the convex polygon L, that have the form presented in the figure 2 or the form that we can see in the figure 3:

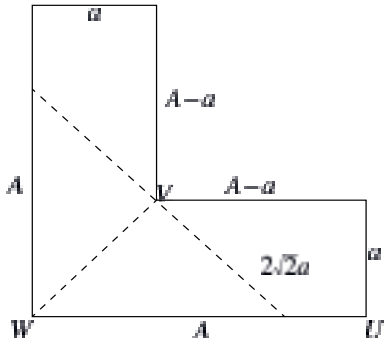

Fig. 2 $A \geq 2a$

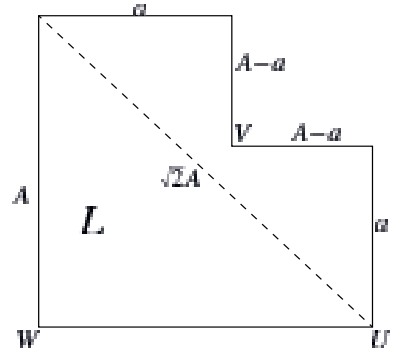

Fig. 3 $A < 2a$

We denote that the computation of the probability $p(s)$ that the polygon L intersects a segment of length greater than or equal to $s \leq diam(L)$ on a line of $\mathcal{R}_D$ is the most easy in the cases of the figures 2 and 3 that in the case of the figure 1, because the polygons in the figures 2 and 3 have a symmetry compared to the line determinate of V and W.

2 General considerations

The dimensions of L are

- for the figure 2 the follow: $a, a\sqrt{2}, 2\sqrt{2}\,a,\ A-a,\ \sqrt{A^2-2Aa+2a^2}$,

$$A \ \text{ and } \ \frac{A}{A-a}\sqrt{A^2-2Aa+2a^2} = diam(L),$$

- for the figure 3 the follow: $a, a\sqrt{2}\,,\ A-a,\ \sqrt{A^2-2Aa+2a^2},\ A\,,$

$$\frac{A}{a}\sqrt{A^2-2Aa+2a^2},\ \sqrt{A^2+a^2},\ \sqrt{2}\,A = diam(L).$$

For each pair (A,a) with $A>a$ we always have

$$\max(a, A-a) < \sqrt{A^2-2Aa+2a^2} < A < \sqrt{A^2+a^2}.$$

Moreover, for $A \geq 2a$ we have

$$\max(2\sqrt{2}\,a, \sqrt{A^2+a^2}) < \frac{A}{A-a}\sqrt{A^2-2Aa+2a^2} = diam(L),$$

and for $A<2a$ we have

$$A < \min(\frac{A}{a}\sqrt{A^2-2Aa+2a^2},\ \sqrt{A^2+a^2}) \leq$$

$$\max(\frac{A}{a}\sqrt{A^2-2Aa+2a^2},\ \sqrt{A^2+a^2}) < \sqrt{2}\,A = diam(L).$$

The other relations between the dimensions of L depend on quotient $\frac{A}{a}$. The equivalences

$$2\sqrt{2}\,a \leq A-a \iff \left(2\sqrt{2}+1\right)a \leq A,$$

$$2\sqrt{2}\,a \leq \sqrt{A^2-2Aa+2a^2} \iff \left(\sqrt{7}+1\right)a \leq A,$$

$$2\sqrt{2}\,a \leq \sqrt{A^2+a^2} \iff \sqrt{7}a \leq A,$$

$$\sqrt{2}\,a \leq A-a \iff \left(\sqrt{2}+1\right)a \leq A,$$

$$\sqrt{A^2+a^2} \leq \frac{A}{a}\sqrt{A^2-2Aa+2a^2} \iff \frac{\sqrt{5}+1}{2}a \leq A,$$

$$\sqrt{2}\,a \leq \frac{A}{a}\sqrt{A^2-2Aa+2a^2} \iff 0 \leq \left(\frac{A}{a}\right)^4 - 2\left(\frac{A}{a}\right)^3 + 2\left(\frac{A}{a}\right)^2 - 2 \iff \lambda_0 a \leq A,$$

where $\lambda_0 \approx 1,338$ is the only solution greater than 1 of the equation

$$\lambda^4 - 2\lambda^3 + 2\lambda^2 - 2 = 0,$$

give us therefore the values for the quotient $\frac{A}{a}$:

$$\lambda_0,\ \frac{\sqrt{5}+1}{2}, \sqrt{2}+1, \sqrt{7}, \sqrt{7}+1 \text{ and } 2\sqrt{2}+1.$$

.

Moreover we must consider also the values $1,\ \sqrt{2},\ 2,$ and $2\sqrt{2}$.

In this way we obtain ten subintervals

$$]1,\lambda_0]\,,\quad \left[\lambda_0,\sqrt{2}\right]\,,\quad \left[\sqrt{2},\frac{\sqrt{5}+1}{2}\right]\,,\quad \left[\frac{\sqrt{5}+1}{2},2\right]\,,$$

$$\left[2,\sqrt{2}+1\right]\,,\left[\sqrt{2}+1,\sqrt{7}\right]\,,\quad \left[\sqrt{7},2\sqrt{2}\right]\,,$$

$$\left[2\sqrt{2},\sqrt{7}+1\right]\,,\quad \left[\sqrt{7}+1,2\sqrt{2}+1\right] \text{ and } \left[2\sqrt{2}+1,+\infty\right[$$

of $]1,+\infty[$. The form of clains of inequalities between the dimensions of L depend on the belonging to the quotient $\dfrac{A}{a}$ to any of these ten subintervals.

I if $\dfrac{A}{a}\geq 2\sqrt{2}+1,$ therefore we have

$$0<a<a\sqrt{2}\,<2\sqrt{2}a\leq A-a<\sqrt{A^2-2Aa+2a^2}<$$
$$A<\sqrt{A^2+a^2}<\frac{A}{A-a}\sqrt{A^2-2Aa+2a^2},$$

II if $\dfrac{A}{a}\in\left[\sqrt{7}+1,2\sqrt{2}+1\right]$, therefore we have

$$0<\sqrt{2}a<A-a\leq 2\sqrt{2}a\leq\sqrt{A^2-2Aa+2a^2}<$$
$$A<\sqrt{A^2+a^2}<\frac{A}{A-a}\sqrt{A^2-2Aa+2a^2},$$

III if $\dfrac{A}{a}\in\left[2\sqrt{2},\sqrt{7}+1\right]$, therefore we have

$$0<a<\sqrt{2}a<A-a<\sqrt{A^2-2Aa+2a^2}\leq$$
$$2\sqrt{2}a\leq A<\sqrt{A^2+a^2}<\frac{A}{A-a}\sqrt{A^2-2Aa+2a^2},$$

IV if $\dfrac{A}{a}\in\left[\sqrt{7},2\sqrt{2}\right]$, therefore we have

$$0<a<\sqrt{2}a<A-a<\sqrt{A^2-2Aa+2a^2}<$$
$$A\leq 2\sqrt{2}a\leq\sqrt{A^2+a^2}<\frac{A}{A-a}\sqrt{A^2-2Aa+2a^2},$$

V if $\dfrac{A}{a}\in\left[\sqrt{2}+1,\sqrt{7}\right]$, therefore we have

$$0<a<\sqrt{2}a\leq A-a<\sqrt{A^2-2Aa+2a^2}<$$
$$A<\sqrt{A^2+a^2}\leq 2\sqrt{2}a<\frac{A}{A-a}\sqrt{A^2-2Aa+2a^2},$$

VI if $\frac{A}{a} \in \left[2, \sqrt{2}+1\right]$, therefore we have

$$0 < a \leq A - a \leq \sqrt{2}a < \sqrt{A^2 - 2Aa + 2a^2} <$$
$$A < \sqrt{A^2 + a^2} < 2\sqrt{2}a < \frac{A}{A-a}\sqrt{A^2 - 2Aa + 2a^2},$$

VII if $\frac{A}{a} \in \left[\frac{\sqrt{5}+1}{2}, 2\right]$, therefore we have

$$0 < A - a \leq a < \sqrt{A^2 - 2Aa + 2a^2} \leq \sqrt{2}a <$$
$$A < \sqrt{A^2 + a^2} \leq \frac{A}{a}\sqrt{A^2 - 2Aa + 2a^2} < \sqrt{2}A,$$

VIII if $\frac{A}{a} \in \left[\sqrt{2}, \frac{\sqrt{5}+1}{2}\right]$, therefore we have

$$0 < A - a < a < \sqrt{A^2 - 2Aa + 2a^2} < \sqrt{2}a \leq$$
$$A < \frac{A}{a}\sqrt{A^2 - 2Aa + 2a^2} \leq \sqrt{A^2 + a^2} < \sqrt{2}A,$$

IX if $\frac{A}{a} \in \left[\lambda_0, \sqrt{2}\right]$, therefore we have

$$0 < A - a < a < \sqrt{A^2 - 2Aa + 2a^2} < A \leq \sqrt{2}a \leq$$
$$\frac{A}{a}\sqrt{A^2 - 2Aa + 2a^2} < \sqrt{A^2 + a^2} < \sqrt{2}A,$$

X if $\frac{A}{a} \in \left]1, \lambda_0\right]$, therefore we have

$$0 < A - a < a < \sqrt{A^2 - 2Aa + 2a^2} < A <$$
$$\frac{A}{a}\sqrt{A^2 - 2Aa + 2a^2} \leq \sqrt{2}a < \sqrt{A^2 + a^2} < \sqrt{2}A.$$

We denote with φ the angle between the direction of the lines of $\mathcal{R}_D$ and the side WU. Because L is symmetric compared to the line between W and V, we obtain all the possible positions of L compared to $\mathcal{R}_D$ exactly one time, if φ varies in the interval $\left[-\frac{\pi}{4}, \frac{\pi}{4}\right]$.

To facilitate the calculations we denote the angle $\varphi \in \left[-\frac{\pi}{4}, 0\right[$ with $-\Psi$, therefore Ψ varies between 0 and $\frac{\pi}{4}$.

We denote with $d_s(\varphi)$ and $\delta_s(\Psi)$ the maximum distance between two parallel segments of length s, which make an angle φ respectively Ψ with WU. For different values of s, φ and Ψ we compute $d_s(\varphi)$ and $\delta_s(\Psi)$ using the expressions of $x_s(\varphi)$, $y_s(\varphi)$, $z_s(\varphi)$ and $w_s(\varphi)$ respectively $u_s(\Psi)$ and $v_s(\Psi)$:

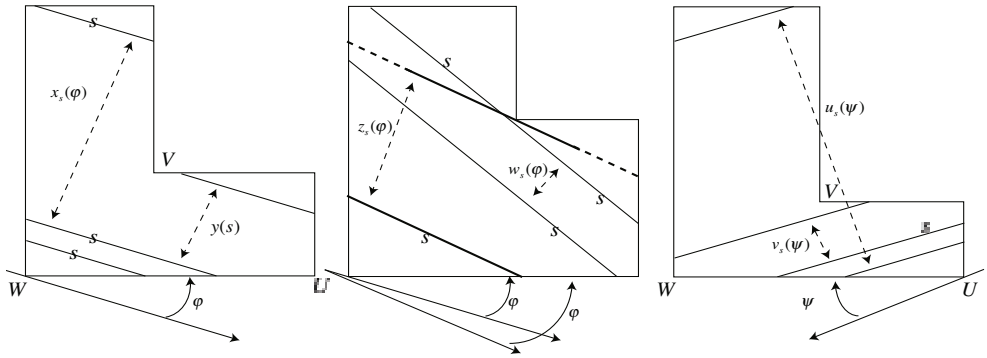

fig.4

We have:

$$x_s(\varphi) = A\cos\varphi + a\sin\varphi - s\sin 2\varphi,$$

$$y_s(\varphi) = A\sin\varphi + a\cos\varphi - s\sin 2\varphi,$$

$$z_s(\varphi) = \sqrt{2}a\sin\left(\varphi + \frac{\pi}{4}\right) - \frac{s}{2}\sin 2\varphi =$$

$$a\sin\varphi + a\cos\varphi - \frac{s}{2}\sin 2\varphi,$$

$$w_s(\varphi) = \sqrt{2}A\sin\left(\varphi + \frac{\pi}{4}\right) - s\sin 2\varphi =$$

$$A\sin\varphi + A\cos\varphi - s\sin 2\varphi,$$

$$u_s(\Psi) = A\sin\Psi + A\cos\Psi - s\sin 2\Psi,$$

$$v_s(\Psi) = A\sin\Psi + a\cos\Psi - s\sin 2\Psi.$$

The probability that we should search is given by the formula

$$p(s) = \frac{2}{\pi D}\left[\int_0^{\frac{\pi}{4}} d_s(\varphi)\ d\varphi + \int_0^{\frac{\pi}{4}} \delta_s(\Psi)\ d\Psi\right]. \tag{1}$$

The expressions of d_s and δ_s does not change, if s is between two dimensions that derive from one of the chain of inequalities given in I, II,...X.

For the expression of d_s, the diagonal $\sqrt{A^2+a^2}$ does not play any role. For δ_s we use only the dimensions 0, a , $\sqrt{2}a$, A and $\sqrt{A^2+a^2}$; $\delta_s = 0$ if $s \geq \sqrt{A^2+a^2}$.

We determine the probability $p(s)$ computing

$$\int_0^{\frac{\pi}{4}} d_s(\varphi)\ d\varphi$$

and then

$$\int_0^{\frac{\pi}{4}} \delta_s(\Psi)\ d\Psi$$

for all the pair of the dimensions that derive from L in the ten chains of inequalities.

3 Subcases for d_s

We need angles $\varphi_0, \varphi_1, \varphi_2, \varphi_3, \varphi_4$, and φ_5 when they are in the interval $\left[0, \frac{\pi}{4}\right]$; they are uniquely determined by the formulas

$$\cos\varphi_0 = \frac{a}{s}, \qquad \sin\varphi_1 = \frac{a}{s},$$

$$\cos\varphi_2 = \frac{A-a}{s}, \qquad \frac{1}{\sin\varphi_3} + \frac{1}{\cos\varphi_3} = \frac{s}{a},$$

$$\cos\varphi_4 = \frac{a}{\sqrt{A^2 - 2Aa + 2a^2}} \quad \text{and} \quad \cos\varphi_5 = \frac{A}{s}.$$

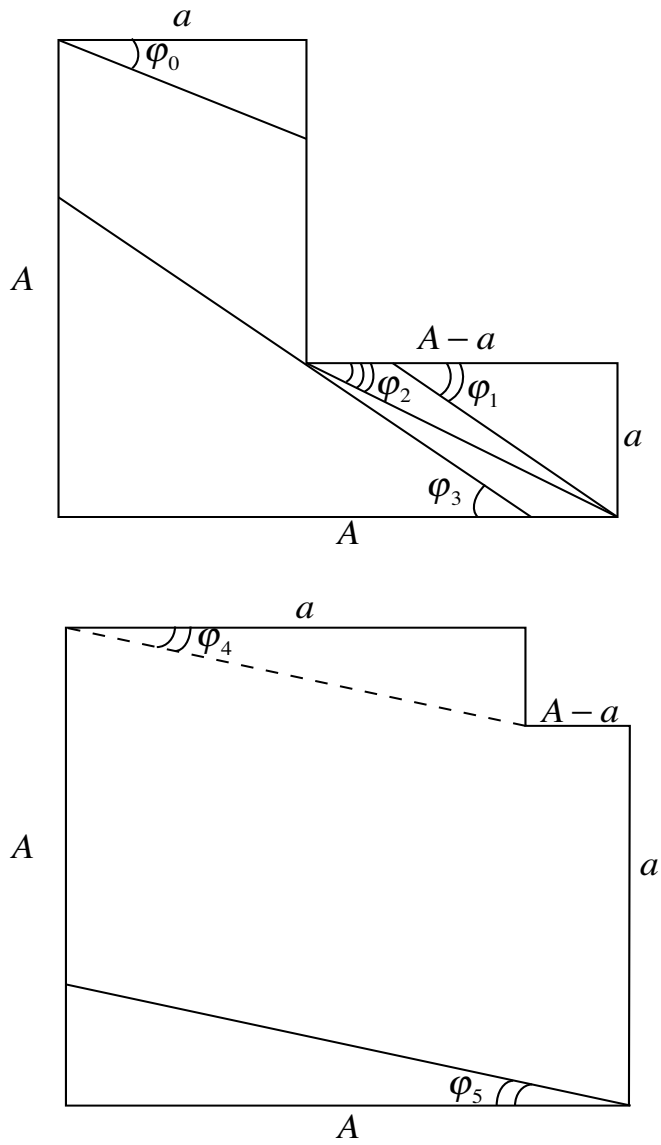

fig.5 - The angles φ_1, φ_2,..., φ_5

If the angles exist in $\left[0, \frac{\pi}{4}\right]$ we have $\varphi_1 \leq \varphi_3$ and $\varphi_5 < \varphi_2$;moreover we have

$$\varphi_2 \leq \varphi_0 \iff 2a \leq A,$$
$$\varphi_5 \leq \varphi_4 \iff s \leq \frac{A}{a}\sqrt{A^2 - 2Aa + 2a^2},$$
$$\varphi_2 \leq \varphi_1 \iff s \leq \sqrt{A^2 - 2Aa + 2a^2}.$$

$(d1)$ If $0 \leq s \leq \min(a, A-a)$ or $A-a \leq s \leq a$ there is

$$d_s(\varphi) = x_s(\varphi)$$

if $\varphi \in \left[0, \frac{\pi}{4}\right]$.

$$\int_0^{\frac{\pi}{4}} d_s(\varphi)\ d\varphi = \int_0^{\frac{\pi}{4}} x_s(\varphi)\ d\varphi = \frac{\sqrt{2}}{2}A + \left(1 - \frac{\sqrt{2}}{2}\right)a - \frac{s}{2}.$$

$(d2)$ If $a \leq s \leq \min\left(\sqrt{2}a, A-a\right)$ there is

$$d_s(\varphi) = \begin{cases} y_s(\varphi) & \text{if } 0 \leq \varphi \leq \varphi_0, \\ x_s(\varphi) & \text{if } \varphi_0 \leq \varphi \leq \frac{\pi}{4}. \end{cases}$$

$$\int_0^{\frac{\pi}{4}} d_s(\varphi)\ d\varphi = \int_0^{\varphi_0} y_s(\varphi)\ d\varphi + \int_{\varphi_0}^{\frac{\pi}{4}} x_s(\varphi)\ d\varphi = \left(1 - \cos\varphi_0 - \sin\varphi_0 + \frac{\sqrt{2}}{2}\right)A +$$

$$\left(\sin\varphi_0 + \cos\varphi_0 - \frac{\sqrt{2}}{2}\right)a - \frac{s}{2}.$$

$(d3)$ If $\sqrt{2}a \leq s \leq \min\left(A-a, 2\sqrt{2}a\right)$ there is

$$d_s(\varphi) = \begin{cases} y_s(\varphi) & \text{if } 0 \leq \varphi \leq \varphi_1, \\ z_s(\varphi) & \text{if } \varphi_1 \leq \varphi \leq \frac{\pi}{4}. \end{cases}$$

$$\int_0^{\frac{\pi}{4}} d_s(\varphi)\ d\varphi = \int_0^{\varphi_1} y_s(\varphi)\ d\varphi + \int_{\varphi_1}^{\frac{\pi}{4}} z_s(\varphi)\ d\varphi =$$

$$(1 - \cos\varphi_1)A + a\cos\varphi_1 - \frac{1}{4}(2 - \cos 2\varphi_1)s.$$

$(d4)$ If $a \leq A-a \leq s \leq \min\left(\sqrt{2}a, \sqrt{A^2 - 2Aa + 2a^2}\right)$ there is

$$d_s(\varphi) = \begin{cases} z_s(\varphi) & \text{if } 0 \leq \varphi \leq \varphi_2, \\ y_s(\varphi) & \text{if } \varphi_2 \leq \varphi \leq \varphi_0, \\ x_s(\varphi) & \text{if } \varphi_0 \leq \varphi \leq \frac{\pi}{4}. \end{cases}$$

$$\int_0^{\frac{\pi}{4}} d_s(\varphi)\ d\varphi = \left(\frac{\sqrt{2}}{2} + \cos\varphi_2 - \cos\varphi_0 - \sin\varphi_0\right)A +$$

$$\left(1 - \frac{\sqrt{2}}{2} - \cos\varphi_2 + \sin\varphi_0 + \cos\varphi_0\right)a -$$

$$\frac{1}{4}\left(1+\cos^2\varphi_2\right)s.$$

($d5$) If $A-a\leq a\leq s\leq \min\left(\sqrt{2}a,\sqrt{A^2-2Aa+2a^2}\right)$ there is

$$d_s(\varphi)=\begin{cases} z_s(\varphi) & \text{if } 0\leq\varphi\leq\varphi_0,\\ x_s(\varphi) & \text{if } \varphi_0\leq\varphi\leq\dfrac{\pi}{4}.\end{cases}$$

$$\int_0^{\frac{\pi}{4}} d_s(\varphi)\ d\varphi=\left(\frac{\sqrt{2}}{2}-\sin\varphi_0\right)+\left(1-\frac{\sqrt{2}}{2}+\sin\varphi_0\right)-\frac{1}{4}\left(1+\cos 2\varphi_0\right)s.$$

($d6$) If $2\sqrt{2}a\leq s\leq A-a$ there is

$$d_s(\varphi)=\begin{cases} y_s(\varphi) & \text{if } 0\leq\varphi\leq\varphi_1,\\ z_s(\varphi) & \text{if } \varphi_1\leq\varphi\leq\varphi_3,\\ 0 & \text{if } \varphi_3\leq\varphi\leq\dfrac{\pi}{4}.\end{cases}$$

$$\int_0^{\frac{\pi}{4}} d_s(\varphi)\ d\varphi=\left(1-\cos\varphi_1\right)A+\left(\cos\varphi_1+\sin\varphi_3-\cos\varphi_3\right)a-$$

$$\frac{1}{4}\left(2-\cos 2\varphi_1-\cos 2\varphi_3\right)s.$$

($d7$) If $\max\left(2\sqrt{2}a,\sqrt{A^2-2Aa+2a^2}\right)\leq s\leq A$ there is

$$d_s(\varphi)=\begin{cases} z_s(\varphi) & \text{if } 0\leq\varphi\leq\varphi_3,\\ 0 & \text{if } \varphi_3\leq\varphi\leq\dfrac{\pi}{4}.\end{cases}$$

$$\int_0^{\frac{\pi}{4}} d_s(\varphi)\ d\varphi=\left(1+\sin\varphi_3-\cos\varphi_3\right)a-$$

$$\frac{1}{4}\left(1-\cos 2\varphi_3\right)s.$$

($d8$) If $2a\leq A\leq s\leq 2\sqrt{2}a$ there is

$$d_s(\varphi)=\begin{cases} 0 & \text{if } 0\leq\varphi\leq\varphi_5,\\ z_s(\varphi) & \text{if } \varphi_5\leq\varphi\leq\dfrac{\pi}{4}.\end{cases}$$

$$\int_0^{\frac{\pi}{4}} d_s(\varphi)\ d\varphi=\left(\cos\varphi_5-\sin\varphi_5\right)a-\frac{s}{4}\cos 2\varphi_5.$$

($d9$) If $A \leq s \leq \min\left(2a, \frac{A}{a}\sqrt{A^2 - 2Aa + 2a^2}\right)$ there is

$$d_s(\varphi) = \begin{cases} 0 & \text{if } 0 \leq \varphi \leq \varphi_5, \\ z_s(\varphi) & \text{if } \varphi_5 \leq \varphi \leq \varphi_4, \\ w_s(\varphi) & \text{if } \varphi_4 \leq \varphi \leq \frac{\pi}{4}. \end{cases}$$

$$\int_0^{\frac{\pi}{4}} d_s(\varphi)\ d\varphi = (\cos\varphi_4 - \sin\varphi_4)\, A +$$
$$(\sin\varphi_4 - \cos\varphi_4 + \cos\varphi_5 - \sin\varphi_5)\, a -$$
$$\frac{1}{4}(\cos 2\varphi_4 + \cos 2\varphi_5)\, s.$$

($d10$) If $2a \leq A$ and $\max\left(2a, 2\sqrt{2}a\right) \leq s \leq \frac{A}{A-a}\ \sqrt{A^2 - 2Aa + 2a^2}$ there is

$$d_s(\varphi) = \begin{cases} 0 & \text{if } 0 \leq \varphi \leq \varphi_5, \\ z_s(\varphi) & \text{if } \varphi_5 \leq \varphi \leq \varphi_3, \\ 0 & \text{if } \varphi_3 \leq \varphi \leq \frac{\pi}{4}. \end{cases}$$

$$\int_0^{\frac{\pi}{4}} d_s(\varphi)\ d\varphi = (\cos\varphi_5 - \cos\varphi_3 + \sin\varphi_3 - \sin\varphi_5)\, a -$$
$$\frac{1}{4}(\cos 2\varphi_5 - \cos 2\varphi_3)\, s.$$

($d11$) If $\max\left(2\sqrt{2}a, A - a\right) \leq s \leq \sqrt{A^2 - 2Aa + 2a^2}$ there is

$$d_s(\varphi) = \begin{cases} z_s(\varphi) & \text{if } 0 \leq \varphi \leq \varphi_2, \\ y_s(\varphi) & \text{if } \varphi_2 \leq \varphi \leq \varphi_1, \\ z_s(\varphi) & \text{if } \varphi_1 \leq \varphi \leq \varphi_3, \\ 0 & \text{if } \varphi_3 \leq \varphi \leq \frac{\pi}{4}. \end{cases}$$

$$\int_0^{\frac{\pi}{4}} d_s(\varphi)\ d\varphi = (\cos\varphi_2 - \cos\varphi_1)\, A +$$
$$(1 + \cos\varphi_1 - \cos\varphi_2 + \sin\varphi_3 - \cos\varphi_3)\, a -$$
$$\frac{1}{4}(1 + \cos 2\varphi_2 - \cos 2\varphi_1 - \cos 2\varphi_3)\, s.$$

($d12$) If $\max\left(\sqrt{2}a, A - a\right) \leq s \leq \min\left(\sqrt{A^2 - 2Aa + 2a^2}, 2\sqrt{2}a\right)$ there is

$$d_s(\varphi) = \begin{cases} z_s(\varphi) & \text{if } 0 \leq \varphi \leq \varphi_2, \\ y_s(\varphi) & \text{if } \varphi_2 \leq \varphi \leq \varphi_1, \\ z_s(\varphi) & \text{if } \varphi_1 \leq \varphi \leq \frac{\pi}{4}. \end{cases}$$

$$\int_0^{\frac{\pi}{4}} d_s(\varphi)\ d\varphi = (\cos\varphi_2 - \cos\varphi_1)\, A + (1 + \cos\varphi_1 - \cos\varphi_2)\, a - \frac{1}{4}(1 + \cos 2\varphi_2 - \cos 2\varphi_1)\, s.$$

($d13$) If $\sqrt{A^2 - 2Aa + 2a^2} \leq s \leq \min\left(2\sqrt{2}a, A\right)$ there is

$$d_s(\varphi) = z_s(\varphi) \text{ if } 0 \leq \varphi \leq \frac{\pi}{4}.$$

$$\int_0^{\frac{\pi}{4}} d_s(\varphi)\ d\varphi = a - \frac{s}{4}.$$

($d14$) If $\sqrt{A^2 - 2Aa + 2a^2} \leq s \leq A \leq 2a$ there is

$$d_s(\varphi) = \begin{cases} z_s(\varphi) & \text{if } 0 \leq \varphi \leq \varphi_4, \\ w_s(\varphi) & \text{if } \varphi_4 \leq \varphi \leq \frac{\pi}{4}. \end{cases}$$

$$\int_0^{\frac{\pi}{4}} d_s(\varphi)\ d\varphi = (\cos\varphi_4 - \sin\varphi_4)\, A + (1 + \sin\varphi_4 - \cos\varphi_4) - \frac{1}{4}(1 - \cos 2\varphi_4)\, s.$$

($d15$) If $\frac{A}{a}\sqrt{A^2 - 2Aa + 2a^2} \leq s \leq \sqrt{2}A$ (and therefore $A \leq 2a$) there is

$$d_s(\varphi) = \begin{cases} 0 & \text{if } 0 \leq \varphi \leq \varphi_5, \\ w_s(\varphi) & \text{if } \varphi_5 \leq \varphi \leq \frac{\pi}{4}. \end{cases}$$

$$\int_0^{\frac{\pi}{4}} d_s(\varphi)\ d\varphi = (\cos\varphi_5 - \sin\varphi_5)\, a - \frac{s}{2}\cos 2\varphi_5.$$

Remark: If s is equal to a dimension of L, the integral $\int_0^{\frac{\pi}{4}} d_s(\varphi)\ d\varphi$ is computed at least in two different subcases; the result must be also of geometric reasons, because $s \longrightarrow \int_0^{\frac{\pi}{4}} d_s(\varphi)\ d\varphi$ is a continuous function. This phenomenon, that needs also like a proof, takes place for example

- if $s = a$,therefore $\varphi_0 = 0$ and the formulas given of ($d1$) and ($d2$) coincide;

- if $s=\sqrt{2}a$,therefore $\varphi_0=\varphi_1=\frac{\pi}{4}$ and $(d2)$ and $(d3)$ give the same result for $\int\limits_0^{\frac{\pi}{4}} d_s(\varphi)\ d\varphi$;

- if $s=\sqrt{2}a=A-a$,therefore $\varphi_2=0$and also $(d4)$ give the result of $(d2)$ and $(d3)$;

- if $A-a=a$,therefore $\varphi_0=\varphi_2=0$and the formulas of $(d4)$ and $(d5)$ coincide;

- if $s=2\sqrt{2}a$,we obtain the same result

i) from $(d3)$ and $(d6)$, because we have $\varphi_3=\dfrac{\pi}{4}$,

ii) from $(d6)$ and $(d7)$, because we have $\varphi_1=0$,

iii) from $(d7)$ and $(d8)$, because we have $\varphi_3=\dfrac{\pi}{4}$ and $\varphi_6=0$.

- If moreover $s=A=2\sqrt{2}a$, the formulas that are in $(d7)$ and $(d8)$ coincide with the formula (d_{10});

- if $2\sqrt{2}a\leq A-a=s$,therefore $\varphi_2=0$ and from $(d6)$ and $(d11)$ we obtain the same value for $\int\limits_0^{\frac{\pi}{4}} d_s(\varphi)\ d\varphi$;

- if $\sqrt{2}a\leq A-a\leq s=2\sqrt{2}a$,the formulas of $(d11)$ and $(d12)$ give the same result , because $\varphi_3$is egual to $\dfrac{\pi}{4}$;

- if $\sqrt{A^2-2Aa+2a^2}\leq 2\sqrt{2}a=s\leq A$,so $(d7)$ and (d_{13}) give the same result , because $\varphi_3=\dfrac{\pi}{4}$, if moreover $s=A$,therefore also $(d8)$ gives the same result of $(d7)$ and $(d11)$;

- if $\sqrt{A^2-2Aa+2a^2}\leq 2\sqrt{2}a=s=A$, therefore also $(d8)$ gives the same result of $(d7)$ and $(d11)$;

- if $s=A\leq 2a$ from (d_9) and (d_{14}) we obtain the same result, because we have $\varphi_5=0$;

- if $s=\frac{A}{a}\sqrt{A^2-2Aa+2a^2}=2a$ we have $\varphi_4=\dfrac{\pi}{4}$ and therefore from $(d9)$ and $(d15)$ we obtain the same result for the integral.

4 Subcases for δ_s

In this case we consider (if exist in the interval $\left[0,\dfrac{\pi}{4}\right]$) the angles Ψ_0,Ψ_1 and Ψ_2 only determined between the formulas

$$\cos\Psi_0=\frac{a}{s},\quad \sin\Psi_1=\frac{a}{s},\quad \cos\Psi_2=\frac{A}{s}.$$

We have $\Psi_0\leq\Psi_1$and $\Psi_2\leq\Psi_0$if the two angles in the written inequality exist.

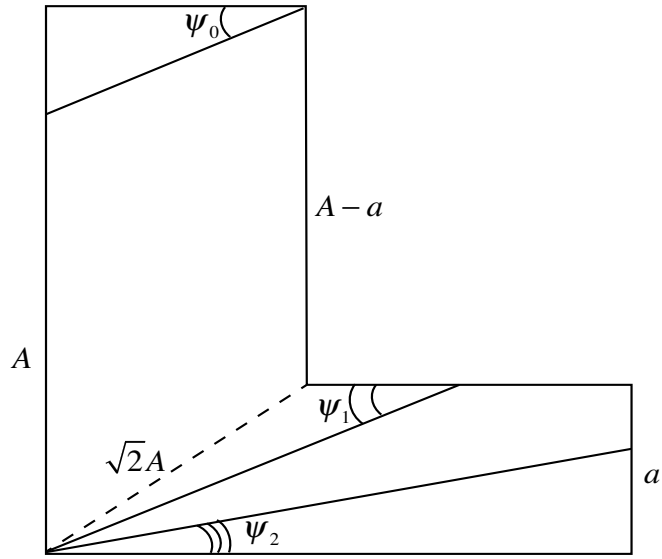

fig.6 - The angles Ψ_0, Ψ_1 and Ψ_2

($\delta 1$) If $0 \leq s \leq a$ there is $\delta_s(\Psi) = u_s(\Psi)$ if $0 \leq \Psi \leq \frac{\pi}{4}$.

$$\int_0^{\frac{\pi}{4}} \delta_s(\Psi)\ d\Psi = \int_0^{\frac{\pi}{4}} u_s(\Psi)\ d\Psi = A - \frac{s}{2}.$$

($\delta 2$) If $a \leq s \leq \min\left(\sqrt{2}a, A\right)$ there is

$$\delta_s(\Psi) = \begin{cases} v_s(\Psi) & \text{if } 0 \leq \Psi \leq \Psi_0, \\ u_s(\Psi) & \text{if } \Psi_0 \leq \Psi \leq \dfrac{\pi}{4}. \end{cases}$$

$$\int_0^{\frac{\pi}{4}} \delta_s(\Psi)\ d\Psi = \int_0^{\Psi_0} v_s(\Psi)\ d(\Psi) + \int_{\Psi_0}^{\frac{\pi}{4}} u_s(\Psi)\ d(\Psi) =$$

$$(1 - \sin\Psi_0)\, A + a \sin\Psi_0 - \frac{s}{2}.$$

($\delta 3$) If $\sqrt{2}a \leq s \leq A$ there is

$$\delta_s(\varphi) = \begin{cases} v_s(\Psi) & \text{if } 0 \leq \Psi \leq \Psi_1, \\ 0 & \text{if } \Psi_1 < \Psi \leq \dfrac{\pi}{4}. \end{cases}$$

$$\int_0^{\frac{\pi}{4}} \delta_s(\Psi)\ d\Psi = (1 - \cos\Psi_1)\, A + a \sin\Psi_1 - \frac{1}{2}(1 - \cos 2\Psi_1)\, s.$$

($\delta 4$)

$$a \leq A \leq s \leq \sqrt{2}a$$

$$\delta_s(\varphi) = \begin{cases} 0 & \text{if } 0 \leq \Psi \leq \Psi_2, \\ v_s(\Psi) & \text{if } \Psi_2 \leq \Psi \leq \Psi_0, \\ u_s(\Psi) & \text{if } \Psi_0 \leq \Psi \leq \dfrac{\pi}{4}. \end{cases}$$

$$\int_0^{\frac{\pi}{4}} \delta_s(\Psi)\ d\Psi = (\cos\Psi_2 - \sin\Psi_0)A + (\sin\Psi_0 - \sin\Psi_2)a - \frac{s}{2}\cos 2\Psi_2.$$

($\delta 5$) If $\max\left(\sqrt{2}a, A\right) \leq s \leq \sqrt{A^2+a^2}$ there is

$$\delta_s(\varphi) = \begin{cases} 0 & \text{if } 0 \leq \Psi \leq \Psi_2, \\ v_s(\Psi) & \text{if } \Psi_2 \leq \Psi \leq \Psi_1, \\ 0 & \text{if } \Psi_1 \leq \Psi \leq \dfrac{\pi}{4}. \end{cases}$$

$$\int_0^{\frac{\pi}{4}} \delta_s(\Psi)\ d\Psi = (\cos\Psi_2 - \cos\Psi_1)A +$$

$$(\sin\Psi_1 - \sin\Psi_2)a - \frac{1}{2}(\cos 2\Psi_2 - \cos 2\Psi_1)s.$$

Remark: The integral $\int_0^{\frac{\pi}{4}} \delta_s(\Psi)\ d\Psi$ defines a continuous function on $\left[0, \sqrt{A^2+a^2}\right]$ because

- ($\delta 1$) and ($\delta 2$)give the same result if $s = a$;
- ($\delta 2$) and ($\delta 3$)coincide if $s = \sqrt{2}a$ because $\Psi_0 = \Psi_1 = \dfrac{\pi}{4}$;
- from ($\delta 2$) and ($\delta 4$) we obtain for $s = A$ at first $\Psi_2 = 0$ and so the same value for $\int_0^{\frac{\pi}{4}} \delta_s(\Psi)\ d\Psi$;

if $\sqrt{2}a \leq A = s$ we have from ($\delta 3$) and ($\delta 5$) the same result for the integral of δ_s.

5 The searched probability

For every s of one interval of every chain I, II,,...X if we obtain from subcases $(d1), ..., (d15)$ and $(\delta 1), ..., (\delta 5)$ using the formula (1) the probability $p(s)$ that L determines on a line of $\mathcal{R}_D$ a secant of length greater than or equal to s.We want to give for this last statement some examples:

Proposition 1. If $s \leq a$ or if $A - a \leq s \leq a$ from ($d1$) and ($\delta 1$) we have

$$p(s) = \frac{1}{\pi D}\left[\left(2+\sqrt{2}\right)A + \left(2-\sqrt{2}\right)a - 2s\right]. \tag{2}$$

Proposition 2. If $a \leq s \leq A - a \leq \sqrt{2}a$ from $(d2)$ and $(\delta 2)$ we obtain

$$p(s) = \frac{1}{\pi D}\left[4A + \left(\sqrt{2} - \frac{2a}{s} - 4\sqrt{1 - \frac{a^2}{s^2}}(A - a)\right) - 2s\right]. \tag{3}$$

Proposition 3. If $\sqrt{2}a \leq s \leq A - a \leq 2\sqrt{2}a$,therefore from $(d3)$ and $(\delta 3)$ we have

$$p(s) = \frac{1}{\pi D}\left[4\left(1 - \sqrt{1 - \frac{a^2}{s^2}}\right)A + 2a\sqrt{1 - \frac{a^2}{s^2}} - \frac{a^2}{s} - \frac{s}{2}\right]. \tag{4}$$

Proposition 4. If $a \leq A - a \leq s \leq \min\left(\sqrt{2}a, \sqrt{A^2 - 2Aa + 2a^2}\right)$, therefore from $(d4)$ and $(\delta 2)$ we obtain

$$p(s) = \frac{1}{\pi D}\left[2(A + a) + \left(\sqrt{2} - \frac{2a}{s} - 4\sqrt{1 - \frac{a^2}{s^2}}\right)(A - a)\right. .$$
$$\left. + \frac{3}{2}\left(\frac{(A - a)^2}{s} - s\right)\right] \tag{5}$$

Proposition 5. If $\frac{\sqrt{5}+1}{2}a \leq A \leq 2a$ and $\frac{A}{a}\sqrt{A^2 - 2Aa + 2a^2} \leq s \leq \sqrt{2}A$,therefore from $(d15)$ we have

$$p(s) = \frac{1}{\pi D}\left[s - \frac{2A(A - a)}{s} - 2a\sqrt{1 - \frac{a^2}{s^2}}\right]. \tag{6}$$

Remark. If $s = 0$ we get from (2) for the probability $p(0)$ that a line of $\mathcal{R}_D$ intersects L

$$p(0) = \frac{1}{\pi D}\left[\left(2 + \sqrt{2}\right)A + \left(2 - \sqrt{2}\right)a\right]. \tag{7}$$

We consider the convex hull $co(L)$ of L

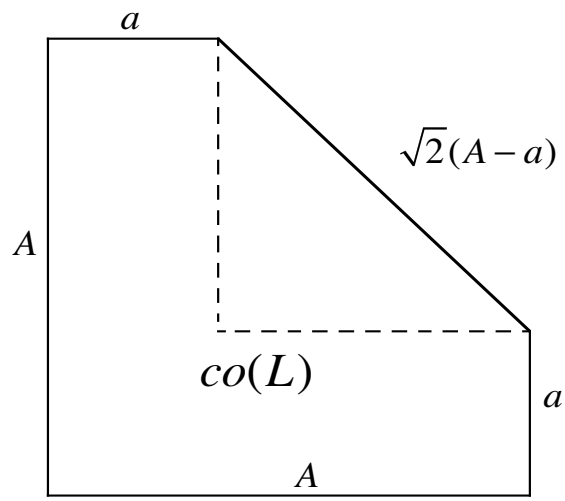

fig.7 - The convex hull of L

Because the hull of L has the perimeter $\left(2+\sqrt{2}\right)A+\left(2-\sqrt{2}\right)a$ we obtain $p\left(0\right)$ by a Cauchy formula the same result, and so also a confirmation for our result.

6 The distribution function of the chord in L

The fuction F which associates to every number $s\in\left[0,diam\left(L\right)\right]$ the probability that any line that cuts L determines in L a chord of length greater than or equal to s. This conditional probability can be to compute using a lattice $\mathcal{R}_D$ of Buffon with $D>diam\left(L\right)$ by the formula

$$F\left(s\right)=1-\frac{p\left(s\right)}{p\left(0\right)}=1-\frac{p\left(s\right)\cdot\pi D}{\left(2+\sqrt{2}\right)A+\left(2-\sqrt{2}\right)a}. \tag{8}$$

If $s\leq a$ or if $A-a\leq s\leq a$ we obtain from the proposition1

$$F\left(s\right)=\frac{s}{\left(2+\sqrt{2}\right)A+\left(2-\sqrt{2}\right)a}. \tag{9}$$

The density f of the distribution of the chord in L is the derivate of F, therefore $F'=f$. Only in the situation $s\leq a$ or $A-a\leq s\leq a$ the density is constant, therefore

$$f\left(s\right)=\frac{1}{\left(2+\sqrt{2}\right)A+\left(2-\sqrt{2}\right)a}.$$

In all the other case f is not a constant, bacause $F\left(s\right)$ is a function of $\sin\varphi_j\left(s\right)$ and $\cos\varphi_j\left(s\right)$, $j=0,1,...5$ and of $\sin\Psi_k\left(s\right)$ and $\cos\Psi_k\left(s\right)$, $k=0,1,2$.

These functions depend on s in the nonlinear way ; therefore we have

$$[\cos\varphi_0(s)]' = \frac{a}{s^2}\sqrt{1-\frac{a}{s^2}},$$

$$[\sin\varphi_1(s)]' = -\frac{a}{s^2}\sqrt{1-\frac{a^2}{s^2}}, ...,$$

$$[\cos\Psi_2(s)]' = \frac{A}{s^2}\sqrt{1-\frac{A^2}{s^2}}.$$

References

[1] V. Conserva and A. Duma, Intersections of a small convex body in a plane lattice, Suppl. Rend. Circ. Mat. Palermo, Serie II, 80, 2008, pp. 75-82.

[2] A. Duma, Problems of Buffon tye for non small needles, Rend. Circ. Mat. Palermo, Serie II, Tomo XLVIII, 1999, pp. 23-40.

[3] A. Duma and S. Rizzo, Chord lenght distribution function for an arbitrary triangle, Suppl. Rend. Circ. Mat. Palermo, Serie II, 81, 2009, pp. 141-157.

[4] A.Duma and S. Rizzo, La funzione di distribuzione di una corda su un trapezio rettangolo, Preprint 2010.

[5] A. Duma and M. Stoka, Schnitte eines kleinen gleichseitigen Dreiecks mit den Gittern von Buffon und Laplace, Seminarberichte der Fernuniversität, 2008, pp. 13-22.

[6] H. S. Harutyunyan and V. K. Ohanyan, The chord length distribution function for regular polygons, Adv. in Appl. Probab., 41, 2 (2009), pp. 358-366.

[7] W. Gille, N. G. Aharonyan and H. S. Harutyunyan, Chord length distribution of pentagonal and hexagonal rods: relation to small-angle scattering, J. Appl. Cryst., 42,(2009), pp. 326-328.

[8] M. Pettineo, Geometric probability problems for Buffon and Laplace grid, Suppl. Rend. Circ. Mat. Palermo, Serie II, 80, 2008, pp. 267-274.

[9] L. Sorrenti, On some geometric and algebraic models for image analysis, Communications in Applied and Industrial Mathematics, DOI: 10.1685/2010CAIM484, ISSN 2038-0909, 1, 2010, pp. 225-236.

[10] L. Sorrenti, Chord lenght distribution functions for an isosceles trapezium, Preprint 2010.

[11] M. Stoka, Probabilites geometriques de type Buffon dans le plan euclidien, Atti Acc. Sci. Torino, 110, pp. 53-59, 1975-76.

RENDICONTI DEL CIRCOLO MATEMATICO DI PALERMO
Serie II, Suppl. 83 (2011), pp. 41-55

Geometric Probabilities for a Cluster of Needles and a Lattice of Parallel Planes

Uwe Bäsel

Abstract

n needles ($1 \leq n < \infty$, ℓ_i = length of needle i) with a common endpoint are placed at random into a lattice $\mathcal{R}_a$ of equidistant parallel planes with distance a. The probabilities of exactly i intersections between the needles and $\mathcal{R}_a$ are calculated.

For $\ell_1 = \ldots = \ell_n$ the limit distribution of the relative number of intersections as $n \to \infty$ is derived.

AMS Classification: 60D05, 52A22, 78M05

AMS 2000 Subject Classification: geometric probability, stochastic geometry, random sets and random convex sets, method of moments

1 Introduction

We consider a cluster $\mathcal{Z}_n$ of n needles ($1 \leq n < \infty$) placed at random into a lattice $\mathcal{R}_a$ of parallel and equidistant planes (see figure 1):

$$\mathcal{R}_a = \{(x, y, z) \in \mathbb{R}^3 \,|\, x = ka, k \in \mathbb{Z}\}\,.$$

Each needle of $\mathcal{Z}_n$ is fixed with one endpoint in the centre C of $\mathcal{Z}_n$ and can rotate independently about this centre. ℓ_i denotes the length of needle i. We assume $\max((\ell_j + \ell_k) \leq a;\ j,\ k \in \{1, 2, \ldots, n\})$ so that $\mathcal{Z}_n$ can intersect at most one of the planes of $\mathcal{R}_a$ (except sets with measure zero). A *random placement of $\mathcal{Z}_n$ into $\mathcal{R}_a$* is defined as follows: After placing $\mathcal{Z}_n$ into $\mathcal{R}_a$ the coordinate x of the centre point C is a random variable uniformly distributed in $[0, a]$. The second endpoint of the needle i is uniformly distributed upon the sphere with radius ℓ_i and centre point C. We denote by d_i, $1 \leq i \leq n$, the signed projection of the needle i onto the x-axis. From the last assumption and geometrical considerations it follows that each d_i is uniformly distributed in $[-\ell_i, \ell_i]$. All $n+1$ random variables $x, d_1, \ldots, d_n$ are assumed to be stochastically independent.

In the section 2 the intersection probabilities between a cluster $\mathcal{Z}_n$ with $\ell_1 = \ldots = \ell_n$ and the lattice $\mathcal{R}_a$ are calculated. In section 3 the distribution of the relative number of intersections and the limit distribution as $n \to \infty$ are derived. Section 4 deals with $\mathcal{Z}_n$, whose needles have different lengths.

Diaconis [4] derived the distribution of the number of intersections for a needle of length ℓ and a lattice of parallel lines of distance d apart with $\ell > d$. He showed,

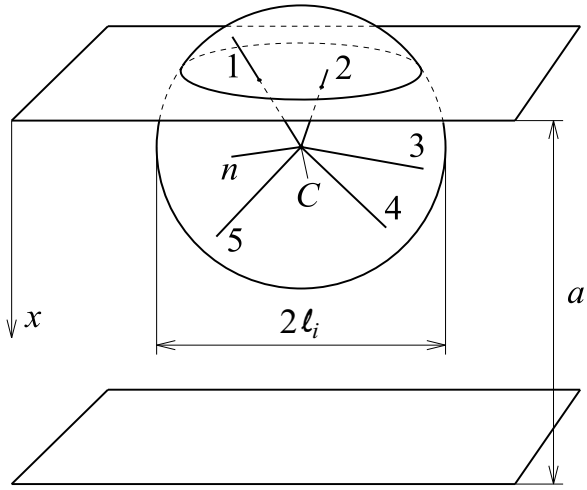

Figure 1: Lattice $\mathcal{R}_a$ and cluster $\mathcal{Z}_n$

that this distribution converges weakly to an arc sine law as $\ell/d \to \infty$. Further intersection probabilities are to be found e. g. in [5], [6], [7], [11], [12] and [13].

2 Intersection probabilities

Theorem 1. *A cluster $\mathcal{Z}_n$ with $\ell := \ell_1 = \ldots = \ell_n$ is placed at random into the lattice $\mathcal{R}_a$ with $\lambda = \ell/a \le 1/2$. The probabilities $p_n(i)$ of exactly i intersections between $\mathcal{Z}_n$ and $\mathcal{R}_a$ are given by*

$$p_n(0) = 1 - 2\lambda\left(1 - \frac{2 - 2^{-n}}{n+1}\right),$$

$$p_n(i) = 2^{1-n}\lambda\binom{n}{i}\sum_{\nu=0}^{n-i}\binom{n-i}{\nu}\frac{\nu!\,i!}{(\nu+i+1)!}\,,\ \text{if } 1 \le i \le n\,.$$

The expectation $\mathrm{E}(Z_n)$ and the variance $\mathrm{Var}(Z_n)$ of the number Z_n of the intersections between $\mathcal{Z}_n$ and $\mathcal{R}_a$ are

$$\mathrm{E}(Z_n) = n\,\frac{\lambda}{2} \quad \text{and} \quad \mathrm{Var}(Z_n) = \frac{n\lambda}{2}\left(\frac{n+2}{3} - \frac{n\lambda}{2}\right)$$

respectively.

Proof. Due to the symmetry of the problem it is sufficient to consider only x with $0 < x \le a/2$. A single needle whose point C has fixed coordinate x with $0 < x \le \ell$ intersects the lattice, if its endpoint is in a spherical segment above the plane (see figure 1). The surface area of this segment is $2\pi\ell(\ell - x)$. The surface area of the sphere with radius ℓ is $4\pi\ell^2$. Since the endpoint of the needle is uniformly

distributed on the surface of the sphere, the probability that the needle intersects the plane is

$$\frac{2\pi\ell(\ell-x)}{4\pi\ell^2}=\frac{\ell-x}{2\ell}\,.$$

For $0<x\le\ell$ the probability of no intersections is

$$1-\frac{\ell-x}{2\ell}=\frac{\ell+x}{2\ell}\,.$$

If $\ell<x\le a/2$ the probability that the needle intersects the plane is equal to zero.

With $p_n(i\,|\,x)$ we denote the conditional probability of exactly i intersections between $\mathcal{Z}_n$ and $\mathcal{R}_a$ for fixed x and have

$$p_n(i)=\int_{x=0}^{a/2}p_n(i\,|\,x)f(x)\,\mathrm{d}x\,,$$

where f is the density function of x:

$$f(x)=\begin{cases}2/a & \text{for}\quad 0\le x\le a/2\,,\\ 0 & \text{else}\,.\end{cases}$$

For $1\le i\le n$ we have

$$p_n(i\,|\,x)=\begin{cases}\displaystyle\binom{n}{i}\left(\frac{\ell-x}{2\ell}\right)^i\left(\frac{\ell+x}{2\ell}\right)^{n-i} & \text{for}\quad 0<x\le\ell\,,\\ 0 & \text{for}\quad \ell<x\le a/2\,,\end{cases}$$

therefore

$$p_n(i)=\frac{2^{1-n}}{a}\binom{n}{i}\int_{x=0}^{\ell}\left(1-\frac{x}{\ell}\right)^i\left(1+\frac{x}{\ell}\right)^{n-i}\mathrm{d}x\,.$$

With the substitution $y=x/\ell$ ($\mathrm{d}x=\ell\,\mathrm{d}y$) and $\lambda=\ell/a$ we get

$$\begin{aligned}
p_n(i)&=2^{1-n}\lambda\binom{n}{i}\int_0^1(1-y)^i(1+y)^{n-i}\,\mathrm{d}y\\
&=2^{1-n}\lambda\binom{n}{i}\int_0^1\sum_{\nu=0}^{n-i}\binom{n-i}{\nu}y^\nu(1-y)^i\,\mathrm{d}y\\
&=2^{1-n}\lambda\binom{n}{i}\sum_{\nu=0}^{n-i}\binom{n-i}{\nu}\int_0^1 y^\nu(1-y)^i\,\mathrm{d}y\\
&=2^{1-n}\lambda\binom{n}{i}\sum_{\nu=0}^{n-i}\binom{n-i}{\nu}\mathrm{B}(\nu+1,i+1)\qquad[3,\text{ p. }70]\\
&=2^{1-n}\lambda\binom{n}{i}\sum_{\nu=0}^{n-i}\binom{n-i}{\nu}\frac{\Gamma(\nu+1)\Gamma(i+1)}{\Gamma(\nu+i+2)}\\
&=2^{1-n}\lambda\binom{n}{i}\sum_{\nu=0}^{n-i}\binom{n-i}{\nu}\frac{\nu!\,i!}{(\nu+i+1)!}\,,
\end{aligned}$$

where B and Γ are the beta and gamma function respectively. For $i = 0$ we find

$$p_n(0\,|\,x) = \begin{cases} \left(\dfrac{\ell + x}{2\ell}\right)^n & \text{for} \quad 0 < x \le \ell\,, \\ 1 & \text{for} \quad \ell < x \le a/2\,, \end{cases}$$

hence with the substitution $y = x/\ell$ and $\lambda = \ell/a$

$$\begin{aligned} p_n(0) &= \frac{2^{1-n}}{a} \int_{x=0}^{\ell} \left(1 + \frac{x}{\ell}\right)^n \mathrm{d}x + \frac{2}{a} \int_{x=\ell}^{a/2} 1 \,\mathrm{d}x \\ &= 2^{1-n}\lambda \int_{y=0}^{1} (1+y)^n \,\mathrm{d}x + 1 - 2\lambda \\ &= \frac{2^{1-n}\lambda}{n+1}\big(2^{n+1} - 1\big) + 1 - 2\lambda = 1 - 2\lambda\left(1 - \frac{2 - 2^{-n}}{n+1}\right). \end{aligned}$$

For the first and second moment of Z_n we get

$$\begin{aligned} \mathrm{E}(Z_n) = \sum_{i=0}^{n} i p_n(i) &= 2^{1-n}\lambda \sum_{i=1}^{n} i \binom{n}{i} \int_0^1 (1-y)^i (1+y)^{n-i} \,\mathrm{d}y \\ &= 2^{1-n}\lambda \int_0^1 \sum_{i=1}^{n} i \binom{n}{i} (1-y)^i (1+y)^{n-i} \,\mathrm{d}y \\ &= 2^{1-n}\lambda \int_0^1 2^{n-1} n(1-y) \,\mathrm{d}y \ {}^{1} \\ &= -n\lambda \int_0^1 (y-1) \,\mathrm{d}y = n\,\frac{\lambda}{2} \end{aligned}$$

and

$$\begin{aligned} \mathrm{E}\big(Z_n^2\big) = \sum_{i=0}^{n} i^2 p_n(i) &= 2^{1-n}\lambda \sum_{i=1}^{n} i^2 \binom{n}{i} \int_0^1 (1-y)^i (1+y)^{n-i} \,\mathrm{d}y \\ &= 2^{1-n}\lambda \int_0^1 \sum_{i=1}^{n} i^2 \binom{n}{i} (1-y)^i (1+y)^{n-i} \,\mathrm{d}y \\ &= 2^{1-n}\lambda \int_0^1 2^{n-2} n[(n-1)y^2 - 2ny + n + 1] \,\mathrm{d}y \ {}^{1} \\ &= \frac{1}{6} n(n+2)\lambda \end{aligned}$$

respectively. Therefore we have

$$\mathrm{Var}(Z_n) = \mathrm{E}\big(Z_n^2\big) - \big(\mathrm{E}(Z_n)\big)^2 = \frac{n\lambda}{2}\left(\frac{n+2}{3} - \frac{n\lambda}{2}\right). \qquad \square$$

[1] These sums were calculated with Mathematica. $\mathrm{E}(Z_n)$ also follows from the additivity of the expectation.

Special cases: For $n = 1$, $n = 2$, $n = 3$ and $n = 10$ the calculation of the intersection probabilities and variances yields the following results:

$\underline{n = 1:}$

$$p_1(0) = 1 - \frac{\lambda}{2}\,, \quad p_1(1) = \frac{\lambda}{2}\,, \quad \mathrm{Var}(Z_1) = \frac{\lambda}{4}\,(2-\lambda)\,.$$

$p_1(1)$ can also be deduced as special case of results of Stoka [13], Santaló [12, p. 250] and Duma/Stoka [6], [7].

$\underline{n = 2:}$

$$p_2(0) = 1 - \frac{5\lambda}{6}\,, \quad p_2(1) = \frac{2\lambda}{3}\,, \quad p_2(2) = \frac{\lambda}{6}\,, \quad \mathrm{Var}(Z_2) = \frac{\lambda}{3}\,(4-3\lambda)\,.$$

$\underline{n = 3:}$

$$p_3(0) = 1 - \frac{17\lambda}{16} = 1 - 1{,}0625\lambda\,,\ p_3(1) = \frac{11\lambda}{16} = 0{,}6875\lambda\,,$$

$$p_3(2) = \frac{5\lambda}{16} = 0{,}3125\lambda\,,\ p_3(3) = \frac{\lambda}{16} = 0{,}0625\lambda\,,\ \mathrm{Var}(Z_3) = \frac{\lambda}{4}\,(10-9\lambda)\,.$$

$\underline{n = 10:}$

$$p_{10}(0) = 1 - \frac{9217\lambda}{5632} \approx 1 - 1{,}63654\lambda\,, \quad p_{10}(1) = \frac{509\lambda}{1408} \approx 0{,}361506\lambda\,,$$

$$p_{10}(2) = \frac{1981\lambda}{5632} \approx 0{,}35174\lambda\,, \qquad p_{10}(3) = \frac{227\lambda}{704} \approx 0{,}322443\lambda\,,$$

$$p_{10}(4) = \frac{743\lambda}{2816} \approx 0{,}263849\lambda\,, \qquad p_{10}(5) = \frac{2\lambda}{11} \approx 0{,}181818\lambda\,,$$

$$p_{10}(6) = \frac{281\lambda}{2816} \approx 0{,}0997869\lambda\,, \qquad p_{10}(7) = \frac{29\lambda}{704} \approx 0{,}0411932\lambda\,,$$

$$p_{10}(8) = \frac{67\lambda}{5632} \approx 0{,}0118963\lambda\,, \qquad p_{10}(9) = \frac{3\lambda}{1408} \approx 0{,}00213068\lambda\,,$$

$$p_{10}(10) = \frac{\lambda}{5632} \approx 0{,}000177557\lambda\,, \qquad \mathrm{Var}(Z_{10}) = 5\lambda(4-5\lambda)\,.$$

3 Distribution functions

As in the last preceding section we assume $\ell := \ell_1 = \ldots = \ell_n$. In the following let X_n denote the ratio

$$\frac{\text{number of intersections between } \mathcal{Z}_n \text{ and } \mathcal{R}_a}{n}\,.$$

We consider the distribution functions

$$F_n(x) = P(X_n \le x) = \begin{cases} 0 & \text{for} \quad -\infty < x < 0\,, \\ \displaystyle\sum_{i=0}^{\lfloor nx \rfloor} p_n(i) & \text{for} \quad 0 \le x < 1\,, \\ 1 & \text{for} \quad 1 \le x < \infty\,. \end{cases}$$

Since it is possible to write $p_n(0)$ in the form

$$p_n(0) = 1 - 2\lambda + 2^{1-n}\lambda \binom{n}{0} \sum_{\nu=0}^{n-0} \binom{n-0}{\nu} \frac{\nu!\,0!}{(\nu+0+1)!}$$

we have

$$F_n(x) = \begin{cases} 0 \text{ for } -\infty < x < 0\,, \\ 1 - 2\lambda + 2^{1-n}\lambda \sum_{i=0}^{\lfloor nx \rfloor} \binom{n}{i} \sum_{\nu=0}^{n-i} \binom{n-i}{\nu} \frac{\nu!\,i!}{(\nu+i+1)!} \text{ for } 0 \le x < 1\,, \\ 1 \text{ for } 1 \le x < \infty\,. \end{cases}$$

Now we investigate the asymptotic behaviour of F_n as $n \to \infty$.

Theorem 2. *As $n \to \infty$, the random variables X_n converge weakly to the random variable X, whose distribution function is given by*

$$F(x) = \begin{cases} 0 & \text{for } -\infty < x < 0\,, \\ 1 - 2\lambda(1-2x) & \text{for } 0 \le x < 1/2\,, \\ 1 & \text{for } 1/2 \le x < \infty\,. \end{cases}$$

Moreover, it holds the uniform convergence $\lim_{n\to\infty} \sup_{x\in\mathbb{R}} |F_n(x) - F(x)| = 0$.

Proof. The proof of the weak convergence is based on the method of moments and is similar to the proof in [1]. According to the Fréchet-Shohat theorem (see e.g. [10, pp. 81/82]) we have to show that for each $k \in \mathbb{N}$ the sequence of moments $\mathrm{E}(X_n^k) = \int_{-\infty}^{\infty} x^k \,\mathrm{d}F_n(x)$ converges to $\mathrm{E}(X^k) = \int_{-\infty}^{\infty} x^k \,\mathrm{d}F(x)$ as $n \to \infty$ and the moments $\mathrm{E}(X^k)$, $k \in \mathbb{N}$, uniquely determine F.

Since F is a distribution function that is constant outside the interval $[0, 1/2]$, it is uniquely determined by its moments. These moments are given by

$$\begin{aligned} \mathrm{E}(X^k) &= \int_{-\infty}^{\infty} x^k \,\mathrm{d}F(x) = 4\lambda \int_0^{1/2} x^k \,\mathrm{d}x = 4\lambda \frac{1}{k+1} \left(\frac{1}{2}\right)^{k+1} \\ &= \frac{\lambda}{(k+1)2^{k-1}}\,,\ k \in \mathbb{N}\,. \end{aligned} \tag{1}$$

For the moments $\mathrm{E}(X_n^k)$, $k \in \mathbb{N}$, we find

$$\mathrm{E}(X_n^k) = \mathrm{E}\big[\mathrm{E}(X_n^k \,|\, x)\big] = \frac{2}{a} \int_0^{\ell} \mathrm{E}(X_n^k \,|\, x) \,\mathrm{d}x\,,$$

where $\mathrm{E}(X_n^k \,|\, x)$ is the conditional k-th moment of X_n for the cluster centre in fixed x. We have

$$\mathrm{E}(X_n^k \,|\, x) = \sum_{i=0}^{n} \left(\frac{i}{n}\right)^k p_n(i \,|\, x) = \sum_{i=0}^{n} \left(\frac{i}{n}\right)^k \binom{n}{i} \left(\frac{\ell - x}{2\ell}\right)^i \left(\frac{\ell + x}{2\ell}\right)^{n-i}. \tag{2}$$

By Z_i, $i \in \{1, \ldots, n\}$, we denote the random number of intersections between needle i and $\mathcal{R}_a$ for the cluster center with fixed x and by M_n the arithmetic mean $(Z_1 + \ldots + Z_n)/n$. We have $\mathrm{E}(Z_i) = (\ell - x)/(2\ell) = \mathrm{E}(Z_i^2)$ and therefore $\mathrm{Var}(Z_i) = \mathrm{E}(Z_i^2) - [\mathrm{E}(Z_i)]^2 = (\ell - x)/(2\ell) - [(\ell - x)/(2\ell)]^2$. Furthermore we find

$$\mathrm{E}(M_n) = \mathrm{E}(Z_1/n) + \ldots + \mathrm{E}(Z_n/n) = \mathrm{E}(Z_1) = \frac{\ell - x}{2\ell}\,.$$

Since the random variables $Z_1, \ldots, Z_n$ are independent and identically distributed we have

$$\begin{aligned} \mathrm{Var}(M_n) &= \mathrm{Var}(Z_1/n) + \ldots + \mathrm{Var}(Z_n/n) = \frac{1}{n}\,\mathrm{Var}(Z_1) \\ &= \frac{1}{n}\left[\frac{\ell - x}{2\ell} - \left(\frac{\ell - x}{2\ell}\right)^2\right] \le \frac{1}{n} \end{aligned}$$

and therefore $\mathrm{Var}(M_n) \to 0$ as $n \to \infty$. From [8, p. 219] it follows that (2) converges uniformly to $[(\ell - x)/(2\ell)]^k$ as $n \to \infty$.

Now we get

$$\begin{aligned} \lim_{n\to\infty} \mathrm{E}(X_n^k) &= \lim_{n\to\infty} \frac{2}{a}\int_0^\ell \mathrm{E}(X_n^k \,|\, x)\,\mathrm{d}x = \frac{2}{a}\int_0^\ell \lim_{n\to\infty} \mathrm{E}(X_n^k \,|\, x)\,\mathrm{d}x \\ &= \frac{2}{a}\int_0^\ell \left(\frac{\ell - x}{2\ell}\right)^k \mathrm{d}x = 2^{1-k}\lambda \int_0^1 (1 - y)^k\,\mathrm{d}y \\ &= \frac{\lambda}{(k+1)2^{k-1}}\,,\ k \in \mathbb{N}\,. \end{aligned} \tag{3}$$

The comparison of (3) with (1) shows, that $\lim_{n\to\infty} \mathrm{E}(X_n^k) = \mathrm{E}(X^k)$ for $k \in \mathbb{N}$. It follows that F_n converges weakly to F as $n \to \infty$.

From the weak convergence it follows that F_n converges uniformly to F in all points of continuity of F. F is a continuous function, if $\lambda = 1/2$. If $\lambda \neq 1/2$, F is continuous except in the point 0. For $x = 0$ we find

$$\begin{aligned} \lim_{n\to\infty} F_n(0) = \lim_{n\to\infty} p_n(0) &= \lim_{n\to\infty}\left[1 - 2\lambda\left(1 - \frac{2 - 2^{-n}}{n+1}\right)\right] \\ &= 1 - 2\lambda + 2\lambda \lim_{n\to\infty}\left(\frac{2}{n+1} - \frac{1}{(n+1)2^n}\right) = 1 - 2\lambda = F(0)\,. \end{aligned}$$

Hence the convergence $F_n \to F$ is completely uniform. So the proof is finished. □

The diagrams in the figures 2 and 3 show examples of distribution functions F_n and F.

Remark. According to the Lebesgue decomposition theorem (see [2, p. 35]) it is possible to write F uniquely in the form $F = \alpha_1 F_d + \alpha_2 F_{ac} + \alpha_3 F_s$, $0 \le \alpha_i \le 1$, $\alpha_1 + \alpha_2 + \alpha_3 = 1$ with distribution functions F_d, F_{ac} and F_s, where F_d is discrete,

F_{ac} is absolutely continuous and F_s is singular. One finds

$$F_d(x) = \begin{cases} 0 & \text{for} \quad -\infty < x < 0\,, \\ 1 & \text{for} \quad 0 \le x < \infty\,, \end{cases} \qquad F_{ac}(x) = \begin{cases} 0 & \text{for} \quad -\infty < x < 0\,, \\ 2x & \text{for} \quad 0 \le x < 1/2\,, \\ 1 & \text{for} \quad 1/2 \le x < \infty \end{cases}$$

and $\alpha_1 = 1 - 2\lambda$, $\alpha_2 = 2\lambda$, $\alpha_3 = 0$.

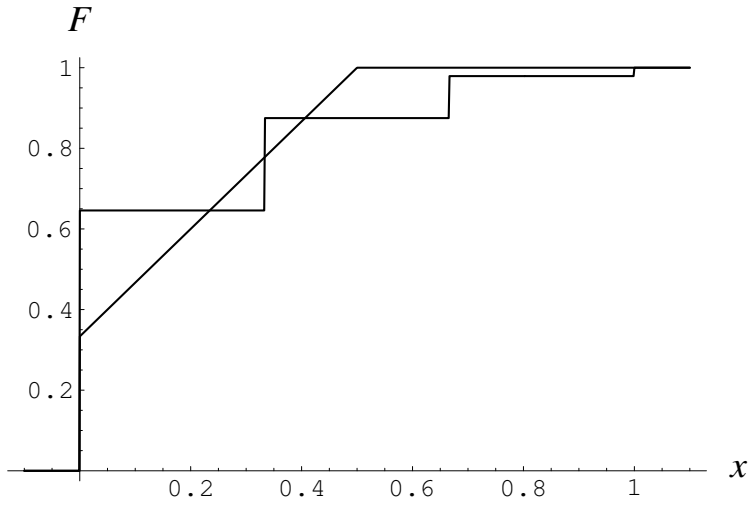

Figure 2: F_3 and F for $\lambda = 1/3$

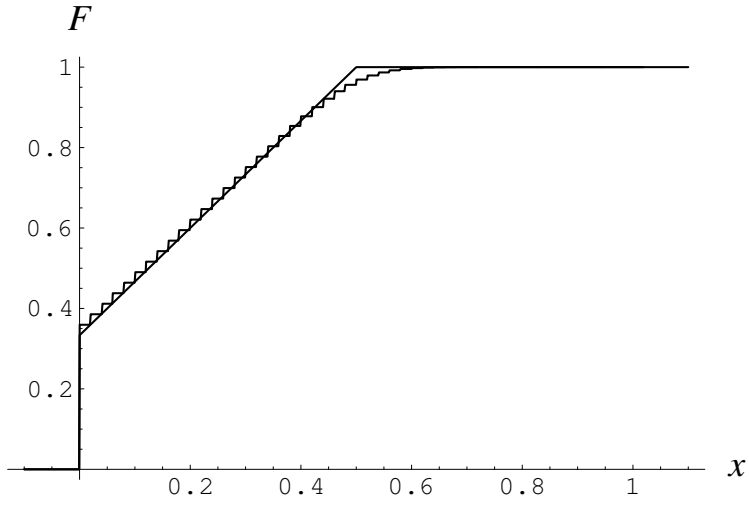

Figure 3: F_{50} and F for $\lambda = 1/3$

4 Clusters of needles with different lengths

Now we consider a cluster $\mathcal{Z}_n$ of needles with different lenghts. A_i denotes the event that needle i intersects $\mathcal{R}_a$. We number the needles in such a way, that $\ell_1 \geq \ell_2 \geq \cdots \geq \ell_n > 0$. To simplify notation, we define

$$J_k := \{(j_1, \ldots, j_k) \,|\, 1 \leq j_1 < \cdots < j_k \leq n\}\,.$$

Theorem 3. *The probabilities $p(i)$ of exactly i, $1 \leq i \leq n$, intersections between $\mathcal{Z}_n$ and $\mathcal{R}_a$ are for*

$$\max((\ell_j + \ell_k) \leq a;\; j,\, k \in \{1, 2, \ldots, n\})$$

given by

$$p(i) = \sum_{k=i}^{n} (-1)^{i+k} \binom{k}{i} \sum_{J_k} P(A_{j_1} \cap \cdots \cap A_{j_k}) \tag{4}$$

with

$$P(A_{j_1} \cap \cdots \cap A_{j_k}) = \frac{\ell_{j_k}}{2^{k-1} a \prod_{m=1}^{k-1} \ell_{j_m}} \sum_{\nu=1}^{k} \frac{(-1)^{\nu-1}\, \ell_{j_k}^{\nu-1}}{\nu(\nu+1)} \sum_{I_{k-\nu}} \prod_{\rho=1}^{k-\nu} \ell_{i_\rho}\,, \tag{5}$$

where $I_{k-\nu} := \{(i_1, \ldots, i_{k-\nu}) \,|\, i_1 < \cdots < i_{k-\nu}\}$ is any subset of J_{k-1} with $1 \leq \nu \leq k$.

Proof. Formula (4) is the inclusion-exclusion principle (see [15]). So we have to calculate the probabilities $P(A_{j_1} \cap \cdots \cap A_{j_k})$ for $\ell_{j_1} \geq \cdots \geq \ell_{j_k}$. For fixed x, $0 < x \leq a/2$, (see fig. 1) the conditional probability $P(A_{j_1} \cap \cdots \cap A_{j_k} \,|\, x)$ is

$$P(A_{j_1} \cap \cdots \cap A_{j_k} \,|\, x) = \begin{cases} \prod_{\rho=1}^{k} (\ell_{j_\rho} - x)/(2\,\ell_{j_\rho})\,, & \text{if} \quad 0 < x < \ell_{j_k}\,, \\ 0\,, & \text{if} \quad \ell_{j_k} \leq x \leq a/2\,. \end{cases}$$

So we have

$$\begin{aligned} P(A_{j_1} \cap \cdots \cap A_{j_k}) &= \frac{2}{a} \int_0^{\ell_{j_k}} P(A_{j_1} \cap \cdots \cap A_{j_k} \,|\, x)\, \mathrm{d}x \\ &= \frac{2}{a} \int_0^{\ell_{j_k}} \frac{\ell_{j_1} - x}{2\ell_{j_1}} \cdots \frac{\ell_{j_k} - x}{2\ell_{j_k}}\, \mathrm{d}x \\ &= \frac{1}{2^{k-1} a\, \ell_{j_1} \cdots \ell_{j_k}} \underbrace{\int_0^{\ell_{j_k}} (\ell_{j_1} - x) \cdots (\ell_{j_k} - x)\, \mathrm{d}x}_{=:\,\mathcal{I}}\,. \end{aligned}$$

For the calculation of the integral $\mathcal{I}$ we consider it as a function of the parameter ℓ_{j_k} and differentiate with respect to ℓ_{j_k} (see [9, pp. 688-689]):

$$\mathcal{I}'(\ell_{j_k}) = \int_0^{\ell_{j_k}} \frac{\partial}{\partial \ell_k} \big[(\ell_{j_1} - x) \cdots (\ell_{j_k} - x)\big]\, \mathrm{d}x$$

$$
\begin{aligned}
&= \int_0^{\ell_{j_k}} (\ell_{j_1} - x) \cdots (\ell_{j_{k-1}} - x)\,\mathrm{d}x \\
&\quad + \underbrace{1 \cdot (\ell_{j_1} - \ell_{j_k}) \cdots (\ell_{j_k} - \ell_{j_k}) \;-\; 0 \cdot \ell_{j_1} \cdots \ell_{j_k}}_{0} \\
&= \int_0^{\ell_{j_k}} \sum_{\nu=1}^{k} (-1)^{\nu-1}\, x^{\nu-1} \sum_{I_{k-\nu}} \prod_{\rho=1}^{k-\nu} \ell_{i_\rho}\,\mathrm{d}x \\
&= \sum_{\nu=1}^{k} (-1)^{\nu-1}\, \frac{\ell_{j_k}^{\nu}}{\nu} \sum_{I_{k-\nu}} \prod_{\rho=1}^{k-\nu} \ell_{i_\rho}\,.
\end{aligned}
$$

We integrate this expression with respect to ℓ_{j_k} and get

$$
\begin{aligned}
\mathcal{I}(\ell_{j_k}) &= \sum_{\nu=1}^{k} (-1)^{\nu-1}\, \frac{\ell_{j_k}^{\nu+1}}{\nu(\nu+1)} \sum_{I_{k-\nu}} \prod_{\rho=1}^{k-\nu} \ell_{i_\rho} \;+\; C \\
&= \ell_{j_k}^2 \sum_{\nu=1}^{k} (-1)^{\nu-1}\, \frac{\ell_{j_k}^{\nu-1}}{\nu(\nu+1)} \sum_{I_{k-\nu}} \prod_{\rho=1}^{k-\nu} \ell_{i_\rho} \;+\; C\,.
\end{aligned}
$$

For $\ell_{j_k} = 0$ we have

$$
\int_0^{\ell_{j_k}} (\ell_{j_1} - x) \cdots (\ell_{j_k} - x)\,\mathrm{d}x = 0
$$

and

$$
\ell_{j_k}^2 \sum_{\nu=1}^{k} (-1)^{\nu-1}\, \frac{\ell_{j_k}^{\nu-1}}{\nu(\nu+1)} \sum_{I_{k-\nu}} \prod_{\rho=1}^{k-\nu} \ell_{i_\rho} = 0\,.
$$

Hence the constant C of integration is equal to zero. It follows

$$
\begin{aligned}
P(A_{j_1} \cap \cdots \cap A_{j_k}) &= \frac{1}{2^{k-1} a\, \ell_{j_1} \cdots \ell_{j_k}}\, \ell_{j_k}^2 \sum_{\nu=1}^{k} \frac{(-1)^{\nu-1} \ell_{j_k}^{\nu-1}}{\nu(\nu+1)} \sum_{I_{k-\nu}} \prod_{\rho=1}^{k-\nu} \ell_{i_\rho} \\
&= \frac{\ell_{j_k}}{2^{k-1} a \prod_{m=1}^{k-1} \ell_{j_m}} \sum_{\nu=1}^{k} \frac{(-1)^{\nu-1}\, \ell_{j_k}^{\nu-1}}{\nu(\nu+1)} \sum_{I_{k-\nu}} \prod_{\rho=1}^{k-\nu} \ell_{i_\rho}
\end{aligned}
$$

and the proof is complete. □

Special cases: At first we consider the special case $n = 3$. One finds

$$
\begin{aligned}
&P(A_1) = \frac{\ell_1}{2a}\,,\quad P(A_2) = \frac{\ell_2}{2a}\,,\quad P(A_3) = \frac{\ell_3}{2a}\,,\quad P(A_1 \cap A_2) = \frac{(3\ell_1 - \ell_2)\ell_2}{12a\ell_1}\,, \\
&P(A_1 \cap A_3) = \frac{(3\ell_1 - \ell_3)\ell_3}{12a\ell_1}\,,\quad P(A_2 \cap A_3) = \frac{(3\ell_2 - \ell_3)\ell_3}{12a\ell_2}\,, \\
&P(A_1 \cap A_2 \cap A_3) = \frac{\left[6\ell_1\ell_2 - 2(\ell_1 + \ell_2)\ell_3 + \ell_3^2\right]\ell_3}{48a\ell_1\ell_2}\,.
\end{aligned}
$$

With the inclusion-exclusion principle in the form of equation (4) and $\lambda_1 := \ell_1/a$, $\lambda_i := \ell_i/\ell_1$, $i \in \{2, \dots n\}$, we get

$$p(1) = \frac{\lambda_1\big[8\lambda_2^3 + \lambda_3^2(2+3\lambda_3) + 2\lambda_2(12 - 3\lambda_3 + \lambda_3^2)\big]}{48\lambda_2}\,,$$
$$p(2) = \frac{\lambda_1\big[-4\lambda_2^3 + \lambda_3^2(2-3\lambda_3) + 2\lambda_2(6\lambda_2 + 3\lambda_3 + \lambda_3^2)\big]}{48\lambda_2}\,,$$
$$p(3) = \frac{\lambda_1\lambda_3\big[2\lambda_2(3-\lambda_3) - \lambda_3(2-\lambda_3)\big]}{48\lambda_2}\,.$$

Note that from $\ell_3 \le \ell_2$ it follows that $\lambda_3 \le \lambda_2$. So these formulas are valid for $(\lambda_2, \lambda_3) \in \mathcal{F} := \{(x,y) \in \mathbb{R}^2 \mid 0 < x \le 1\,,\ 0 < y \le x)$.

Now we consider $p(1)$ as function $f : \mathcal{F} \to [0,1]$ and ask for the values of λ_2 and λ_3 for which f has extrema. One finds for the system of equations

$$\left.\begin{aligned} f_{\lambda_2}(\lambda_2,\lambda_3) := \frac{\partial f(\lambda_2,\lambda_3)}{\partial\lambda_2} &= \frac{\lambda_1\big[16\lambda_2^3 - \lambda_3^2(2+3\lambda_3)\big]}{48\lambda_2^2} = 0 \\ f_{\lambda_3}(\lambda_2,\lambda_3) := \frac{\partial f(\lambda_2,\lambda_3)}{\partial\lambda_3} &= \frac{\lambda_1\big[\lambda_2(-6+4\lambda_3) + \lambda_3(4+9\lambda_3)\big]}{48\lambda_2} = 0 \end{aligned}\right\}$$

the solution $\lambda_2 = \lambda_3 = 2/13 \approx 0,153846$ as the only solution in $\mathcal{F}$. For this point we find

$$f_{\lambda_2\lambda_2} f_{\lambda_3\lambda_3} - f_{\lambda_2\lambda_3}^2 = 1079\lambda_1^2/2304 > 0 \quad \text{and} \quad f_{\lambda_2\lambda_2} = \lambda_1 > 0\,.$$

Hence $f = p(1)$ has its minimum in $\mathcal{F}$ in $(\lambda_2, \lambda_3) = (2/13, 2/13)$ with $p(1) = 77\lambda_1/156 \approx 0,493590\lambda_1$. An easy calculation shows that $p(1)$ has its maximum in $\mathcal{F}$ in $(\lambda_2, \lambda_3) = (1,1)$ with $p(1) = 11\lambda_1/16 = 0,6875\lambda_1$. This is the probability $p_3(1)$ from section 3. Furthermore for $(\lambda_2, \lambda_3) = (1,1)$ one gets $p(2) = p_3(2) = 5\lambda_1/16$ and $p(3) = p_3(3) = \lambda_1/16$ as maxima of $p(2)$ and $p(3)$ in $\mathcal{F}$ respectively.

The diagrams in the figures $4, \dots, 6$ show contourplots of $p(1), \dots, p(3)$ as functions of λ_2 and λ_3. The diagram in figure 7 shows the contourplot of the probability $P(A_1 \cup A_2 \cup A_3)$ of at least one intersection.

The expectation of the number Z of intersections is given by

$$\mathrm{E}(Z) = \frac{\ell_1 + \ell_2 + \ell_3}{2a} = \frac{\lambda_1}{2}(1 + \lambda_2 + \lambda_3)\,.$$

Now we consider the special case $\ell := \ell_1 = \ldots = \ell_n$. At first we calculate $P(A_{j_1} \cap \cdots \cap A_{j_k})$ with formula (5). We find

$$\sum_{I_{k-\nu}} \prod_{\rho=1}^{k-\nu} \ell_{i_\rho} = \binom{k-1}{k-\nu} \ell^{k-\nu} = \binom{k-1}{(k-1)-(k-\nu)} \ell^{k-\nu} = \binom{k-1}{\nu-1} \ell^{k-\nu}$$

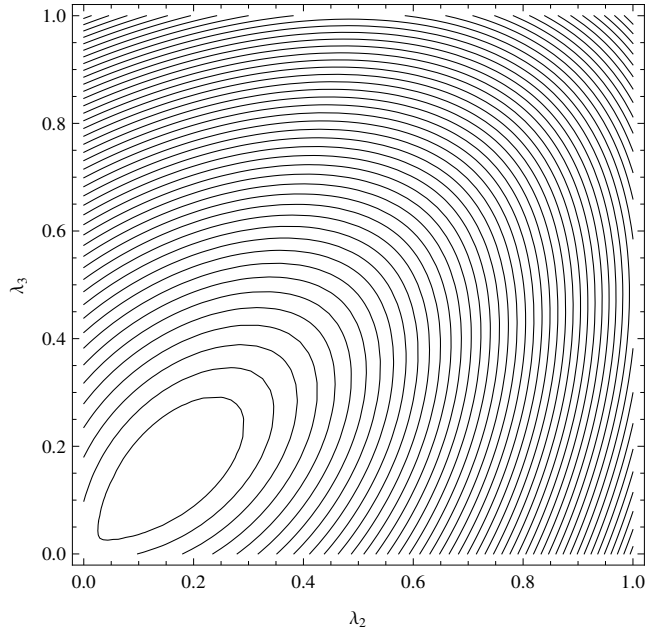

Figure 4: Contourplot of $p(1)$

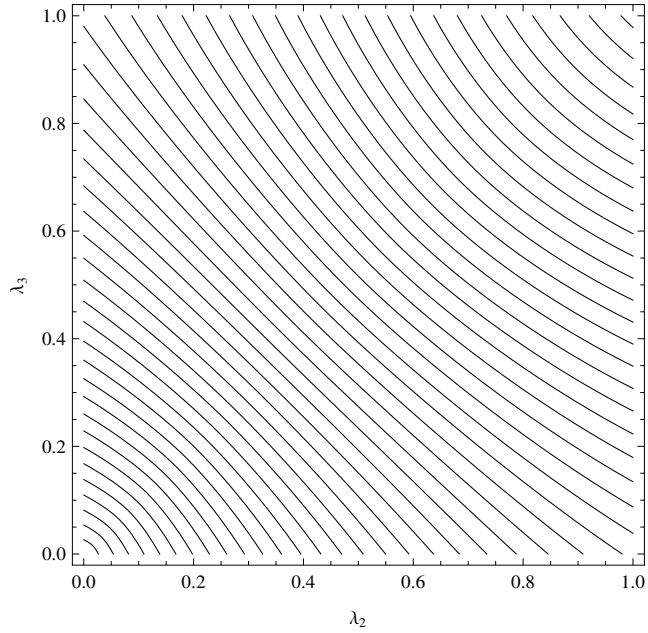

Figure 5: Contourplot of $p(2)$

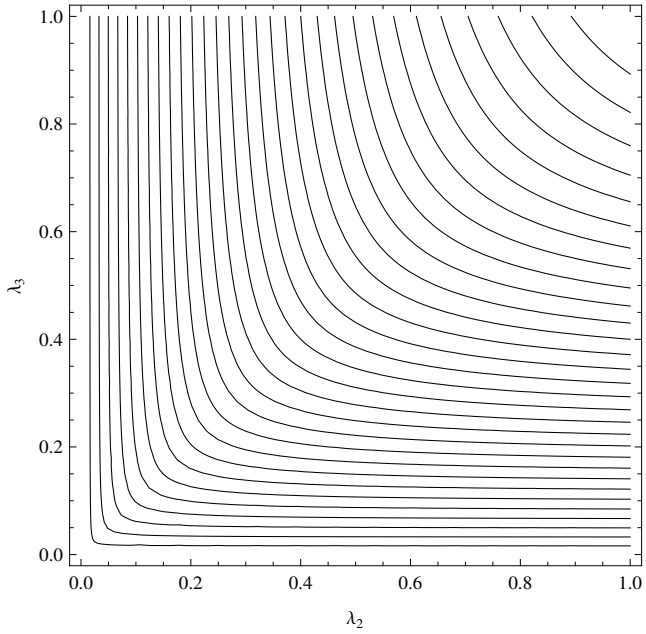

Figure 6: Contourplot of $p(3)$

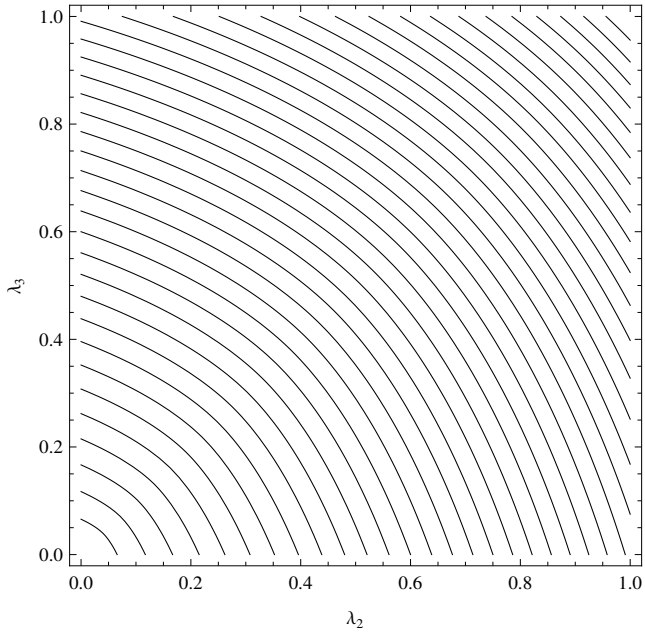

Figure 7: Contourplot of $P(A_1 \cup A_2 \cup A_3)$

and therefore with $\lambda = \ell/a$

$$P(A_{j_1} \cap \cdots \cap A_{j_k}) = \frac{\lambda}{2^{k-1}} \sum_{\nu=1}^{k} \frac{(-1)^{\nu-1}}{\nu(\nu+1)} \binom{k-1}{\nu-1} = \frac{\lambda}{2^{k-1}(k+1)},$$

where the sum was calulated with Mathematica. Furthermore we have

$$\sum_{J_k} P(A_{j_1} \cap \cdots \cap A_{j_k}) = \binom{n}{k} \frac{\lambda}{2^{k-1}(k+1)}$$

and with formula (4) for $1 \le i \le n$

$$p(i) = \lambda \sum_{k=i}^{n} \frac{(-1)^{i+k}}{2^{k-1}(k+1)} \binom{k}{i} \binom{n}{k}.$$

With

$$\binom{k}{i}\binom{n}{k} = \binom{n}{i}\binom{n-i}{k-i}$$

we finally get

$$p(i) = 2\lambda \binom{n}{i} \sum_{k=i}^{n} \frac{(-1)^{i+k}}{2^k(k+1)} \binom{n-i}{k-i},$$

which provides a different representation of the result of theorem 1.

References

[1] U. Bäsel: Geometric Probabilities for a Cluster of Needles and a Lattice of Rectangles, *Rend. Circ. Mat. Palermo*, Serie II, Suppl. **81** (2009), 29-38.

[2] A. A. Borowkow: *Wahrscheinlichkeitstheorie. Eine Einführung*, Akademie-Verlag, Berlin, 1976.

[3] I. N. Bronstein, K. A. Semendjajew: *Taschenbuch der Mathematik*, 24. Aufl., Teubner, Leipzig, 1989.

[4] P. Diaconis: Buffon's Problem with a Long Needle. *J. Appl. Prob.*, **13** (1976), 614-618.

[5] A. Duma, M. I. Stoka: Hitting Probabilities for Random Ellipses and Ellipsoids. *J. Appl. Prob.*, **30** (1993), 971-974.

[6] A. Duma, M. I. Stoka: Geometric Probabilities for Convex Bodies of Revolution in the Euclidean Space E_3, *Rend. Circ. Mat. Palermo*, Serie II, Suppl. **65** (2000), 109-115.

[7] A. Duma, M. I. Stoka: Geometric Probabilities for Convex Bodies of Large Revolution in the Euclidean Space E_3 (II), *Beiträge zur Algebra und Geometrie/Contributions to Algebra and Geometry*, **43** (2002) No. 2, 339-349.

[8] W. Feller: *An Introduction to Probability Theory and Its Applications*, Vol. II, 2nd edn. John Wiley & Sons, New York, 1971.

[9] G. M. Fichtenholz: *Differential- und Integralrechnung II*, VEB Deutscher Verlag der Wissenschaften, Berlin 1964.

[10] J. Galambos: *Advanced Probability Theory*, 2nd edn. Marcel Dekker, New York, Basel, Hong Kong, 1995.

[11] A. M. Mathai: *An Introduction to Geometrical Probability*, Gordon and Breach, Australia, 1999.

[12] L. A. Santaló: *Integral Geometry and Geometric Probability*, Addison-Wesley, London, 1976.

[13] M. I. Stoka: Une extension du problème de l'aiguille de Buffon dans l'espace euclidien $\mathbb{R}^n$, *Boll. Unione Mat. Italiana* **10** (1974), 386-389.

[14] M. I. Stoka: Probabilités géométriques de type 'Buffon' dans le plan euclidien, *Atti Accad. Sci. Torino* **110** (1975/76), 53-59.

[15] W. Szpankowski: *Inclusion-Exclusion Principle,* Purdue University, www.cs.purdue.edu/homes/spa/papers/chap3.ps

Uwe BÄSEL

Leipzig University of Applied Sciences
Department of Mechanical
and Energy Engineering,
04251 Leipzig, Germany

baesel@me.htwk-leipzig.de

RENDICONTI DEL CIRCOLO MATEMATICO DI PALERMO
Serie II, Suppl. 83 (2011), pp. 57-64

Models associated with extended exponential smoothing

Denis Bosq

Université Pierre et Marie Curie, Paris 6, France

Abstract

We study an extended form of exponential smoothing which is more flexible than the original one: let $(X_t,\, t \in \mathbb{Z})$ be a real stochastic process, observed until time n, consider the predictor of X_{n+1} defined as

$$X^*_{n+1} = \alpha \sum_{j=0}^{\infty} \beta^j X_{n-j}, \quad (\alpha \in \mathbb{R},\, \beta \in \mathbb{R})$$

where the series is supposed to be convergent in mean square. We look for stochastic models such that X^*_{n+1} is the best linear predictor of X_{n+1}, given $X_t,\, t \leq n$.

We obtain various ARIMA models depending on (α, β). In this context we study estimation of (α, β). Finally, extension to functional stochastic processes is considered.

Keywords exponential smoothing, prediction, forecasting, estimation, ARIMA, Hilbertian ARIMA.

MSC2010 classification 62M20, 62F10.

1 Exponential smoothing

The well known *exponential smoothing* (ES) is commonly used to forecast economic series. That genuine method has been introduced and studied by R.Brown (1962): given the observed random variables $X_0, X_1, ..., X_n$, one constructs a predictor of the non-observed random variable X_{n+1} by setting

$$\hat{X}_{n+1} = (1-\beta) \sum_{j=0}^{n} \beta^j X_{n-j}, \quad (0 < \beta < 1)\,. \tag{1}$$

In the current paper, we propose a more general theoretical form of ES and extend it to the functional case.

Let $X = (X_t,\, t \in \mathbb{Z})$ be a real stochastic process observed until time n; consider the predictor X^*_{n+1} of X_{n+1} defined by

$$X^*_{n+1} = \alpha \sum_{j=0}^{\infty} \beta^j X_{n-j}, \quad (\alpha \in \mathbb{R},\, \beta \in \mathbb{R}), \tag{2}$$

where the series is supposed to be convergent in mean-square. In (2) we use the convention $0^0 = 1$. Note that (1) corresponds with a truncated form of (2) in the special case where $\alpha = 1 - \beta$ and $0 < \beta < 1$.

Our purpose is to find stochastic models such that X^*_{n+1} is the *best linear predictor* (BLP) of X_{n+1}, given $X_t, t \leq n$.

If X is stationary, we exhibit such models in Section 2. Estimation of (α, β) is considered in Section 3. We look at the non-stationary case in Section 4. Finally, Section 5 is devoted to the infinite dimensional situation.

2 Stationary models

Note first that the predictor defined by (2) is flexible. For example, if $X_1, ..., X_n$, X_{n+1} are i.i.d. and $X_t = 0, t \leq 0$, the choice $\beta = 1$ and $\alpha = \frac{1}{n}$ gives $X^*_{n+1} = \bar{X}_n$. On the contrary, $\alpha = 1$ and $\beta = 0$ yields $X^*_{n+1} = X_n$. Note also that ES is *recursive*:

$$X^*_{n+1} = \alpha X_n + \beta X^*_n, \;\; n \in \mathbb{Z}. \tag{3}$$

Now the following statement exhibits the model associated with ES if X is supposed to be *(weakly) stationary* (see Brockwell and Davies (1991) (BD) for the definitions here and below).

Proposition 2.1. *Suppose that* $0 < |\beta| < 1$, $|\alpha + \beta| < 1$, $\alpha \neq 0$. *If* X *is a regular zero-mean stationary process with innovation* $\epsilon = (\epsilon_t, t \in \mathbb{Z})$ *and such that* X^*_{n+1} *is BLP for every* n, *then* X *is ARMA (1,1):*

$$X_t - (\alpha + \beta) X_{t-1} = \epsilon_t - \beta \epsilon_{t-1}, \;\; t \in \mathbb{Z}. \tag{4}$$

Conversely, if X *satisfies* (4), *then* X^*_{n+1} *is BLP for every* n.

Proof. First, stationarity of X and condition $|\beta| < 1$ yield L^2- convergence of the series in (2). Now, since X is regular with innovation ϵ, one has

$$X_t = X^*_t + \epsilon_t, \;\; t \in \mathbb{Z}, \tag{5}$$

where

$$X^*_t = \alpha \sum_{j=0}^{\infty} \beta^j X_{t-1-j}.$$

hence

$$\epsilon_t = X_t - \alpha X_{t-1} - \alpha\beta X_{t-2} - \alpha\beta^2 X_{t-3} - ..., \tag{6}$$

Now set

$$R(z) = 1 - \alpha z - \alpha\beta z^2 - \alpha\beta^2 z^3 - ... = \frac{1-(\alpha+\beta)\,z}{1-\beta z},\ \ |z| < 1, \qquad (7)$$

and let B be the backward operator defined by

$$B(X_t) = (X_{t-1}).$$

From (6) and (7) it follows that

$$(\epsilon_t) = (I - (\alpha+\beta)B)\ (I-\beta B)^{-1}\,(X_t),$$

where I is identity, which is equivalent to (4).

Conversely, if (4) holds, (6) follows and, from (5), one get (2). □

In some special cases the model is more simple:

– If $\alpha = 0$ then $X_t^* = 0$, thus

$$X_t = \epsilon_t\ \ t \in \mathbb{Z};$$

– If $\beta = 0,\ 0 < |\alpha| < 1$, the model is AR(1):

$$X_t = \alpha X_{t-1} + \epsilon_t\ \ t \in \mathbb{Z};$$

– If $\alpha + \beta = 0,\ 0 < |\beta| < 1$, then

$$X_t = \epsilon_t - \beta\epsilon_{t-1},\ \ t \in \mathbb{Z};$$

and the model is MA(1).

The case $|\alpha+\beta| \geq 1$, which leads to a non-stationary model, appears in Section 4.

3 Estimating the parameters

If X is gaussian, the parameters α, β and $\sigma^2 = E\epsilon_t^2$ can be estimated by maximum likelihood (see Gourieroux and Monfort (1990)(GM)).

In the general case, one may use empirical methods: let $\gamma_k = E(X_0 X_k)$,$k \in \mathbb{N}$ be the autocovariance of X. From (4) we have:

$$\begin{cases} \gamma_0 &= (\alpha+\beta)\,\gamma_1 + (1-\alpha\beta)\,\sigma^2 \\ \gamma_1 &= (\alpha+\beta)\gamma_0 - \beta\,\sigma^2 \\ \gamma_k &= (\alpha+\beta)^{k-1}\gamma_1,\ \ k \geq 2 \end{cases}$$

it follows that

$$\begin{cases} \alpha+\beta & = \frac{\gamma_2}{\gamma_1} \\ \beta\sigma^2 & = \frac{\gamma_0\gamma_2-\gamma_1^2}{\gamma_1} \\ (1-\alpha\beta)\,\sigma^2 & = \gamma_0-\gamma_2 \end{cases} \tag{8}$$

Thus, an estimator of (α,β,σ^2) can be constructed by substituting $\gamma_0,\gamma_1,\gamma_2$ for the empirical covariances

$$\hat{\gamma}_k = \frac{1}{n-k+1}\sum_{i=0}^{n-k} X_i X_{i+k};\ \ k=0,1,2;\ n\geq 2.$$

Note that the system (8) is somewhat difficult to solve.

Now, consistency and asymptotic normality of the obtained estimator $\left(\hat{\alpha},\,\hat{\beta},\,\hat{\sigma}^2\right)$ come from general results concerning estimation of ARMA processes (see BD and GM).

Finally, if $|\alpha\beta|$ is small, one may neglect it and uses the estimators:

$$\begin{aligned} \tilde{\alpha} &= \frac{\hat{\gamma}_1^2-\hat{\gamma}_2^2}{\hat{\gamma}_1(\hat{\gamma}_0-\hat{\gamma}_2)}\,, \\ \tilde{\beta} &= \frac{\hat{\gamma}_0\hat{\gamma}_2-\hat{\gamma}_1^2}{\hat{\gamma}_1(\hat{\gamma}_0-\hat{\gamma}_2)}\,, \\ \tilde{\sigma}^2 &= \hat{\gamma}_0-\hat{\gamma}_2\,. \end{aligned}$$

4 The non-stationary case

If the case $|\alpha+\beta|\geq 1$, we take $X_t=0$, $t<0$ and we suppose that $EX_t=0$, $0<\left|EX_t^2\right|<\infty$, $t\geq 0$. Then X_{n+1}^* is given by

$$X_{n+1}^* = \alpha\sum_{j=0}^{n}\beta^j X_{n-j},\ \ n\in\mathbb{Z}, \tag{9}$$

note that, in particular, one has $X_0^*=0$.

Proposition 4.1. *If $|\alpha+\beta|\geq 1$ and the BLP is given by* (9)*, then*

$$X_t-(\alpha+\beta)X_{t-1} = \epsilon_t-\beta\epsilon_{t-1},\ \ t\geq 1, \tag{10}$$

where

$$\epsilon_t = X_t-X_t^*,\ \ t\geq 0. \tag{11}$$

Moreover

$$V_t := sp\left\{X_0,...,X_t\right\} = sp\left\{\epsilon_0,...,\epsilon_t\right\},\ \ t\geq 0 \tag{12}$$

and

$$\epsilon_s\perp\epsilon_t,\ \ s\neq t.$$

Proof. From (11) one has

$$\epsilon_t - \beta\epsilon_{t-1} = (X_t - X_t^*) - \beta\left(X_{t-1} - X_{t-1}^*\right), \ t \geq 1,$$

and (9) yields (10).

Now (10) and an easy induction give

$$X_t = \epsilon_t + \alpha \sum_{j=0}^{t-1} (\alpha+\beta)^j \epsilon_{t-1-j}, \ t \geq 1,$$

when (11) implies

$$\epsilon_t = X_t - \alpha \sum_{j=0}^{t-1} \beta^j X_{t-1-j}, \ t \geq 1,$$

and, since $X_0 = \epsilon_0$, (12) follows.

Finally, X_t^* being the orthogonal projection of X_t on V_{t-1}, it follows that

$$\epsilon_t = X_t - X_t^* \perp V_{t-1},$$

hence

$$\epsilon_s \perp \epsilon_t, \ s \neq t.$$

□

Now, with an additional assumption, (ϵ_t) becomes a white noise. Let us set

$$Y_t = X_t - (\alpha+\beta) X_{t-1}, \ t \in \mathbb{Z}, \tag{13}$$

note that $Y_0 = X_0 = \epsilon_0$ and $Y_t = 0 \ t < 0$.

Corollary 4.2. *If* $Y_t = X_t - (\alpha+\beta)X_{t-1}, \ t \geq 1$ *is stationary and non-degenerated, and if* $\beta \neq 0$, *then* $(\epsilon_t, \ t \geq 1)$ *is the innovation of* $(Y_t, \ t \geq 1)$.

Proof. First we show that $(\epsilon_t, \ t \geq 0)$ is a white noise. From Proposition 4.1 it suffices to verify that $E\epsilon_t^2$ is strictly positive and does not depend on t. We have

$$c_1 := E(Y_t Y_{t+1}) = E\left[(\epsilon_t - \beta\epsilon_{t-1})(\epsilon_{t+1} - \beta\epsilon_t)\right] = -\beta E\epsilon_t^2, \ t \geq 1.$$

hence

$$E\epsilon_t^2 = -c_1\beta^{-1}, \ t \geq 1.$$

On the other hand

$$c_0 := EY_2^2 = E\left(\epsilon_2 - \beta\epsilon_1\right)^2 = -c_1\beta^{-1}(1+\beta^2) > 0, \tag{14}$$

since (Y_t) is not degenerated.

Finally $Y_1 = \epsilon_1 - \beta\epsilon_0$ yields

$$-c_1\beta^{-1}(1+\beta^2) = -c_1\beta^{-1} + \beta^2 E\epsilon_0^2$$

which implies

$$E\epsilon_0^2 = -c_1\beta^{-1}.$$

Now, set

$$W_t = sp\{Y_0, ..., Y_t\}, \ t \geq 0,$$

then $W_t \subseteq V_t$, and since

$$\epsilon_t = \sum_{j=0}^{t} \beta^j Y_{t-j}, \ t \geq 0,$$

it follows that

$$W_t = V_t, \ t \geq 0.$$

Finally from $Y_t = \epsilon_t - \beta\epsilon_{t-1}$,we deduce that the best linear predictor of Y_t given W_{t-1} is

$$Y_t^* = -\beta\epsilon_{t-1}, \ t \geq 1$$

(recall that $Y_0 = \epsilon_0$). □

In the special case where $0 < \beta < 1$ and $\alpha = 1 - \beta$, one obtains the IMA(1,1) defined by

$$X_t - X_{t-1} = \epsilon_t - \beta\epsilon_{t-1}, \ t \geq 1,$$

a well known result (cf Brown (1962)).

Note that, (Y_t) being a one-sided MA(1), there is no condition concerning β. If one wants to extend (Y_t), in order to obtain a two-sided MA(1), it is necessary to suppose that $0 < |\beta| < 1$ (cf BD) or at least that $|\beta| = 1$ (cf Blanke and Bosq (2010)).

We now give some ideas concerning *Estimation*. In the non-stationary case, estimation of the parameters is somewhat intricate. However(10) implies

$$E(X_tX_{t-2}) = (\alpha+\beta)\, E(X_{t-1}X_{t-2}), \ t \geq 2,$$

then, a reasonable empirical estimator of $\theta = \alpha + \beta$ is

$$\hat{\theta} = \frac{\sum_{t=2}^{n} X_tX_{t-2}}{\sum_{t=2}^{n} X_{t-1}X_{t-2}}, \tag{15}$$

now, under conditions in the corollary, one may claim that $\left(X_t - \hat{\theta}X_{t-1}\right)$ is approximately a MA(1) process, for which estimation of β and $E\epsilon_t^2$ are classical (cf BD or GM).

5 Exponential smoothing in a Hilbert space

That final section deals with (extended) exponential smoothing in a function space. In order to be concise enough, we use notation in Bosq and Blanke (2007).

Suppose that each X_t takes its values in a separable real Hilbert space H, and that α and β are now in $\mathcal{L}$ (the space of continuous linear operators from H to H). We define ES by putting

$$X_{n+1}^* = \alpha \left(\sum_{j=0}^{\infty} \beta^j (X_{n-j}) \right),$$

provided the series converges in the space $L_H^2(\Omega, A, P)$. Our main assumption is

$$\alpha\beta = \beta\alpha,$$

it easily follows that

$$X_{n+1}^* = \alpha(X_n) + \beta(X_n^*),$$

and Proposition 2.1 becomes:

Proposition 5.1. *Suppose that* $\left\|\beta^{j_0}\right\|_{\mathcal{L}} < 1$ *and* $\left\|(\alpha+\beta)^{j_0}\right\|_{\mathcal{L}} < 1$ *for some integer* j_0*, and that* $\alpha \neq 0$*. If* (X_t) *is a regular zero-mean stationary process with innovation* (ϵ_t) *and such that* X_{n+1}^**is BLP for every* n*, then* (X_t) *is an ARMAH (1,1):*

$$X_t - (\alpha+\beta)(X_{t-1}) = \epsilon_t - \beta(\epsilon_{t-1}), \quad t \in \mathbb{Z}. \tag{16}$$

Conversely, if (X_t) *satisfies* (16)*,* X_{n+1}^* *is BLP for every* n*.*

We omit the proof since it is almost similar to the proof of Proposition 1. Also, the special cases are analogous.

Concerning estimation, one defines the cross autocovariance operators (C_k) of (X_t) by

$$C_k(x) = E\left(\prec X_0, x \succ X_k\right), \; x \in H \;\;, k \in \mathbb{N},$$

where $\prec .,. \succ$denotes the scalar product in H. Then (16) allows to obtain the following system

$$\begin{cases} C_0 &= (\alpha+\beta)\, C_1 + (I - \alpha\beta)\, C_\epsilon \\ C_1 &= (\alpha+\beta)\, C_0 - \beta C_\epsilon \\ C_k &= (\alpha+\beta)^{k-1}\, C_1, \;\; k \geq 2 \end{cases}$$

where $C_\epsilon$is the autocovariance operator of ϵ_t.

It is not possible to directly obtain a system similar to (8) since the operators C_k and C_ϵ are not invertible. Then, in order to solve the above system, one have to project on a d_n- dimensional subspace of H, where d_n is small with respect to n . We omit the technical details.

References

D. Blanke and D. Bosq. Moving average with roots of modulus one and polynomial regression. To appear.

D. Bosq and D. Blanke. *Prediction and inference in large dimensions.* Wiley series in probability and statistics. Wiley-Dunod, 2007.

P. J. Brockwell and R. A. Davis. *Time Series : Theory and Methods.* Springer-Verlag, New-York, 2nd edition, 1991.

R.G. Brown. *Smoothing, forecasting, and prediction of discrete time series.* Prentice-Hall, New York, 1962.

C. Gourieroux and A. Monfort. *Séries temporelles et modèles dynamiques.* Economica, 1990.

RENDICONTI DEL CIRCOLO MATEMATICO DI PALERMO
Serie II, Suppl. 83 (2011), pp. 65-82

A Buffon type problem for an irregular lattice I

Giuseppe Caristi* and Marius Stoka**
*Department S.E.A.
University of Messina
e-mail: gcaristi@unime.it
**Accademia delle Scienze di Torino

Abstract

In this paper we consider a lattice with fundamental cell is composed by an isosceles triangle and an isosceles trapezium represented in fig. 1 and fig. 16 and we compute the probabilty that a segment of random position and with costant lenght intersects a side of the lattice.

Keywords: Geometric Probability, stochstic geometry, random sets, integral geometry.

1 Obstacles isosceles triangles

Let $R_1\,(a,\alpha;m)$ be a lattice with fundamental cell C_{01} composed by an isosceles triangle with base $a/2$ and angles $\alpha,\alpha,\pi-2\alpha$ and a trapezium with bases a and $a/2$ and angles $\alpha,\alpha,\pi-\alpha,\pi-\alpha$, $\left(\frac{\pi}{4}\leq\alpha\leq\frac{\pi}{3}\right)$, represented in fig. 1;

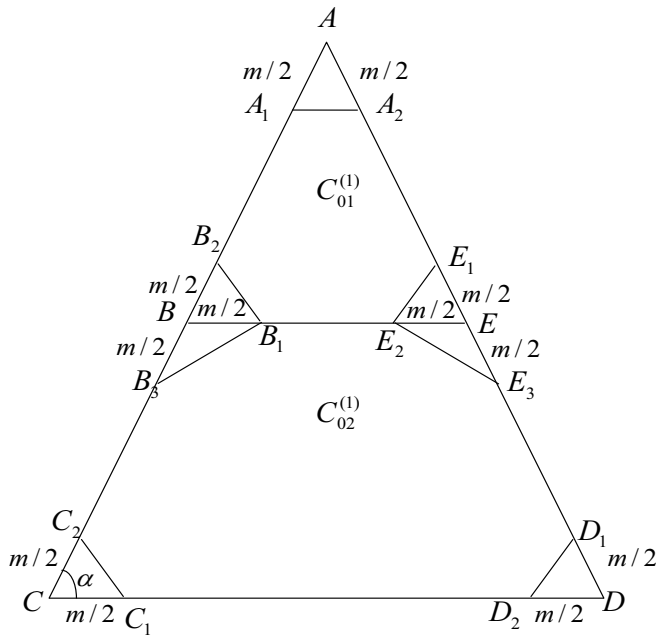

fig.1

The seven obstacles are isoscele triangles with equal side $m/2$.
We have

$$|AB| = |BC| = |AE| = |ED| = \frac{a}{4\cos\alpha},$$

$$|A_1A_2| = m\cos\alpha, \qquad |B_1B_3| = |E_2E_5| = m\cos\frac{\alpha}{2},$$

$$|B_1B_2| = |C_1C_2| = |D_1D_2| = |E_1E_2| = m\sin\frac{\alpha}{2}. \tag{1}$$

Denoting with o_1 the obstacle AA_1A_2, with o_2 the obstacle BB_1B_2 and with o_3 the obstacle BB_1B_3 we have that

$$area\ o_1 = \frac{m^2}{8}\sin 2\alpha, \quad area\ o_2 = area\ o_3 = \frac{m^2}{8}\sin\alpha. \tag{2}$$

With these values follow that

$$area\ C_{01} = \frac{a^2}{4}tg\alpha - \frac{m^2}{4}\sin\alpha\,(3+\cos\alpha)\,. \tag{3}$$

In similar way, denoting with $C_{01}^{(1)}$ the polygon $A_1B_2B_1E_2E_1A_2A_1$ and with $C_{01}^{(2)}$ the polygon $B_1B_3C_2C_1D_2D_1E_5E_2B_1$, we have that

$$area\ C_{01}^{(1)} = \frac{a^2}{16}tg\alpha - \frac{m^2}{4}\sin\alpha\,(1+\cos\alpha)\,,$$

$$area\ C_{01}^{(2)} = \frac{3a^2}{16} tg\alpha - \frac{m^2}{2} \sin\alpha. \tag{4}$$

Consider now, a segment s of random position and with constant lenght $l < \min\left(\frac{a}{2} - m, \frac{a}{4\cos\alpha} - m\right)$; we want compute the probability $P_{int}^{(1)}$ that the segment s intersect a side of the fundamental cell C_{01}.

The position of the segment s is determinated by the middle point O and by the angle φ that it forms with the side CD (or BE) of the cell C_{01}.

In order to compute the probability $P_{int}^{(1)}$ we consider the limit positions of the segment s, for a fixed value of φ in the polygon $C_{01}^{(1)}$ and for the limit positions of s, for teh same value of φ in the polygon $C_{01}^{(2)}$ (see fig. 2):

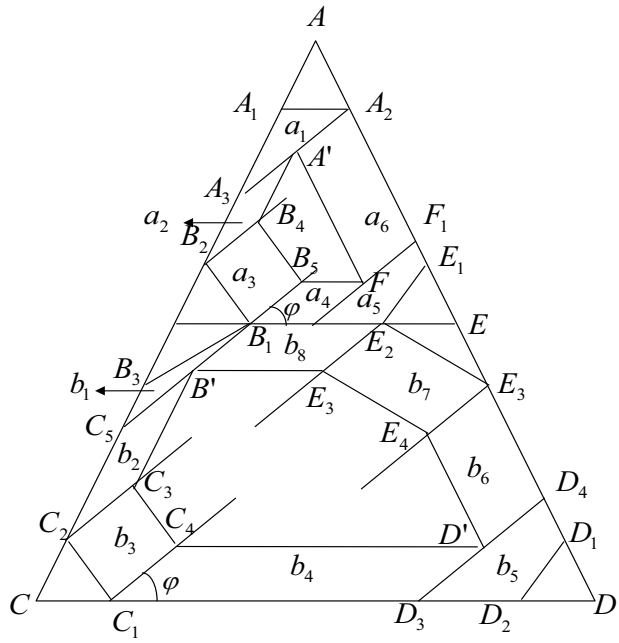

fig.2

Denoting with $\widehat{C}_{01}^{(1)}(\varphi)$ the determinated figure by the limit positions of s in the first case and with $\widehat{C}_{01}^{(2)}(\varphi)$ the determinated figure by limit positions of s in the second case, the fig. 2 give us:

$$area\ \widehat{C}_{01}^{(1)}(\varphi) = \frac{a^2}{16} tg\alpha - \frac{m^2}{4} \sin\alpha\,(1 + \cos\alpha) -$$

$$[areaa_1(\varphi) + areaa_2(\varphi) + ... + areaa_6(\varphi)] \tag{5}$$

and

$$area\ \widehat{C}_{01}^{(2)}(\varphi) = \frac{3a^2}{16} tg\alpha - \frac{m^2}{2} \sin\alpha -$$

$$[areab_1(\varphi) + areab_2(\varphi) + ... + areab_8(\varphi)]. \tag{6}$$

In the figure

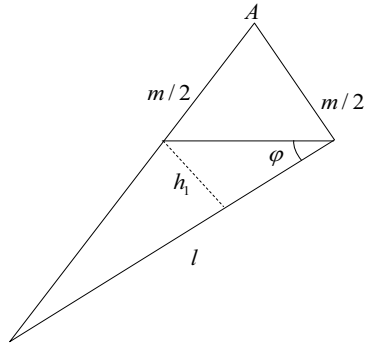

fig.3

the triangle $A_1A_2A_3$ give us

$$\frac{|A_1A_3|}{\sin\varphi} = \frac{l}{\sin\alpha},$$

then

$$|A_1A_3| = \frac{l\sin\varphi}{\sin\alpha}. \tag{7}$$

Considering (1) we have that

$$h_1 = |A_1A_2|\sin\varphi = m\cos\alpha\sin\varphi.$$

Then

$$areaa_1(\varphi) = \frac{lh_1}{2} = \frac{m\cos\alpha}{2} l\sin\varphi. \tag{8}$$

In oreder to compute $areaa_2(\varphi)$, we consider the figure

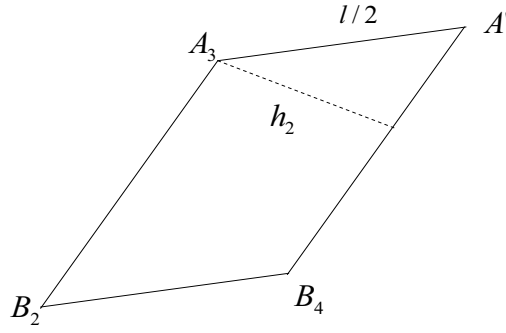

fig.4

We have that

$$\widehat{A_3B_2B_4} = \widehat{A_1A_3A_2} = \alpha - \varphi$$

and

$$h_2 = \frac{l}{2}\sin(\alpha - \varphi).$$

By (1) and (6) we obtain that

$$|A_3B_2| = |AB| - m - |A_1A_3| = \frac{a}{4\cos\alpha} - m - \frac{l\sin\varphi}{\sin\alpha},$$

and then we have that:

$$areaa_2(\varphi) = \left(\frac{a}{4\cos\alpha} - m - \frac{l\sin\varphi}{\sin\alpha}\right) \cdot \frac{l}{2}\sin(\alpha - \varphi). \tag{9}$$

Now we consider the figure

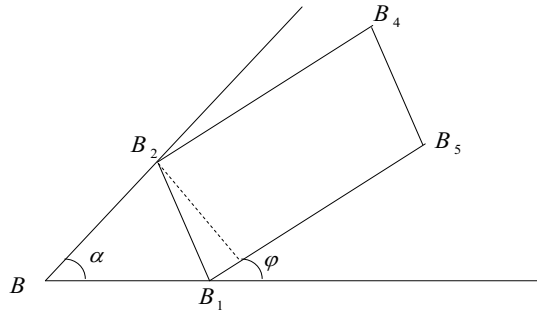

fig.5

we have that:

$$\widehat{BB_1B_2} = \frac{\pi}{2} - \frac{\alpha}{2}, \qquad \widehat{B_2B_1B_5} = \pi - \left(\frac{\pi}{2} - \frac{\alpha}{2} + \varphi\right) = \frac{\pi}{2} - \varphi + \frac{\alpha}{2},$$

and with the relation (1)

$$h_3 = |B_1B_2|\sin\left(\frac{\pi}{2} - \varphi + \frac{\alpha}{2}\right) = m\sin\frac{\alpha}{2}\cos\left(\varphi - \frac{\alpha}{2}\right),$$

then

$$areaa_3(\varphi) = \frac{lh_3}{2} = \frac{m\sin\frac{\alpha}{2}}{2}\cos\left(\varphi - \frac{\alpha}{2}\right). \tag{10}$$

The figure

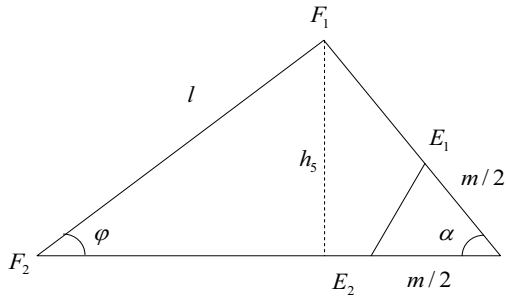

fig.6

give us that:

$$\widehat{F_2F_1E} = \pi - (\varphi + \alpha)$$

and

$$h_5 = l \sin \varphi.$$

By triangle EF_1F_2 follow that:

$$\frac{|EF_2|}{\sin(\varphi + \alpha)} = \frac{|EF_1|}{\sin \varphi} = \frac{l}{\sin \alpha},$$

then

$$|EF_1| = \frac{l \sin \varphi}{\sin \alpha}, \qquad |EF_2| = \frac{l \sin(\varphi + \alpha)}{\sin \alpha}. \tag{11}$$

Considering the (2) we have that:

$$areaa_5(\varphi) = \frac{|EF_2| \cdot h_5}{2} - areaAA_1A_2 =$$

$$\frac{l^2 \sin \varphi \sin(\varphi + \alpha)}{2 \sin \alpha} - \frac{m^2}{8} \sin 2\alpha. \tag{12}$$

From figure

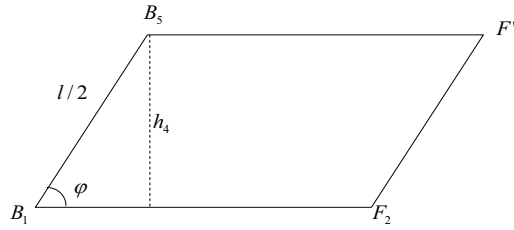

fig.7

and by (11) follow that:

$$h_4 = \frac{l}{2} \sin \varphi,$$

$$|B_1F_2| = |BE| - \frac{m}{2} - \frac{l\sin(\varphi+\alpha)}{\sin\alpha} = \frac{a}{2} - \frac{m}{2} - \frac{l\sin(\varphi+\alpha)}{\sin\alpha},$$

then

$$areaa_4(\varphi) = |B_1F_2| \cdot h_4 = \left[a - m - \frac{2l\sin(\varphi+\alpha)}{\sin\alpha}\right] \cdot \frac{l}{4}\sin\varphi. \qquad (13)$$

From the figure

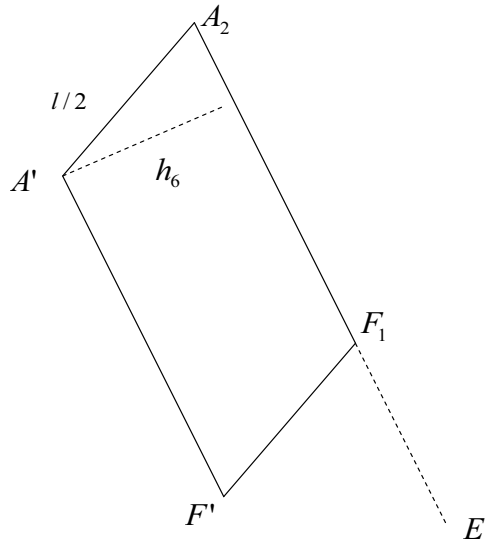

fig.8

and by relation (1) and (11) we obtain that:

$$\widehat{A'A_2F_1} = \widehat{F_2F_1E} = \pi - (\varphi+\alpha),$$

$$h_6 = \frac{l}{2}\sin\widehat{A'A_2F} = \frac{l}{2}\sin(\varphi+\alpha),$$

$$|A_2F_1| = |AE| - \frac{m}{2} - |EF_1| = \frac{a}{4\cos\alpha} - \frac{m}{2} - \frac{l\sin\varphi}{\sin\alpha},$$

then

$$areaa_6(\varphi) = \left(\frac{a}{2\cos\alpha} - m - \frac{2l\sin\varphi}{\sin\alpha}\right) \cdot \frac{l}{4}\sin(\varphi+\alpha). \qquad (14)$$

Considering in the relation (5) the relations (8), (9), (10), (12), (13) and (14) we obtain that:

$$area\widehat{C}_{01}^{(1)}(\varphi) = \frac{a^2}{16} \cdot tg\alpha - \frac{m^2}{4}\sin(1+\cos\alpha) -$$

$$\left[\left(atg\alpha - \frac{5m}{2}\sin\alpha\right) \cdot \frac{l}{4}\cos\varphi + \left(a - \frac{m}{2} + \frac{5m}{2}\cos\alpha\right) \cdot\right.$$

$$\frac{l}{4}\sin\varphi - \frac{l^2}{2}\sin 2\varphi - \frac{m^2}{8}\sin 2\alpha\Big]. \tag{15}$$

The figure

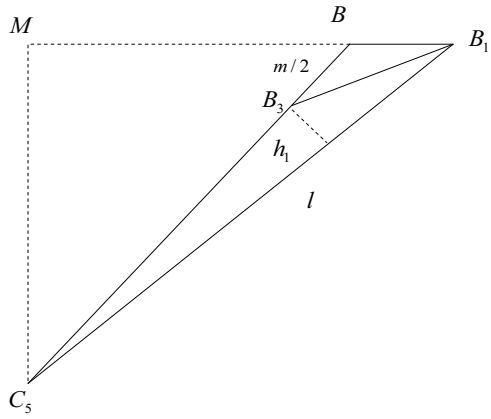

fig.9

give us that

$$\widehat{C_5B_1M} = \varphi, \qquad |C_5M| = l\sin\varphi.$$

Then, considering of the relation (2) we have that:

$$areab_1(\varphi) = areaBB_1C_5 - \frac{m^2}{8}\sin\alpha = \frac{|BB_1|\cdot|MC_5|}{2} - \frac{m^2}{8}\sin\alpha,$$

i.e.

$$areab_1(\varphi) = \frac{ml\sin\varphi}{4} - \frac{m^2}{8}\sin\alpha. \tag{16}$$

In order to compute $b_2(\varphi)$ we considering the figure

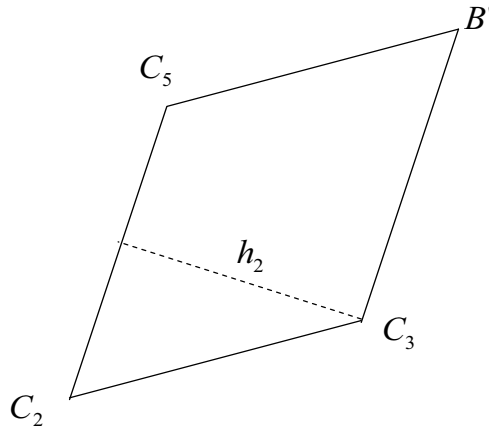

fig.10

and follow that:

$$\widehat{C_5C_2C_3} = \widehat{A_1A_3A_4} = \alpha - \varphi, \qquad k_2 = \frac{l}{2}\sin(\alpha - \varphi).$$

Moreover, the triangle BB_1C_5 give us that:

$$\frac{|BC_5|}{\sin\varphi} = \frac{l}{\sin(\pi - \alpha)},$$

i.e.

$$|BC_5| = \frac{l\sin\varphi}{\sin\alpha}.$$

This relation and the (1) give us

$$|C_2C_5| = |BC| - \frac{m}{2} - |BC_5| = \frac{a}{4\cos\alpha} - \frac{m}{2} - \frac{l\sin\varphi}{\sin\alpha}.$$

Then

$$areab_2(\varphi) = k_2 \cdot |C_2C_5| = \left(\frac{a}{4\cos\alpha} - \frac{m}{2} - \frac{l\sin\varphi}{\sin\alpha}\right) \cdot \frac{l}{2}\sin(\alpha - \varphi). \qquad (17)$$

The figure 2 and relation (10) give us that:

$$areab_3(\varphi) = areaa_3(\varphi) = \frac{ml\sin\frac{\alpha}{2}}{2} \cdot \cos\left(\varphi - \frac{\alpha}{2}\right). \qquad (18)$$

Considering the figure

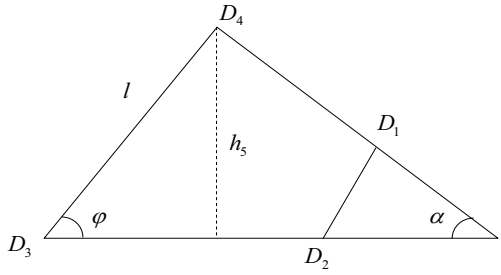

fig.11

we can write that:

$$k_5 = l\sin\varphi, \qquad \widehat{DD_4D_3} = \pi - (\alpha + \varphi).$$

The triangle DD_3D_4 give us that:

$$\frac{|DD_3|}{\sin(\alpha + \varphi)} = \frac{l}{\sin\alpha} = \frac{DD_4}{\sin\varphi},$$

then

$$|DD_3| = \frac{l \sin(\alpha + \varphi)}{\sin \alpha}, \qquad |DD_4| = \frac{l \sin \varphi}{\sin \alpha}. \tag{19}$$

The by the (2)

$$areab_5(\varphi) = areaDD_3D_4 - areaDD_1D_2,$$

i.e.

$$areab_5(\varphi) = \frac{l^2 \sin(\varphi + \alpha) \sin \varphi}{2 \sin \alpha} - \frac{m^2}{8} \sin \alpha. \tag{20}$$

Compute now the $areab_4(\varphi)$. The figure

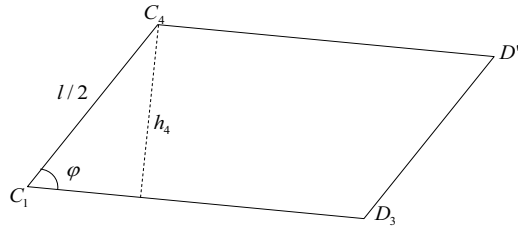

fig.12

and the relation (19) give us that:

$$k_4 = \frac{l}{2} \sin \varphi, \qquad |C_1D_3| = a - \frac{m}{2} - |DD_3| = a - \frac{m}{2} - \frac{l \sin(\varphi + \alpha)}{\sin \alpha},$$

then

$$areab_4(\varphi) = |C_1D_3| \cdot k_4 = \left[a - \frac{m}{2} - \frac{l \sin(\varphi + \alpha)}{\sin \alpha} \right] \cdot \frac{l}{2} \sin \varphi. \tag{21}$$

Considering the figure

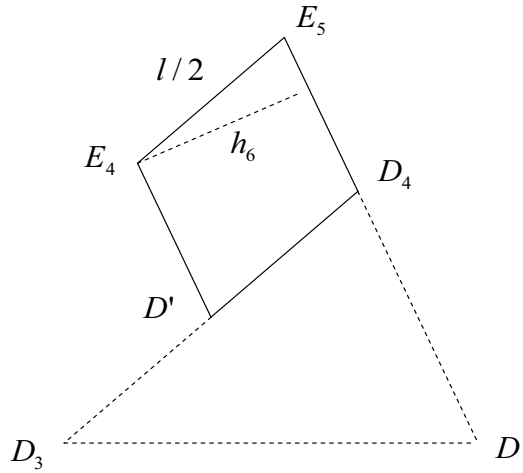

fig.13

by relations (1) and (19) we can write that:

$$\widehat{E_4E_5D_4} = \widehat{DD_4D_3} = \pi - (\varphi + \alpha),$$

$$k_6 = \frac{l}{2}\sin\widehat{E_4E_5D_4} = \frac{l}{2}\sin(\varphi + \alpha),$$

$$|D_4E_5| = |BC| - \frac{m}{2} - |DD_4| = \frac{a}{4\cos\alpha} - \frac{m}{2} - \frac{l\sin\varphi}{\sin\alpha},$$

then

$$areab_6(\varphi) = k_6 \cdot |D_4E_5| = \left(\frac{a}{4\cos\alpha} - \frac{m}{2} - \frac{l\sin\varphi}{\sin\alpha}\right) \cdot \frac{l}{2}\sin(\varphi + \alpha). \qquad (22)$$

The figure

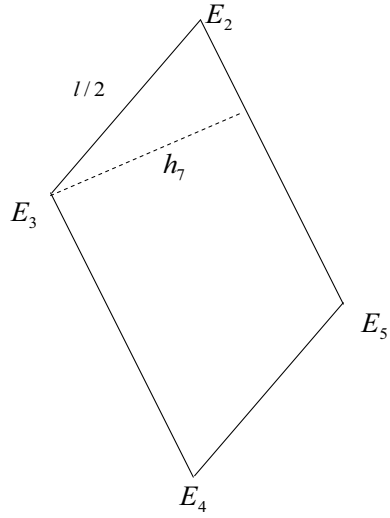

fig.14

give us the $areab_7(\varphi)$. By relation (1) we have that

$$|E_2E_5| = m\cos\frac{\alpha}{2},$$

and

$$\widehat{E_3E_2E_5} = \pi - \widehat{E_2E_5E_4}, \qquad \widehat{E_2E_5E_4} = \pi - \left(\frac{\alpha}{2} + \widehat{E_4E_5D_4}\right) = \frac{\alpha}{2} + \varphi,$$

then

$$\widehat{E_3E_2E_5} = \pi - \frac{\alpha}{2} - \varphi,$$

and consequently

$$k_7 = \frac{l}{2}\sin\left(\varphi + \frac{\alpha}{2}\right).$$

We have that:

$$areab_7(\varphi) = |E_2E_5| \cdot k_7 = \frac{m\cos\frac{\alpha}{2}}{2} \cdot \sin\left(\varphi + \frac{\alpha}{2}\right). \tag{23}$$

The figure

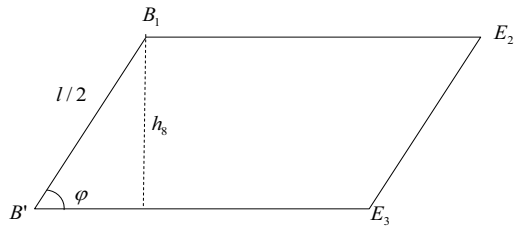

fig.15

give us

$$k_8 = \frac{l}{2}\sin\varphi, \qquad |B_1E_2| = |BE| - m = \frac{a}{2} - m,$$

then

$$areab_8(\varphi) = \left(\frac{a}{2} - m\right) \cdot \frac{l}{2}\sin\varphi. \tag{24}$$

Considering in the relation (6) the expressions (16), (17), (18), (20), (21), (22), (23), and (24) we obtain that:

$$areaC_{01}^{(2)}(\varphi) = \frac{3a^2}{16}tg\alpha - \frac{m^2}{2}\sin\alpha -$$

$$\left[\frac{al}{4}(tg\alpha \cdot \cos\varphi + 3\sin\varphi) - \frac{l^2}{2}\sin 2\varphi - \frac{m^2}{4}\sin\alpha\right]. \tag{25}$$

Denoting with $M^{(1)}$ the set of segments s which have the middle point O in he fundamental cell C_{01}, with $N_1^{(1)}$ the set of segments s completely contanined in $C_{01}^{(1)}$ and with $N_2^{(1)}$ the set of segment s completely contained in $C_{01}^{(2)}$, we have [2] that:

$$P_{int}^{(1)} = 1 - \frac{\mu\left(N_1^{(1)}\right) + \mu\left(N_2^{(1)}\right)}{\mu\left(M^{(1)}\right)}, \tag{26}$$

where μ is the Lebesgue measure in Euclidean plane.

In order to compute the measures $\mu\left(M^{(1)}\right), \mu\left(N_1^{(1)}\right)$ and $\mu\left(N_2^{(1)}\right)$ we use the kinematic Poincaré measure [1]:

$$dK = dx \wedge dy \wedge d\varphi,$$

where x, y are the coordinates of the point and φ is the defined angle.

Since $\varphi \in [0,\ \alpha]$, we have that:

$$\mu\left(M^{(1)}\right) = \int_0^{\alpha} d\varphi \iint\limits_{\{(x,y)\in C_{01}\}} dxdy = \int_0^{\alpha} (areaC_{01})\, d\varphi = \alpha areaC_{01}. \tag{27}$$

Considering the relation (15) we have that:

$$\mu\left(N_1^{(1)}\right) = \int_0^{\alpha} d\varphi \iint\limits_{\left\{(x,y)\in C_{01}^{(1)}\right\}} dxdy = \int_0^{\alpha} \left(areaC_{01}^{(1)}\right) d\varphi =$$

$$\alpha\left[\frac{a^2}{16}\cdot tg\alpha - \frac{m^2}{4}\sin\alpha\,(1+\cos\alpha)\right] - \left\{\left[a\frac{\sin^2\alpha}{\cos\alpha} + (a-3m)\,(1-\cos\alpha)\right]\cdot \right.$$

$$\left. \frac{l}{4} - \frac{l^2}{2}\sin^2\alpha - \frac{m^2}{8}\alpha\sin 2\alpha\right\}. \tag{28}$$

In the same way by relation (25), we can write that:

$$\mu\left(N_2^{(1)}\right) = \int_0^{\alpha} d\varphi \iint\limits_{\left\{(x,y)\in \widehat{C}_{02}^{(1)}\right\}} dxdy = \int_0^{\alpha} \left(area\widehat{C}_{02}^{(1)}\right) d\varphi =$$

$$\alpha\left(\frac{3a^2}{16}tg\alpha - \frac{m^2}{2}\sin\alpha\right) -$$

$$\left[\left(\frac{1}{\cos\alpha} - 4\cos\alpha + 3\right)\cdot\frac{al}{4} - \frac{l^2}{2}\sin^2\alpha - \frac{m^2}{4}\alpha\sin\alpha\right]. \tag{29}$$

The relations (3), (25), (27), (28), and (29) give us that:

$$P_{int}^{(1)} = \frac{1}{\alpha\left[a^2 tg\alpha - m^2\sin\alpha\,(3+\cos\alpha)\right]}\cdot$$

$$\left\{\left[\frac{2a}{\cos\alpha} + a + 3 - 3m - (2a+m)\cos\alpha\right] l -\right.$$

$$\left. 4l^2\sin^2\alpha - m^2\alpha\sin\alpha\,(1+\cos\alpha)\right\}. \tag{30}$$

For $m \to 0$, the obstacles became points and the probability (30) became:

$$P^{(1)} = \frac{\left(\frac{2a}{\cos\alpha} + a + 3 - 2a\cos\alpha\right) l - 4l^2\sin^2\alpha}{\alpha a^2 tg\alpha}. \tag{31}$$

Moreover, considering the limit values of α, we have that:

$$P_1^{(1)} = \frac{4\left[a\left(\sqrt{2}+1\right)+3\right] l - 8l^2}{\pi a^2}$$

for $\alpha = \frac{\pi}{4}$, and

$$P_2^{(1)} = \frac{\left[(4a+3)\,l - 3l^2\right]\sqrt{3}}{\pi a^2}$$

for $\alpha = \frac{\pi}{3}$.

2 Obstacles triangles and circular sectors

Let $R_2\,(a,\alpha;m)$ be the lattice with fundamental cell C_{02} rappresented in fig. 16

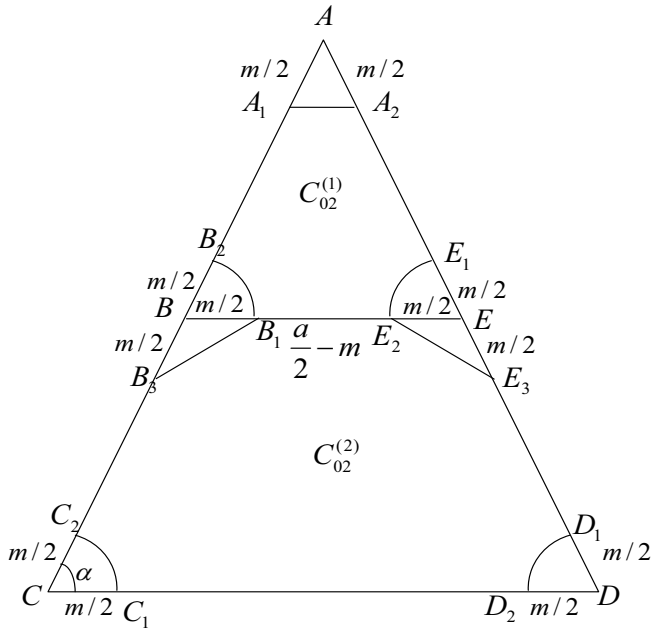

fig.16

The obstacles are isosceles triangles denoting same in section 1, with σ_1 and σ_2 and four circular sectors of radius $m/2$, equals, denoting with o_3.

Considering the relation (2), we have that:

$$areao_1 = \frac{m^2}{8}\sin 2\alpha, \qquad areao_3 = \frac{m^2}{8}\sin\alpha. \tag{32}$$

In the same way

$$areao_2 = \frac{\alpha m^2}{8}.$$

By these values follow that:

$$areaC_{02} = \frac{a^2}{4}tg\alpha - \frac{m^2}{8}\sin 2\alpha - \frac{m^2}{4}\sin\alpha - \frac{\alpha m^2}{2},$$

i.e.

$$areaC_{02} = \frac{a^2}{4}tg\alpha - \frac{m^2}{4}\sin\alpha\,(1+\cos\alpha) - \frac{\alpha m^2}{2}. \tag{33}$$

Denoting with $C_{02}^{(1)}$ the figure $A_1B_2B_1E_2E_1A_2A_1$ and with $C_{02}^{(2)}$ the figure $B_1B_3C_2C_1D_2D_1E_3E_2B_1$, we have that:

$$areaC_{02}^{(1)} = \frac{a^2}{16}tg\alpha - \frac{m^2}{4}\left(\sin\alpha\cos\alpha + \alpha\right), \tag{34}$$

and

$$areaC_{02}^{(2)} = \frac{3a^2}{16} tg\alpha - \frac{m^2}{4} (\sin\alpha + \alpha) . \tag{35}$$

We want to compute the probability $P_{int}^{(2)}$ that a segment s of random position and of constant lenght $l < \min\left(\frac{a}{2} - m, \frac{a}{4\cos\alpha} - m\right)$ intersects a side of the lattice R_2, i.e. the ptobability $P_{int}^{(2)}$ that the segment s intersects a side of the fundamental cell C_{02}.

Denoting with φ the angle that the segment s forms with the side CD (or BE) of the cell C_{02} and with O the middle point of the segment s.

Denoting with $\widehat{C}_{02}^{(1)}(\varphi)$, (respectivament $\widehat{C}_{02}^{(2)}(\varphi)$), the detrminated figure of the limit positions of the segment s for a fixed value of φ, in $C_{02}^{(1)}$, (respectivament $\widehat{C}_{02}^{(2)}(\varphi)$):

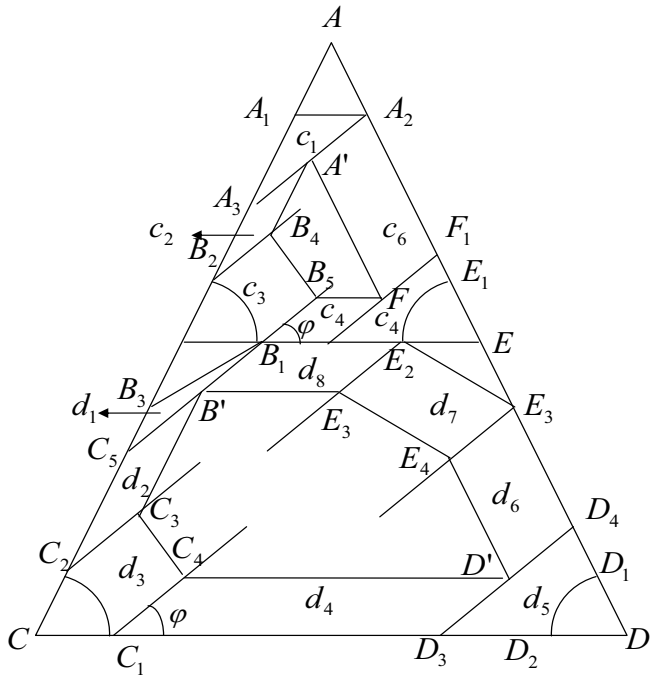

fig.17

Follow that:

$$area\widehat{C}_{02}^{(1)}(\varphi) = \frac{a^2}{16} tg\alpha - \frac{m^2}{4} (\sin\alpha\cos\alpha + \alpha) -$$
$$[areac_1(\varphi) + areac_2(\varphi) + ... + areac_6(\varphi)] , \tag{36}$$

and

$$area\widehat{C}_{02}^{(2)}(\varphi) = \frac{3a^2}{16} tg\alpha - \frac{m^2}{4} (\sin\alpha + \alpha) -$$

$$[aread_1(\varphi) + aread_2(\varphi) + ... + aread_8(\varphi)]. \tag{37}$$

The fig. 2 and 17 give us that:

$$areac_1(\varphi) = areaa_1(\varphi), \quad areac_2(\varphi) = areaa_2(\varphi),$$
$$areac_4(\varphi) = areaa_4(\varphi), \quad areac_6(\varphi) = areaa_6(\varphi), \tag{38}$$

and

$$aread_1(\varphi) = areab_1(\varphi), \ aread_2(\varphi) = areab_2(\varphi), \ aread_4(\varphi) = areab_4(\varphi),$$
$$aread_6(\varphi) = areab_6(\varphi), \ aread_7(\varphi) = areab_7(\varphi), \ aread_8(\varphi) = areab_8(\varphi). \tag{39}$$

We have that:

$$area\overset{\frown}{B_1B_2} = \frac{m^2}{8}(\alpha - \sin\alpha),$$

then

$$\begin{aligned} areac_3(\varphi) &= areaa_3(\varphi) - \frac{m^2}{8}(\alpha - \sin\alpha), \\ areac_5(\varphi) &= areaa_5(\varphi) - \frac{m^2}{8}(\alpha - \sin\alpha), \end{aligned} \tag{40}$$

and

$$\begin{aligned} aread_3(\varphi) &= areab_3(\varphi) - \frac{m^2}{8}(\alpha - \sin\alpha), \\ aread_5(\varphi) &= areab_5(\varphi) - \frac{m^2}{8}(\alpha - \sin\alpha). \end{aligned} \tag{41}$$

The relations (38) and (40) give us

$$areac_1(\varphi) + areac_2(\varphi) + ... + areac_6(\varphi) =$$
$$areaa_1(\varphi) + areaa_2(\varphi) + ... + areaa_6(\varphi) - \frac{m^2}{4}(\alpha - \sin\alpha), \tag{42}$$

and by relations (39) and (41) follow that:

$$aread_1(\varphi) + aread_2(\varphi) + ... + aread_8(\varphi) =$$
$$areab_1(\varphi) + areab_2(\varphi) + ... + areab_8(\varphi) - \frac{m^2}{4}(\alpha - \sin\alpha). \tag{43}$$

The relations (36) and (42) give us that:

$$area\widehat{C}_{02}^{(1)}(\varphi) = \frac{a^2}{16}tg\alpha - \frac{m^2}{4}(\sin\alpha\cos\alpha + \alpha) -$$
$$\left[areaa_1(\varphi) + areaa_2(\varphi) + ... + areaa_6(\varphi) - \frac{m^2}{4}(\alpha - \sin\alpha)\right],$$

or, considering the (5),

$$area\widehat{C}_{01}^{(2)}(\varphi) = area\widehat{C}_{01}^{(1)} - \frac{m^2}{4}(\alpha - \sin\alpha). \tag{44}$$

In the same way, by relations (37) and (43) follow that:

$$areaC_{02}^{(2)}(\varphi) = \frac{3a^2}{16}tg\alpha - \frac{m^2}{4}(\sin\alpha + \alpha) -$$

$$\left[areab_1(\varphi) + areab_2(\varphi) + ... + areab_8(\varphi) - \frac{m^2}{4}(\alpha - \sin\alpha)\right],$$

i.e., considering the (6),

$$area\widehat{C}_{02}^{(2)}(\varphi) = area\widehat{C}_{01}^{(2)}(\varphi). \tag{45}$$

We have that:

$$P_{int}^{(2)} = 1 - \frac{\mu\left(N_1^{(2)}\right) + \mu\left(N_2^{(2)}\right)}{\mu\left(M^{(2)}\right)}, \tag{46}$$

where

$$\mu\left(M^{(2)}\right) = \int_0^{\alpha} (areaC_{02})\, d\varphi = \alpha areaC_{02},$$

$$\mu\left(N_1^{(2)}\right) = \int_0^{\alpha} \left[area\widehat{C}_{02}^{(1)}(\varphi)\right] d\varphi = \mu\left(N_1^{(1)}\right) - \frac{m^2}{4}\alpha(\alpha - \sin\alpha), \tag{47}$$

$$\mu\left(N_2^{(2)}\right) = \int_0^{\alpha} \left[area\widehat{C}_{02}^{(2)}(\varphi)\right] d\varphi = \mu\left(N_2^{(1)}\right).$$

With these values the relation (46) became

$$P_{int}^{(2)} = 1 - \frac{\mu\left(N_1^{(2)}\right) + \mu\left(N_2^{(1)}\right) - \frac{m^2}{4}\alpha(\alpha - \sin\alpha)}{\alpha areaC_{02}}.$$

Considering of the relation (27) we can write that:

$$P_{int}^{(2)} = 1 - \frac{areaC_{01}}{areaC_{02}}\left[1 - P_{int}^{(1)}\right] + \frac{m^2(\alpha - \sin\alpha)}{areaC_{02}}. \tag{48}$$

From here follow that:

$$P_{int}^{(2)} \geq P_{int}^{(1)}.$$

For $m = 0$ we have that $areaC_{02} = areaC_{01}$ and the relation (48) give us that:

$$P^{(1)} = P^{(2)}.$$

References

[1] Poincaré H., Calcul des probabilités, ed. 2, Carré, Paris, 1912.

[2] Stoka M., Probabilités géométriques de type Buffon dans le plan euclidien, Atti Acc. Sci. Torino, T. 110, pp. 53-59, 1976-1976.

RENDICONTI DEL CIRCOLO MATEMATICO DI PALERMO
Serie II, Suppl. 83 (2011), pp. 83-93

A Buffon type problem for an irregular lattice II

Giuseppe Caristi* and Marius Stoka**
*Department S.E.A.
University of Messina
e-mail: gcaristi@unime.it
**Accademia delle Scienze di Torino

Abstract

In this paper we consider a lattice with fundamental cell is composed by two isosceles trapezium represented in fig. 1 and we compute the probabilty that a segment of random position and with costant lenght intersects a side of the lattice.

Keywords: Geometric Probability, stochstic geometry, random sets, integral geometry

Let $R_1(a, \alpha, \beta; m)$ be a lattice with fundamental cell C_0 composed by an isosceles trapezium $C_0^{(1)}$ with bases $2a$ and a and angles $\alpha, \alpha, \pi - \alpha, \pi - \alpha$, $\left(\frac{\pi}{4} \leq \alpha \leq \frac{\pi}{3}\right)$ and an isosceles trapezium with bases $2a$ and a and angles $\beta, \beta, \pi - \beta, \pi - \beta$, $(\beta \leq \alpha)$, represented in fig. 1;

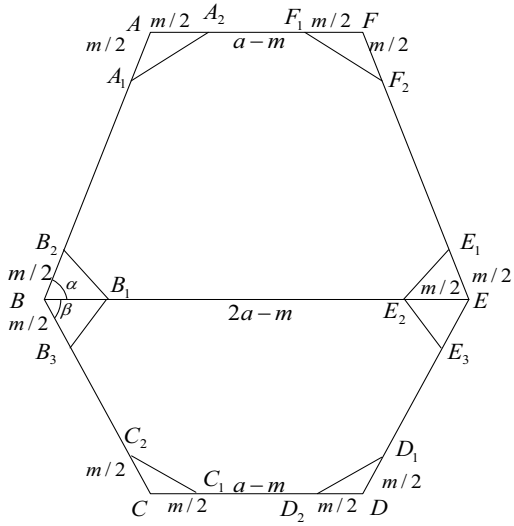

fig.1

The eight obstacles are isoscele triangles with equal side $m/2$.

We have

$$|AB| = |EF| = \frac{a}{2\cos\alpha},$$

$$|BC| = |DE| = \frac{a}{2\cos\beta}, \qquad |B_1B_2| = |E_1E_2| = m\sin\frac{\alpha}{2},$$

$$|B_1B_3| = |E_2E_3| = m\sin\frac{\beta}{2}, \qquad |A_1A_2| = |F_1F_2| = m\cos\frac{\alpha}{2},$$

$$|C_1C_2| = |D_1D_2| = m\cos\frac{\beta}{2}. \tag{1}$$

Denoting with o_1 the obstacle AA_1A_2, with o_2 the obstacle BB_1B_2, with o_3 the obstacle BB_1B_3 and with o_4 the obstacle CC_1C_2 we have that

$$area\ o_1 = area\ o_2 = \frac{m^2}{8}\sin\alpha, \quad area\ o_3 = area\ o_4 = \frac{m^2}{8}\sin\beta. \tag{2}$$

With these values follow that

$$area\ C_0^{(1)} = \frac{3a^2}{4}tg\alpha - \frac{m^2}{2}\sin\alpha, \quad area\ C_0^{(2)} = \frac{3a^2}{4}tg\beta - \frac{m^2}{2}\sin\beta \tag{3}$$

and we have that:

$$area\ C_0 = \frac{a^2}{4}\left(tg\alpha + tg\beta\right) - \frac{m^2}{2}\left(\sin\alpha + \sin\beta\right). \tag{4}$$

Consider now, a segment s of random position and with constant lenght $l < \min\left(a - m, \frac{a}{2\cos\beta} - m\right)$; we want compute the probability P_{int} that the segment s intersect a side of the fundamental cell C_0.

The position of the segment s is determinated by the middle point O and by the angle φ that it forms with the side BC of the cell C_0.

In order to compute the probability P_{int} we consider the limit positions of the segment s, for a fixed value of φ in the polygon $C_0^{(1)}$ and for the limit positions of s, for the same value of φ in the polygon $C_0^{(2)}$ (see fig. 2):

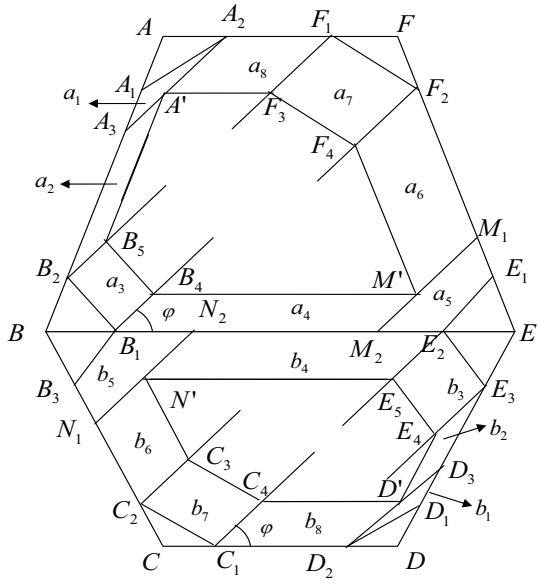

fig.2

Denoting with $\widehat{C}_0^{(1)}(\varphi)$ the determinated polygon by the limit positions of s in the first case and with $\widehat{C}_0^{(2)}(\varphi)$ the determinated polygon by limit positions of s in the second case, the fig. 2 give us:

$$area\ \widehat{C}_0^{(1)}(\varphi) = areaC_0^{(1)} - [areaa_1(\varphi) + areaa_2(\varphi) + ... + areaa_8(\varphi)] \quad (5)$$

and

$$area\ \widehat{C}_0^{(2)}(\varphi) = areaC_0^{(2)} - [areab_1(\varphi) + areab_2(\varphi) + ... + areab_8(\varphi)]. \quad (6)$$

Considering the figure

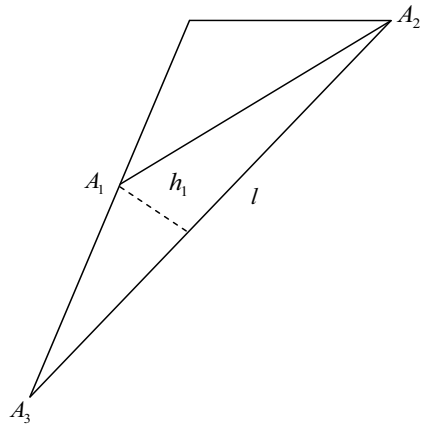

fig.3

we have that

$$\widehat{A_3AA_2} = \pi - \alpha, \quad \widehat{AA_1A_2} = \widehat{AA_2A_1} = \frac{\alpha}{2}, \quad \widehat{AA_2A_3} = \varphi, \quad \widehat{A_1A_2A_3} = \varphi - \frac{\alpha}{2},$$

$$\widehat{A_2A_1A_3} = \pi - \frac{\alpha}{2}, \quad \widehat{A_1A_3A_2} = \pi - \left(\varphi - \frac{\alpha}{2} + \pi - \frac{\alpha}{2}\right) = \alpha - \varphi.$$

By triangle $A_1A_2A_3$ follow that

$$\frac{|A_1A_3|}{\sin\left(\varphi - \frac{\alpha}{2}\right)} = \frac{l}{\sin\frac{\alpha}{2}} = \frac{m\cos\frac{\alpha}{2}}{\sin(\alpha - \varphi)}.$$

Then

$$|A_1A_3| = \frac{l\sin\left(\varphi - \frac{\alpha}{2}\right)}{\sin\frac{\alpha}{2}} \tag{7}$$

and the condition

$$2l\sin(\alpha - \varphi) = m\sin\alpha. \tag{8}$$

Considering the relation (2) we have that

$$h_1 = |A_1A_2|\sin\left(\varphi - \frac{\alpha}{2}\right) = m\cos\frac{\alpha}{2}\sin\left(\varphi - \frac{\alpha}{2}\right),$$

then

$$areaa_1(\varphi) = \frac{lh_1}{2} = \frac{ml}{2}\cos\frac{\alpha}{2}\sin\left(\varphi - \frac{\alpha}{2}\right). \tag{9}$$

The figure

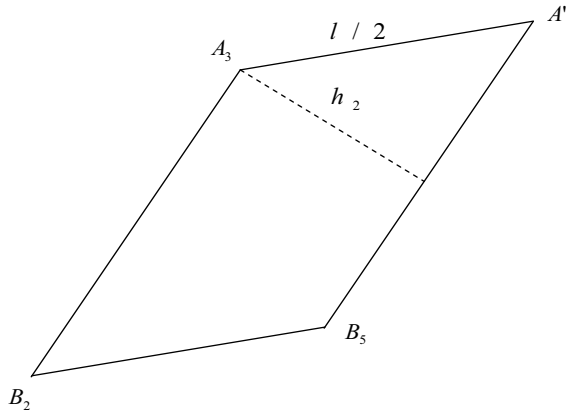

fig.4

give us that

$$\widehat{B_2A_3A'} = \pi - \widehat{A_1A_3A_2} = \pi - \alpha + \varphi, \qquad \widehat{A_3A'B_5} = \alpha - \varphi,$$

then

$$h_2 = \frac{l}{2}\sin(\alpha - \varphi).$$

Moreover by (7) we obtain that

$$|A_3B_2| = |AB| - m - |A_1A_3| = \frac{a}{2\cos\alpha} - m - \frac{l\sin\left(\varphi - \frac{\alpha}{2}\right)}{\sin\frac{\alpha}{2}},$$

and then we have that:

$$areaa_2(\varphi) = |A_3B_2| \cdot h_2 = \left(\frac{a}{2\cos\alpha} - m - \frac{l\sin\left(\varphi - \frac{\alpha}{2}\right)}{\sin\frac{\alpha}{2}}\right) \cdot \frac{l}{2}\sin(\alpha - \varphi).$$

Considering the relation (8) we obtain that:

$$areaa_2(\varphi) = \frac{al}{4\cos\alpha}\sin(\alpha - \varphi) - \frac{ml}{4}\left[\sin(\alpha - \varphi) + \sin\varphi\right]. \tag{10}$$

Now we consider the figure

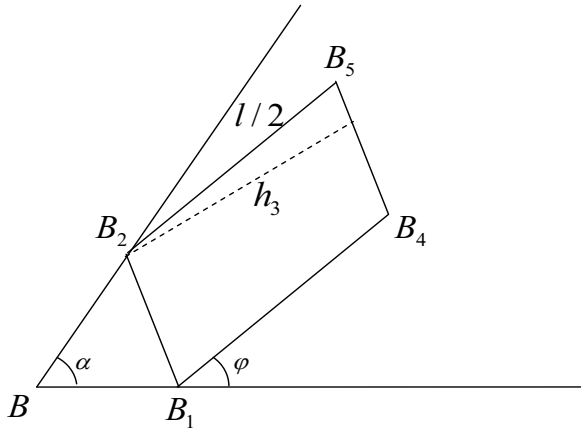

fig.5

we have that:

$$\widehat{B_2B_1B_4} = \pi - \left(\frac{\pi}{2} - \frac{\alpha}{2} + \varphi\right) = \frac{\pi}{2} - \varphi + \frac{\alpha}{2},$$

then

$$h_3 = \frac{l}{2}\sin\widehat{B_2B_1B_4} = \frac{l}{2}\cos\left(\varphi - \frac{\alpha}{2}\right).$$

Then

$$areaa_3(\varphi) = h_3\,|B_1B_2| = \frac{ml}{2}\sin\frac{\alpha}{2}\cos\left(\varphi - \frac{\alpha}{2}\right). \tag{11}$$

Consider now the figure

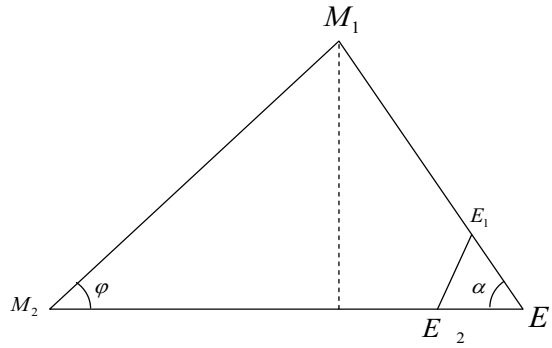

fig.6

By triangle EF_1F_2 follow that:

$$\frac{|EM_2|}{\sin(\varphi+\alpha)} = \frac{|EM_1|}{\sin\varphi} = \frac{l}{\sin\alpha},$$

then

$$|EM_1| = \frac{l \sin \varphi}{\sin \alpha}, \qquad |EM_2| = \frac{l \sin (\varphi + \alpha)}{\sin \alpha}. \tag{12}$$

and

$$h_5 = l \sin \varphi.$$

Consequently

$$areaa_5 (\varphi) = \frac{l^2 \sin \varphi \sin (\varphi + \alpha)}{2 \sin \alpha} - areaEE_1E_2,$$

i.e.

$$areaa_5 (\varphi) = \frac{l^2 \sin \varphi \sin (\varphi + \alpha)}{2 \sin \alpha} - \frac{m^2}{8} \sin \alpha. \tag{13}$$

In order to compute $areaa_4 (\varphi)$, we consider the figure

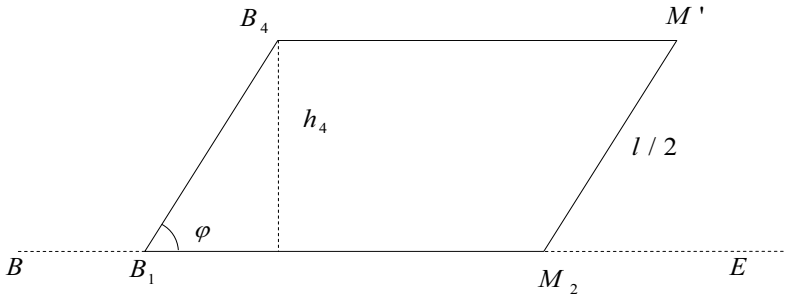

fig.7

and by (12) follow that:

$$h_4 = \frac{l}{2} \sin \varphi,$$

$$|B_1M_2| = 2a - \frac{m}{2} - |EM_2| = 2a - \frac{m}{2} - \frac{l \sin (\varphi + \alpha)}{\sin \alpha},$$

then

$$areaa_4 (\varphi) = \left[2a - \frac{m}{2} - \frac{l \sin (\varphi + \alpha)}{\sin \alpha} \right] \cdot \frac{l}{2} \sin \varphi. \tag{14}$$

From the figure

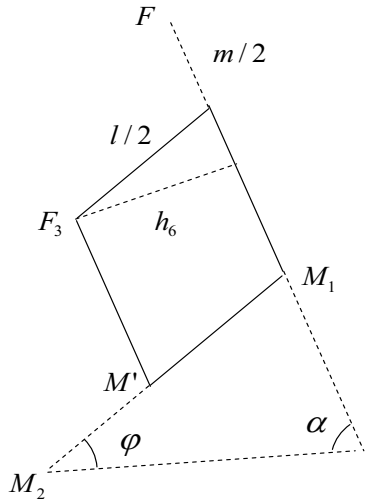

fig.8

and by (12) we obtain that:

$$\widehat{F_3F_2M_1} = \pi - (\varphi + \alpha)\,,$$

$$h_6 = \frac{l}{2}\sin(\varphi + \alpha)\,,$$

$$|F_2M_1| = |AB| - \frac{m}{2} - |EM_1| = \frac{a}{2\cos\alpha} - \frac{m}{2} - \frac{l\sin\varphi}{\sin\alpha},$$

then

$$areaa_6(\varphi) = \left(\frac{a}{2\cos\alpha} - \frac{m}{2} - \frac{2l\sin\varphi}{\sin\alpha}\right)\cdot\frac{l}{2}\sin(\varphi + \alpha)\,. \tag{15}$$

The figure

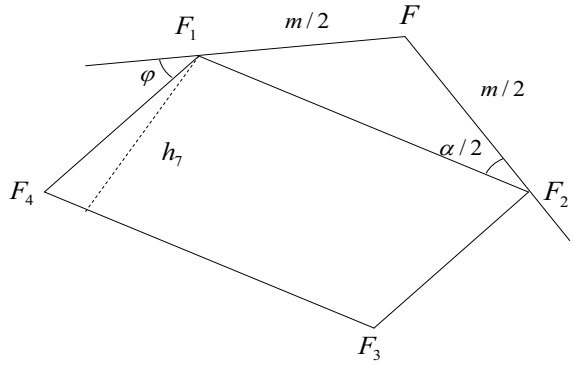

fig.9

give us that

$$\widehat{F_4F_1F_2} = \pi - \left(\varphi + \frac{\alpha}{2}\right), \quad \widehat{F_1F_4F_3} = \pi - \widehat{F_4F_1F_2} = \varphi + \frac{\alpha}{2},$$

$$h_7 = \frac{l}{2}\sin\left(\varphi + \frac{\alpha}{2}\right).$$

Then by (1) we have that

$$areaa_7(\varphi) = |F_1F_2| \cdot h_7 = \frac{m\cos\frac{\alpha}{2}}{2} \cdot l\sin\left(\varphi + \frac{\alpha}{2}\right). \tag{16}$$

Moreover, by figure

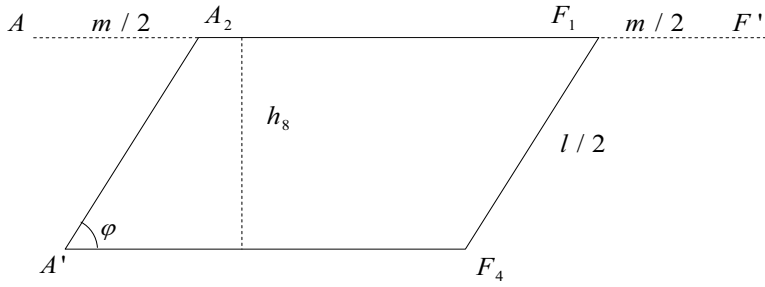

fig.10

follow that

$$|A_2F_1| = a - m, \qquad h_8 = \frac{l}{2}\sin\varphi,$$

then

$$areaa_8(\varphi) = \frac{a-m}{2} \cdot l\sin\varphi. \tag{17}$$

Considering in the relation (5) the relations (9), (10), (11), (13), (14), (15), (16) and (17) we obtain that:

$$area\widehat{C}_0^{(1)}(\varphi) = areaC_0^{(1)} - \left\{\frac{atg\alpha}{2}l\cos\varphi + \left(3a - \frac{m}{2} + \frac{m\cos\alpha}{2}\right) \cdot l\sin\varphi - \right.$$

$$\left. \frac{l^2}{4}\left[\sin 2\varphi + ctg\alpha \cdot (1 - \cos 2\varphi)\right] - \frac{m^2}{8}\sin\alpha\right\}. \tag{18}$$

Denoting with M_1 the set of segments s which have the middle point O in he fundamental cell $C_0^{(1)}$, with M_2 the set of segments s which have the middle point O in he fundamental cell $C_0^{(2)}$,with N_1 the set of segments s completely contanined in $C_0^{(1)}$ and with N_2 the set of segment s completely contained in $C_0^{(2)}$, we have [2] that:

$$P_{int} = 1 - \frac{\mu(N_1) + \mu(N_2)}{\mu(M_1) + \mu(M_2)}, \tag{19}$$

where μ is the Lebesgue measure in Euclidean plane.

In order to compute the measures $\mu(M_1), \mu(M_2), \mu(N_1)$ and $\mu(N_2)$ we use the kinematic Poincaré measure [1]:

$$dK = dx \wedge dy \wedge d\varphi,$$

where x, y are the coordinates of the point and φ is the defined angle.

Since $\varphi \in [0,\ \alpha]$, we have that:

$$\mu(M_1) = \int_0^{\alpha} d\varphi \iint\limits_{\left\{(x,y)\in \widehat{C}_0^{(1)}(\varphi)\right\}} dxdy = \int_0^{\alpha} \left(area\widehat{C}_0^{(1)}\right) d\varphi = \alpha area C_0^{(1)} \tag{20}$$

and considering the relation (18) we have that:

$$\mu(N_1) = \int_0^{\alpha} d\varphi \iint\limits_{\left\{(x,y)\in \widehat{C}_0^{(1)}\right\}} dxdy = \int_0^{\alpha} \left(area\widehat{C}_0^{(1)}(\varphi)\right) d\varphi = \alpha area C_0^{(1)} -$$

$$\left[\left(3 - 3\cos\alpha + \frac{\sin^2\alpha}{2\cos\alpha}\right) al - \frac{\alpha ctg\alpha - \cos 2\alpha}{4} l^2 - \frac{m^2}{8}\alpha \sin 2\alpha\right]. \tag{21}$$

Replacing α with β we obtain that:

$$\mu(M_2) = \beta area C_0^{(2)}, \tag{22}$$

$$\mu(N_2) = \beta area C_0^{(2)} -$$

$$\left[\left(3 - 3\cos\beta + \frac{\sin^2\beta}{2\cos\beta}\right) al - \frac{\beta ctg\alpha - \cos 2\beta}{4} l^2 - \frac{m^2}{8}\beta \sin 2\beta\right]. \tag{23}$$

The relations (19), (20), (21), (22) and (23) give us that:

$$P_{int} = \frac{1}{3a^2(\alpha tg\alpha\beta tg\beta) - 2m^2(\alpha\sin\alpha + \beta\sin\beta)} \cdot$$

$$\left\{\left[6 - 3(\cos\alpha + \cos\beta) + \frac{\sin^2\alpha}{2\cos\alpha} + \frac{\sin^2\beta}{2\cos\beta}\right] al -\right.$$

$$\left.\frac{\alpha ctg\alpha + \beta ctg\beta - \cos 2\alpha + \cos 2\beta}{4} l^2 - \frac{m^2}{8}\alpha(\alpha\sin\alpha + \beta\sin\beta)\right\}. \tag{24}$$

For $m \to D$, the probability (24) became:

$$P = \frac{4}{3a^2(\alpha tg\alpha\beta tg\beta)} \left\{\left[6 - 3(\cos\alpha + \cos\beta) + \frac{\sin^2\alpha}{2\cos\alpha} + \frac{\sin^2\beta}{2\cos\beta}\right] al - .\right.$$

$$\left.\frac{\alpha ctg\alpha + \beta ctg\beta - \cos 2\alpha + \cos 2\beta}{4} l^2\right\}.$$

References

[1] Poincaré H., Calcul des probabilités, ed. 2, Carré, Paris, 1912.

[2] Stoka M., Probabilités géométriques de type Buffon dans le plan euclidien, Atti Acc. Sci. Torino, T. 110, pp. 53-59, 1976-1976.

RENDICONTI DEL CIRCOLO MATEMATICO DI PALERMO
Serie II, Suppl. 83 (2011), pp. 95-109

ON JONES $S(E)$-TRIPLES AND $S(E)$-QUADRUPLES IN RINGS

ZVONKO ČERIN AND GIAN MARIO GIANELLA

Abstract. Let x be an element of a commutative ring Q with the identity e and let R be its subring contining e. In this paper we study basic properties of the triples (u, v, w) and the quadruples (u, v, w, z) of elements of the polynomial ring $R[x]$ with the property that x is a transcendental element over the ring R and $u\,v + e$, $v\,w + e$, $w\,z + e$, $u\,w + e$ and $v\,z + e$ are squares and u, v and w are linear polynomials. We find the whole family of such triples and quadruples parametrized by three arbitrary elements a, b and c in R. In the special case when the ring R is the integers $\mathbb{Z}$, the famous Jones quadruple $(x, x+2, 4x+4, 4(x+1)(2x+1)(2x+3))$ is included in this family. We study these triples and quadruples of linear polynomials in great detail. Many properties and identities for their components and various sums and products are established.

1. Introduction

Let R be a ring. For its subset P, an $n \in R$ and a natural number m, we say that $a \in R^m$ is a $P(n)$-m-*tuple* provided $a_i\,a_j + n$ is from P for each pair of different indices i and j. An interesting special case is when P is the subset $S = \{x^2 : x \in R\}$ of all squares of R.

In the special case when R is the ring of integers $\mathbb{Z}$, then the $S(1)$-m-tuples are called Diophantine m-tuples to honor the hellenic mathematician Diophantus of Alexandria who first found that $(\frac{1}{16}, \frac{33}{16}, \frac{17}{4}, \frac{105}{16})$ is the $S(1)$-quadruple of rationals ([2], [1]). It is interesting that this $S(1)$-quadruple is the value of the Jones Diophantine quadruple

$$(x, x+2, 4x+4, 4(x+1)(2x+1)(2x+3))$$

of polynomials for $x = \frac{1}{16}$ (see [8] and [9]).

In this paper we shall assume (as in [7, Chapter III, §4]) that

- Q is commutative ring with identity e,

1991 *Mathematics Subject Classification.* Primary 11B37, 11B39, 11D09.

Key words and phrases. Ring, polynomial ring, squares, $P(n)$-triple, Euler triple, basic symmetric functions, determinants, generalized determinants, vector cross-product.

- R is a subring of Q and $e \in R$,
- $x \in Q$ is a transcendental element over a ring R,

and search for the $S(e)$-quadruples (u, v, w, z) in the polynomial ring $R[x]$ such that u, v and w are linear. In fact, we shall construct two families of such quadruples that use elements a, b and c of the ring R as parameters.

2. Construction of the $S(e)$-quadruples in $R[x]$

In order to construct $S(e)$-quadruples in $R[x]$, we shall first describe two families of $S(e)$-triples in $R[x]$ and then apply the Arkin-Hoggatt-Strauss upgrading to get the quadruples. The idea comes from the observation that the equations (for complex numbers)

$$[(a+d)x+f][(a+d+a(2\,c+1))x+g]+1=(h\,x+k)^2,$$

$$[(a+d+a(2\,c+1))x+g](a\,x+b)+1=(u\,x+v)^2,$$

$$(a\,x+b)[(a+d)x+f]+1=(p\,x+q)^2,$$

have essentially two solutions in d, f and g. Hence, if $a, b, c \in R$ and $M = a\,x + b$, then

$$\lambda_\pm = \lambda_\pm(a,\, b,\, c,\, x) = \big(M,\, c^2\,M \pm 2\,c,\, (c+e)^2\,M \pm 2(c+e)\big)$$

are $S(e)$-triples in $R[x]$.

Indeed, if $\mathfrak{a} = \lambda_+$ and $\mathfrak{b} = \lambda_-$, then the components satisfy

$$\mathfrak{a}_2\mathfrak{a}_3 + e = (c_\square M + c_2)^2, \qquad \mathfrak{b}_2\mathfrak{b}_3 + e = (c_\square M - c_2)^2,$$

$$\mathfrak{a}_3\mathfrak{a}_1 + e = (c_1 M + e)^2, \qquad \mathfrak{b}_3\mathfrak{b}_1 + e = (c_1 M - e)^2,$$

$$\mathfrak{a}_1\mathfrak{a}_2 + e = (cM + e)^2, \qquad \mathfrak{b}_1\mathfrak{b}_2 + e = (cM - e)^2,$$

where $c_\square = c(c+e)$, $c_1 = c + e$ and $c_2 = 2\,c + e$.

The verification of the first relation is as follows: Since

$$\mathfrak{a}_2\mathfrak{a}_3 + e = (c^2M + 2c)[(c+e)^2M + 2(c+e)] + e =$$
$$c_\square(c_\square M^2 + 2c_2M + 4e) + e = c_\square^2M^2 + 2c_\square c_2M + 4c_\square + e,$$

$(c_\square M + c_2)^2 = c_\square^2M^2 + 2c_\square c_2M + c_2^2$ and $4c_\square + e = c_2^2$, it follows that the first equality holds. The remaining five are proved similarly.

Let $\widetilde{\lambda}_{\pm1} = c_\square\, M \pm c_2$, $\widetilde{\lambda}_{\pm2} = c_1 M \pm e$ and $\widetilde{\lambda}_{\pm3} = c\,M \pm e$. Hence,

$$\Lambda_+ = A = A(a,b,c,x) = (\lambda_{+\,1},\, \lambda_{+\,2},\, \lambda_{+\,3},\, 4\,\widetilde{\lambda}_{+1}\,\widetilde{\lambda}_{+2}\,\widetilde{\lambda}_{+3}),$$

$$\Lambda_- = B = B(a,b,c,x) = (\lambda_{-\,1},\, \lambda_{-\,2},\, \lambda_{-\,3},\, 4\,\widetilde{\lambda}_{-1}\,\widetilde{\lambda}_{-2}\,\widetilde{\lambda}_{-3})$$

are the Arkin-Hoggatt-Strauss upgrading of the Diophantine triples $\lambda_\pm$ to the Diophantine quadruples $\Lambda_\pm$.

The first property of the triples $\mathfrak{a}$ and $\mathfrak{b}$ is that they are the Euler $S(e)$-triples. In other words, there is a $z \in R$ such that the triples $\mathfrak{a}$ and $\mathfrak{b}$ have the form (u, v, w) with $uv + e = z^2$ and $w = u + v + 2z$ (see [5]).

Property 1. *For $a, b, c \in R$ and $x \in Q$, the following relations hold:*

$$\mathfrak{a}_1 + \mathfrak{a}_2 + 2\,\widetilde{\mathfrak{a}}_3 = \mathfrak{a}_3, \qquad \mathfrak{b}_1 + \mathfrak{b}_2 + 2\,\widetilde{\mathfrak{b}}_3 = \mathfrak{b}_3.$$

Proof. In order to prove the first equality, note that the difference

$$\mathfrak{a}_3 - (\mathfrak{a}_1 + \mathfrak{a}_2 + 2\,\widetilde{\mathfrak{a}}_3)$$

is $c_2Me - c_2M = 0$. The other equality is proved similarly. □

Similarly, the quadruples A and B are the Euler $S(e)$-quadruples. In other words, there is an $h \in R$ such that the quadruples A and B have the form (u, v, w, z) with $vw + e = (u + h)^2$, $wu + e = (v + h)^2$, $uv + e = h^2$, $w = u + v + 2h$ and $z = 4h(u + h)(v + h)$. In view of the Property 1, it suffices to establish the following property.

Let E denote either A or B. Besides the notation $c_\square = c(c + e)$, $c_1 = c + e$ and $c_2 = 2c + e$, we also need $c_u = uc + e$ and $c_{u,v} = uc + ve$. When $E = A$, we take the upper sign while lower sign is selected for $E = B$.

Property 2. *For $a, b, c \in R$ and $x \in Q$, the following relations hold:*

$$E_3E_4 + e = [2c_1M(c_\square M \pm c_3) + c_{4,3}]^2,$$
$$E_4E_1 + e = [2M(c_\square M \pm c_2) + e]^2,$$
$$E_2E_4 + e = [2cM(c_\square M \pm c_{3,2}) + c_4]^2.$$

Proof. In order to prove the second equality, note that the difference

$$[2M(c_\square M \pm c_2) + e]^2 - e$$

is the product $4M(c_\square M + c_2)[M(c_\square M + c_2) + e]$ that we recognize as E_4E_1. The other two equalities are proved similarly. □

Notice that when the ring R is the integers $\mathbb{Z}$ and $a = 1$, $b = 0$ and $c = 1$, then the quadruple A is the Jones quadruple.

The articles [3] and [4] describe a method of extending any Euler $S(e)$-quadruple (u, v, w, z) with $uv + e = h^2$, $vw + e = (u + h)^2$, $wu + e = (v + h)^2$, $w = u + v + 2h$ and $z = 4h(u + h)(v + h)$ to a family

$$(u, v, w, z)[m] = (u, um^2 + 2hm + v, um^2 + 2(u + h)m + w,$$
$$4[um^2 + (2h + u)m + v + h][um + u + h][um + h])$$

of Euler $S(e)$-quadruples, where $m \in R$.

The identities $E[m] = E(a, b, c + m, x)$ show that if we apply this method of extension to the $S(e)$-quadruples E we shall not get anything new.

The functions $\Lambda_\pm$ determine the functions $\widetilde{\Lambda}_\pm : R^3 \times Q \to Q^6$, where $\widetilde{A} = \widetilde{\Lambda}_+(a, b, c, x)$ and $\widetilde{B} = \widetilde{\Lambda}_-(a, b, c, x)$ have the components

$$\widetilde{E}_1 = cM \pm e, \qquad \widetilde{E}_2 = c_\square M \pm c_2, \qquad \widetilde{E}_3 = 2c_1 M(c_\square M \pm c_3) + c_{4,3},$$

$$\widetilde{E}_4 = 2M\widetilde{E}_2 + e, \qquad \widetilde{E}_5 = c_1 M \pm e, \qquad \widetilde{E}_6 = 2cM(c_\square M \pm c_{3,2}) + c_4,$$

given in the first two properties. In different words, the coordinates of the sextuple $\widetilde{E}$ satisfy the following six relations: $\widetilde{E}_1^2 = E_1\, E_2 + e$, $\widetilde{E}_2^2 = E_2\, E_3 + e$, $\widetilde{E}_3^2 = E_3\, E_4 + e$, $\widetilde{E}_4^2 = E_4\, E_1 + e$, $\widetilde{E}_5^2 = E_1\, E_3 + e$ and $\widetilde{E}_6^2 = E_2\, E_4 + e$.

For $a, b, c \in R$ and $x \in Q$, let $c^A = A(a, b, c, x)$, etc. This alternative notation for various quadruples is used in situations when only the variable c is important.

The next property shows that the functions A and $\widetilde{A}$ can be derived from the function B and $\widetilde{B}$ and vice versa. The interpretation of the first identity is: The second components of $B(a, b, -c, x)$ and $A(a, b, c, x)$ are equal.

Property 3. *For $a, b, c \in R$ and $x \in Q$, it holds:*

$$A_2 = (-c)_2^B, \;\; B_2 = (-c)_2^A, \;\; A_3 = (-c_{1,2})_3^B = B_3 + 4c_1, \;\; A_4 = (-c_1)_4^B,$$

$$\widetilde{A}_1 = \widetilde{B}_1 + 2e, \quad \widetilde{A}_2 = (-c_1)_2^{\widetilde{B}} = \widetilde{B}_2 + 2c_2, \quad \widetilde{A}_3 = \widetilde{B}_3 + 4c_3(\widetilde{B}_5 + e),$$

$$\widetilde{A}_4 = (-c_1)_4^{\widetilde{B}} = \widetilde{B}_4 + 4c_2 B_1, \;\; \widetilde{A}_5 = \widetilde{B}_5 + 2e, \;\; \widetilde{A}_6 = \widetilde{B}_6 + 4c_{3,2}(\widetilde{B}_1 + e),$$

$$B_3 = (-c_{1,2})_3^A, \quad B_4 = (-c_1)_4^A, \quad \widetilde{B}_2 = (-c_1)_2^{\widetilde{A}}, \quad \widetilde{B}_4 = (-c_1)_4^{\widetilde{A}}.$$

Proof. Since $B_2 = c^2 M - 2c$, it is clear that $B(a, b, -c, x)_2$ is $c^2 M + 2c$, i. e., the second component A_2 of the quadruple A. The same switch of signs clearly happens also in the second identity. For the third identity, note that $B_3 = c_1^2 M - 2c_1$ and that the equation $u + e = -c - e$ has the solution $u = -c - 2e = -c_{1,2}$. Fortunately, for this u in place of c in $-2c_1$ we get $2c_1$. It follows that $B(a, b, -c_{1,2}, x)_2 = A(a, b, c, x)_2$. The other identities have similar proofs. □

Let $d_1 = c_\square + e$ and $d_2 = 2\, c_\square + e$. The following relations for the basic symmetric functions of the triples $\mathfrak{a} = \lambda_+$ and $\mathfrak{b} = \lambda_-$ involve the numbers $d_1, d_2, c_1, c_2, \ldots$. Perhaps, the most interesting are the three cases when the right hand sides are squares.

Let σ_1, σ_2, σ_3, $\sigma_4 : R^4 \to R$ be the basic symmetric functions defined for $x = (a, b, c, d)$ from R^4 by $x_{\sigma_4} = abcd$, $x_{\sigma_3} = bcd + acd + abd + abc$, $x_{\sigma_2} = ab + bc + cd + da + ac + bd$ and $x_{\sigma_1} = a + b + c + d$. Let us also

define functions $\sigma_3^*, \sigma_2^*, \sigma_1^* : R^4 \to R$ by $x_{\sigma_3^*} = bcd - acd + abd - abc$, $x_{\sigma_2^*} = ab - bc + cd - da + ac - bd$ and $x_{\sigma_1^*} = a - b + c - d$. Note that $x_{\sigma_1^*}$ is the determinant of the 1×4 matrix $[a, b, c, d]$ (see [10]).

We use the same notation for the basic symmetric functions in three variables σ_1, σ_2, $\sigma_3 : R^3 \to R$ defined for $x = (a, b, c)$ by $x_{\sigma_1} = a + b + c$, $x_{\sigma_2} = bc + ca + ab$, and $x_{\sigma_3} = a\,b\,c$. Let the functions σ_1^*, $\sigma_2^* : R^3 \to R$ be defined by $x_{\sigma_1^*} = a - b + c$ and $x_{\sigma_2^*} = b\,c - c\,a + a\,b$. Note that $x_{\sigma_1^*}$ is the determinant of the 1×3 matrix $[a, b, c]$ (see [10]).

Of course, the values of these functions depend on the kind of objects we operate on. For the triples they have one meaning and on the quadruples they have another similar effect.

Property 4. *For $a, b, c \in R$ and $x \in Q$,*

$$\mathfrak{a}_{\sigma_1^*} - \mathfrak{b}_{\sigma_1^*} = 4e, \qquad \mathfrak{a}_{\sigma_1} - \mathfrak{b}_{\sigma_1} = 4c_2, \qquad \mathfrak{a}_{\sigma_1} + \mathfrak{b}_{\sigma_1} = 4d_1M,$$

$$\mathfrak{a}_{\sigma_1^*} + \mathfrak{b}_{\sigma_1^*} = 4c_1M, \quad \mathfrak{a}_{\sigma_2} - \mathfrak{b}_{\sigma_2} = 4c_2d_1M, \quad \mathfrak{a}_{\sigma_2} + \mathfrak{b}_{\sigma_2} = 2d_1^2M^2 + 8c_\square,$$

$$\mathfrak{a}_{\sigma_3} - \mathfrak{b}_{\sigma_3} = 4c_\square c_2M^2, \qquad \mathfrak{a}_{\sigma_3} + \mathfrak{b}_{\sigma_3} = 2c_\square M(c_\square M^2 + 4e),$$

$$\mathfrak{a}_{\sigma_1}\,\mathfrak{b}_{\sigma_1} + 4c_2^2 = 4d_1^2M^2, \quad \mathfrak{a}_{\sigma_2}\,\mathfrak{b}_{\sigma_2} - 16\,c_1^2 = d_1^2M^2(d_1^2M^2 - 4\,d_2),$$

$$\mathfrak{a}_{\sigma_3}\,\mathfrak{b}_{\sigma_3} - 16\,c_\square^2\,M^2 = c_\square^2M^4(c_\square^2\,M^2 - 4\,d_2), \quad \mathfrak{a}_{\sigma_1^*}\,\mathfrak{b}_{\sigma_1^*} + 4e = 4c_1^2M^2.$$

Proof. Since $\mathfrak{a}_{\sigma_1} = 2(d_1M + c_2)$ and $\mathfrak{b}_{\sigma_1} = 2(d_1M - c_2)$, it follows that the second, the third and the ninth formulae hold. Similarly, the identities $\mathfrak{a}_{\sigma_1^*} = 2(c_1M + e)$ and $\mathfrak{b}_{\sigma_1^*} = 2(c_1M - e)$ imply that the first, the fourth and the last formulae are true. The higher symmetric functions are treated similarly with somewhat more complicated expressions. □

We shall now consider sums of powers of $\mathfrak{a}_{\sigma_1}$, $\mathfrak{b}_{\sigma_1}$, $\mathfrak{a}_{\sigma_1^*}$, $\mathfrak{b}_{\sigma_1^*}$, $\widetilde{\mathfrak{a}}_{\sigma_1}$, $\widetilde{\mathfrak{b}}_{\sigma_1}$, $\widetilde{\mathfrak{a}}_{\sigma_1^*}$ and $\widetilde{\mathfrak{b}}_{\sigma_1^*}$. Let $U = d_1\,M$, $V = U^2$, $u = c_2^2$ and $v = u^2$.

Property 5. *For $a, b, c \in R$ and $x \in Q$,*

$$(\mathfrak{a}_{\sigma_1})^2 + (\mathfrak{b}_{\sigma_1})^2 = 8(V + u), \quad (\mathfrak{a}_{\sigma_1})^3 + (\mathfrak{b}_{\sigma_1})^3 = 16\,U(V + 12d_1 - 9e),$$

$$(\mathfrak{a}_{\sigma_1})^4 + (\mathfrak{b}_{\sigma_1})^4 = 32V[V + 24d_1 - 18e] + 32v,$$

$$(\mathfrak{a}_{\sigma_1})^5 + (\mathfrak{b}_{\sigma_1})^5 = 64\,U[V^2 + 10\,V\,u + 5\,v].$$

Proof. Since $\mathfrak{a}_{\sigma_1} = 2(d_1M + c_2)$ and $\mathfrak{b}_{\sigma_1} = 2(d_1M - c_2)$, it follows that $(\mathfrak{a}_{\sigma_1})^2 + (\mathfrak{b}_{\sigma_1})^2 = 8(d_1^2M^2 + c_2^2) = 8(V + u)$. The higher powers give more complicated expressions that with our notation lead to the above identities. □

We can similarly get the formulas for $(\mathfrak{a}_{\sigma_1^*})^k + (\mathfrak{b}_{\sigma_1^*})^k$, $(\widetilde{\mathfrak{a}}_{\sigma_1})^k + (\widetilde{\mathfrak{b}}_{\sigma_1})^k$ and $(\widetilde{\mathfrak{a}}_{\sigma_1^*})^k + (\widetilde{\mathfrak{b}}_{\sigma_1^*})^k$ $(k = 2, 3, 4, 5)$.

In the next three results we consider products of components of A, B and $\widetilde{A}$, $\widetilde{B}$. They are differences of squares.

Property 6. *For $a, b, c \in R$ and $x \in Q$,*

$$A_2\, B_2 + 4\, c^2 = c^4\, M^2, \qquad A_3\, B_3 + 4c_1^2 = c_1^4\, M^2,$$

$$A_4\, B_4 + 16\, c_2^2 = 16\, M^2\, (c_\square^2\, M^2 - 3\, c_\square - e)^2.$$

Proof. Since $A_2 = c^2 M + 2c$ and $B_2 = c^2 M - 2c$, it follows that $A_2 B_2 = c^4 M^2 - 4c^2$, i. e., the first equality holds. The third and the fourth components are treated similarly. □

Property 7. *For $a, b, c \in R$ and $x \in Q$,*

$$\widetilde{A}_1\, \widetilde{B}_1 + e = c^2\, M^2, \qquad \widetilde{A}_3\, \widetilde{B}_3 + 4c_1^2 c_3^2 M^2 = (2c_1 c_\square M^2 + c_{4,3})^2,$$

$$\widetilde{A}_2\, \widetilde{B}_2 + c_2^2 = c_\square^2\, M^2, \qquad \widetilde{A}_4\, \widetilde{B}_4 + 4c_2^2 M^2 = (2c_\square M^2 + e)^2,$$

$$\widetilde{A}_5\, \widetilde{B}_5 + e = c_1^2 M^2, \qquad \widetilde{A}_6\, \widetilde{B}_6 + 4c^2 c_{3,2}^2 M^2 = (2cc_\square M^2 + c_4)^2.$$

Proof. Since $\widetilde{A}_1 = cM + e$ and $\widetilde{B}_1 = cM - e$, it follows that $\widetilde{A}_1 \widetilde{B}_1 = c^2 M^2 - e$, i. e., the first equality holds.

Also, since $\widetilde{A}_4 = 2c_\square M^2 + 2c_2 M + e$ and $\widetilde{B}_4 = 2c_\square M^2 - 2c_2 M + e$, we get $\widetilde{A}_4 \widetilde{B}_4 = (2c_\square M^2 + e)^2 - 4c_2^2 M^2$, i. e., the fourth equality is true. The other components are treated similarly. □

3. Squares from components

The next item is related to the basic property $E_2 E_3 + e = \widetilde{E}_1^2$ and shows that from the second and the third components of $E(a, b, u, x)$ and E it is possible to get complete squares in many ways.

Property 8. *For $a, b, c, u \in R$ and $x \in Q$,*

$$E(a, b, c + u + e, x)_2\, E_3 + u^2 = (E_3 + u\, \widetilde{E}_5)^2,$$

$$E_2\, E(a, b, c + u - e, x)_3 + u^2 = (E_2 + u\, \widetilde{E}_1)^2.$$

Proof. Let $E = A$. The sum $A(a, b, c + u + e, x)_2\, A_3 + u^2$ is the square of $c_1(c_1 + u)M + 2c_1 + u$ that is clearly $A_3 + u\, \widetilde{A}_5$. The remaining three formulae have similar proofs. □

It is possible to get complete squares also from products of the second and the third with the fourth component of both A and B.

Property 9. *For $a, b, c, u \in R$ and $x \in Q$,*

$$E(a, b, c + u, x)_2\, E_4 + 4u(u - e)\widetilde{E}_1 \widetilde{E}_5 + e = [\widetilde{E}_3 + 2(u - e)\widetilde{E}_1 \widetilde{E}_5]^2,$$

$$E(a, b, c + u, x)_3\, E_4 + 4u(u + e)\widetilde{E}_1 \widetilde{E}_5 + e = (\widetilde{E}_3 + 2u\widetilde{E}_1 \widetilde{E}_5)^2.$$

Proof. Let $E = A$. Then $A(a,b,c+u+e,x)_3\, A_4 + 4u(u+e)\widetilde{A}_1\widetilde{A}_5 + e$ is the square of $2c_\square(c_1+u)M^2 + 2(3c_\square + c_1 + uc_2)M + 2u + c_{4,3}$ that is clearly $\widetilde{A}_3 + 2u\widetilde{A}_1\widetilde{A}_5$. The remaining three formulae have similar proofs. □

4. Volumes and areas of tetrahedra

Let $\mathfrak{a}' = \lambda_+(a',\, b',\, c',\, x')$, $\mathfrak{b}' = \lambda_-(a',\, b',\, c',\, x')$ and $M' = a'\,x' + b'$.

For triples $u, v, w, z \in R^3$, let $|u,v,w,z|$ and $||u,v,w,z||$ denote the (oriented) volume and the sum of the squares of areas of sides of the tetrahedron with vertices u, v, w and z. In other words, $|u,v,w,z|$ is the value of the 4×4-matrix with rows (u_1,u_2,u_3,e), (v_1,v_2,v_3,e), (w_1,w_2,w_3,e) and (z_1,z_2,z_3,e). Also, the square of the area $||u,v,w||$ of a triangle with vertices u, v and w is the sum

$$\begin{vmatrix} u_2 & u_3 & e \\ v_2 & v_3 & e \\ w_2 & w_3 & e \end{vmatrix}^2 + \begin{vmatrix} u_3 & u_1 & e \\ v_3 & v_1 & e \\ w_3 & w_1 & e \end{vmatrix}^2 + \begin{vmatrix} u_1 & u_2 & e \\ v_1 & v_2 & e \\ w_1 & w_2 & e \end{vmatrix}^2 .$$

Note that in the 3-dimensional Euclidean space the above volume is divided by 6 and the square of the area of a triangle by 4. Since in rings division need not be possible, we have dropped these rational factors.

Property 10. *For $a, a', b, b', c, c' \in R$ and $x, x' \in Q$,*

$$|\mathfrak{a},\mathfrak{b},\mathfrak{a}',\mathfrak{b}'| = -2|\widetilde{\mathfrak{a}},\widetilde{\mathfrak{b}},\widetilde{\mathfrak{a}}',\widetilde{\mathfrak{b}}'| = 16(M'-M)(c-c'),$$

$$||\mathfrak{a},\mathfrak{b},\mathfrak{a}',\mathfrak{b}'|| - 2||\widetilde{\mathfrak{a}},\widetilde{\mathfrak{b}},\widetilde{\mathfrak{a}}',\widetilde{\mathfrak{b}}'|| = 32(M'-M)^2(c-c')^2.$$

Proof. Let $c'_\square = c'(c'+e)$, $c'_1 = c'+e$, etc. Let m_1 and m_2 denote the matrices

$$\begin{pmatrix} M & c^2M + 2c & c_1^2M + 2c_1 & e \\ M & c^2M - 2c & c_1^2M - 2c_1 & e \\ M' & (c')^2M' + 2c' & (c'_1)^2M' + 2c'_1 & e \\ M' & (c')^2M' - 2c' & (c'_1)^2M' - 2c'_1 & e \end{pmatrix}$$

and

$$\begin{pmatrix} c_\square M + c_2 & c_1M + e & cM + e & e \\ c_\square M - c_2 & c_1M - e & cM - e & e \\ c'_\square M' + c'_2 & c'_1M' + e & c'M' + e & e \\ c'_\square M' - c'_2 & c'_1M' - e & c'M' - e & e \end{pmatrix}.$$

Then $|\mathfrak{a},\mathfrak{b},\mathfrak{a}',\mathfrak{b}'| = \det m_1$ and $|\widetilde{\mathfrak{a}},\widetilde{\mathfrak{b}},\widetilde{\mathfrak{a}}',\widetilde{\mathfrak{b}}'| = \det m_2$. The routine calculation of determinants reveals that the first formula holds. Even more tedious is the check of the second relation. However, with the help from computers, this task is also easily accomplished. □

For $a, b, c \in R$, $x \in Q$ and a natural number $k \in \mathbb{N}$, let

$$\mathfrak{u}_\pm = \lambda_\pm(a, 2k^2b^2, 2\,c_\square, x) \qquad \text{and} \qquad \mathfrak{u}'_\pm = \lambda_\pm(a, 2k^2b^2, 2\,c_\square, -x).$$

The next result is an interesting case when the volume of a tetrahedron from the products of $\mathfrak{u}_\pm$ and $\mathfrak{u}'_\pm$ is a complete square.

Let $\ltimes$ and $\rtimes$ denote binary operations on R^3 defined by

$$(a, b, c) \ltimes (u, v, w) = (b\,w - c\,v, c\,u - a\,w, a\,v - b\,u),$$

$$(a, b, c) \rtimes (u, v, w) = (b\,w + c\,v, c\,u + a\,w, a\,v + b\,u).$$

Note that restricted on the space $\mathbb{R}^3$ the product $\ltimes$ is the familiar vector cross-product.

Property 11. *For $a, b, c \in R$, $x \in Q$ and $k \in \mathbb{N}$,*

$$|\mathfrak{u}_+ \ltimes \mathfrak{u}_-, \mathfrak{u}_+ \rtimes \mathfrak{u}_-, \mathfrak{u}'_+ \ltimes \mathfrak{u}'_-, \mathfrak{u}'_+ \rtimes \mathfrak{u}'_-| = (64\,k\,a\,b\,c_\square\,c_2\,d_2\,x)^2.$$

Proof. Let $\omega_\pm = 2k^2b^2 \pm ax$. Then $\mathfrak{u}_+ \ltimes \mathfrak{u}_- = 4\omega_+(2c_\square d_2, d_2, -2c_\square)$, $\mathfrak{u}_+ \rtimes \mathfrak{u}_- = 2(4c_\square d_2(c_\square d_2\omega_+^2 - 2e), d_2^2\omega_+^2, 4c_\square^2\omega_+^2)$, $\mathfrak{u}'_+ \ltimes \mathfrak{u}'_- = 4\omega_-(2c_\square d_2, d_2, -2c_\square)$ and $\mathfrak{u}'_+ \rtimes \mathfrak{u}'_- = 2(4c_\square d_2(c_\square d_2\omega_-^2 - 2e), d_2^2\omega_-^2, 4c_\square^2\omega_-^2)$. It follows that the tetrahedron with vertices $\mathfrak{u}_+ \ltimes \mathfrak{u}_-$, $\mathfrak{u}_+ \rtimes \mathfrak{u}_-$, $\mathfrak{u}'_+ \ltimes \mathfrak{u}'_-$ and $\mathfrak{u}'_+ \rtimes \mathfrak{u}'_-$ is the square of $64\,k\,a\,b\,c_\square\,c_2\,d_2\,x$. □

5. Equal products of differences and sums

For $a, b, c, z, w \in R$ and $x, y \in Q$, let $\mathfrak{d}_\pm = \lambda_\pm(a, b, c, x - y)$, $\mathfrak{s}_\pm = \lambda_\pm(a, b, c, x + y)$, $\mathfrak{d}^*_\pm = \lambda_\pm(a, b - z, c, x)$, $\mathfrak{s}^*_\pm = \lambda_\pm(a, b + z, c, x)$, $\mathfrak{d}^\bullet_\pm = \lambda_\pm(a - w, b, c, x)$, $\mathfrak{s}^\bullet_\pm = \lambda_\pm(a + w, b, c, x)$. The following surprising chains of equalities define triples $\mathfrak{u}$ and $\widetilde{\mathfrak{u}}$.

Property 12. *For $a, b, c, z, w \in R$ and $x, y \in Q$, the following holds:*

$$\mathfrak{u} = \mathfrak{d}_+ \ltimes \mathfrak{s}_- = \mathfrak{s}_+ \ltimes \mathfrak{d}_- = \mathfrak{d}^*_+ \ltimes \mathfrak{s}^*_- = \mathfrak{s}^*_+ \ltimes \mathfrak{d}^*_- = \mathfrak{d}^\bullet_+ \ltimes \mathfrak{s}^\bullet_- = \mathfrak{s}^\bullet_+ \ltimes \mathfrak{d}^\bullet_-,$$

$$\widetilde{\mathfrak{u}} = \widetilde{\mathfrak{d}}_+ \ltimes \widetilde{\mathfrak{s}}_- = \widetilde{\mathfrak{s}}_+ \ltimes \widetilde{\mathfrak{d}}_- = \widetilde{\mathfrak{d}}^*_+ \ltimes \widetilde{\mathfrak{s}}^*_- = \widetilde{\mathfrak{s}}^*_+ \ltimes \widetilde{\mathfrak{d}}^*_- = \widetilde{\mathfrak{d}}^\bullet_+ \ltimes \widetilde{\mathfrak{s}}^\bullet_- = \widetilde{\mathfrak{s}}^\bullet_+ \ltimes \widetilde{\mathfrak{d}}^\bullet_-.$$

Proof. Let $d = x - y$ and $s = x + y$. Since $\mathfrak{d}_+$ has the components $ad + b$, $c(acd + bc + 2e)$ and $c_1(ac_1d + bc + b + 2e)$ and the triple $\mathfrak{s}_-$ has the components $as + b$, $c(acs + bc - 2e)$ and $c_1(ac_1s + bc + b - 2e)$, the product $\mathfrak{d}_+ \ltimes \mathfrak{s}_-$ is $\mathfrak{u} = 4M(c_\square, c_1, -c)$.

Similarly, since $\widetilde{\mathfrak{d}}_+$ has the components $ac_\square d + c(bc + b + 2e) + e$, $ac_1d + bc + b + e$ and $acd + bc + e$ and the triple $\widetilde{\mathfrak{s}}_-$ has the components $ac_\square s + c(bc + b - 2e) - e$, $ac_1s + bc + b - e$ and $acs + bc - e$, the product $\widetilde{\mathfrak{d}}_+ \ltimes \widetilde{\mathfrak{s}}_-$ is $\widetilde{\mathfrak{u}} = -2M(1, c^2, -c_1^2)$.

All other products in the first of the above two chains reduce to $\mathfrak{u}$ while those from the second chain reduce to $\widetilde{\mathfrak{u}}$. □

The following result gives values of basic symmetric functions for triples $\mathfrak{u}$ and $\widetilde{\mathfrak{u}}$.

Property 13. *For $a, b, c \in R$ and $x \in Q$, the following holds:*

$$\mathfrak{u}_{\sigma_1^*} = 4(c_\square - c_2)M, \qquad \widetilde{\mathfrak{u}}_{\sigma_1^*} = 4\,c_\square\,M, \qquad \mathfrak{u}_{\sigma_1} = 4\,d_1\,M, \qquad \mathfrak{u}_{\sigma_2} = 0,$$
$$\widetilde{\mathfrak{u}}_{\sigma_1} = 4\,c\,M, \qquad \mathfrak{u}_{\sigma_2^*} = 32\,c\,c_\square\,M^2, \qquad \widetilde{\mathfrak{u}}_{\sigma_2^*} = 4\,[c_\square^2 - 2c_\square - e]\,M^2,$$
$$\widetilde{\mathfrak{u}}_{\sigma_2} = -4[c_\square^2 + 2c_\square + c_2^2]M^2, \qquad \mathfrak{u}_{\sigma_3} = -64\,c_\square^2\,M^3, \qquad \widetilde{\mathfrak{u}}_{\sigma_3} = 8\,c_\square^2\,M^3.$$

Proof. We shall only prove that $\mathfrak{u}_{\sigma_2} = 0$. Since $\mathfrak{u} = 4M(c_\square, c_1, -c)$, we have $\mathfrak{u}_{\sigma_2} = 16M^2(c_\square c_1 - c_\square c - c_1 c) = 16M^2[(c^2 + c)(c + e) - (c^2 + c)c - (c + e)c] = 0$. □

6. Sums and differences in the third variable

We now turn to the third variable c and explore the effect of adding and subtracting another element d from it.

For $a, b, c, d \in R$ and $x \in Q$, let $\mathfrak{d}_\pm = \lambda_\pm(a, b, c - d, x)$, $\mathfrak{s}_\pm = \lambda_\pm(a, b, c + d, x)$, $\widetilde{\mathfrak{d}}_\pm = \widetilde{\lambda}_\pm(a, b, c - d, x)$, $\widetilde{\mathfrak{s}}_\pm = \widetilde{\lambda}_\pm(a, b, c + d, x)$, $\mathfrak{u} = \mathfrak{d}_+ \ltimes \mathfrak{s}_-$, $\mathfrak{v} = \mathfrak{s}_+ \ltimes \mathfrak{d}_-$, $\mathfrak{p} = \mathfrak{d}_+ \rtimes \mathfrak{s}_-$, $\mathfrak{q} = \mathfrak{s}_+ \rtimes \mathfrak{d}_-$, $\widetilde{\mathfrak{u}} = \widetilde{\mathfrak{d}}_+ \ltimes \widetilde{\mathfrak{s}}_-$, $\widetilde{\mathfrak{v}} = \widetilde{\mathfrak{s}}_+ \ltimes \widetilde{\mathfrak{d}}_-$, $\widetilde{\mathfrak{p}} = \widetilde{\mathfrak{d}}_+ \rtimes \widetilde{\mathfrak{s}}_-$ and $\widetilde{\mathfrak{q}} = \widetilde{\mathfrak{s}}_+ \rtimes \widetilde{\mathfrak{d}}_-$.

For $a = (a_1, a_2, a_3)$ and $b = (b_1, b_2, b_3)$ in R^3, let

$$a \cdot b = \begin{vmatrix} a_2 & a_3 \\ b_2 & b_3 \end{vmatrix} + \begin{vmatrix} a_3 & a_1 \\ b_3 & b_1 \end{vmatrix} + \begin{vmatrix} a_1 & a_2 \\ b_1 & b_2 \end{vmatrix},$$
$$a : b = \begin{vmatrix} a_2 & a_3 \\ b_2 & b_3 \end{vmatrix} - \begin{vmatrix} a_3 & a_1 \\ b_3 & b_1 \end{vmatrix} + \begin{vmatrix} a_1 & a_2 \\ b_1 & b_2 \end{vmatrix}.$$

Note that $a \cdot b$ is the determinant of the rectangular 2×3 matrix with rows a and b (see [10]).

Property 14. *For $a, b, c, d \in R$ and $x \in Q$, if $\overline{M} = dM$, then*

$$\mathfrak{u} \cdot \mathfrak{v} = 64\,c_2\,\overline{M}\left(e - \overline{M}^2\right), \qquad \widetilde{\mathfrak{u}} \cdot \widetilde{\mathfrak{v}} = 16\,c_{2,3}\,\overline{M}\left(\overline{M}^2 - e\right),$$
$$\mathfrak{p} \cdot \mathfrak{q} = 32\,c_2\,dM^3\left(c_\square - d^2\right), \qquad \widetilde{\mathfrak{p}} \cdot \widetilde{\mathfrak{q}} = 16\,c\,\overline{M}\left(c_1\,c_{2,-1}M^2 - 2e\right),$$
$$\mathfrak{u} : \mathfrak{v} = 64\,\overline{M}\left(e - \overline{M}^2\right), \qquad \widetilde{\mathfrak{u}} : \widetilde{\mathfrak{v}} = 16\,c_2\,\overline{M}\left(\overline{M}^2 - e\right),$$
$$\mathfrak{p} : \mathfrak{q} = 32\,\overline{M}\left((3c_\square^2 + c - d_2 d^2 - d^4)M^2 - 4(c_\square - d^2)\right),$$
$$\widetilde{\mathfrak{p}} : \widetilde{\mathfrak{q}} = 16\,c_2\,\overline{M}\left(c_\square\,M^2 - 2e\right).$$

Proof. Since $\mathfrak{u} = \mathfrak{d}_+ \ltimes \mathfrak{s}_- = 4(e - \overline{M})((c_\square - d^2)M + 2d, c_1 M, -cM)$ and $\mathfrak{v} = \mathfrak{s}_+ \ltimes \mathfrak{d}_- = 4(e + \overline{M})((c_\square - d^2)M - 2d, c_1 M, -cM)$, it follows that $\mathfrak{u} \cdot \mathfrak{v} = 64\,c_2\,\overline{M}\left(e - \overline{M}^2\right)$. The other identities in this property are proved similarly. □

Property 15. *For $a, b, c, d \in R$ and $x \in Q$,*

$$\widetilde{\mathfrak{p}}_{\sigma_1^*} = \widetilde{\mathfrak{q}}_{\sigma_1^*} = 2\left(2c_\square\, M^2 - e\right),$$
$$\widetilde{\mathfrak{p}}_{\sigma_1} + 2\,c_{4,3} = 4c_1 M\left[(c_\square - d^2)M + 2\,d\right],$$
$$\widetilde{\mathfrak{q}}_{\sigma_1} + 2\,c_{4,3} = 4c_1 M\left[(c_\square - d^2)M - 2\,d\right].$$

Proof. Let $\delta = c - d$ and $\zeta = c + d$. Since $\widetilde{\mathfrak{d}}_+ = (\delta(\delta+e)M + 2\delta + e, (\delta+e)M + e, \delta M + e)$ and $\widetilde{\mathfrak{s}}_- = (\zeta(\zeta+e)M - 2\zeta - e, (\zeta+e)M - e, \zeta M - e)$, the product $\widetilde{\mathfrak{p}} = \widetilde{\mathfrak{d}}_+ \rtimes \widetilde{\mathfrak{s}}_-$ is the triple with the components $2(c_\square - d^2)M^2 + 4\overline{M} - 2e$, $2\delta\zeta c_1 M^2 + 4c_1\overline{M} - 2c_2$ and $2c(\delta+e)(\zeta+e)$ $M^2 + 4c\overline{M} - 2c_2$. It follows that $\widetilde{\mathfrak{p}}_{\sigma_1^*}$ is equal $2\,(2c_\square\, M^2 - e)$. The other claims in this property are proved similarly. □

In the next property we collect formulas for some symmetric sums of the products $\mathfrak{g} = \mathfrak{a} \rtimes \mathfrak{b}$ and $\widetilde{\mathfrak{g}} = \widetilde{\mathfrak{a}} \rtimes \widetilde{\mathfrak{b}}$. In the Property 13, we found those sums for the products $\mathfrak{u} = \mathfrak{a} \ltimes \mathfrak{b}$ and $\widetilde{\mathfrak{u}} = \widetilde{\mathfrak{a}} \ltimes \widetilde{\mathfrak{b}}$.

Property 16. *For $a, b, c, x \in R$,*

$$\mathfrak{g}_{\sigma_1^*} + 8\,c_\square = 2(c_\square^2 - c_2)M^2, \qquad \widetilde{\mathfrak{g}}_{\sigma_1^*} + 2e = 4\,c_\square\, M^2,$$
$$\mathfrak{g}_{\sigma_1} + 8\,c_\square = 2\,d_1^2\, M^2, \qquad \widetilde{\mathfrak{g}}_{\sigma_1} + 2\,c_{4,3} = 4\,c_\square c_1\, M^2,$$
$$\mathfrak{g}_{\sigma_2} = 8\,c_\square\, M^2\left(c_\square d_1 M^2 - 2d_2\right), \quad \mathfrak{g}_{\sigma_3} = 8\,c_\square^3\, M^4(c_\square\, M^2 - 4e).$$

Proof. The product $\mathfrak{g}$ has the components $2c_\square(c_\square M^2 - 4e)$, $2c_1^2 M^2$ and $2c^2 M^2$. It follows that $\mathfrak{g}_{\sigma_1} + 8\,c_\square = 2M^2(c_\square^2 + c_1^2 + c^2) = 2d_1^2 M^2$. Also, the product $\widetilde{\mathfrak{g}}$ has the components $2(c_\square M^2 - e)$, $2(cc_\square M^2 - c_2)$ and $2(c_1 c_\square M^2 - c_2)$. It follows that $\widetilde{\mathfrak{g}}_{\sigma_1} + 2\,c_{4,3} = 4\,c_\square c_1\, M^2$. The other identities in this property are proved similarly. □

7. Values in sums and products

In this section we shall show that the last variable x has the property that the value of the sums σ_1 and σ_1^* for the functions $\mathfrak{a}$, $\mathfrak{b}$, $\widetilde{\mathfrak{a}}$ and $\widetilde{\mathfrak{b}}$ in the quadruples $(a, b, c, x + \bar{x})$ and $(a, b, c, x\,\bar{x})$ can be recovered from their values at (a, b, c, x) and $(a, b, c, \bar{x})$.

Let $d_x = x - \bar{x}$, $p_x = x\,\bar{x}$ and $s_x = x + \bar{x}$. Let $\mathfrak{f}$ be either $\mathfrak{a}$ or $\mathfrak{b}$. If $\mathfrak{f} = \mathfrak{a}$, then $\mathfrak{f}' = \mathfrak{b}$ and if $\mathfrak{f} = \mathfrak{b}$, then $\mathfrak{f}' = \mathfrak{a}$.

Property 17. *For $a, b, c \in R$ and $x, \bar{x} \in Q$, for $\mathfrak{h}$ either $\mathfrak{f}$ or $\widetilde{\mathfrak{f}}$ and for σ either σ_1 or σ_1^*,*

$$a\,d_x\,(s_x^{\mathfrak{h}})_\sigma = [a(s_x + \bar{x}) + 2\,b]\,x_\sigma^{\mathfrak{h}'} - [a(s_x + x) + 2\,b]\,\bar{x}_\sigma^{\mathfrak{h}'},$$
$$a\,d_x\,(p_x^{\mathfrak{h}})_\sigma = [a(p_x + \bar{x}) + 2\,b]\,x_\sigma^{\mathfrak{h}'} - [a(p_x + x) + 2\,b]\,\bar{x}_\sigma^{\mathfrak{h}'}.$$

Proof. Let $\mathfrak{h} = \mathfrak{a}$ and $\sigma = \sigma_1$. Since $(s_x^{\mathfrak{a}})_{\sigma_1} = 2[d_1\,(s_M - b) + c_2]$, $x_{\sigma_1}^{\mathfrak{b}} = 2[d_1\,M - c_2]$ and $\bar{x}_{\sigma_1}^{\mathfrak{b}} = 2[d_1\,\bar{M} - c_2]$, where $\bar{M}$ denotes $a\,\bar{x} + b$, we get easily the first formula in this case.

Similarly, let $\mathfrak{h} = \mathfrak{b}$, $\sigma = \sigma_1^*$ and $P = a\,p_x + b$. Since $(p_x^{\mathfrak{b}})_{\sigma_1^*} = 2(c_1\,P - e)$, $x_{\sigma_1^*}^{\mathfrak{a}} = 2(c_1 M + e)$ and $\bar{x}_{\sigma_1^*}^{\mathfrak{a}} = 2(c_1\,\bar{M} + e)$, we conclude that the second formula holds in this case. □

The above formulas are remarkable for many cases which fall under the same form. The following two results are less uniform but in some respects are simpler. We select the sign + for $\mathfrak{f} = \mathfrak{a}$ and − for $\mathfrak{f} = \mathfrak{b}$.

Property 18. *For $a, b, c \in R$ and $x, \bar{x} \in Q$,*

$$(s_x^{\mathfrak{f}})_{\sigma_1} + 2\,b\,d_1 = x_{\sigma_1}^{\mathfrak{f}'} + \bar{x}_{\sigma_1}^{\mathfrak{f}'} \pm 6\,c_2,$$

$$(s_x^{\mathfrak{f}})_{\sigma_1^*} + 2\,b\,c_1 = x_{\sigma_1^*}^{\mathfrak{f}'} + \bar{x}_{\sigma_1^*}^{\mathfrak{f}'} \pm 6\,e,$$

$$(s_x^{\widetilde{\mathfrak{f}}})_{\sigma_1} + b\,(c_\square + c_2) = x_{\sigma_1}^{\widetilde{\mathfrak{f}}'} + \bar{x}_{\sigma_1}^{\widetilde{\mathfrak{f}}'} \pm 3c_{2,3},$$

$$(s_x^{\widetilde{\mathfrak{f}}})_{\sigma_1^*} + b\,(c_\square - e) = x_{\sigma_1^*}^{\widetilde{\mathfrak{f}}'} + \bar{x}_{\sigma_1^*}^{\widetilde{\mathfrak{f}}'} \pm 3\,c_2.$$

Proof. Let $\mathfrak{f} = \mathfrak{a}$. Using the values for $(s_x^{\mathfrak{a}})_{\sigma_1}$, $x_{\sigma_1}^{\mathfrak{b}}$ and $\bar{x}_{\sigma_1}^{\mathfrak{b}}$ from the previous proof, we get $(s_x^{\mathfrak{a}})_{\sigma_1} - x_{\sigma_1}^{\mathfrak{b}} - \bar{x}_{\sigma_1}^{\mathfrak{b}} = 6\,c_2 - 2\,b\,d_1$.

Similarly, let $\mathfrak{f} = \mathfrak{b}$. This time, using analogous values for $(s_x^{\mathfrak{b}})_{\sigma_1^*}$, $x_{\sigma_1^*}^{\mathfrak{a}}$ and $\bar{x}_{\sigma_1^*}^{\mathfrak{a}}$, we get $x_{\sigma_1^*}^{\mathfrak{a}} + \bar{x}_{\sigma_1^*}^{\mathfrak{a}} - (s_x^{\mathfrak{b}})_{\sigma_1^*} = 2bc_1 + 6e$. □

Property 19. *For $a, b, c \in R$ and $x, \bar{x} \in Q$,*

$$2(p_x^{\mathfrak{f}})_{\sigma_1} + 2\,b\,d_1(s_x - 2e) = \bar{x}\,x_{\sigma_1}^{\mathfrak{f}'} + x\,\bar{x}_{\sigma_1}^{\mathfrak{f}'} \pm 2\,c_2(s_x + 2\,e),$$

$$2(p_x^{\mathfrak{f}})_{\sigma_1^*} + 2\,b\,c_1(s_x - 2e) = \bar{x}\,x_{\sigma_1^*}^{\mathfrak{f}'} + x\,\bar{x}_{\sigma_1^*}^{\mathfrak{f}'} \pm 2(s_x + 2\,e),$$

$$2(p_x^{\widetilde{\mathfrak{f}}})_{\sigma_1} + b\,(c_\square + c_2)(s_x - 2e) = \bar{x}\,x_{\sigma_1}^{\widetilde{\mathfrak{f}}'} + x\,\bar{x}_{\sigma_1}^{\widetilde{\mathfrak{f}}'} \pm (c_2 + 2)(s_x + 2\,e),$$

$$2(p_x^{\widetilde{\mathfrak{f}}})_{\sigma_1^*} + b\,(c_\square - e)(s_x - 2e) = \bar{x}\,x_{\sigma_1^*}^{\widetilde{\mathfrak{f}}'} + x\,\bar{x}_{\sigma_1^*}^{\widetilde{\mathfrak{f}}'} \pm c_2(s_x + 2\,e).$$

Proof. Let $\mathfrak{f} = \mathfrak{b}$. Using the values for $(p_x^{\mathfrak{b}})_{\sigma_1^*}$, $x_{\sigma_1^*}^{\mathfrak{a}}$ and $\bar{x}_{\sigma_1^*}^{\mathfrak{a}}$ from the proof of Properties 18 and 19, we get

$$\bar{x}\,x_{\sigma_1^*}^{\mathfrak{a}} + x\,\bar{x}_{\sigma_1^*}^{\mathfrak{a}} - 2(p_x^{\mathfrak{b}})_{\sigma_1^*} = 2\,bc_1(s_x - 2) + 2(s_x + 2\,e).$$

□

The second variable b in $\mathfrak{f}(a, b, c, x)$ has analogous property as the fourth variable x. Let $s_b^{\mathfrak{h}} = \mathfrak{h}(a, s_b, c, x)$, $\bar{b}^{\mathfrak{h}'} = \mathfrak{h}'(a, \bar{b}, c, x)$, etc.

Property 20. *For $a, b, \bar{b}, c \in R$ and $x \in Q$, for $\mathfrak{h}$ either $\mathfrak{f}$ or $\widetilde{\mathfrak{f}}$ and for σ either σ_1 or σ_1^*,*

$$d_b\,(s_b^{\mathfrak{h}})_\sigma = (2\,a\,x + s_b + \bar{b})\,b_\sigma^{\mathfrak{h}'} - (2\,a\,x + s_b + b)\,\bar{b}_\sigma^{\mathfrak{h}'},$$

$$d_b\,(p_b^{\mathfrak{h}})_\sigma = (2\,a\,x + p_b + \bar{b})\,b_\sigma^{\mathfrak{h}'} - (2\,a\,x + p_b + b)\,\bar{b}_\sigma^{\mathfrak{h}'}.$$

Proof. Let $\mathfrak{h} = \mathfrak{a}$ and $\sigma = \sigma_1$. Since $(s_b^{\mathfrak{a}})_{\sigma_1} = 2[d_1(s_b + 2\,a\,x) + c_2]$ and $b_{\sigma_1}^{\mathfrak{b}} = 2[d_1(b + 2\,a\,x) - c_2]$, we get easily the first formula in this case.

Similarly, let $\mathfrak{h} = \mathfrak{b}$, $\sigma = \sigma_1^*$. Since $(p_b^{\mathfrak{b}})_{\sigma_1^*} = 2[c_1(p_b + 2\,a\,x) - e]$ and $b_{\sigma_1^*}^{\mathfrak{a}} = 2[c_1(b + 2\,a\,x) + e]$, we conclude that the second formula holds in this case. □

The first variable a in $\mathfrak{f}(a, b, c, x)$ also has analogous property as the second and the fourth variables b and x. Let $s_a^{\mathfrak{h}} = \mathfrak{h}(s_a, b, c, x)$, $\bar{a}^{\mathfrak{h}'} = \mathfrak{h}'(\bar{a}, b, c, x)$, etc.

Property 21. *For $a, \bar{a}, b, c \in R$ and $x \in Q$, for $\mathfrak{h}$ either $\mathfrak{f}$ or $\widetilde{\mathfrak{f}}$ and for σ either σ_1 or σ_1^*,*

$$x\,d_a\,(s_a^{\mathfrak{h}})_\sigma = [x(s_a + \bar{a}) + 2\,b]\,a_\sigma^{\mathfrak{h}'} - [x(s_a + a) + 2\,b]\,\bar{a}_\sigma^{\mathfrak{h}'}.$$

$$x\,d_a\,(p_a^{\mathfrak{h}})_\sigma = [x(p_a + \bar{a}) + 2\,b]\,a_\sigma^{\mathfrak{h}'} - [x(p_a + a) + 2\,b]\,\bar{a}_\sigma^{\mathfrak{h}'}.$$

Proof. Let $\mathfrak{h} = \mathfrak{a}$ and $\sigma = \sigma_1$. Since $(s_a^{\mathfrak{a}})_{\sigma_1} = 2[d_1(b + s_a\,x) + c_2]$ and $a_{\sigma_1}^{\mathfrak{b}} = 2[d_1 M - c_2]$, we get easily the first formula in this case.

Similarly, let $\mathfrak{h} = \mathfrak{b}$, $\sigma = \sigma_1^*$. Since $(p_a^{\mathfrak{b}})_{\sigma_1^*} = 2[c_1(p_a\,x + b) - e]$ and $a_{\sigma_1^*}^{\mathfrak{a}} = 2[c_1 M + e]$, we conclude that the second formula holds in this case. □

The third variable c in the function $\mathfrak{f}(a, b, c, x)$ is different from the other three variables a, b and x. As in Properties 18 and 19, we have four separate cases both for sums and for products. Let $s_c^{\mathfrak{f}} = \mathfrak{f}(a, b, s_c, x)$, $\bar{c}^{\mathfrak{f}'} = \mathfrak{f}'(a, b, \bar{c}, x)$, etc.

Property 22. *For $a, b, c, \bar{c} \in R$ and $x \in R$,*

$$d_c(2\,p_c + s_c - e)(s_c^{\mathfrak{f}})_{\sigma_1} = (s_c + \bar{c} + 1)(\bar{c}_2\,c + 2\,\bar{d}_1)\,c_{\sigma_1}^{\mathfrak{f}'} - (s_c + c_1)(c_2\,\bar{c} + 2\,d_1)\bar{c}_{\sigma_1}^{\mathfrak{f}'},$$

$$d_c(s_c^{\mathfrak{f}})_{\sigma_1^*} = (s_c + \bar{c} + 2e)c_{\sigma_1^*}^{\mathfrak{f}'} - (s_c + c + 2e)\bar{c}_{\sigma_1^*}^{\mathfrak{f}'},$$

$$d_c(2\,p_c + 3\,s_c + 7e)(s_c^{\widetilde{\mathfrak{f}}})_{\sigma_1} =$$

$$(s_c + \bar{c} + 3e)[2\,p_c + 3\,s_c + 2\,\bar{c}_3 + \bar{c}]\,c_{\sigma_1}^{\widetilde{\mathfrak{f}}'} - (s_c + c + 3e)[2\,p_c + 3\,s_c + 2\,d_1 + c]\bar{c}_{\sigma_1}^{\widetilde{\mathfrak{f}}'},$$

$$d_c(2\,p_c + s_c + 3e)(\widetilde{s_c^{\mathfrak{f}}})_{\sigma_1^*} =$$
$$(s_c + \bar{c}_1)[\bar{c}_2\,c + 2\,\bar{c}_1 - 2e]\,\widetilde{c^{\mathfrak{f}'}_{\sigma_1^*}} - (s_c + c_1)[c_2\,\bar{c} + 2\,c_\square - 2e]\widetilde{\bar{c}^{\mathfrak{f}'}_{\sigma_1^*}}.$$

Proof. Let $\mathfrak{f} = \mathfrak{a}$. Since $(s_c^{\mathfrak{a}})_{\sigma_1} = 2[(2\,p_c + d_1 + \bar{d}_1 - e)M + 2\,s_c + e]$ and $c^{\mathfrak{b}}_{\sigma_1} = 2[d_1\,M - c_2]$, we get that the difference

$$(s_c + \bar{c}_1)(\bar{c}_2\,c + 2\,\bar{d}_1)\,c^{\mathfrak{b}}_{\sigma_1} - (s_c + c_1)(c_2\,\bar{c} + 2\,d_1)\bar{c}^{\mathfrak{b}}_{\sigma_1}$$

is the product $d_c(2\,p_c + s_c - e)(s_c^{\mathfrak{a}})_{\sigma_1}$. □

Property 23. *For $a, b, c, \bar{c} \in R$ and $x \in Q$,*

$$d_c(2\,p_c + s_c - e)(p_c^{\mathfrak{f}})_{\sigma_1} =$$
$$(p_c + \bar{c}_1)(p_c\,\bar{c}_2 + \bar{c} + 2e)\,c^{\mathfrak{f}'}_{\sigma_1} - (p_c + c_1)(p_c\,c_2 + c + 2e)\bar{c}^{\mathfrak{f}'}_{\sigma_1},$$
$$d_c(p_c^{\mathfrak{f}})_{\sigma_1^*} = (p_c + \bar{c} + 2e)c^{\mathfrak{f}'}_{\sigma_1^*} - (p_c + c + 2e)\bar{c}^{\mathfrak{f}'}_{\sigma_1^*},$$

$$d_c(2\,p_c + 3\,s_c + 7e)(\widetilde{p_c^{\mathfrak{f}}})_{\sigma_1} =$$
$$(p_c+\bar{c}+3e)[p_c(2\,\bar{c}+3e)+3\bar{c}+2e]\,\widetilde{c^{\mathfrak{f}'}_{\sigma_1}} - (p_c+c+3e)[p_c(2\,c+3e)+c_{3,2}]\widetilde{\bar{c}^{\mathfrak{f}'}_{\sigma_1}},$$

$$d_c(2\,p_c + s_c + 3e)(\widetilde{p_c^{\mathfrak{f}}})_{\sigma_1^*} =$$
$$(p_c + \bar{c}_1)[p_c\,\bar{c}_2 + \bar{c} - 2e]\,\widetilde{c^{\mathfrak{f}'}_{\sigma_1^*}} - (p_c + c_1)[p_c\,c_2 + c - 2e]\widetilde{\bar{c}^{\mathfrak{f}'}_{\sigma_1^*}}.$$

Proof. Let $\mathfrak{f} = \mathfrak{b}$. Since $(p_c^{\mathfrak{b}})_{\sigma_1^*} = 2[(p_c + e)M - e]$ and the sums $c^{\mathfrak{a}}_{\sigma_1^*}$ and $\bar{c}^{\mathfrak{a}}_{\sigma_1^*}$ are $2[c_1 M + e]$ and $2[\bar{c}_1 M + e]$, we get that the difference $(p_c + \bar{c} + 2)c^{\mathfrak{a}}_{\sigma_1^*} - (p_c + c + 2e)\bar{c}^{\mathfrak{a}}_{\sigma_1^*}$ is the product $d_c(p_c^{\mathfrak{b}})_{\sigma_1^*}$. □

8. Squares from symmetric sums

In this section we shall show that from basic symmetric functions of the triples $\lambda_\pm$ and quadruples $\overrightarrow{\lambda_\pm}$ it is possible to get many squares. For example, from Jones linear polynomials x, $x + 2$ and $4x + 4$ we get a square $9(x + 1)^2$ by taking the sum of products of three pairs $x(x + 2) + x(4x + 4) + (x + 2)(4x + 4)$ and add 1 (apply Property 25 for $u = 0$ and $v = 1$). Another possibility is to get $(x^4 + 3x + 3)^2$ by taking the sum of x^8 and the product of x^4 with the sum $6x + 6$ of polynomials and the sum of products of three pairs and add 1 as before (apply Property 25 for $u = x^4$ and $v = 1$).

Property 24. *For $a, b, c, u, v \in R$ and $x \in Q$, the triples $\lambda_\pm$ satisfy the relations*

$$u^2 + u\,v\,\sigma_1(\lambda_\pm) + v^2(\sigma_2(\lambda_\pm) + e) = [u + v(d_1\,M \pm c_2)]^2\,,$$

$$4\,u^2 + u\,v\,(\sigma_1(\lambda_\pm)^2 - 4e) + v^2\,\sigma_2(\lambda_\pm)^2 = \\ [2\,u + v(d_1\,M \pm 2c_1)(d_1\,M \pm 2c)]^2\,,$$

Proof. The difference of the left hand side in the first identity

$$u^2 + u\,v\,\sigma_1(\lambda_\pm) + v^2(\sigma_2(\lambda_\pm) + e)$$

and its right hand side $[u + v(d_1\,M \pm c_2)]^2$ has the form $we - w$, where $w = 2v(c_1M + e)[v(c^2 + e)M + 2vc + u]$. Hence, these sides are indeed equal. The second identity has a similar proof. □

Let $S_\pm = 2\,c_\square\,M^2(c_\square\,M \pm 2\,c_2) + (11\,c_\square + 3e)M \pm 3\,c_2$. Notice that $S_\pm = \widetilde{E}_2\widetilde{E}_4 + 2\widetilde{E}_2 + E_1$.

Property 25. *For $a, b, c, u, v \in R$ and $x \in Q$, the quadruples $\overrightarrow{\lambda_\pm}$ satisfy the relations*

$$u^2 + u\,v\,\sigma_1(\overrightarrow{\lambda_\pm}) + v^2(\sigma_2(\overrightarrow{\lambda_\pm}) + \sigma_4(\overrightarrow{\lambda_\pm}) + e) = (u + v\,S_\pm)^2\,,$$

$$u\,\sigma_1(\overrightarrow{\lambda_\pm})^2 + (v^2 - 4\,u)(\sigma_2(\overrightarrow{\lambda_\pm}) + \sigma_4(\overrightarrow{\lambda_\pm}) + e) = (v\,S_\pm)^2\,,$$

$$u\,\sigma_1(\overrightarrow{\lambda_\pm})^2 + (v^2 - 4\,u)\sigma_2(\overrightarrow{\lambda_\pm}) + 4\,(v^2 - u)\,\sigma_4(\overrightarrow{\lambda_\pm}) + v^2 - 4\,u = \\ [v(2\,S_\pm - 3d_1M \mp 3\,c_2)]^2\,.$$

Proof. The difference of the left hand side in the first identity

$$u^2 + u\,v\,\sigma_1(\overrightarrow{\lambda_+}) + v^2(\sigma_2(\overrightarrow{\lambda_+}) + \sigma_4(\overrightarrow{\lambda_+}) + e)$$

and its right hand side $(u + v\,S_+)^2$ has the form $we - w$, where w is the sum $\sum_{i=0}^{5} k_i\,M^i$ with coefficients $k_0 = 8c_2\,u + c_{8,5}c_{8,3}\,v$, $k_1 = (cc_{24,46} + 8e)u + 6c_2(cc_{6,27} + 5e)v$, $k_2 = 4c_\square c_2\,u + (c^3c_{240,722} + cc_{600,184} + 16e)v$, $k_3 = 8c_\square c_2(cc_{10,21} + 3e)v$, $k_4 = 4c_\square^2(cc_{14,25} + 4e)v$ and $k_5 = 4c_\square^3 c_2 v$. Hence, these sides are indeed equal. The remaining two identities have similar proofs. □

In particular, when $v = e$ and $u = 0$, we get the following statement.

Property 26. *For $a, b, c \in R$ and $x \in Q$,*

$$E_{\sigma_2} + E_{\sigma_4} + e = (\widetilde{E}_2\,\widetilde{E}_4 + 2\,\widetilde{E}_2 + E_1)^2.$$

The sum $E_{\sigma_2} + 4\,E_{\sigma_4} + e$ is also the complete square. The proof of this is almost identical with the proof of the Property 25.

Property 27. *For $a, b, c \in R$ and $x \in Q$,*

$$E_{\sigma_2} + 4\,E_{\sigma_4} + e = (2\,\widetilde{E}_1\,\widetilde{E}_3 - \widetilde{E}_2 - 2\,\widetilde{E}_1 - E_1)^2.$$

On the other hand, we have the following factorization.

Property 28. *For $a, b, c \in R$ and $x \in Q$,*

$$E_{\sigma_2} + 5\,E_{\sigma_4} + e = [2c_\square M(c_\square M^2 \pm 2c_2) + (9c_\square + e)M \pm c_2] \\ [10c_\square M(c_\square M^2 \pm 2c_2) + (49c_\square + 9e)M \pm 9c_2].$$

Proof. The method for the verification of this identity is identical to the method used for the Property 25. In the difference of the left hand side and the right hand side we replace the powers of e with e to get the expression of the form $w\,e - w$, for some element $w \in R$. □

References

[1] A. Baker and H. Davenport, *The equations $3\,x^2 - 2 = y^2$ and $8\,x^2 - 7 = z^2$*, Quart. J. Math. Oxford Ser. (2) **20** (1969), 129-137.

[2] E. Brown, *Sets in which $x\,y + k$ is always a square*, Mathematics of Computation, **45** (1985), 613-620.

[3] Z. Čerin, *The extensions of the Euler triples*, (preprint).

[4] Z. Čerin, *On extended Euler quadruples*, (preprint).

[5] L. Euler, *Commentationes Arithmeticae I*, In Opera Omnia, Series I, volume II, B.G. Teubner, Basel, 1915.

[6] V. E. Hoggatt and G. E. Bergum, *A problem of Fermat and the Fibonacci sequence*, Fibonacci Quart. **15** (1977), 323-330.

[7] N. Jacobson, *Lectures in Abstract Algebra*, Van Nostrand, London 1966.

[8] B. W. Jones, *A variation on a problem of Davenport and Diophantus*, Quart. J. Math. Oxford Ser. (2), **27** (1976), 349-353.

[9] L. Jones, *A Polynomial Approach to a Diophantine Problem*, Math. Mag. **72** (1999), 52-55.

[10] M. Radić, *A definition of determinant of rectangular matrix*, Glasnik Mat. 1 (21) (1966), 17-22.

Kopernikova 7, 10010 Zagreb, CROATIA, Europe
E-mail address: cerin@math.hr

Dipartimento di Matematica, Universita di Torino, Torino, Italy
E-mail address: gianella@dm.unito.it

RENDICONTI DEL CIRCOLO MATEMATICO DI PALERMO
Serie II, Suppl. 83 (2011), pp. 111-129

L'OTTIMIZZAZIONE DEGLI INTERVENTI MANUTENTIVI SULLE LINEE FERROVIARIE CON L'UTILIZZO DI UN MODELLO MARKOVIANO: ANALISI DI UN CASO STUDIO

FERDINANDO CORRIERE* - DARIO DI VINCENZO*
(*) Dipartimento Città e Territorio – Università degli Studi di Palermo

Sommario - Riprendendo, gli esiti di una memoria già presentata in occasione dell'VI International Conference of *"Stochastic Geometry, Convex Bodies, Empirical Measure & Applications To Mechanics And Engineering Of Train-Transport",* viene adesso perfezionata ed applicata ad un caso reale di studio, rappresentato da una delle principali linee ferroviarie siciliane, una metodologia basata su processi decisionali markoviani, che consente l'ottimizzazione della programmazione degli interventi manutentivi.
Da un analisi critica dei dati assunti dai diversi parametri geometrici del binario, nel caso studio relativo alla linea PA-ME periodicamente rilevati attraverso treni diagnostici ad alto rendimento, si è verificata la possibilità, con le metodiche della programmazione dinamica applicata ai processi decisionali, di individuare la migliore politica di intervento tale da garantire sempre opportuni livelli di sicurezza d'esercizio e di qualità di marcia, con il minor numero di interventi ottimizzando, pertanto, le risorse disponibili ed i protocolli manutentivi.

Abstract - From the results of a memory already introduced in the VI International Conference of *"Stochastic Geometry, Convex Bodies, Empirical Measure & Applications To Mechanics And Engineering Of Train-Transport",* it's improved now and applied to a real case of study, that is one of the principal Sicilian railway lines, a methodology based on Markovian decisional trials, that allows to optimize the planning of the maintenance interventions.
A critical analysis of the different geometric parameters data, monitored by diagnostic trains at high-performance on the railway track of the study-case related to the line PA-ME, is made up.
Is, then, emphasized the possibility, with the dynamic planning methodic applied to the decisional trials, to individuate the best politics of such intervention as a tool for guarantee opportune safety levels in the exercise and in the quality of march, optimizing, therefore, the available resources and the maintenance protocols.

1. EXPERIMENTAL ANALYSIS OF A CASE STUDY.

To verify the practical validity of the model of decisional optimization, based on the Markov's chains type, and proposed on the occasion of the VI International Conference of *"Stochastic Geometry, Convex Bodies, Empirical Measure & Applications To Mechanics And Engineering Of Train-Transport"*, is chosen to effect an experimental analysis on a railway line in exercise, so that to make a will its applicability on a real case of railway management

1.1. The line Palermo-Messina.

To verify the practical validity of the model of decisional optimization, based on the markov's chains, and proposed on the occasion of the You International Conference of "Stochastic Geometry, Convex Bodies, Empirical Measure & Applications To Mechanics And Engineering Of Train-Transport, is chosen to effect an experimental analysis on a railway line in exercise, so that to make a will its applicability on a real case of railway management.

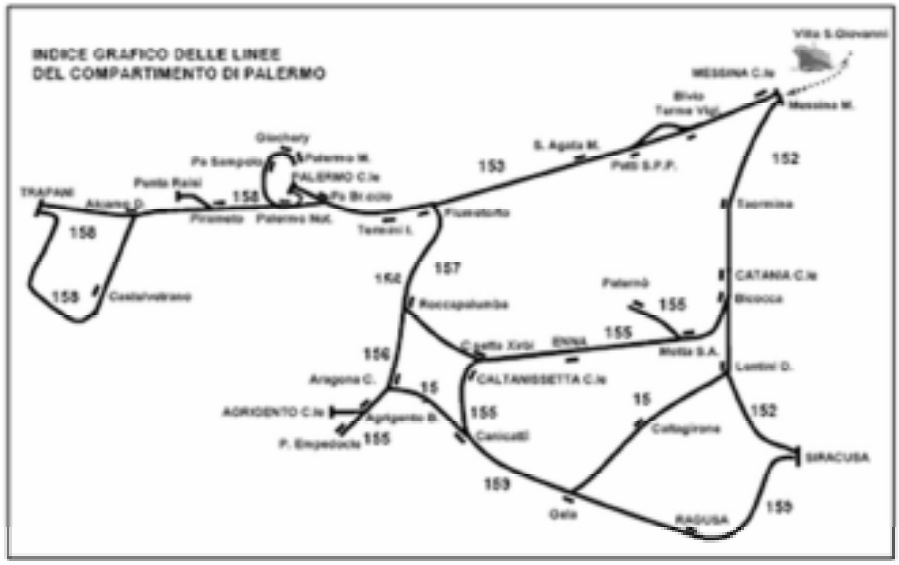

Figure 2: Identification of the line of the Compartment of Palermo.

Staz. Ini	Staz. Fin	Km	Traz.	Binari	Rango A max	Massa assiale
Messina Centrale	Villafranca	18,0	Elettr.	2	81	C3
Villafranca	Rometta	3,0	Elettr.	1	81	C3
Rometta	S.Filippo/S.Lucia	10,0	Elettr.	1	105	C3
S.Filippo/S.Lucia	Milazzo	4,0	Elettr.	2	150	C3
Milazzo	Barcellona	9,0	Elettr.	2	138	C3
Barcellona	Terme Vigliatore	8,0	Elettr.	2	138	C3
Terme Vigliatore	Oliveri Tindari	7,0	Elettr.	1	102	C3
Oliveri Tindari	Patti	18,0	Elettr.	1	102	C3
Patti	Capo D'orlando	22,0	Elettr.	1	101	C3
Capo D'orlando	Santa Agata Di M.	14,0	Elettr.	1	101	C3
Santa Agata Di M.	S. Stefano Camastra	25,0	Elettr.	1	96	C3
S. Stefano Camastra	Cefalu'	30,0	Elettr.	1	96	C3
Cefalu'	Fiumetorto	23,0	Elettr.	1	123	C3
Fiumetorto	Termini Imerese	6,0	Elettr.	2	123	C3
Termini Imerese	Altavilla Milicia	16,0	Elettr.	2	123	C3
Altavilla Milicia	Bagheria	7,0	Elettr.	2	123	C3
Bagheria	Palermo	14,0	Elettr.	2	127	C3

Fonte: Elaborazione su dati RFI 2002 (www.rfi.it).

Table 1: Characteristics of the line Messina Palermo

The different ones drawn that they compose the whole line Palermo Messina with the relative characteristics I am of you bring in the tab.1.

Already in 2004 part was taken to two runs of verification by Palermo to Messina, you effects with the diagnostic car to high-performance Talete connected in tandem with the car Aldebaran, so that to be able the first one to effect a relief of the geometry of the platform, of the usury of the rails, and of the levels of comfort, the second to analyze the electric characteristics, geometric and of deterioration of the line of contact.

Subsequently to the two runs of verification had been delivered the in relief data to the Department during the execution of the same and those related to the two preceding annuities.

To such initial data, they are assistant of the others, that the Compartment RFI in Palermo has furnished City and Territory to the Department. These to be related to the values assumed by the different in relief geometric parameters during the diagnostic reliefs had actually effected on the line since 2004 to 2007, contained further also the historian of the maintenance interventions had realized today actually since 2002 to, with the location, the typology and the costs of the performed interventions.

It is so can constitute a bank you date, of the defects and of the maintenance interventions performed, relative to a period of inclusive general time among 2002 and 2007.

1.2. The typology of data.

The data, related to the values of usury of the rails and to those assumed by the different analyzed geometric parameters (Rail gauge, Skew, Alignment sx and dx, Longitudinal Level sx and dx, Transversal Level sx and dx, Slanting, Discard of Transversal level, Defect him raising and Horizontal Usury, Vertical, and to 45° sx and dx), have been furnished in the form of files manageable through the program VISIONA of RFI, that allows to visualize the graphs with continuous longitudinal development and to complete through the software of visualization and elaboration the necessary activities of analysis.

The data related to the maintenance interventions performed and to the values assumed by the indexes of quality of the platform, have

been furnished instead in formed .xls.

The available Database, as it regards the diagnostic reliefs, it consists of n. 19 parameters (among geometry and usury) relative to every meter of platform, therefore in total around 2.000.000 records are managed for every run of relief. For examples are brought the measures related to 30 m of platform of the line S.Nicola - Trabia (equal platform) between the progressive 26,810 and the progressive 26,840. You first chart shows the values of rail gauge and slanting, the second the values of transversal level, alignment and longitudinal level, the third one the values of usury of the rails.

Gives the fragmentation of the data, due also to the continuous execution of the reliefs along the whole line, dates not always the presence of a general different number of runs of verification on the different ones drawn of the line and a greater or smaller number of information on the maintenance interventions performed on the single drawn, in the considered temporal arc, is chosen to complete a study particularly detailed of the drawn inclusive among Palermo and Fiumetorto, of which it had him the most greater number of data, that introduces a notable heterogeneity in the layout (straight, curves with great, middle and small rays), and different works of art (bridges in c.a., metallic bridges, bridges in masonry, galleries, etc..).

1.3. Analysis of the data related to the geometric parameters.

The in relief data through the diagnostic Talete carriage are analyzed bushels and elaborate for single geometric parameter, appraising the assumed values and comparing them with those of reference.

Effecting a comparison among the in relief values to the different dates, for every single geometric parameter, they are been able to always find not some tied up problem list to the precise location of the defect and this because of one perfect setting of the progressive initial mileage and to the possible jam of the tools of relief. In terms practical such problem is turned into the real difficulty of I compare some values assumed in the time with the purpose to appraise the evolution of the defect in a datum point of the superstructure and the goodness of the maintenance interventions performed.

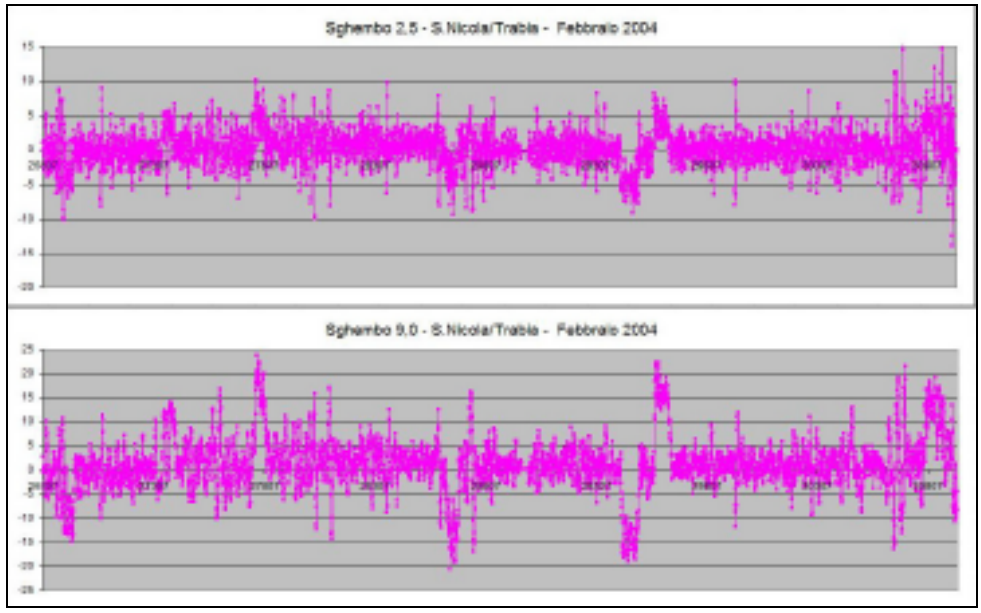

Figure 3: Values of skew in base 9,0mt, line S.Nicola-Trabia - Feb.2004.

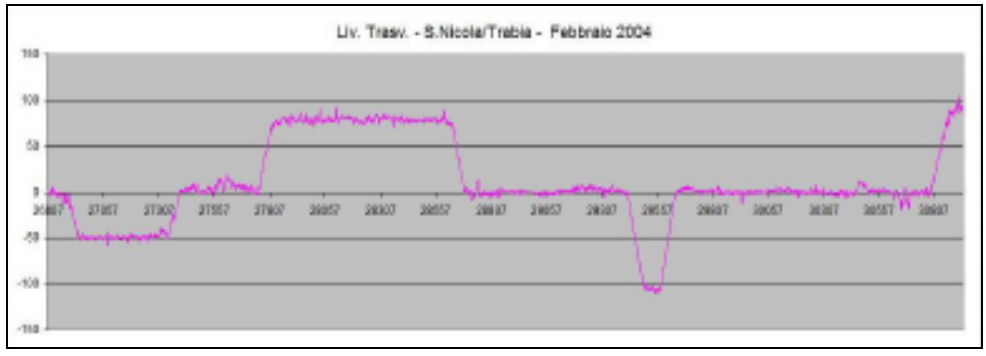

Figure 4: Values of Transversal Level, line S.Nicola-Trabia - Feb.2004.

Analyzing in fact for datum geometric parameter, the courses of the values assumed along the progressive one to every effected relief, comparing them among them, has been possible to find some bewilderments of the values along the progressive one, mostly appraisable if they are taken in reference less punctual geometric parameters.

From the analysis for instance of the slanting one in base 9,0 rather than 2,5 mt. they are been able to mostly underline such

bewilderments, that resulted to be evident even more from an analysis of the Transversal Level. It is so looked for of timing the various reliefs, using as reference the Transversal Level, whose course is tightly tied to the course plane-altimetric of the layout.

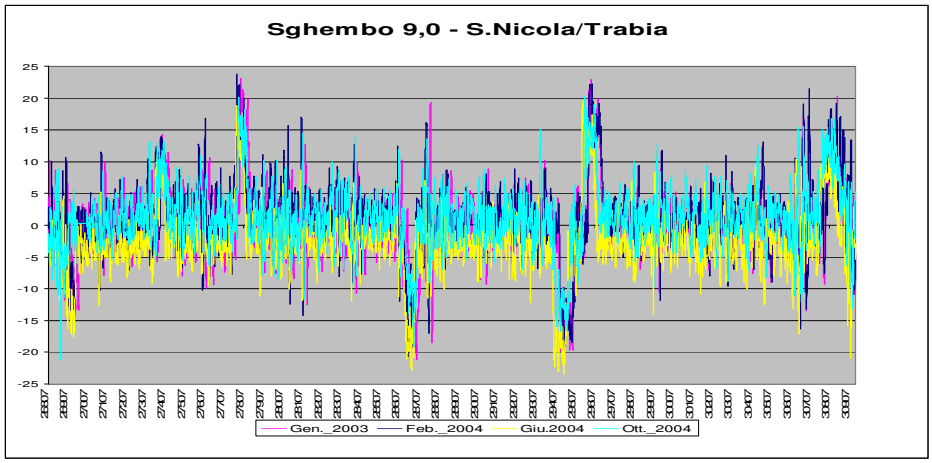

Figure 5: Values of skew in base 9,0mt. Line S.Nicola-Trabia from Jen.2003 until Oct.2004.

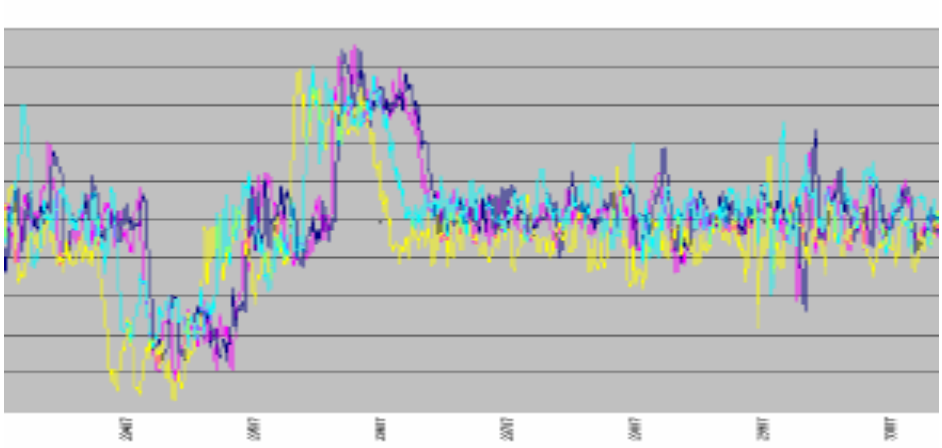

Figure 6: Zoom of the values sideways by 9.0 mt. line S.Nicola-Trabia from Jen.2003 until Oct.2004.

They is so in relief, from a relief to the other, bewilderments along the progressive mileage at times in positive of the order of +35 mt and at times in negative of the order also of -75 mt. Obviously this

is born from the lack of a system GPS on board of the Talete carriage that integrates him with the odometric wheel that measures the progressive one, as it already happens on the diagnostic Archimede train or on diagnostic means of new construction.

From the analysis of the values of transversal level noticed in the four runs of verification effected on S.Nicola-Trabia line, that the values introduced some anomalies in two cases on the four examined. In the relief of June 2004, in fact, the values normally resulted out rather staircase in comparison to the in relief values, while in the relief of October 2004 the same result to exactly be opposed.

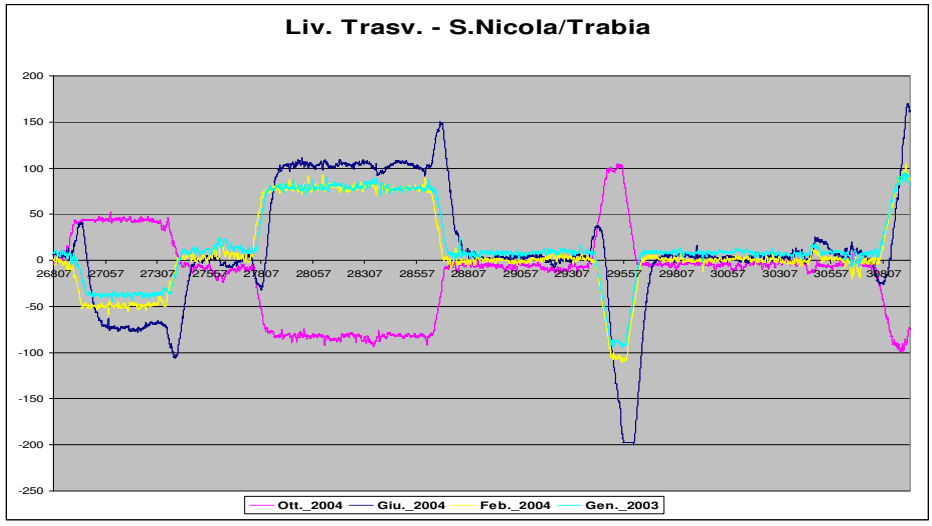

Figure7: Transversal level values, line S.Nicola-Trabia Jen.2003 - Oct.2004.

Therefore an inversion of the relative data is effected to Oct.2004 and is realized a timing of the same appraising the points of peak and the position of the curves, eliminating at the same time the wrong data, and getting so the graph in following figure, mostly notices where her to him not reliability of the in relief data to the date of Giu.2004, perpetually distant from the normal noticed values.

Is ascertained then that to the timing of the relative data to a single geometric parameter it didn't correspond that of the other parameters, that resulted to have discards of mileage of different entity. All of this therefore it transforms him in an excessive riskiness of the since the realization of some evaluation makes impossible regarding the evolution of the defect in the time and to the goodness

of the performed interventions if the defect is appraised by a punctual point of view. It stays however to specify that this however not affect the operational goodness of the interventions to be realized for eliminating the defects found following a run of verification, in how much as a rule such interventions they interest developments of draws some order of the hundred meters. While for the reliefs performed by the Archimede train such riskiness it doesn't subsist sight the presence of a G.P.S. differential integrated to the odometric wheel.

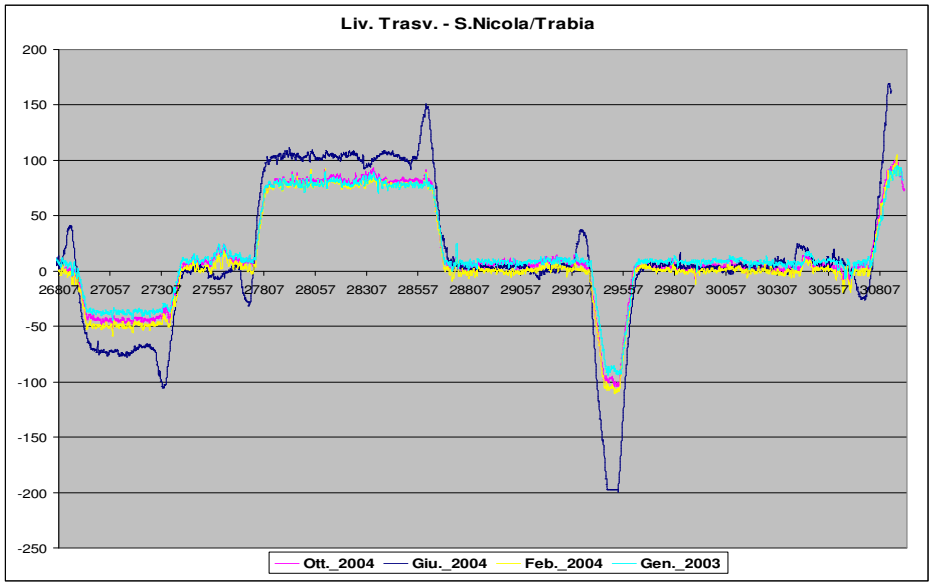

Figure 8: Transversal level value changed, line S.Nicola-Trabia Gen.2003 - Ott.2004

Is ascertained then that to the timing of the relative data to a single geometric parameter it didn't correspond that of the other parameters, that resulted to have discards of mileage of different entity. All of this therefore it transforms him in an excessive riskiness of the since the realization of some evaluation makes impossible regarding the evolution of the defect in the time and to the goodness of the performed interventions if the defect is appraised by a punctual point of view. It stays however to specify that this however not affect the operational goodness of the interventions to be realized for eliminating the defects found following a run of verification, in how much as a rule such interventions they interest developments of draws

some order of the hundred meters. While for the reliefs performed by the Archimede train such riskiness it doesn't subsist sight the presence of a G.P.S. differential integrated to the odometric wheel.

1.4. Analysis of the data related to the IQB

To allow a global evaluation of the level of I degrade some superstructure in every single draws and its temporal evolution, is preferred to make reference to the index of Quality of the Platform in draws IQBT.

As already says, the IQBT and the IQBS are of the synthetic indexes of the geometric quality of the platform. They founds him on the elaboration of the resultant data from the geometric reliefs of the platform, and they makes reference to the standard deviation of some geometric parameters: alignment, longitudinal level, raising to level of attention.

The indexes of quality damage a middle and global judgment on the geometric quality of the platform, keeping in mind only of some parameters, that are those tractable with the most common maintenance intervention: the tamping.

For such motives a careful examination of the values of the Indexes of quality of the platform is conducted extrapolated by the data noticed by the runs of verification of the Talete carriage, in the period of reference.

For every run of verification they are drawn therefore the values of IQBT and relative IQBS, for every draws, to every run of effected verification and have been compared with those of reference given by RFI.

From an united analysis for drawn of the IQBT, has been possible to verify the course of the indexes of quality of the platform in the time, for every draws, verifying the subsistence of a distorted relief, that of June 2004, as already noticed by the analysis of the values of transversal level.

You is to the point purged the date-basic one of the diagnostic reliefs, of all that distorted data or not reliable. From a further anal of the course of the IQB in the time, has been possible to notice as the sensitive improvements found for draws her Casteldaccia-S.Flavia and Trabia-S.Nicola coincides with the interventions of renewal of the equal platform realized between the end of 2006 and the beginning of 2007.

This has confirmed therefore as the qualitative state of the railway superstructure is fully described by the indexes of quality of the platform, really for its nature and for that of the most greater part of the maintenance interventions that realizes him during the ordinary maintenance of the same superstructure.

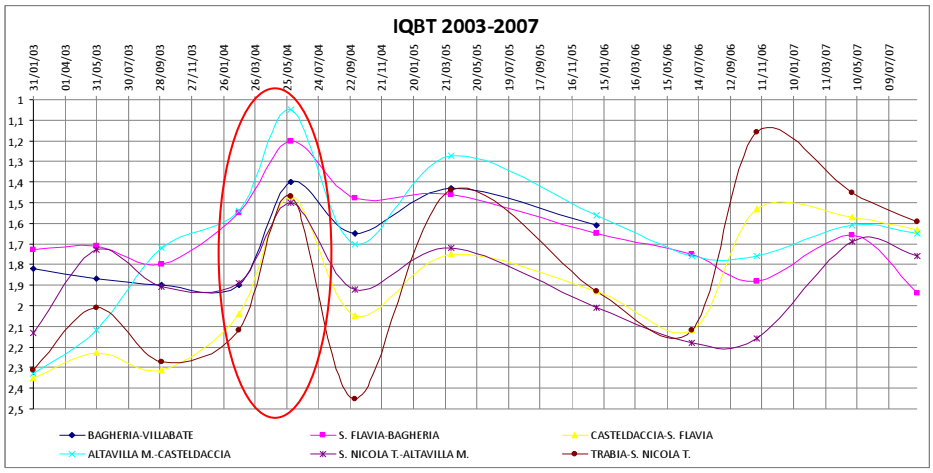

Figure 9: IQBT Values, Palermo-Fiumetorto, (2003-2007).

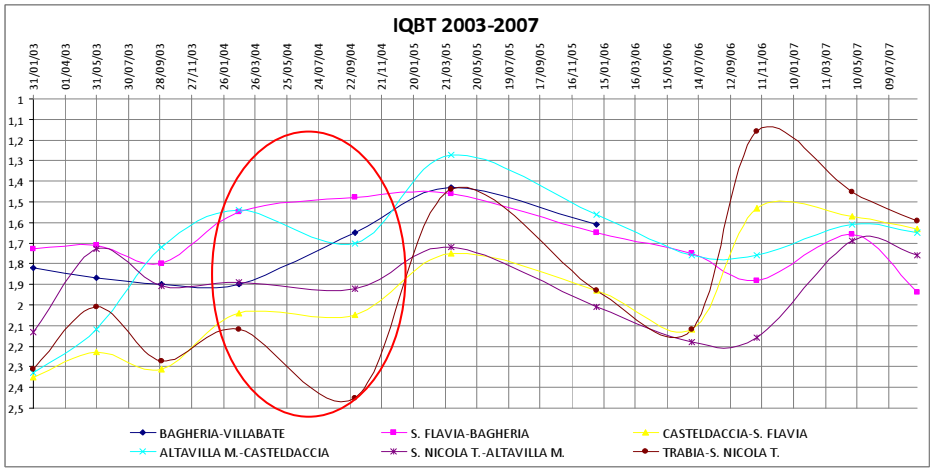

Figure 10: IQBT values, Palermo-Fiumetorto, (2003-2007).

1.5. The calibration of the markovian model for the definition of the trial excellent maintenance.

With the purpose to accomplishedly describe the concrete possibility of use of the mathematical model proposed in the VI International Conference of *"Stochastic Geometry, Convex Bodies, Empirical Measure & Applications To Mechanics And Engineering Of Train-Transport"*[1], in this paper are underlined in the succession the application steps of the method, with the application of the same to a real case.

Taking back the indicators of is proposed by RFI, for the single geometric parameters and holding in account how much foreseen by the sub-directional operational procedure RFI DMAIMSD PS IFS 002 0, is chosen to classify the states of the superstructure making reference to the index of Quality of the Platform. I am so also defined for the IQB, four states in which to classify the level of degrades some superstructure through the opportune definition of four values of thresholds:

Status	Threshold degradation	value
0	Optimum level	IQB ril. = 1,2
1	Threshold of concern	IQB ril. = IQB rif. = 1,8
2	Intervention threshold	IQB ril. = 1,25*IQB rif.= 2,25
3	Security Threshold	IQB ril. = 1,5*IQB rif. = 2,7

Table 6: System status and corresponding threshold values of decay.

From an analysis of the data in possession related to the indexes of quality of the platform noticed and to the interventions of performed tamping, parameterizing the variation of the quality of the platform (IQB) due to the realization of the intervention, has been possible to reconstruct the curve of decadence of the index of Quality of the Platform in Draws.

---

[1] F. Corriere, D. Di Vincenzo – *"A markovian model as a tool for optimization of maintenance planning on the railway lines"* – VI International Conference of *"Stochastic Geometry, Convex Bodies, Empirical Measure & Applications To Mechanics And Engineering Of Train-Transport*", Milazzo 27/05 -03/06 2007 – Rendiconti del Circolo Matematico di Palermo – Serie II – Numero 80 – Anno 2008;

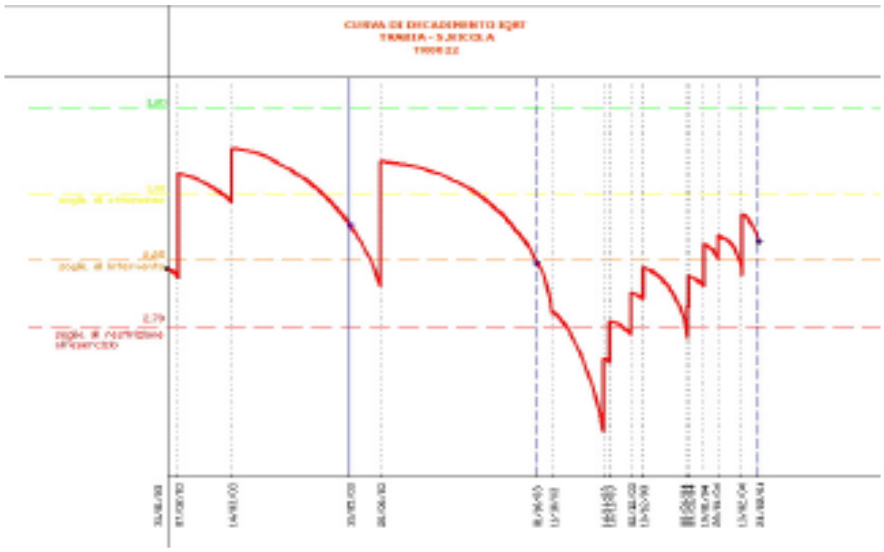

Figure 3: Curves of decay line Trabia-S.Nicola, (2003-2004).

Through the knowledge of the function of decadence F and from the statistic analysis of the data gotten by the measures of the structural and functional characteristics (monitoring and relief of the indicators of quality) has been possible to define the probabilities of transition for the index of quality of the platform in drawn by every state toward the other states both in presence of the maintenance intervention both in presence of the execution of a simple monitoring; the probability of transition represents in conclusion the possibility of success of the intervention for assigned level of cost or, in other words an indicator of the effectiveness of the intervention.

Supposing as already says that to the beginning of every period t the infrastructure is inspected to mean of diagnostic cars to high-performance and classified in one of the four been considered. After the observation of the qualitative state of the superstructure, must be undertakes the decision to continue to use the same one without any intervention up to the next period of inspection (action *c*) or to effect a maintenance intervention to restore the best structural and functional conditions (action *m*). we Suppose, besides, that in the state 0 the action c is allowed only while in the state 3 the action m is allowed only.

If then choosing the action c is incurred in every period in the costs of management equal to 90, 180 and 450 monetary unities when he is respectively in the states 0, 1 and 2. While choosing the action m, the maintenance he will effect with which will be wanted to restore the optimal level of the superstructure (is 0); the maintenance will involve some costs of intervention equal to 1800, 2250 and 2700 monetary unities according to whether are respectively found there in the states 1,2 and 3 when her the action m is undertaken.

The costs C(i,k) and the probabilities Pij(k) I am therefore summaries in the following chart, are assumed where that k = 0,1 respectively for the actions "*c*" and "*m*", and that is, besides, i=0,1,2,3 the states of the system.

Stato	**Azione**	**Costi**	**Probabilità di transizione**			
i	***k***	***C(i,k)***	$P_{i0}(k)$	$P_{i1}(k)$	$P_{i2}(k)$	$P_{i3}(k)$
0	*c*	90	0,73	0,20	0,07	0,00
1	*c*	180	0,00	0,65	0,30	0,05
	m	1890	0,85	0,15	0,00	0,00
2	*c*	450	0,00	0,00	0,55	0,45
	m	2340	0,75	0,18	0,07	0,00
3	*m*	2790	0,68	0,19	0,08	0,05

Table 7: Probability of transiction and Cost.

It intends us therefore to determine that excellent politics of substitution that the middle cost of every period makes least.

The function objective to minimize for the problem in examination it will be:

$$\min \Phi = 90x_{00}+180x_{10}+1890x_{11}+450x_{20}+2340x_{21}+2790x_{31}$$

While the conditions to be respected will be :

The condition (5a) can find expression, with limited reference to the initial state j = 0, the following formal expression:

$$\begin{aligned} x_{00}+x_{01} = \quad & x_{00}\,P_{00}(0) + x_{01}\,P_{00}(1) + \\ & x_{10}\,P_{10}(0) + x_{11}\,P_{10}(1) + \\ & x_{20}\,P_{20}(0) + x_{21}\,P_{20}(1) + \\ & x_{30}\,P_{30}(0) + x_{31}\,P_{30}(1) \end{aligned}$$

e così allo stesso modo per gli stati *1,2 e 3* si avrà:

$$\begin{aligned} x_{10}+x_{11} = \quad & x_{00}\,P_{00}(0) + x_{01}\,P_{00}(1) + \\ & x_{10}\,P_{10}(0) + x_{11}\,P_{10}(1) + \\ & x_{20}\,P_{20}(0) + x_{21}\,P_{20}(1) + \\ & x_{30}\,P_{30}(0) + x_{31}\,P_{30}(1) \\ x_{20}+x_{21} = \quad & x_{00}\,P_{00}(0) + x_{01}\,P_{00}(1) + \\ & x_{10}\,P_{10}(0) + x_{11}\,P_{10}(1) + \\ & x_{20}\,P_{20}(0) + x_{21}\,P_{20}(1) + \\ & x_{30}\,P_{30}(0) + x_{31}\,P_{30}(1) \\ x_{30}+x_{31} = \quad & x_{00}\,P_{00}(0) + x_{01}\,P_{00}(1) + \\ & x_{10}\,P_{10}(0) + x_{11}\,P_{10}(1) + \\ & x_{20}\,P_{20}(0) + x_{21}\,P_{20}(1) + \\ & x_{30}\,P_{30}(0) + x_{31}\,P_{30}(1) \end{aligned}$$

that is:

$$-0{,}27x_{00}-x_{01}+0{,}85x_{11}+0{,}75x_{21}+0{,}68x_{31} = 0$$

$$0{,}20x_{00}-0{,}35x_{11}-0{,}85x_{11}+0{,}18x_{21}+0{,}19x_{31} = 0$$

$$0{,}07x_{00}+0{,}30x_{10}-0{,}45x_{20}-0{,}93x_{21}+0{,}08x_{31} = 0$$

$$0{,}05x_{10}+0{,}45x_{20}-x_{30}-0{,}95x_{31} = 0$$

Furthermore under the conditions that:

$$\sum_i \sum_k x_{ik} = 1$$

and

$$x_{1k} > 0 \qquad \text{per ogni } i,\ k$$

The solution of the problem, gotten through the *algorithm of the simplesso*, using special software of calculation (LINDO 6.1) it will furnish the vector $x^*=(x_{ik})$ of the distribution limit of probability that minimizes the monthly middle cost .

As already says the vector x * it will have the ownership (Dantzig and Wolfe) that for every the, the x_{ik} will be zero peers except that for an alone value of k.

In such way the politics defined by the conditioned probability to undertake the action k in the state j, is not- randomized, that is, the action that it prescribes when he is in the state j it is a deterministic function of j.

$$D^*_{jk} = \frac{x^*_{jk}}{\sum_{k=1}^{K} x^*_{jk}}$$

The solution of the problem of linear planning furnishes the followings results:

(*i*,*k*)	**(0,0)**	**(1,0)**	**(1,1)**	**(2,0)**	**(2,1)**	**(3,1)**
x^*_{ik}	0,471	0,358	0	0	0,152	0,019
D^*_{ik}	1	1	0	0	1	1

Then, the conditioned probabilities D_{jk} derived by the excellent solution define the following Political R: to keep on holding the superstructure in the states 0 and 1, to effect the interventions of maintenance in the states 2 and 3. The middle cost of every period will be equal to 516,09 unities of cost

Comparing besides the curve of ideal decadence gotten through the decisional model with that that describes the course given by the actions of intervention really performed in the case study, it is noticed as the first one allows: a saving of around the 15% of the general resources, a value of the IQBT never to the last level of quality and a better final value of that real. .

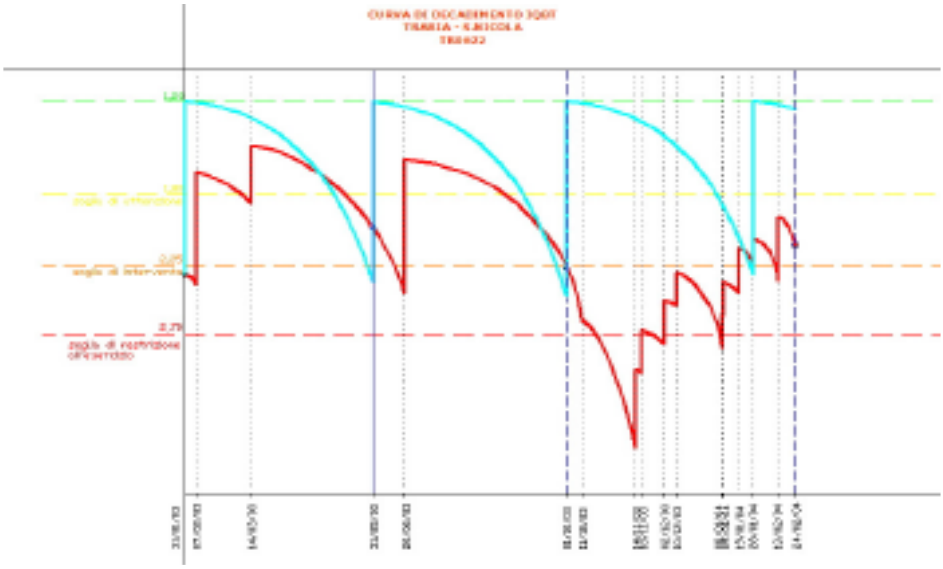

Figure 12: Comparison of decay curves for line Trabia-S.Nicola, (2003-2004).

2. Opinion.

Objective fundamental of a railway maintenance plain is that to succeed in assuring and, eventually, to restore the correct standards of comfort and safety necessary for an optimal exercise of the system to bound guide.

For monitor the superstructure and its state of efficiency are regularly effected some ordinary or extraordinary runs of verification with special diagnostic means to high-performance, following which the presence of remarkable defects is appraised, for which will be had to effect within times narrow interventions of corrective maintenance. In operation of the values assumed by the various parameters that introduce non remarkable defects are programmed interventions according to a so-called logic of maintenance "on condition."

The performed interventions, kind if in a logic of ready intervention, they don't allow however, in the most greater part of the cases, lasting benefits in the time and they involve a difficulty organization of the same with a waste of the available resources. It results therefore clear as is never necessary to succeed in also optimizing the resources thanks to the help of specific systems of

support to the decisions. This to allow the realization of those actions of functional retraining that assures the necessary conditions of reliability of the manufactured article and at the same time optimizes the employment of the aforesaid resources.

The necessity to opportunely analyze, in the phase of maintenance management of a superstructure, the manifold technical and economic aspects that intervene in the optimization of the intervention maintenance, involve the demand to individualize special mathematical criterions that allow to preliminarily appraise the best strategies of intervention, in relationship to the peculiarities of the problem in study.

For what is asked in fact it is to succeed, thanks to the software help of data processing and the programs of mathematical modeling, to simulate the behavior of the critical elements of the superstructure, succeeding to "to foretell" among how much time the breakdown will introduce him, so that to prevent and to plan to the best the interventions to perform during the useful life of the good. Such new system of diagnostic it is said " predictive diagnostic".

The mathematical formulation of the proposed problem, ago reference to the theory of the processes of decision of Markov and it allows an opportune analytical interpretation of the decisional rules.

The developed study, has allowed to reach to the definition of a special model that, beginning from the integrated analysis of the manifold components that characterize the state of I degrade some superstructure, it elaborates the best politics of intervention under the profile of the quality of march for the consumer and of the safety of exercise to the smaller middle cost for unity of time (maximum efficiency) under optimal conditions under the profile of the employment of the economic resources.

Particularly, then, from a critical analysis of the data that are noticed by the diagnostic means, the demand is underlined to accomplishedly characterize the performances assumed by every geometric parameter of the order of the platform and to examine the values assumed by the index IQB for the planning of the maintenance interventions.

To make, therefore, of easy and immediate use the results which is reached for by analytical, it is also looked out upon, in a case study example, the solution of the problem of linear planning with the relative results, coming, so, to the characterization of those specific functional rules that determine the excellent politics of intervention

through the maximization of the function objective and under conditions of not casualness (the action is deterministic function of the state j in which the superstructure is found).

It results therefore possible to define a strategy of intervention on the whole line beginning from the punctual knowledge of the states of I degrade of the single drawn optimizing at the same time the entity of the general expense in the optimality of the result in terms of efficiency of the superstructure.

For the attainment of such finalities it is opportune that they are developed new techniques of management of the maintenance that integrate the actual diagnostic methodologies to intelligent technological systems (ITS) that programs in dynamic way the maintenance interventions and the runs of verification to effect, integrated to systems of data handling type G.I.S., for which becomes the availability of a greater number of equipments of relief substantial, also installed on traditional convoy opportunely adapted, and endowed with systems G.P.S.

This would also benefit obviously to a greater control of the goodness of the maintenance interventions performed, and therefore to a best respect of the indicators of effectiveness of the intervention for assigned level of cost and for every draws examined.

RENDICONTI DEL CIRCOLO MATEMATICO DI PALERMO
Serie II, Suppl. 83 (2011), pp. 131-145

Riformattati

FIRST PASSAGE PHENOMENA FROM THE NEW PERSPECTIVE AND GENERALIZED MAXIMAL LOSS

Tadeusz Czernik
Department of Applied Mathematics
University of Economics, Katowice, Poland
tadeusz.czernik@ue.katowice.pl

This paper investigates the first passage phenomena (sometimes called first exit time or stopping problem). We propose the new method for formulating and solving problems connected with first passage phenomena. As an example we apply this method to calculation of probabilistic properties of the Generalized Maximal Loss.

Keywords: first passage time, stochastic differential equation, generalized function, risk
JEL Classification: C02, G11

1. Introduction.

Observing the phenomenon of reality that surrounds us, we often meet to those whose behaviour cannot be predicted (with certainty). This may results either from ignorance of deterministic mechanisms of evolution as well as the fact that the well-known deterministic mechanism is disturbed by random factors. Examples of these include prices of financial instruments [1] and risk processes (the terminology specific to the actuarial science) [2].

Random evolution does not mean the lack of possibility to evaluate some of the characteristics and regularities of the analyzed phenomenon. To investigate quantitatively the regularities of random

phenomena, the mathematical model should be constructed. This paper will discuss the probability of leaving a certain area by the economical process and the associated risk measure: the Generalized Maximum Loss (Generalized Maximal Loss - GML) that can be used for example in technical analysis of financial instruments, portfolio construction and risk analysis.

The essence of technical analysis is the use of regularity in prices of financial instruments to anticipate price trends. Among other things, we can ask the questions: whether the value of shares leaves trend channel (Fig. 1), what is the time during which the share price will not leave the trend channel, or whether it leaves the trend channel through lower boundary.

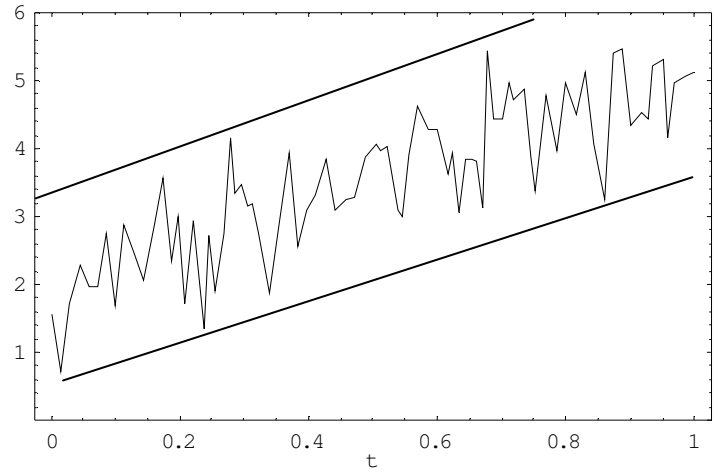

Fig.1 Trend channel

Many risk measures exists, one of the most frequently used by investors is the variance or standard deviation [3], [4], [5]. However, in accordance with modern risk theories, the variance is a measure of uncertainty rather than risk.

Value at Risk (VaR) is one of the modern risk measures [6], [7]. It has many generalizations, Maximum Loss among others (Maximal Loss - ML) [8], [9], [10]. The Maximum Loss is defined as follows:

$$P\left(S_0 - \inf_{t' \in [0,t]} S(t') < ML(\alpha, t) \right) = 1 - \alpha \qquad (1)$$

where:

S_0 - initial value of the equity price,

$ML(\alpha,t)$ Maximum Loss (Maximal Loss) on the time horizon t and the level of acceptance α.

We propose certain generalization of the Maximum Loss:

$$P\left(S_0 - \inf_{t'\in[\tau,t]} S(t') < GML(\alpha,\tau,t)\right) = 1-\alpha \tag{2}$$

where:

τ - the beginning of observation interval of the price of the instrument for its minimal value,

$GML(\alpha,\tau,t)$ - proposed generalization of the maximum loss.

Since in the limiting cases, $\tau \to 0^+$ and $\tau \to t^-$ we obtain accordingly the Maximum Loss and the Value at Risk (VaR), we can conclude that the proposed quantity is a generalization of both the Maximum Loss and Value at Risk, making it extremely attractive from both theoretical and practical point of view.

Since most stochastic models of the dynamics of financial instruments is based on the Wiener process we take into account processes whose evolution is described by ordinary stochastic differential equation (in a sense of Ito) [11], [12], [13]:

$$dS = a(S,t)dt + b(S,t)dW \tag{3}$$

where:

S - equity price,

W - Wiener process.

Under some conditions the solution of the above equation exists and is unique. Moreover solution S_t is a Markov process with almost all continuous realizations. There are many generalizations of the above evolution equation: jump-diffusion and regime-switching among others [14], [15]. Proposed method can also be used in these cases.

2. First passage time - new solution method.

First passage phenomena arises in many fields: pricing exotic instruments [1], [16], credit risk management [17], [18], [19],

portfolio optimization [8], [9], [10], ruin probabilities in insurance [2], [20], [21], [22], queues [23] and not to mention applications in other sciences such as physics [24], [25] biology, social sciences and medicine.

First passage probability (1) (first exit probability) is usually obtained by using elegant martingale technique or by solving so called Pontriagin's equations [26]. The proposed method requires only knowledge of evolution equation of the occupation probability (Kolmogorov's forward equation, also known as Fokker-Planck equation or diffusion equation) and generalized function theory [27], [28], [29]. The method involves modifying the stochastic evolution equation (3) so that the process after reaching a specific set remained in there.

In a case of Generalized Maximal Loss, modification takes the form (for the sake of simplicity we assume for the moment the barrier at level $S = 0$, hence we cannot interpret S as equity price; of course it is not a problem, because we can always transform original variable):

$$dS = a_m(S,t)dt + b_m(S,t)dW \tag{4}$$

where:

$$a_m(S,t) = a(S,t) - a(S,t)\theta_+(-S)\theta_+(t-\tau)$$

$$a_m(S,t) = a(S,t) - a(S,t)\theta_+(-S)\theta_+(t-\tau)$$

$$\theta_+(S) = \begin{cases} 0 \ for \ S < 0 \\ 1 \ for \ S \geq 0 \end{cases}.$$

Above modification means that, when process hits barrier after time τ or its value is less than barrier at time τ, it stops.

Hence we may write corresponding forward Kolmogorov's equation [11]:

$$\begin{aligned} \frac{\partial p(S,t)}{\partial t} = &-\frac{\partial}{\partial S}\left[a_m(S,t)p(S,t)\right] + \\ &+\frac{1}{2}\frac{\partial^2}{\partial S^2}\left[b_m^2(S,t)p(S,t)\right] \end{aligned} \tag{5}$$

with initial condition:

$$p(S,0) = \delta(S - S_0) \tag{6}$$

where $p(S,t)$ is the occupation probability density (or transition density function) and $\delta(S-S_0)$ is a Dirac delta function (distribution, generalized function or atomic measure) with support at point S_0.

Because it is an equation with discontinuous coefficients, solution should be sought in the set of generalized functions. We are looking for solution in the following (distributional or generalized function) form:

$$\begin{aligned} p(S,t) = {} & p_{-}(S,t)\theta_{-}(-S) + \\ & + \alpha(t)\delta(S) + p_{+}(S,t)\theta_{-}(S) \end{aligned} \tag{7}$$

where:

$$\theta_{-}(S) = \begin{cases} 0 \ for \ S \le 0 \\ 1 \ for \ S > 0 \end{cases}$$

$\alpha(t) \ge 0$ - probability that process $S_t = 0$ and integrable functions $p_{\pm}(S,t) \ge 0$ such that (normalization condition):

$$\int_{-\infty}^{0} p_{-}(S,t)dS + \alpha(t) + \int_{0}^{+\infty} p_{+}(S,t)dS = 1 \tag{8}$$

Unfortunately, we face the problem of the multiplication of distribution $p(S,t)$ and discontinuous functions $a_m(S,t)$ and $b_m(S,t)$. It is well known that in Schwartz's distribution theory such operation is not allowed. In the literature there are many solutions to this problem [30], [31]. In this paper we use a measure theoretical generalization of the distribution theory [32]. If we want to multiply the discontinuous function and distribution we have to confine itself to functions $a_m(S,t)$ and $b_m(S,t)$ with bounded variation [32]. In this case we obtain, for example:

$$\theta_{-}(S)\delta(S) = 0 \tag{9}$$

and

$$\theta_{+}(S)\delta(S) = \delta(S). \tag{10}$$

Substituting (7) into (5) we obtain the following formula:

$$\begin{aligned} & G_{-}(S,t)\theta_{-}(-S) + G_{+}(S,t)\theta_{-}(S) + \\ & + H_1(t)\delta(S) + H_2(t)\delta'(S) + H_3(t)\delta''(S) = 0 \end{aligned} \tag{11}$$

where (dependence on (S,t) was suppressed, dot and prime mean respectively time and space derivative):

$$G_{-}(S,t) = -\dot{p} - (ap)'(1-\theta_{+}(t-\tau)) + \\ + \frac{1}{2}(b^2 p)''(1-\theta_{+}(t-\tau))$$

$$G_{+}(S,t) = -\dot{p} - (ap)' + \frac{1}{2}(b^2 p)''$$

$$H_3(t) = \frac{1}{2}b^2(0,t)\alpha(t)(1-\theta_{+}(t-\tau))$$

$$H_2(t) = \frac{1}{2}\left[-b^2(0,t)p_{-}(0,t)(1-\theta_{+}(t-\tau)) + \right. \\ \left. + b^2(0,t)p_{+}(0,t)\right] - a(0,t)\alpha(t)(1-\theta_{+}(t-\tau))$$

$$H_1(t) = \frac{1}{2}\left[\left[b^2 p_{+}\right]'(0,t) + \right. \\ - \left[b^2 p_{-}\right]'(0,t)(1-\theta_{+}(t-\tau))\left.\right] + \\ + a(0,t)p_{-}(0,t)(1-\theta_{+}(t-\tau)) - \\ - a(0,t)p_{+}(0,t) - \dot{\alpha}(t)$$

Using following theorem [33]:

If $g(x)$ is a locally integrable function and β_{ij} are constants, the equality:

$$g(x) + \sum_{i=0}^{n}\sum_{j=1}^{m}\beta_{ij}\delta^{(i)}(x - x_j) = 0 \tag{12}$$

holds iff:

$$\begin{cases} g(x) = 0 \\ \beta_{ij} = 0 \quad i = 0,...,n;\ j = 1,...,m \end{cases} \tag{13}$$

we can rewrite equation (11) as follows:

$$\begin{cases} G_{-}(S,t)=0 \\ G_{+}(S,t)=0 \\ H_1(t)=0 \\ H_2(t)=0 \\ H_3(t)=0 \end{cases}. \tag{14}$$

From $H_3(t)=0$ (assuming diffusion coefficient $b(0,t)\neq 0$) we obtain:

$$\alpha(t)(1-\theta_{+}(t-\tau))=0. \tag{15}$$

Hence:

$$\begin{cases} \alpha(t)=0 \quad if\ t<\tau \\ \alpha(t)\geq 0 \quad if\ t\geq\tau \end{cases} \tag{16}$$

In fact, (15) does not mean that $\alpha(t)\geq 0$ for $t\geq\tau$, but we have to remember that $\alpha(t)$ is the probability of $S_t=0$.

Similarly, from $H_2(t)=0$ we obtain:

$$\begin{cases} p_{-}(0,t)=p_{+}(0,t) \quad for\ t<\tau \\ p_{+}(0,t)=0 \quad for\ t\geq\tau \end{cases} \tag{17}$$

Since we chose barrier level arbitrarily (at point $S=0$), from equality $p_{-}(0,t)=p_{+}(0,t)$ it is apparent that probability distribution function is continuous at points where diffusion coefficient is positive.

Following equations arises from condition $H_1(t)=0$ (where we used (17)):

$$\begin{cases} p'_{-}(0,t)=p'_{+}(0,t) \quad for\ t<\tau \\ \frac{1}{2}b^2(0,t)p'_{+}(0,t)=\dot{\alpha}(t) \quad for\ t\geq\tau \end{cases} \tag{18}$$

From $p_{+}(0,t)=0$ and $\frac{1}{2}b^2(0,t)p'_{+}(0,t)=\dot{\alpha}(t)$, one can also deduce that $\dot{\alpha}(t)\geq 0$ for $t\geq\tau$. Hence $\alpha(t)$ has to be greater than or equal to zero.

The first two conditions, can be written as follows:

$$\begin{cases} \dot{p}_-(S,t) = -\left(a(S,t)p_-(S,t)\right)' + \frac{1}{2}\left(b^2(S,t)p_-(S,t)\right)' \\ \dot{p}_+(S,t) = -\left(a(S,t)p_+(S,t)\right)' + \frac{1}{2}\left(b^2(S,t)p_+(S,t)\right)' \end{cases} \tag{19}$$

for $t < \tau$, and

$$\begin{cases} \dot{p}_-(S,t) = 0 \Rightarrow p_-(S,t) = const = p_-(S,\tau) \\ \dot{p}_+(S,t) = -\left(a(S,t)p_+(S,t)\right)' + \frac{1}{2}\left(b^2(S,t)p_+(S,t)\right)' \end{cases} \tag{20}$$

for $t \geq \tau$.

From the above conditions, we can infer that in case of $t < \tau$, evolution of probability density function $p(S,t)$ satisfies the equation:

$$\dot{p}(S,t) = -\left(a(S,t)p(S,t)\right)' + \frac{1}{2}\left(b^2(S,t)p(S,t)\right) \tag{21}$$

where $p(S,t) = p_-(S,t)\theta_-(-S) + p_+(S,t)\theta_-(S)$ is integrable function (has no distributional component $\alpha(t)\delta(S)$). It's worth noting that the probability distribution function $p(S,t)$ is not defined at point $S = 0$. Of course it is not a problem, because point $S = 0$ is not an atom of a measure $p(S,t)$ ($\alpha(t) = 0$, hence $p(S,t)$ is Lebesgue integrable and there is no need for Lebesgue-Stielties integrability).

Suppose, we've solved above equations, following problems arise: how to interpret solutions, and above all, how to determine the probability $P\left(S_0 - \inf_{t' \in [\tau,t]} S(t') < GML\right)$ defining Generalized Maximum Loss (GML).

For $t < \tau$, the probability of $S_t < 0$ equals to $\int_{-\infty}^{0} p_-(S,t)dS$. Similarly $P(S_t > 0) = \int_{0}^{+\infty} p_+(S,t)dS$ and $P(S_t = 0) = 0$ (these probabilities relate to the both unmodified and modified stochastic dynamic).

Since, the stopping region ($S_t \leq 0$) occurs at time t greater than or equal to τ, the probability of $S_t < 0$ (only modified stochastic

dynamics case) equals to $\int_{-\infty}^{0} p_{-}(S,\tau)dS = const$. Quantity $\alpha(t)$ is the probability of the following random event: $S_t = 0$ for at least one $t \geq \tau$. Integral $\int_{0}^{+\infty} p_{+}(S,t)dS$ is the conditional probability of $S_t > 0 / (\forall t \geq \tau : S_t > 0)$ (in either modified and unmodified stochastic dynamics case).

From the foregoing, one can conclude that, probability $P\left(S_0 - \inf_{t' \in [\tau,t]} S(t') \geq GML \right)$ is given by (for $t \geq \tau$):

$$P\left(S_0 - \inf_{t' \in [\tau,t]} S(t') \geq GML \right) = \alpha(t) + \int_{-\infty}^{0} p_{-}(S,\tau)dS \tag{22}$$

3. Generalized Maximum Loss – geometric Brownian motion case.

The considerations in the previous part of this paper were carried out for any stochastic dynamics, described by equation (3) (provided that there are solutions to that equation, see [11]). In this section, we consider the price of a financial instrument (equity) whose stochastic evolution is described by the stochastic differential equation [1]:

$$dS = \mu S dt + \sigma S dW \tag{23}$$

where:

$\mu = const$ - drift coefficient,

$\sigma = const$ - volatility.

Strong solution [11] is given by:

$$S_t = S_0 e^{\left(\mu - \frac{1}{2}\sigma^2\right)t + \sigma W_t} \tag{24}$$

where S_0 is the initial equity price.

Assume stopping barrier is fixed at point (price) S_b.

The following transformation (monotonic):

$$x = \log \frac{S}{S_b} \tag{25}$$

defines new stochastic process (using Ito theorem [11]):

$$dx = \left(\mu - \frac{1}{2}\sigma^2 \right) dt + \sigma dW \tag{26}$$

whose strong solution is given by:

$$x_t = x_0 + \left(\mu - \frac{1}{2}\sigma^2 \right) t + \sigma W_t \tag{27}$$

where initial value $x_0 = \log \frac{S_0}{S_b}$.

It is clear that:

$$\begin{aligned} &P\left(S_0 - \inf_{t' \in [\tau, t]} S_{t'} < GML \right) = \\ &= P\left(S_0 - \inf_{t' \in [\tau, t]} S_{t'} < S_0 - S_b \right) = 1 - P\left(\inf_{t' \in [\tau, t]} S_{t'} \le S_b \right) \end{aligned} \tag{28}$$

and

$$P\left(\inf_{t' \in [\tau, t]} S_{t'} \le S_b \right) = P\left(\inf_{t' \in [\tau, t]} x_{t'} \le 0 \right) \tag{29}$$

Hence, one can use results from previous part and focus attention on the process x_t.

Forward Kolmogorov equation, corresponding to equation (26) has the form (unmodified stochastic dynamics):

$$\begin{aligned} \frac{\partial p(x,t)}{\partial t} = &- \frac{\partial}{\partial x}\left[\left(\mu - \frac{1}{2}\sigma^2 \right) p(x,t) \right] + \\ &+ \frac{1}{2}\frac{\partial^2}{\partial x^2}\left[\sigma^2 p(x,t) \right] \end{aligned} \tag{30}$$

with initial condition $p(x,0) = \delta(x - x_0)$.

Using a modification technique, described in Part 2 and after some algebra, one obtain for $t < \tau$:

$$\frac{\partial p(x,t)}{\partial t} = -\left(\mu - \frac{1}{2}\sigma^2\right)\frac{\partial}{\partial x}p(x,t) + \\ + \frac{1}{2}\sigma^2\frac{\partial^2}{\partial x^2}p(x,t) \tag{31}$$

where $p(x,t) = p_-(x,t)\theta_-(-x) + p_+(x,t)\theta_-(x)$ with initial condition $p(x,0) = \delta(x - x_0)$.

Well known solution of the equation (31) has the form:

$$p(x,t) = \frac{1}{\sqrt{2\pi t}\sigma}e^{-\frac{\left(x - x_0 - \left(\mu - \frac{1}{2}\sigma^2\right)t\right)^2}{2\sigma^2 t}} \tag{32}$$

For $t \geq \tau$, one can obtain:

$$\begin{cases} p_-(x,\tau) = \dfrac{1}{\sqrt{2\pi\tau}\sigma}e^{-\frac{\left(x - x_0 - \left(\mu - \frac{1}{2}\sigma^2\right)\tau\right)^2}{2\sigma^2\tau}} \\ \dot{p}_+(x,t) = -\left(\mu - \dfrac{1}{2}\sigma^2\right)p'_+(x,t) + \dfrac{1}{2}\sigma^2 p''_+(x,t) \\ p_+(0,t) = 0 \\ p_+(x,\tau) = \dfrac{1}{\sqrt{2\pi\tau}\sigma}e^{-\frac{\left(x - x_0 - \left(\mu - \frac{1}{2}\sigma^2\right)\tau\right)^2}{2\sigma^2 t}}\theta_-(x) \\ \dot{\alpha}(t) = \dfrac{1}{2}\sigma^2 p'_+(0,t) \\ \alpha(\tau) = 0 \end{cases} \tag{33}$$

In order to simplify calculations, we can make a translation of time $t_1 = t - \tau$ and instead of the initial condition

$$p_+(x,\tau) = \frac{1}{\sqrt{2\pi\tau}\sigma}e^{-\frac{\left(x - x_0 - \left(\mu - \frac{1}{2}\sigma^2\right)\tau\right)^2}{2\sigma^2\tau}}\theta_-(x)$$

assume for the moment new initial value condition $p_+(x,t_1 = 0) = \delta(x - x_1)$ where x_1 is chosen arbitrarily but greater than zero (technique similar to conditioning or Green's function method).

Taking the Laplace transform of the

$$\dot{p}_+(x,t_1) = -\left(\mu - \frac{1}{2}\sigma^2\right)p'_+(x,t_1) + \frac{1}{2}\sigma^2 p''_+(x,t_1)$$

with respect to time, one can obtain:

$$\begin{aligned} s\hat{p}_+(x,s) - \delta(x-x_1) = -\left(\mu - \frac{1}{2}\sigma^2\right)\hat{p}'_+(x,s) + \\ + \frac{1}{2}\sigma^2 \hat{p}''_+(x,s) \end{aligned} \tag{34}$$

where $\hat{p}_+(x,s) = \int_0^{+\infty} e^{-st_1} p_+(x,t_1)dt_1$.

Next, taking the Laplace transform of the (34) with respect to x:

$$\begin{aligned} s\tilde{\hat{p}}_+(u,s) - e^{-ux_1} = -\left(\mu - \frac{1}{2}\sigma^2\right)u\tilde{\hat{p}}_+(u,s) + \\ + \frac{1}{2}\sigma^2\left[u^2\tilde{\hat{p}}_+(u,s) - \frac{2}{\sigma^2}s\hat{\alpha}(s)\right] \end{aligned} \tag{35}$$

where $\tilde{\hat{p}}_+(u,s) = \int_0^{+\infty} e^{-ux} p_+(x,s)dx$.

Solving (35) with respect to $\tilde{\hat{p}}_+(u,s)$, we can write:

$$\tilde{\hat{p}}_+(u,s) = \frac{e^{-ux_1} - s\alpha(s)}{s + \left(\mu - \frac{1}{2}\sigma^2\right)u - \frac{1}{2}\sigma^2 u^2} \tag{36}$$

The denumerator has two roots:

$$u_1 = \frac{\left(\mu - \frac{1}{2}\sigma^2\right) + \sqrt{\left(\mu - \frac{1}{2}\sigma^2\right)^2 + 2\sigma^2 s}}{\sigma^2} \tag{37}$$

and

$$u_1 = \frac{\left(\mu - \frac{1}{2}\sigma^2\right) - \sqrt{\left(\mu - \frac{1}{2}\sigma^2\right)^2 + 2\sigma^2 s}}{\sigma^2} \tag{38}$$

Because the image of the required solution must be an analytic

function for all values u and s in the region defined by the inequalities $\mathrm{Re}\,u > c_1$, $\mathrm{Re}\,s > c_2$ (where c_1 and c_2 are two suitably chosen constants) [34], the numerator of the right side of (36) must be equal zero when:

$$u = \frac{\left(\mu - \frac{1}{2}\sigma^2\right) + \sqrt{\left(\mu - \frac{1}{2}\sigma^2\right)^2 + 2\sigma^2 s}}{\sigma^2} \tag{39}$$

In other words:

$$e^{-\frac{\left(\mu-\frac{1}{2}\sigma^2\right)+\sqrt{\left(\mu-\frac{1}{2}\sigma^2\right)^2+2\sigma^2 s}}{\sigma^2}x_1} - s\alpha(s) = 0 \tag{40}$$

Hence, we can write:

$$\alpha(s) = \frac{1}{s} e^{-\frac{\left(\mu-\frac{1}{2}\sigma^2\right)+\sqrt{\left(\mu-\frac{1}{2}\sigma^2\right)^2+2\sigma^2 s}}{\sigma^2}x_1} \tag{41}$$

and

$$\tilde{\tilde{p}}_+(u,s) = \frac{e^{-\frac{\left(\mu-\frac{1}{2}\sigma^2\right)+\sqrt{\left(\mu-\frac{1}{2}\sigma^2\right)^2+2\sigma^2 s}}{\sigma^2}x_1} - s\alpha(s)}{s + \left(\mu - \frac{1}{2}\sigma^2\right)u - \frac{1}{2}\sigma^2 u^2} \tag{42}$$

In order to determine $p_+(x,t_1)$ we have to calculate inverse transforms of the (42). However, from the Generalized Maximum Loss point of view, we do not have to invert (42), because determination of probability $P\left(\inf_{t'\in[\tau,t]} x_{t'} \le 0\right)$ requires only knowledge of $\alpha(t)$ and $p_-(x,\tau)$. Hence, we still need $\alpha(t)$ only. Straightforward calculations gives [35]:

$$\alpha(t_1) = 2e^{\frac{\left(\mu-\frac{1}{2}\sigma^2\right)}{\sigma^2}x_0} \frac{1}{\sqrt{2\pi}} \int_{\sqrt{\frac{x_1^2}{\sigma^2 t_1}}}^{+\infty} e^{-\frac{\left(\mu-\frac{1}{2}\sigma^2\right)^2 x_1^2}{2(\sigma^2)^2 z^2}} e^{-\frac{z^2}{2}} dz \tag{43}$$

Above formula can rewritten as follows:

$$\alpha(t)=N\left(\frac{-x_1-\left(\mu_\Pi-\frac{1}{2}\sigma_\Pi^2\right)(t-\tau)}{\sigma_\Pi\sqrt{t-\tau}}\right)+ \\ +e^{\left(-\frac{2\mu_\Pi}{\sigma_\Pi^2}+1\right)x_1}N\left(\frac{-x_1+\left(\mu_\Pi-\frac{1}{2}\sigma_\Pi^2\right)(t-\tau)}{\sigma_\Pi\sqrt{(t-\tau)}}\right) \tag{44}$$

where $N(x)$ is a cumulative distribution function of the standard normal distribution.

Since, the expression (44) is the conditional probability $P\left(\inf_{t'\in[\tau,t]}x_{t'}\le 0/x_\tau=x_1>0\right)$, we have to return to original initial condition $p_+(x,\tau)=\frac{1}{\sqrt{2\pi\tau}\sigma}e^{-\frac{\left(x-x_0-\left(\mu-\frac{1}{2}\sigma^2\right)\tau\right)^2}{2\sigma^2 t}}\theta_-(x)$:

$$\alpha(t)=\int_0^{+\infty}\left[N\left(\frac{-x_1-\left(\mu_\Pi-\frac{1}{2}\sigma_\Pi^2\right)(t-\tau)}{\sigma_\Pi\sqrt{t-\tau}}\right)+\right. \\ \left.+e^{\left(-\frac{2\mu_\Pi}{\sigma_\Pi^2}+1\right)x_1}N\left(\frac{-x_1+\left(\mu_\Pi-\frac{1}{2}\sigma_\Pi^2\right)(t-\tau)}{\sigma_\Pi\sqrt{(t-\tau)}}\right)\right]. \tag{45}$$
$$\frac{1}{\sqrt{2\pi\tau}\sigma}e^{-\frac{\left(x_1-x_0-\left(\mu-\frac{1}{2}\sigma^2\right)\tau\right)^2}{2\sigma^2\tau}}dx_1$$

Hence, the probability of Generalized Maximum Loss be greater than or equal to S_0-S_b can be expressed as follows:

$$P(GML\ge S_0-S_b)=\alpha(t)+\int_{-\infty}^{0}p_-(S,\tau)dS \tag{46}$$

where $\alpha(t)$ and $p_{-}(S,\tau)$ are given, respectively, by (45) and (33).

It's worth noting, that, $\frac{1}{\sqrt{2\pi\tau}\sigma} e^{-\frac{\left(x-x_0-\left(\mu-\frac{1}{2}\sigma^2\right)\tau\right)^2}{2\sigma^2 t}}$ converges in distributional sense to $\delta(x-x_0)$ as $\tau \to 0^+$. Hence, Generalized Maximal Loss converges to Maximal Loss.

Formula (46) can be used, for example, in risk quantification and portfolio optimization. Technique used to modifying of stochastic differential equation, may also be applied in processes modulated by an additional Markov switching process [36].

SOURCES:

1. Wilmott P., Paul Wilmott on Quantitative Finance, Wiley, 2006,
2. Rolski T., Schmidli H., Schmidt V., Teugels J., Stochastic Processes for Insurance and Finance, Wiley 1999,
3. Chincarini L.B., Kim D., Quantitative Equity Portfolio Management: An Active Approach to Portfolio Construction and Management, McGraw-Hill. 2006,
4. Merton R.C., Continuous-time finance, Blackwell, 2001,
5. Meucci A., Risk and asset allocation, Springer,2005,
6. McNeil A.J., Frey R., Embrechts P., Quantitative risk management. Concepts, techniques, tools. Princeton University Press, 2005,
7. Jorion P., Value at Risk: The New Benchmark for Managing Financial Risk, McGraw-Hill, 2000,
8. Acar E., James S., Maximum loss and maximum drawdown in financial markets. "International Conference Forecasting Financial Markets", London, 1997,
9. Czernik T., Maximal Loss as a risk measure, in Modeling preferences and risk, Trzaskalik T. ed., University of Economics in Katowice, 2003, (in Polish)
10. Czernik T., Portfolio optimization – Maximum Loss, University of Szczecin, 389, 2004, (in Polish),
11. Øksendal B., Stochastic Differential Equations: An Introduction with Applications, Springer, 2010,
12. Gardiner C.W., Handbook of Stochastic Methods, Springer-Verlag, 1985,
13. Pugaczev W.S., Sinicyn I.N., Stochastic differential system, Nauka, 1985 (in Russian),

14. Cont R., Tankov P., Financial modelling with jump processes, Chapman and Hall/CRC, 2004,
15. Mao X., Yuan Ch., Stochastic Differential Equations With Markovian Switching, Imperial College Press, 2006,
16. Zhang P.G., Exotic options. A guide tosecond generation options. World Scientific, 2001.
17. Amman M., Credit risk valuation. Methods, models, and applications, Springer, 2001,
18. Duffie D., Singleton K.J., Credit risk. Pricing, Measurement, and Management, Princeton University Press, 2003,
19. Bielecki T.R., Rutkowski M., Credit Risk: Modeling, Valuation and Hedging, Springer, 2002,
20. Dickson D.C.M., Insurance, risk and ruin, Cambridge University Press, 2005,
21. Panjer H.H., Willmot G.E., Insurance risk models, Society of Actuaries,1992,
22. Asmussen S., Ruin probabilities, World Scientific, 2000,
23. Asmussen S. Applied probability and queues, Springer, 2003,
24. Redner S., A guide to First-Passage processes, Cambridge University Press, 2001,
25. Risken H., The Fokker-Planck Equation: Methods of Solutions and Applications, Springer, 1996,
26. Tihonov W.I., Mironov M.,A., Markov processes, Sovietskoje Radio, 1977, (in Russian),
27. Schwartz L., Mathematics for the physical sciences, Dover, 1966,
28. Zemanian A.H., Distribution theory and transform analysis. An introduction to generalized functions, with applications, Dover, 1965,
29. Brychkov Ju., Prudnikov A.P., Integral transforms of generalized functions, Nauka, 1977, (in Russian),
30. Antosik P., Mikusiński J., Sikorski R., Theory of distributions. The sequential approach. Mir, 1976, (in Russian),
31. Colombeau J.F., New generalized functions and multiplication of distributions, North-Holland,
32. Wyderka Z., Linear differential equations with measures as coefficients and control theory, University of Silesia in Katowice, 1994,
33. Kecs W., Teodorescu P.P., Applications of the theory of distributions in mechanics, Editura Academiei Romane and Abacus Press, 1974,
34. Ditkin V.A., Prudnikov A.P., Operational calculus in two variables and its applications, Pergamon Press, 1962,
35. Prudnikov A.P., Brychkov Yu.A., Marichev A.I., Integrals and series. Inverse Laplace transforms, Gordon and breach Science Publishers, 1992,
36. Czernik T., Risk measures of the family FPRM (First Passage Risk Measures) for markets modulated by Markov processes, working papers, University of Economics in Katowice, 2008

RENDICONTI DEL CIRCOLO MATEMATICO DI PALERMO
Serie II, Suppl. 83 (2011), pp. 147-160

La funzione di distribuzione di una corda in un trapezio rettangolo

Andrei Duma e Sebastiano Rizzo

0. Introduzione

Sia $\mathcal{R}_D$ il reticolo di Buffon formato da rette parallele a distanza D l'una dall'altra. Nei lavori di Conserva, Duma, Pettineo, Rizzo e Stoka pubblicate nel 2007 e 2008 sono state calcolate le probabilità che un poligono convesso P con diametro minore di D (quindi P è "piccolo" rispetto a $\mathcal{R}_D$) intersechi su una delle rette di $\mathcal{R}_D$ un segmento di lunghezza maggiore o uguale ad un numero s, $0 \leq s \leq \operatorname{diam}(P)$. Si può calcolare in maniera analoga la stessa probabilità condizionata se P è un poligono regolare convesso con un numero arbitrario di lati. Se P è un trapezio, per calcolare tale probabilità, occorre considerare un gran numero di casi poiché tra le dimensioni dei lati, delle diagonali e delle altezze sono possibili diverse relazioni. Per tale motivo in tale lavoro si è scelto di considerare un trapezio rettangolo.

1. Il problema

Ci proponiamo di calcolare la probabilità $p(s)$ che il trapezio rettangolo T (vedi fig. 1) con $\operatorname{diam}(T) \leq D$ intersechi un segmento di lunghezza maggiore o uguale al numero s, $0 \leq s \leq \operatorname{diam}(T)$, su una retta di $\mathcal{R}_D$.

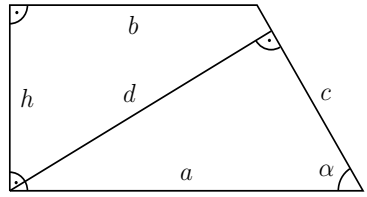

Fig. 1: Il trapezio T

Senza ledere la generalità sia $b \leq a$ dunque $0 < \alpha \leq \frac{\pi}{2}$, $h \leq c$, $b \leq d \leq \min(a, \sqrt{b^2+h^2})$, $\leq \max(a, \sqrt{b^2+h^2}) \leq \sqrt{a^2+h^2}$. Non esistono in generale altre relazioni tra a, b, c, d, h, $\sqrt{b^2+h^2}$ e $\sqrt{a^2+h^2}$. Occorre considerare in maniera separata i due casi $h \leq b$ (e le situazioni I, II,..., VIII) e $h > b$ (e le situazioni $1°, 2°, \ldots, 16°$).

I $\quad h \leq c \leq b \leq d \leq \sqrt{b^2+h^2} \leq a < \sqrt{a^2+h^2}$,

II $\quad h \leq b \leq d \leq c \leq \sqrt{b^2+h^2} \leq a < \sqrt{a^2+h^2}$,

III $\quad h \leq b \leq c \leq d \leq \sqrt{b^2+h^2} \leq a < \sqrt{a^2+h^2}$,

IV $\quad h \leq c \leq b \leq d \leq a \leq \sqrt{b^2+h^2} \leq \sqrt{a^2+h^2}$,

V $\quad h \leq b \leq d \leq c \leq a \leq \sqrt{b^2+h^2} \leq \sqrt{a^2+h^2}$,

VI $\quad h \leq b \leq c \leq d \leq a \leq \sqrt{b^2+h^2} \leq \sqrt{a^2+h^2}$,

VII $h \le b \le d \le \sqrt{b^2+h^2} \le c \le a < \sqrt{a^2+h^2}$,

VIII $h \le b \le d \le a \le c \le \sqrt{b^2+h^2} \le \sqrt{a^2+h^2}$,

e

1° $b < h \le d \le c \le \sqrt{b^2+h^2} \le a < \sqrt{a^2+h^2}$,

2° $b < h \le c \le d \le \sqrt{b^2+h^2} \le a < \sqrt{a^2+h^2}$,

3° $b < h \le d \le c \le a \le \sqrt{b^2+h^2} < \sqrt{a^2+h^2}$,

4° $b < h \le c \le d \le a \le \sqrt{b^2+h^2} < \sqrt{a^2+h^2}$,

5° $b < h \le d \le a \le c \le \sqrt{b^2+h^2} < \sqrt{a^2+h^2}$,

6° $b < h \le d \le a \le \sqrt{b^2+h^2} \le c < \sqrt{a^2+h^2}$,

7° $b < h \le d \le \sqrt{b^2+h^2} \le c \le a < \sqrt{a^2+h^2}$,

8° $b < h \le d \le \sqrt{b^2+h^2} \le a \le c < \sqrt{a^2+h^2}$,

9° $b < d \le h \le a \le c \le \sqrt{b^2+h^2} < \sqrt{a^2+h^2}$,

10° $b < d \le h \le a \le \sqrt{b^2+h^2} \le c < \sqrt{a^2+h^2}$,

11° $b < d < a \le h < \sqrt{b^2+h^2} \le c < \sqrt{a^2+h^2}$,

12° $b < d \le h < \sqrt{b^2+h^2} \le a \le c < \sqrt{a^2+h^2}$,

13° $b < d < a \le h < c \le \sqrt{b^2+h^2} < \sqrt{a^2+h^2}$,

14° $b < d \le h < \sqrt{b^2+h^2} \le c \le a < \sqrt{a^2+h^2}$,

15° $b < d \le h \le c \le a < \sqrt{b^2+h^2} < \sqrt{a^2+h^2}$,

16° $b < d \le a \le c \le h < \sqrt{b^2+h^2} < \sqrt{a^2+h^2}$.

Per ogni situazione dobbiamo considerare 7 sottocasi risultanti dalle relazioni tra s e le dimensioni $a, b, c, d, h, \sqrt{b^2+h^2}$ e $\sqrt{a^2+h^2}$. Per esempio nel caso I $h \le c \le b \le d \le \sqrt{b^2+h^2} \le a < \sqrt{a^2+h^2}$ si hanno i sottocasi $s \le h$, $h \le s \le c$, $c \le s \le b, \ldots, a \le s \le \sqrt{a^2+h^2}$.

Ci sono più di 100 casi diversi, ma per fortuna non sempre occorre fare dei calcoli separati perché alcuni sottocasi si possono calcolare simultaneamente; ciò accade per esempio per i sottocasi "estremi" $s \le \min(b, d)$ e $\max(a, c, \sqrt{b^2+^2}) \le s \le \sqrt{a^2+h^2}$. Faremo i calcoli di $p(s)$ per diversi sottocasi; nei sottocasi rimanenti i calcoli si effettuano in maniera analoga.

Indichiamo con φ l'angolo tra la direzione delle rette di $\mathcal{R}_D$ e il lato orientato a, come nella figura 2.

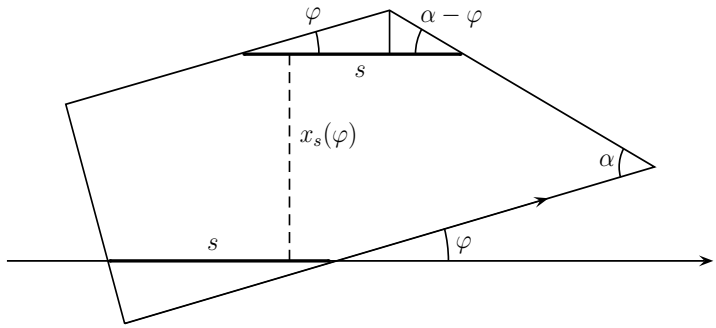

Fig. 2: La definizione di φ e $x_s(\varphi)$

Se φ varia nell'intervallo $[0, \pi[$ si ottengono esattamente una volta tutte le situazioni possibili tra T e $\mathcal{R}_D$. Sia $\varphi \in [0, \pi[$ e indichiamo con $x_s(\varphi)$ la distanza tra due segmenti paralleli di lunghezza s secanti T (come in fig. 2). Secondo una formula di Stoka si ha:

$$p(s) = \frac{\int_0^{\pi} x_s(\varphi)d\varphi}{\int_0^{\pi} D d\varphi} = \frac{1}{\pi D}\int_0^{\pi} x_s(\varphi)d\varphi. \tag{1}$$

Il nostro lavoro si riduce quindi alla determinazione della funzione $x_s(\varphi)$ e al calcolo dell'integrale di $x_s(\varphi)$ tra 0 e π.

2. Il sottocaso $\mathbf{s \leq \min(b, h)}$

La funzione $x_s(\varphi)$ assume diverse espressioni a seconda che φ vari negli intervalli $[0, \alpha]$, $[\alpha, \frac{\pi}{2}]$ e $[\frac{\pi}{2}, \pi[$. Se $\varphi \in [0, \alpha]$ risulta

$$x_s(\varphi) = h\cos\varphi + b\sin\varphi + \frac{s}{2}(-2\sin 2\varphi - \cot\alpha\cos 2\varphi + \cot\alpha), \tag{2}$$

e quindi

$$\int_0^{\alpha} x_s(\varphi)d\varphi = h\sin\alpha + b(1-\cos\alpha) + \frac{s}{4}(2\cos 2\alpha - 2 - \cot\alpha\sin 2\alpha + 2\alpha\cot\alpha). \tag{2'}$$

Se $\varphi \in [\alpha, \frac{\pi}{2}]$ risulta dalla figura 3

$$x_s(\varphi) = a\sin\varphi - \frac{s}{2}(\cot\alpha - \cot\alpha\cos 2\varphi) \tag{3}$$

e quindi

$$\int_{\alpha}^{\frac{\pi}{2}} x_s(\varphi)d\varphi = a\cos\alpha - \frac{s}{4}((\pi - 2\alpha)\cot\alpha + \sin 2\alpha\cot\alpha). \tag{3'}$$

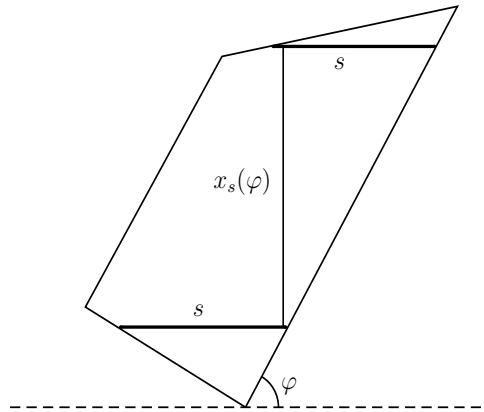

Fig. 3: $\alpha \leq \varphi < \frac{\pi}{2}$

Se $\varphi \in [\frac{\pi}{2}, \pi[$ risulta dalla figura 4

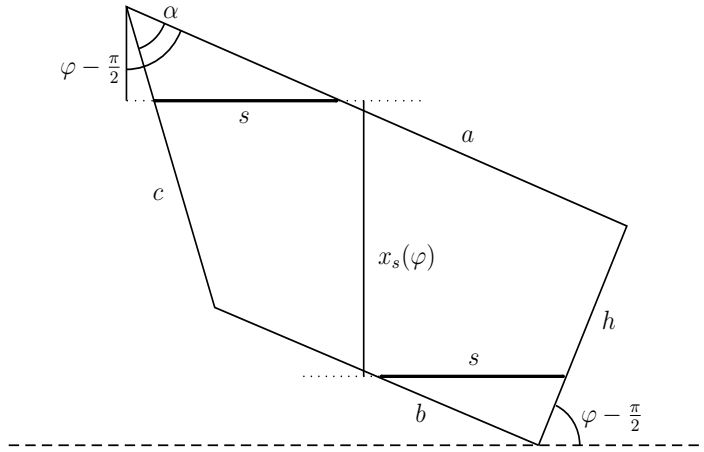

Fig. 4: $\frac{\pi}{2} \leq \varphi < \pi$

$$x_s(\varphi) = a\sin\varphi - h\cos\varphi + s\sin 2\varphi - \frac{s}{2}\cot\alpha + \frac{s}{2}\cot\alpha\cos 2\varphi \tag{4}$$

e quindi

$$\int_{\frac{\pi}{2}}^{\pi} x_s(\varphi)d\varphi = a + h - \frac{s}{4}(4 + \pi\cot\alpha). \tag{4'}$$

In conclusione in questo sottocaso si ha:

$$\int_0^{\pi} x_s(\varphi)d\varphi = a(1+\cos\alpha)+b(1-\cos\alpha)+h(1+\sin\alpha)-\frac{s}{2}\left[3-\cos 2\alpha+(\pi-2\alpha+\sin 2\alpha)\cot\alpha\right],$$

e quindi utilizzando la formula (1):

$$(5)\; p(s) = \frac{a(1+\cos\alpha)+b(1-\cos\alpha)+h(1+\sin\alpha)-\frac{s}{2}[3-\cos 2\alpha+(\pi-2\alpha+\sin 2\alpha)\cot\alpha]}{\pi D}$$

In particolare se $s=0$ si ritrova la formula ben nota

$$p(0) = \frac{a(1+\cos\alpha)+b(1-\cos\alpha)+h(1+\sin\alpha)}{\pi D} = \frac{a+b+c+h}{\pi D}\,.$$

3. Il sottocaso $\mathbf{h \le s \le \min(b,c,d)}$

Questo sottocaso è comune ai casi I e IV. Dobbiamo considerare l'angolo $\varphi_0 \in [\alpha, \frac{\pi}{2}]$ univocamente determinato dalla relazione $s\sin\varphi_0 = h$; per $\varphi \in]\varphi_0, \pi-\varphi_0[$ si ha $s\sin\varphi > h$ e dunque $x_s(\varphi)=0$. Altrimenti si può utilizzare il sottocaso precedente, cioè (2) e (2') per $\varphi\in[0,\alpha]$, (3) per calcolare $\int_\alpha^{\varphi_0} x_s(\varphi)d\varphi$ e (4) per calcolare $\int_{\pi-\varphi_0}^{\pi} x_s(\varphi)d\varphi$. Con

$$(3'')\qquad \int_\alpha^{\varphi_0} x_s(\varphi)d\varphi = a(\cos\alpha-\cos\alpha_0)+\frac{s}{4}(2\alpha-2\varphi_0+\sin 2\varphi_0-\sin 2\alpha)\cot\alpha\,.$$

e

$$(4'')\qquad \int_{\pi-\varphi_0}^{\pi} x_s(\varphi)d\varphi = a(1-\cos\varphi_0) = +h\sin\varphi_0+\frac{s}{4}(2\cos 2\varphi_0-2+\cot\alpha\sin 2\varphi_0 - 2\varphi_0\cot\alpha)$$

abbiamo

$$\int_0^{\pi} x_s(\varphi)d\varphi = a(1-2\cos\varphi_0+\cos\alpha)+b(1-\cos\alpha)+h(\sin\alpha+\sin\varphi_0) + \frac{s}{2}(-2+\cos 2\alpha+\cos 2\varphi_0+(2\alpha-\sin 2\alpha-2\varphi_0+\sin 2\varphi_0)\cot\alpha)$$

e quindi si ottiene:

$$(7)\qquad p(s) = \frac{1}{\pi D}\big[a(1-2\cos\varphi_0+\cos\alpha)+b(1-\cos\alpha)+h(\sin\alpha+\sin\varphi_0) + \frac{s}{2}(-2+\cos 2\alpha+\cos 2\varphi_0+(2\alpha-\sin 2\alpha-2\varphi_0+\sin 2\varphi_0)\cot\alpha)\big]\,.$$

Si osservi (e tale osservazione serve anche come prova della correttezza dei calcoli) che se $s=h$ si ha $\varphi_0=\frac{\pi}{2}$ e quindi la formula (7) coincide con la (5).

4. Il sottocaso $\mathbf{h \le c \le s \le b}$

Questo sottocaso appare nei casi I e IV. Anche qui utilizziamo l'angolo φ_0 definito da $s \sin \varphi_0 = h$, ma questa volta si ha $\varphi_0 \in [0, \alpha]$. Se $\varphi \in [0, \varphi_0]$ e $\varphi \in [\pi - \varphi_0, \pi]$ l'espressione di $x_s(\varphi)$ è data da (2) rispettivamente da (4); con:

$$\int_0^{\varphi_0} x_s(\varphi) d\varphi = b(1 - \cos \varphi_0) + h \sin \varphi_0 + \frac{s}{4}(2 \cos 2\varphi_0 - 2 + 2\varphi_0 \cot \alpha - \cot \alpha \sin 2\varphi_0)$$

e con (4") abbiamo

$$\int_0^{\pi} x_s(\varphi) d\varphi = (a + b)(1 - \cos \varphi_0) + 2h \sin \varphi_0 - s(1 - \cos 2\varphi_0) \tag{8}$$

ne segue

$$p(s) = \frac{1}{\pi D}\left[(a + b)(1 - \cos \varphi_0) + 2h \sin \varphi_0 - s(1 - cos 2\varphi_0)\right]. \tag{9}$$

Se $s = c$, si ha $\varphi_0 = \alpha$ e le formule (7) e (9) forniscono lo stesso risultato

$$p(c) = \frac{1}{\pi D}[(a + b)(1 - \cos \alpha) + 2h \sin \alpha - s(1 - \cos 2\alpha)] \, .$$

5. Il sottocaso $\max(\mathbf{h}, \mathbf{c}, \mathbf{b}) \le \mathbf{s} \le \mathbf{d}$

Questo sottocaso serve per i casi I, III, IV, VI, 2° e 4°. Stavolta oltre all'angolo φ_0 definito come precedentemente, occorre considerare gli angoli φ_1 e φ_2 definiti (vedere anche la figura 5) da $\sin(\alpha - \varphi_1) = b \sin \alpha$ e $s \cos \varphi_2 = b$.

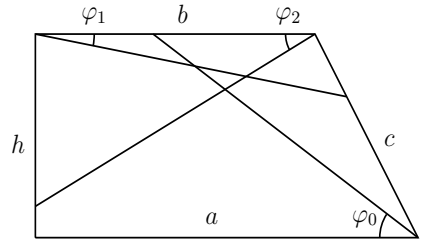

Fig. 5: Gli angoli φ_0, φ_1 e φ_2

Risulta $\varphi_1 \le \varphi_2 \le \varphi_0 \le \alpha$. La distanza $x_s(\varphi)$ tra le due secanti di lunghezza s si calcola per $\varphi \in [\varphi_1, \varphi_2]$ e $\varphi \in [\pi - \varphi_0, \pi - \varphi_2]$ con la formula (2) rispettivamente (4). Quindi:

$$\begin{aligned} \int_{\varphi_1}^{\varphi_0} x_s(\varphi) d\varphi \;\; &= \;\; h(\sin \varphi_0 - \sin \varphi_1) + b(\cos \varphi_1 - \cos \varphi_0) + \frac{s}{4}(2 \cos 2\varphi_0 - \\ &\qquad 2 \cos 2\varphi_1 + (\sin 2\varphi_1 - \sin 2\varphi_0 + 2\varphi_0 - 2\varphi_1) \cot \alpha) \, , \end{aligned} \tag{2"}$$

$$(4''') \qquad \int_{\pi-\varphi_0}^{\pi-\varphi_2} x_s(\varphi)d\varphi = a(\cos\varphi_2 - \cos\varphi_0) + h(\sin\varphi_0 - \sin\varphi_2) + \frac{s}{4}(2\cos 2\varphi_0 - 2\cos 2\varphi_2 + (2(\varphi_2 - \varphi_0) + \sin 2\varphi_0 - \sin 2\varphi_2)\cot\alpha)\ .$$

Quando $\varphi \in [0, \varphi_1]$ si ottiene (vedere anche la figura 6):

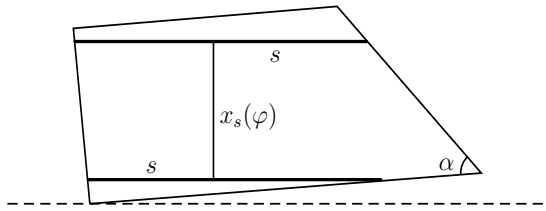

Fig 6: $s > b$ e φ piccolo

$$(10) \qquad x_s(\varphi) = b\tan\alpha\cos\varphi + h\cos\varphi - \frac{s}{2}(1 + \cos 2\varphi)\tan\alpha$$

e quindi

$$(10') \qquad \int_0^{\varphi_1} x_s(\varphi)d\varphi = b\tan\alpha\sin\varphi_1 + h\sin\varphi_1 - \frac{s}{4}(2\varphi_1 + \sin 2\varphi_1)\tan\alpha.$$

L'espressione di $x_s(\varphi)$ quando φ varia nell'intervallo $[\pi - \varphi_2, \pi]$ (vedere anche la fig. 7)

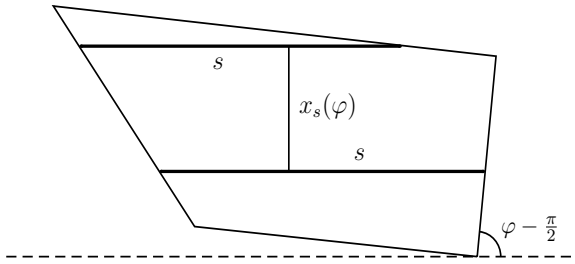

Fig. 7: $s > b$ e φ vicino a π

è

$$(11) \qquad x_s(\varphi) = a\sin\varphi - b\tan\alpha\cos\varphi - h\cos\varphi + s\sin 2\varphi - \frac{s}{\sin 2\alpha} + s\cot 2\alpha\cos 2\varphi.$$

Da cui

$$(11') \qquad \int_{\pi-\varphi_2}^{\pi} x_s(\varphi)d\varphi = a(1 - \cos\varphi_2) + b\tan\alpha\sin\varphi_2 + h\sin\varphi_2 - \frac{s\varphi_2}{\sin 2\alpha} + \frac{s}{2}\cot 2\alpha\sin 2\varphi_2 - \frac{s}{2}(1 - \cos 2\varphi_2)\ ,$$

e quindi

$$\begin{aligned}\int_0^{\pi} x_s(\varphi)d\varphi &= a(1-\cos\varphi_0)+b(\tan\alpha(\sin\varphi_1+\sin\varphi_2)+\cos\varphi_1-\cos\varphi_0)\\ &\quad +2h\sin\varphi_0+\frac{s}{2}(-1-\cos 2\varphi_1+2\cos 2\varphi_0+\cot 2\alpha(\sin 2\varphi_1+\sin 2\varphi_2)\\ &\quad -\frac{\varphi_1+\varphi_2}{\sin 2\alpha}+(\varphi_2-\frac{1}{2}\sin 2\varphi_2)\cot\alpha)\ ,\end{aligned}$$

$$\begin{aligned}p(s) &= \frac{1}{\pi D}[a(1-\cos\varphi_0)+b(\tan\alpha(\sin\varphi_1+\sin\varphi_2)+\cos\varphi_1-\cos\varphi_0)\\ &\quad +2h\sin\varphi_0+\frac{s}{2}(-1-\cos 2\varphi_1+2\cos 2\varphi_0+\cot 2\alpha(\sin 2\varphi_1+\sin 2\varphi_2)\\ &\quad -2\frac{\varphi_1+\varphi_2}{\sin 2\alpha}+(\varphi_2-\frac{1}{2}\sin 2\varphi_2)\cot\alpha)]\ .\end{aligned} \tag{12}$$

Se $h \le c \le b = s \le d$, allora $\varphi_1 = \varphi_2 = 0$ e le formule (9) e (12) danno:

$$p(b) = \frac{a(1-\cos\varphi_0)+b(\cos 2\varphi_0-\cos\varphi_0)+2h\sin\varphi_0}{\pi D}\ .$$

6. Il sottocaso $\max(\mathbf{h},\mathbf{c},\mathbf{d}) \le \mathbf{s} \le \min(\mathbf{a},\sqrt{\mathbf{b^2+h^2}})$

Questa situazione si presenta nei casi I, II, III, IV, V, VI, 1°, 2°, 3°, 4°, 9°, 10°, 15°. Consideriamo gli angoli φ_0, φ_1 e φ_2 definiti come precedentemente ed inoltre l'angolo $\varphi_3 \in [0, \frac{\pi}{2}-\alpha]$ definito da $s\sin(\varphi_3+\alpha) = d$.

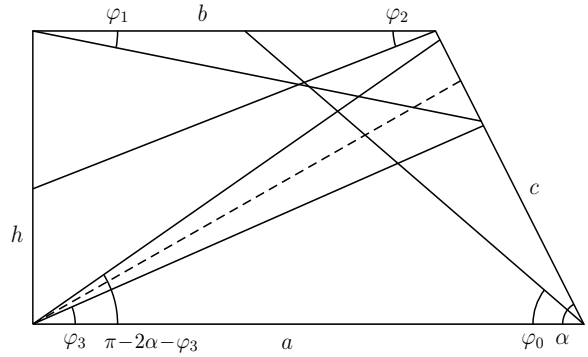

Fig. 8: φ_3 e $\pi-2\alpha-\varphi_3$

In questo caso (vedere anche la Fig. 8) risulta che se $\varphi \in]\varphi_0, \pi-\varphi_0[\cup [2\alpha+\varphi_3, \pi-\varphi_3[$ allora $x_s(\varphi) = 0$. Negli intervalli $[0,\varphi_1[\ ,\ [\varphi_1,\varphi_0]\ ,\ [\pi-\varphi_0,\pi-\varphi_2[\ ,\ [\pi-\varphi_2, 2\alpha+\varphi_3]$ e $[\pi-\varphi_3,\pi[$ la distanza $x_s(\varphi)$ è data da (10), (2), (4), (11) e ancora (11). Con (10'), (2"), (4"') e con

$$(11'') \quad \int_{\pi-\varphi_2}^{2\alpha+\varphi_3} x_s(\varphi)d\varphi = a(-\cos(2\alpha+\varphi_3)-\cos\varphi_2)+b\tan\alpha(\sin\varphi_2-\sin(2\alpha+\varphi_3)),$$
$$+h(\sin\varphi_2-\sin(2\alpha+\varphi_3))-\frac{s}{2}(\cos(4\alpha+2\varphi_3)-\cos 2\varphi_2)-$$
$$\frac{s}{\sin 2\alpha}(2\alpha+\varphi_2+\varphi_3-\pi)+\frac{s}{2}\cot\alpha(\sin(4\alpha+2\varphi_3)+\sin 2\varphi_2)$$

nonché

$$(11''') \quad \int_{\pi-\varphi_3}^{\pi} x_s(\varphi)d\varphi = a(1-\cos\varphi_3)+b\tan\alpha\sin\varphi_3+h\sin\varphi_3$$
$$-\frac{s}{2}(1-\cos 2\varphi_3)-\frac{s}{\sin 2\alpha}\varphi_3+\frac{s}{2}\cot 2\alpha\sin 2\varphi_3$$

si ottiene

$$\int_0^{\pi} x_s(\varphi)d\varphi = a(1-\cos\varphi_0-\cos\varphi_3-\cos(2\alpha+\varphi_3))+b(\cos\varphi_1-\cos\varphi_0+$$
$$+\tan\alpha(\sin\varphi_1+\sin\varphi_2+\sin\varphi_3-\sin(2\alpha+\varphi_3)))+h(2\sin\varphi_0-\sin(2\alpha+\varphi_3)+\sin\varphi_3)+$$
$$+\frac{s}{2}(-1-\cos 2\varphi_1+2\cos 2\varphi_0+\cos 2\varphi_3-\cos(4\alpha+2\varphi_3)-\frac{2}{\sin 2\alpha}(\varphi_1+\varphi_2+2\alpha+2\varphi_3-\pi)$$
$$+(\sin 2\varphi_1+\sin 2\varphi_2+\sin 2\varphi_3+\sin(4\alpha+2\varphi_3))\cot 2\alpha+(\varphi_2-\frac{1}{2}\sin 2\varphi_2)\cot\alpha) =:$$
$$=: A(\varphi_0,\varphi_1,\varphi_2,\varphi_3;s)\ ,$$

e quindi

$$(13) \qquad p(s)=\frac{A(\varphi_0,\varphi_1,\varphi_2,\varphi_3;s)}{\pi D}.$$

Se $\max(h,c,d)=d=s$ allora si ha $\varphi_3+\alpha=\frac{\pi}{2}$ e le formule (12) e (13) forniscono lo stesso risultato di $p(d)$.

7. Il sottocaso $\max(\mathbf{c},\sqrt{\mathbf{b^2+h^2}})\le \mathbf{s}\le \mathbf{a}$

Questo sottocaso riguarda i casi I, II, III, IV, 1°, 2°, 7°, 14°. Poiché $s\ge\max(c,\sqrt{b^2+h^2})$ si ha $\varphi_0\le\pi-2\alpha-\varphi_3$ e dunque $2\alpha+\varphi_3\le\pi-\varphi_0$; ne segue che se $\varphi\in]\varphi_0,\pi-\varphi_3[$ allora $x_s(\varphi)=0$. Negli intervalli $[0,\varphi_1[$, $[\varphi_1,\varphi_0[$ e $[\pi-\varphi_3,\pi[$ si calcola $x_s(\varphi)$ utilizzando rispettivamente (10), (2), (11). Da (10'), (2") e (11"') risulta:

$$\int_0^{\pi} x_s(\varphi)d\varphi = a(1-\cos\varphi_3)+b((\sin\varphi_1+\sin\varphi_3)\tan\alpha+\cos\varphi_1-\cos\varphi_0)+$$
$$h(\sin\varphi_0+\sin\varphi_3)+\frac{s}{2}(-1-\cos 2\varphi_1+\cos 2\varphi_0+\cos 2\varphi_3-\frac{2}{\sin 2\alpha}(\varphi_1+\varphi_3)+$$
$$(\sin 2\varphi_1+\sin 2\varphi_3)\cot 2\alpha+(\varphi_0-\frac{1}{2}\sin 2\varphi_0)\cot\alpha) =: B(\varphi_0,\varphi_1,\varphi_3;s)$$

e dalla (1) si ottiene:

$$p(s) = \frac{B(\varphi_0, \varphi_1, \varphi_3; s)}{\pi D}. \tag{14}$$

Se $c \le \sqrt{b^2+h^2} = s \le a$, allora $\varphi_0 = \varphi_2 = \pi - 2\alpha - \varphi_3$ e le formule (13) e (14) forniscono lo stesso risultato.

8. Il sottocaso $\max(\mathbf{c}, \sqrt{\mathbf{b^2+h^2}}) \le \mathbf{a} \le \mathbf{s} \le \sqrt{\mathbf{a^2+h^2}}$

Questo sottocaso riguarda i casi I, II, III, VII, 1°, 2°, 7°, 15°. Sia $\varphi_4 \in]0, \alpha]$ l'angolo definito da $s\cos\varphi_4 = a$; ne segue $\varphi_4 \le \varphi_1 \le \varphi_0 \le \alpha$ e $x_s(\varphi) = 0$ se $\varphi \in [0, \varphi_4[\cup]\varphi_0, \pi]$. Se $\varphi \in [\varphi_4, \varphi_1]$ vale (10) e dunque:

$$\int_{\varphi_4}^{\varphi_1} x_s(\varphi)d\varphi = b\tan\alpha(\sin\varphi_1 - \sin\varphi_4) + h(\sin\varphi_1 - \sin\varphi_4) - \frac{s}{2}(\varphi_1 - \varphi_4 + \frac{1}{2}(\sin 2\varphi_1 - \sin 2\varphi_4))\tan\alpha\ . \tag{10"}$$

Utilizzando (2") risulta

$$\int_0^{\pi} x_s(\varphi)d\varphi = b(\cos\varphi_1 - \cos\varphi_0 + (\sin\varphi_1 - \sin\varphi_4)\tan\alpha) +$$
$$h(\sin\varphi_0 - \sin\varphi_4) + \frac{s}{2}(\cos 2\varphi_0 - \cos 2\varphi_1 - \frac{2\varphi_1}{\sin 2\alpha} + \sin 2\varphi_1 \cot 2\alpha$$
$$+(\varphi_4 + \frac{1}{2}\sin 2\varphi_4)\tan\alpha - (\varphi_0 - \frac{1}{2}\sin 2\varphi_0)\cot\alpha) =: C(\varphi_0, \varphi_1, \varphi_4; s)$$

e da cui:

$$p(s) = \frac{C(\varphi_0, \varphi_1, \varphi_4; s)}{\pi D}. \tag{15}$$

Nel caso particolare $\max(c, \sqrt{b^2+h^2}) \le a = s$, si ha $\varphi_3 = \varphi_4 = 0$ e le formule (14) e (15) forniscono la stessa probabilità $p(a)$. Se $\sqrt{a^2+h^2} = s$, risulta $\varphi_0 = \varphi_1 = \varphi_4 = \alpha_1$ (dove $\alpha_1 = \arctan(h/a)$), $C(\alpha_1, \alpha_1, \alpha_1; \sqrt{a^2+h^2}) = 0$ e di conseguenza $p(\sqrt{a^2+h^2}) = 0$.

9. Il sottocaso $\max(\mathbf{b}, \mathbf{h}) \le \mathbf{s} \le \min(\mathbf{c}, \mathbf{d})$

Questa situazione si presenta nei casi II, III, V, VI, VII, VIII, 1°, 2°, 3°, 4°, 5°, 6°, 7°, 8°. Per queste relazioni tra b, h, s, c e d si ha $\varphi_1 \le \varphi_2 \le \alpha \le \varphi_0$ e $x_s(\varphi) = 0$ se $\varphi \in]\varphi_0, \pi - \varphi_0[$. La distanza $x_s(\varphi)$ nei seguenti intervalli $[0, \varphi_1[$, $[\varphi_1, \alpha[$, $[\alpha, \varphi_0]$, $[\pi - \varphi_0, \pi - \varphi_2[$ e $[\pi - \varphi_2, \pi[$ ha l'espressione data rispettivamente da (10), (2), (3), (4) e (11) e quindi l'integrale di $x_s(\varphi)$ su tali intervalli é fornito rispettivamente da (10'), (2"'), (3"), (4"') e (11') con

$$(2''') \qquad \int_{\varphi_1}^{\alpha} x_s(\varphi)d\varphi = b(\cos\varphi_1 - \cos\alpha) + h(\sin\alpha - \sin\varphi_1)$$
$$+\frac{s}{2}(\cos 2\alpha - \cos 2\varphi_1 - \frac{1}{2}(\sin 2\alpha - \sin 2\varphi_1)\cot\alpha + (\alpha - \varphi_1)\cot\alpha) \ .$$

Tenendo conto delle formule (10'), (2'''), (3''), (4''') e (11') abbiamo

$$\int_0^{\pi} x_s(\varphi)d\varphi = a(1 + \cos\alpha - 2\cos\varphi_0) + b(\cos\varphi_1 - \cos\alpha + (\sin\varphi_1 + \sin\varphi_2)\tan\alpha)$$
$$+h(\sin\alpha + \sin\varphi_0) - \frac{s}{2}(1 + \cos 2\varphi_1 - (\cos 2\alpha + \cos 2\varphi_0) - (\sin 2\varphi_1 + \sin\varphi_2)\cot 2\alpha$$
$$+2\frac{\varphi_1 + \varphi_2}{\sin 2\alpha} + (\frac{1}{2}\sin 2\alpha - \varphi_2)\cot\alpha + (\varphi_0 - \alpha)\cot\alpha =: D(\varphi_0, \varphi_1, \varphi_2; s)$$

e così la probabilità cercata è:

$$(16) \qquad p(s) = \frac{D(\varphi_0, \varphi_1, \varphi_2; s)}{\pi D} \ .$$

Si osservi la concordanza delle formule (12) e (16) nel caso $\max(b, h) \le s = c \le d$ (e dunque $\varphi_0 = \alpha$.

10. Il sottocaso $\max(\mathbf{a}, \mathbf{c}) \le \mathbf{s} \le \sqrt{\mathbf{b^2 + h^2}}$

Utilizziamo questo sottocaso nei casi IV, V, VI, VIII, 3°, 4°, 5°, 9° e 13° Sia φ_5 l'angolo definito da $s\sin(\varphi_5 + \alpha) = a\sin\alpha$. Risulta (vedere anche la fig. 9) $\varphi_5 \le \varphi_2 \le \varphi_0$ e $\varphi_4 \le \varphi_1 \le \alpha$.

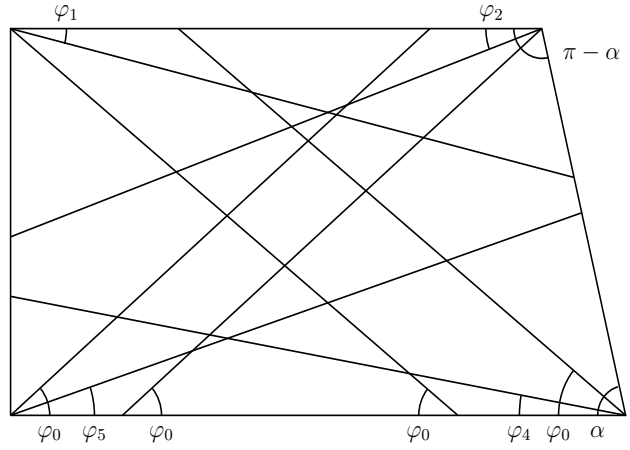

Fig. 9: $\varphi_5 \le \varphi_2 \le \varphi_0,\ \varphi_4 \le \varphi_1 \le \varphi_0 \le \alpha$

Questa volta $x_s(\varphi)$ è zero su $[0, \varphi_4[\cup]\varphi_0, \pi - \varphi_0[\cup]\pi - \varphi_5, \pi]$, mentre su $[\varphi_4, \varphi_1[$, $[\varphi_1, \varphi_0[$, $[\pi - \varphi_0, \pi - \varphi_2[$ e $[\pi - \varphi_2, \pi - \varphi_5]$ l'integrale di $x_s(\varphi)$ si calcola con (10''), (2''), (4''') e (11^{IV}) dove

$$(11^{(\mathrm{IV})}) \qquad \int_{\pi-\varphi_2}^{\pi-\varphi_5} x_s(\varphi)d\varphi = a(\cos\varphi_5 - \cos\varphi_2) + b(\sin\varphi_2 - \sin\varphi_5)\tan\alpha$$
$$+h(\sin\varphi_2 - \sin\varphi_5) - \frac{s}{\sin 2\alpha}(\varphi_2 - \varphi_5) + \frac{s}{2}(\sin 2\varphi_2 - \sin 2\varphi_5 + \cos 2\varphi_2$$
$$- \cos 2\varphi_5)\cot 2\alpha\,.$$

Denotiamo con $E(\varphi_0, \varphi_1, \varphi_2, \varphi_4, \varphi_5; s)$ l'integrale di x_s su $[0, \pi]$, cioè

$$E(\varphi_0, \varphi_1, \varphi_2, \varphi_4, \varphi_5; s) = a(\cos\varphi_5 - \cos\varphi_0) + b((\sin\varphi_1 + \sin\varphi_2 - \sin\varphi_4 - \sin\varphi_5)\tan\alpha$$
$$+ \cos\varphi_1 - \cos\varphi_0) + h(2\sin\varphi_0 - \sin\varphi_4 - \sin\varphi_5) - \frac{s}{2}(\cos 2\varphi_1 + \cos 2\varphi_2 - 2\cos 2\varphi_0$$
$$+\frac{2(\varphi_1 + \varphi_2 - \varphi_5)}{\sin 2\alpha} + (\sin 2\varphi_5 - \sin 2\varphi_2 + \cos 2\varphi_5 - \cos 2\varphi_2 - \sin 2\varphi_1)\cot 2\alpha$$
$$-(\varphi_4 + \frac{1}{2}\sin 2\varphi_4)\tan\alpha + (-\varphi_2 + \frac{1}{2}\sin 2\varphi_2)\cot\alpha)\,.$$

In questo sottocaso risulta

$$(17) \qquad p(s) = \frac{E(\varphi_0, \varphi_1, \varphi_2, \varphi_4, \varphi_5; s)}{\pi D}\,.$$

Nel caso particolare $c \le a = s = \sqrt{b^2 + h^2}$ si ha $\varphi_4 = 0$ e $\varphi_5 = \varphi_2 = \varphi_0$ e quindi si osservi come, in tal caso le formule (15) e (17) coincidono.

11. **Il sottocaso $\mathbf{b \le s \le \min(c, d, h)}$**

Questo sottocaso si presenta in tutti i casi $1°, 2°, \ldots, 16°$. Stavolta non esiste alcun intervallo aperto in cui $x_s(\varphi)$ è zero. L'espressione di $x_s(\varphi)$ su $[0, \varphi_1[\,, [\varphi_1, \alpha[\,, [\alpha\,, \frac{\pi}{2}[\,, [\frac{\pi}{2}, \pi - \varphi_2[$ e $[\pi - \varphi_2, \pi[$ è data rispettivamente da (10), (2), (3), (4) e (11). Utilizziamo gli integrali (10'), (2'''), (3'), (4^{IV}) e (11') dove

$$(4^{\mathrm{IV}}) \qquad \int_{\frac{\pi}{2}}^{\pi-\varphi_2} x_s(\varphi)d\varphi = a\cos\varphi_2 + h(1 - \sin\varphi_2) - \frac{s}{2}(1 + \cos 2\varphi_2 + (\frac{\pi}{2} - \varphi_2 + \frac{1}{2}\sin 2\varphi_2)\cot\alpha)$$

per ottenere:

$$\int_0^{\pi} x_s(\varphi)d\varphi = a(1 + \cos\alpha) + b(\cos\varphi_1 - \cos\alpha + (\sin\varphi_1 + \sin\varphi_2)\tan\alpha)$$
$$+h(1 + \sin\alpha) - \frac{s}{2}(2 + \frac{2(\varphi_1 + \varphi_2)}{\sin 2\alpha} + \cos 2\varphi_1 - \cos 2\alpha + (\sin 2\alpha + \pi - 2\alpha - \varphi_2$$
$$+\frac{1}{2}\sin 2\varphi_2)\cot\alpha - (\sin 2\varphi_1 + \sin 2\varphi_2)\cot 2\alpha) =: F(\varphi_1, \varphi_2; s)\,.$$

Ne segue:

$$p(s) = \frac{F(\varphi_1, \varphi_2; s)}{\pi D} \,. \tag{18}$$

Se $b = h = s$, allora $\varphi_1 = \varphi_2 = 0$ e la formula (18) si riduce alla formula (5).

12. Considerazione degli autori e riassunto

Sono stati considerati finora nove sottocasi che forniscono soluzioni complete per i casi I, II, III, VI e 1°, 2°, 3° e 4°. Ci proponiamo di completare i casi restanti in un successivo lavoro già in fase di stesura.

13. La distribuzione della corda in T

La distribuzione della corda in T è la funzione F che associa ad ogni numero $s, 0 \leq s \leq \sqrt{a^2 + h^2}$ la probabilità che una retta che taglia T determina in T una corda di lunghezza minore o uguale a s.

Consideriamo un reticolo $\mathcal{R}_D$, dove D è un numero arbitrario $D > \sqrt{a^2 + h^2}$. Allora si ha:

$$F(s) = 1 - \frac{p(s)}{p(0)} = 1 - \frac{p(s) \cdot \pi D}{a + b + c + h}. \tag{19}$$

Se $s \leq \min(b, h)$, allora da (5) segue:

$$F(s) = \frac{s}{2} \cdot \frac{3 - \cos 2\alpha + (\pi - 2\alpha + \sin 2\alpha) \cot \alpha}{a + b + c + h}. \tag{20}$$

In particolare per $a = b$ (cioè $\alpha = \frac{\pi}{2}$) si ottiene il risultato già noto: $F(s) = \frac{s}{a+b}$.

La densità f della distribuzione della corda in T, cioè $f = F'$, è costante per $s \leq \min(b, h)$. Se $s > \min(b, h)$ nella formula di $p(s)$ appaiono gli angoli $\varphi_0, \varphi_1, ..., \varphi_5$ che sono dipendenti da s, ma tale dipendenza non è lineare. Per esempio $\varphi_0^{'} = -\frac{h}{s\sqrt{s^2 - h^2}}$. Dunque se $s > \min(b, h)$ la densità f non è costante.

Bibliografia

[C-D] **Conserva, V.; Duma, A.:** Schnitte eines regulären Hexagons in Buffon- und Laplace-Gitter, *Seminarberichte Mathematik, FernUniversität in Hagen, Band 78, 2007, pp. 29-36.*

[D] **Duma, A.:** Problems of Buffon type for "non small" needles, *Rendiconti del Circolo Matematico di Palermo, Serie II, Tomo XLVIII, 1999, pp. 23-40.*

[D-R] **Duma, A.; Rizzo, S.:** Die Sehnenlängenverteilung in einem beliebigen Dreieck, *Seminarberichte Mathematik, FernUniversität in Hagen, Band 80, 2008, pp. 103-120.*

[D-S] **Duma, A.; Stoka, M.:** Schnitte eines "kleinen" gleichseitigen Dreiecks mit dem Gitter von Buffon und Laplace, *Seminarberichte Mathematik, FernUniversität in Hagen, Band 79, 2008, pp. 13-22.*

[P] **Pettineo, M.:** Geometric probability problems for Buffon and Laplace grid. *Suppl. Rendiconti del Circolo matematico di Palermo, Serie II, numero 80, 2008, pp. 267-274.*

[S] **Stoka, M.:** Probabilità e geometria, *Herbita editrice, Palermo, 1982.*

Andrei Duma
Fakultät für
Mathematik und Informatik
FernUniversität in Hagen
58084 Hagen
Deutschland

Sebastiano Rizzo
Dipartimento di Matematica
Università del Salento
Via per Arnesano
73100 Lecce
Italia

RENDICONTI DEL CIRCOLO MATEMATICO DI PALERMO
Serie II, Suppl. 83 (2011), pp. 161-174

THE IMPLIED FORWARD RATE AS AN INDICATOR OF DISTURBANCES IN POLISH INTERBANK MARKET

Ewa Dziwok*
Ph.D., Lecturer, Department of Applied Mathematics,
University of Economics, Katowice, Poland;
ewa.dziwok@ue.katowice.pl

In countries with well developed interbank market the parsimonious models play an important role in the monetary policy. For several years central banks have focused on an extraction of market expectations from term structures, which helps to judge their influence on real economy. With the assumption of PEH (with liquidity premium equal to zero), the implied forward rates are particularly interesting for central banks, especially if the length of calculated implied forward rate matches with the maturity of the central bank's key interest rate. The lower is the difference between an implied forward rate and a reference rate (ex post analysis), the more clear and transparent was monetary policy before a decision-making meeting. If the difference is high, there is a question about the circumstances – sometimes it is inefficiency of the market (illiquidity), sometimes the biases: risk premium caused by lack of trust or a surprising decision of the central bank.

The aim of the paper is twofold: to derive the implied forward rates from the assets' prices with a parametric Svensson model and to show their sensitivity to market disturbances (through ex post analysis of a risk premium – a difference between an implied forward rate and a reference rate).

This paper applies data for several segments of Polish market: interbank deposits forward rate agreements (FRA), interest rate swaps, and coupon bonds. During last two years we found that there is a period of time when a higher positive premium in a form of calculated differences was noticed. The result could be used as a leading indicator of market disturbances – especially for the central bank who wants (like other central bankers

* Ph.D., Lecturer, Department of Applied Mathematics, University of Economics, Katowice, Poland; ewa.dziwok@ue.katowice.pl

around the world) to assure markets that it controls the situation and does not let investors lose the mutual confidence.

Keywords: yield curve estimation, parsimonious models, market expectations
JEL Classification: C53, C92, E43, E58

1. Introduction.

Following the definition suggested by Nawalkha, Soto, Beliaeva (2004), a term structure of interest rates gives the relationship between the yield of the investment with the same credit quality but different term to maturity. There are plenty of methods, widely described by James, Weber (2000) which let create a yield curve but typically it is built with a set of liquid and common assets; every instrument can be considered as a portfolio of zero-coupon bonds (with the maturities adequate to the payment dates). Price of the zero-coupon bond is expressed as a discount factor which represents the relationship between the spot rate and the forward one (Shiller et al. 1983 and 1990, Fama 1976).

Because financial markets offer only discrete data, one of the most important problems to be solved is the model selection for fitting the data. In countries with a well developed debt market central banks use parsimonious models coming from works of Nelson-Siegel (1987) and Svensson (1994) but the method based on cubic splines is also popular (McCulloch 1975, Fisher, Nychka, Zervos 1995, Waggoner 1996). To find the strength and sensitivity of market expectation to market disturbances the construction of a wide range of term structures based on different data is necessary.

The paper is structured as follows: Section 2 provides a general overview of the term structure modelling the evolution of methods and shows the applications from the central bank's point of view, Section 3 shows the methodology of term structure modelling based on parsimonious Svensson model, Section 4 is an empirical one which gives short description of Polish market data used in a further analysis and illustrates an influence of market expectations (fears and believes) on the term structure. The final part covers concluding remarks.

2. Expectations and monetary policy.

Following Tuckman (2002) a forward rate is an agreement made to lend money at some future date. Choudhry (2004) differentiates forward rates taken directly from the market from these implied forward rates which are derived from the spot interest rates (theoretical ones). Because predictive power of implied forward rates (as an estimation of the future spot rates) depends on the efficiency of the market and a kind of biases which may be included in forward rates, various hypotheses try to explain this relation. According to one of them, the pure expectation hypothesis (Lutz 1940-41), the term structure reflects directly the market expectations of future rates with liquidity premium equal to zero.

With the assumption of PEH (Pure Expectation Hypothesis), the implied forward rates are particularly interesting for central banks, especially if the length of calculated implied forward is tantamount to the duration of the central bank's key open market operation. It is very useful for an evaluation of central bank's predictability. The lower is the difference between a reference rate and an implied forward rate (ex post analysis), the clearer and more transparent monetary policy was before a decision-making meeting. If the difference is high, the question arises about the circumstances – sometimes it is an inefficiency of the market (illiquidity), sometimes a bias mentioned earlier: risk premium caused by lack of trust or a decision of the central bank which surprised the market.

It is also possible that market participants could overestimate the scale of central bank decisions as an effect of misunderstandings of the monetary policy. Being familiar with determinants that shaped the term structure, the central bank is able to improve its transparency through official and unofficial messages covering information about future interest rates movements to keep the inter-bank rates as stable as possible (Choudhry 2002).

3. A yield curve construction

To derive the implied forward rates from the assets' prices with a parametric Svensson model first of all one should define the process of zero-coupon yield construction.

Definition 1.

Zero-coupon bond is an instrument with only two cashflows: first – at the beginning of the investment – called the price; the second one is a cashflow which is paid at maturity.

Suppose the price of the zero-coupon bond is denoted as P, with a cashflow c at maturity τ and yield to maturity $i(\tau)$ understood as a spot rate. If the continuously compound interest is taken into account, the price is the discounted value of a future cashflow c:

$$P(\tau) = c \cdot e^{-i(\tau)\cdot\tau} \tag{1}$$

where:

$P(\tau)$ - price of the zero-coupon bond with maturity τ

c – cashflow at time τ

$i(\tau)$ - spot rate

It is important (according to Audley, Chin, and Ramamurthy, 2002) that under continuous compounding, the spot rate is understood as the continuously compounded instantaneous rate of return. Graphically, the spot rate may be visualized as the yield corresponding to the point at which the spot yield curve intercepts the yield axis.

Definition 2

The function $\delta : \Re_+ \to (0;1]$ is called the discount function if it fulfills following criteria:

(1) $\delta(0) = 1$

(2) $\delta(\tau)$ is a decreasing function of τ

Here, for our purposes the discount function which represents continuously compound interest will be expressed as:

$$\delta(\tau) = e^{-i(\tau)\cdot\tau} \tag{2}$$

Lemma:

Every default-free coupon bond can be described as a portfolio of zero-coupon bonds (with the maturities adequate to the payment dates).

Proof: If P is a coupon bond with a set of future cashflows c_j, observed at time τ_j, $j = 1,2,...,k$ and let (for simplicity) spot rates $i_j(\tau_j) = i_j$, $j = 1,2,...,k$, then the price of coupon bond could be expressed as a present value of cashflows:

$$P = c_1 \cdot e^{-i_1\tau_1} + c_2 \cdot e^{-i_2\tau_2} + ... + c_k \cdot e^{-i_k\tau_k}$$

According to formula 1, the coupon bond can be described as a linear combination of discount factors δ_j, $j = 1,2,...,k$:

$$P = c_1 \cdot \delta_1 + c_2 \cdot \delta_2 + ... + c_k \cdot \delta_k$$

Definition 3

The instantaneous forward rate $f(\tau) \equiv f_{\tau,\tau+\Delta\tau}$, defined by O. de La Grandville (2001), is understood as the marginal rate of return implied for infinitesimally short period (length of investment) $\Delta\tau \to 0$.

$$i(\tau) = \frac{1}{\tau}\int_0^{\tau} f(m)\,dm \tag{3}$$

The existence of inter-relation between discount factor $\delta(\tau)$, spot rate $i(\tau)$ and forward one $f(\tau)$ (in continuous time) could be – after the formulas (1)-(3) illustrated as below:

$$P(\tau) = \delta(\tau) = e^{-i(\tau)\cdot\tau} = e^{-\int_0^{\tau} f(m)dm} \tag{4}$$

where: $P(\tau)$ - price of a bond

$\delta(\tau)$ - discount factor

$i(\tau)$ - spot rate

$f(\tau)$ - forward rate

τ - term to maturity

The term structure construction begins by gathering the sample of the instrument to be used. In Polish money market, which is analyzed here, there is lack of short term data (apart from money market fixing quotations), that is why all available quotations were taken into account with no quality check.

Suppose that there is a set of k instruments, with market values

P_l, $l = 1,2,...,k$ and cashflows $c_{l,j}$ for bond l at time τ_j, $j = 1,2,...,k$. Let $C = \{c_{l,j}\}_{l=1,...,k,\, j=1,...,k}$ is a cashflow matrix, generally sparse one with most entries zero and $P = \{P_l\}_{l=1,...,k}$ is the price vector. The knowledge of *C* and *P* determines the discount factors:

$$P = C \cdot [\delta(\tau_1) \quad \delta(\tau_2) \quad \dots \quad \delta(\tau_k)]^T \tag{5}$$

To fit the curve it is necessary to choose an interpolation method, (a form of a theoretical function) which let receive discount factors $\bar{\delta}(\tau)$ for all maturities (between zero and infinity). McCulloch (1971, 1975) used a piecewise polynomial function, but the main problem was the instability of this model and high possibility of unrealistic, negative forward rates (through formula4).

An idiosyncrasy of parametric models (which this article focuses on) involves their simplicity and small number of parameters to be estimated. Additionally the functional form determines three main features (smoothness, flexibility and stability) expected from correctly estimated curve (Anderson, Sleath, 2001).

Table 1. Estimation criteria in case of parametric models[1]

Model	Parametric models	
	Nelson-Siegel	Svensson
Smoothness	+	+
Flexibility	+	-
Stability	-	-/+

Source: Based on Anderson N., Sleath J., (2001) *New estimates of the UK real and nominal yield curves*. Bank of England Working Paper

The utilization of parametric models (here the Svensson model) allows to calculate forward rates directly (and then via formula 4, to receive discount factors). It guarantees different shapes of a theoretical term structure.

For the further analysis the Svensson model with six

[1] The Nelson-Sigel model uses only four parameters. See e.g.: C. R. Nelson, A. F. Siegel, *Parsimonious Modeling of Yield Curves.* Journal of Business, 1985, Vol. 60, No. 4, s. 473-489

parameters which describes the discount factor $\overline{\delta}(\tau) = \overline{\delta}(\tau \mid \beta_0, \beta_1, \beta_2, \beta_3, v_1, v_2)$ is taken into account:

$$f(\tau) = \beta_0 + (\beta_1 + \beta_2 \frac{\tau}{v_1}) \cdot e^{-\frac{\tau}{v_1}} + \beta_3 \frac{\tau}{v_2} \cdot e^{-\frac{\tau}{v_2}} \qquad (6)$$

where:

$f(\tau)$ - instantaneous forward rate

$[\beta_0, \beta_1, \beta_2, \beta_3, v_1, v_2]$ – vector of parameters describing the curve:

β_0 - parameter indicates a limit in infinity, $\beta_0 > 0$

β_1 - indicates a limit in infinity, $\beta_0 + \beta_1 \geq 0$

β_2 - parameter indicates a strength of first curvature

β_3 - indicates a strength of second curvature

v_1 - indicates a place of first curvature, $v_1 > 0$

v_2 - indicates a place of second curvature, $v_2 > v_1$

According the formula (4) a whole set of discount factors (for all cashflows) could be calculated from forward rates. Then a vector of theoretical prices $\overline{P} = \left\{\overline{P_l}\right\}_{l=1,\ldots,k}$ can be described as a product of a cash flow matrix C multiplied by a vector of discount factors (in a functional form):

$$\overline{P} = C \cdot \left[\overline{\delta}(\tau_1) \quad \overline{\delta}(\tau_2) \quad \ldots \quad \overline{\delta}(\tau_k)\right]^T \qquad (7)$$

A set of parameters: $[\beta_0, \beta_1, \beta_2, \beta_3, v_1, v_2]$ is estimated by minimizing mean square errors between market prices and theoretical ones (taken from the fitted curve):

$$\frac{\sum_{l=1}^{k} (P_l - \overline{P_l})^2}{k} \rightarrow \min \qquad (8)$$

where: $P_l - \overline{P_l}$ – a price error of l-th bond

$i_l - \overline{i_l}$ – a yield error of l-th bond

k – number of bonds

When a vector of discount factors is known, it is easy to construct a set of zero-coupon rates (by given formula 4) and then implied forward term structure which let analyse a current situation in the market.

$$i(\tau_l) = -\frac{\ln \delta(\tau_l)}{\tau_l} \qquad \text{for every cashflow times } \tau_l \text{ ; } l=1,2...m \quad (9)$$

According to rules laid down for the National Bank of Poland this analysis uses a Svensson model (due to its simplicity and small number of parameters to estimate). To calculate the implied forward rate, the estimation of six parameters [β_0; β_1; β_2; β_3; v_1; v_2] is needed such that they let minimize the difference between theoretical and market prices of given papers.

Generally a term structure is typically built with a set of liquid and common assets; the problem arises in a case of non-liquid market (as in Poland) with a small number of data. One of solutions is to analyze several types of models and then to choose this one which let achieve the best approximation.

4. Data and results

For several years Polish money market has become one of the most important places of trade in Eastern Europe attracting both speculators and long term investors. Following the openness and liberalization, Polish market has started to be more liquid and can be used as a source of market participant's behavior.

Four types of instruments were taken into a forthcoming research. They vary in terms of their liquidity, maturity, representativeness, and default risk.

Interbank lending rates are represented by WIBOR (Warsaw InterBank Offer Rate) – a panel of rates calculated and published each day at 11.00 a.m. of Warsaw time by Reuters service[2]. Contrary to the LIBOR, the WIBOR rate is an average of quotations provided by chosen banks which received a Primary Dealers status. The maturities of WIBOR rates have been changed during last years (first time WIBOR was published on 15 of March 1993), and nowadays they range from overnight to one year. As a representative of the interbank market, the WIBOR rates reflect default risk affected by a quoting bank's condition (an interbank loan is unsecured) and liquidity of the market. Because the shortest, overnight rate illustrates the demand for liquidity and strongly depends on the obligatory reserve maintenance period, its volatility is very high. For the purposes of following research only rates from

[2] www.reuters.pl

T/N to one year were taken (eight in total: T/N, 1-week, 2-weeks, 1-month, 3-, 6-, 9-months, one year). According to formula (2) they let to create the square diagonal matrix of cash flows (with eight columns and rows) and following (3) with (4) and (5) the instantaneous implied forward rate could be achieved (it is an equivalent of the overnight rate in the future, thus the beginning of both spot and forward rate is at the same point). The existing instantaneous forward rate let to receive (with the formula 6) 7-days implied forward rate on any day in the future.

FRA rates are derived from cash market and reflect the current price of money for an agreed term in future. As an over-the counter derivative contract between two parties it carries credit and liquidity risk, but in term of value at risk is lower than connected cash market's instruments thanks to the construction of the contract (there is only an exchange of difference of interest in a form of settlement or compensation payment). In Poland an existing FRA market is very liquid mainly as a result of an activity of short-term foreign investors (speculators) whose generate almost 80%-90% of transactions. In this paper five contracts were taken (1x2, 1x4, 3x6, 6x9, and 9x12) which let to derive seven theoretical discount factors (as an equivalent of 1, 2, 3, 4, 6, 9, 12-months). The further procedure was as before.

Swap rates is an agreement for exchange interest payments (fixed versus floating) The only payments that are exchanged between the counterparties are the interest ones, not the principal thus as in FRA case the default risk connected with this asset is lower in terms of value at risk. The Polish interest rate swap market has been increasing for several years and has become very popular among both domestic and foreign investors. For the purposes of following research fixed-lag swap rates were taken, ranged from one to ten years (six in total: 1-year, 2-, 3-, 4-, 5- and 10-years). Lack of short term rates biases the approximation results – the constructed term structure is very volatile on its short end.

Government bonds (both coupon and zero coupon ones) are the papers issued by government of Poland and thus in this country they are treated as free of credit risk. The problem of representativeness was solved by taking the fixing rates from a non-regulated organised market (MTS Poland Market), which provides wholesale electronic trading of Polish treasury bills and bonds. In spite of the MTS Poland Market is an integral part of the Primary Dealer system (developed by the Ministry of Finance in

cooperation with the National Bank of Poland, the National Depository for Securities, and banking environment), its liquidity is not satisfactory – the MTS Poland Market contains only around 20%-25% of bond's trade (the rest is dealt in the interbank market without a fixing). The prices used in the research are fixing prices set during each trading day by MTS Poland Market.[3] The created term structure – in spite of lack of observed rates – was derived from coupon bonds so there were a set of cash flows paid in a term up to one year.

Since 1999 due to the implementation of the direct inflation targeting strategy (DIT, IT) into Polish monetary policy, the National Bank of Poland defines the inflation target and then adjusts basic interest rates in order to maximize the probability of achieving the target. The NBP maintains interest rates at a level consistent with the adopted inflation target by influencing the level of nominal short-term interest rates in the money market. The minimum yield of the 7-days open market operations is one of the instruments used by the NBP to determine interest rates in the market (the reference rate adopted by the Monetary Policy Council).

The research takes into account eighteen Monetary Policy Council decision-making meetings held between January 2008 and June 2009 and the dates two weeks before. For each of these particular days, four implied forward term structures were constructed using different sources of data: inter-bank deposit rates, FRA, swap rates and coupon bonds. Having four estimated vectors of parameters for each of eighteen dates, a set of 7-days implied forward rates (for every $\tau \in (\frac{1}{365}; \frac{28}{365})$) was calculated (from formula 9):

$$f_{asset(i)}(\tau, \tau + \frac{7}{365}) = \frac{365}{7} \frac{\ln \delta(\tau + \frac{7}{365})}{\ln \delta(\tau)} \tag{10}$$

where:

$f_{asset(i)}$ - estimated 7-days forward rate for i-th asset

Chart 1. 7-days forward curves estimated two weeks before open central bank meeting based on four different assets

[3] www.mtspoland.com

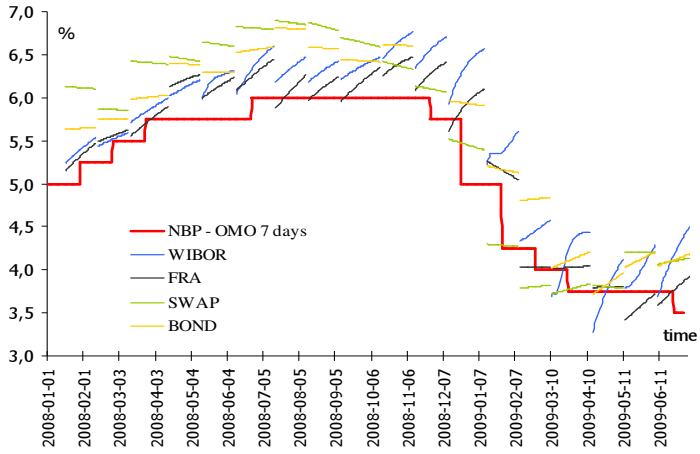

Source: own computations based on bond data

Looking at Chart 1 we can see how market participants estimated 7-days rate depending on the data taking into account (four different types of assets). They are compared with an official 7-days reference rate. The point in the middle of each curve shows the expected 7-day rate for that day when the Monetary Policy Council meeting takes place. Formally it could be shown in a form of following formula:

$$f_{asset(i)}\left(\tfrac{14}{365},\tfrac{21}{365}\right)=\tfrac{365}{7}\frac{\ln\delta\left(\tfrac{21}{365}\right)}{\ln\delta\left(\tfrac{14}{365}\right)} \tag{11}$$

Statistically there are no significant differences between the data - but we can notice that WIBOR is the worst one, but no instruments clearly dominated. It means that market's participants almost always recognize the direction of future monetary policy decisions, but sometimes they were surprised by the scale of the movement. It is necessary to remember that the data biases might be connected with a scale of liquidity in emerging markets and number of data (the set of data used in these calculations is small and could be not enough to representative the behavior of the market).

Additionally, the difference between an implied 7-days forward rate (calculated in a form 11) and the reference NBP rate settled on that day was taken into account (calculated for 18 dates and four assets: WIBOR, FRA, swap and coupon bonds). We want to examine if the disturbances in financial markets have an influence on these differences.

Chart 2. A difference between implied 7-days forward and the reference rate (in basis points).

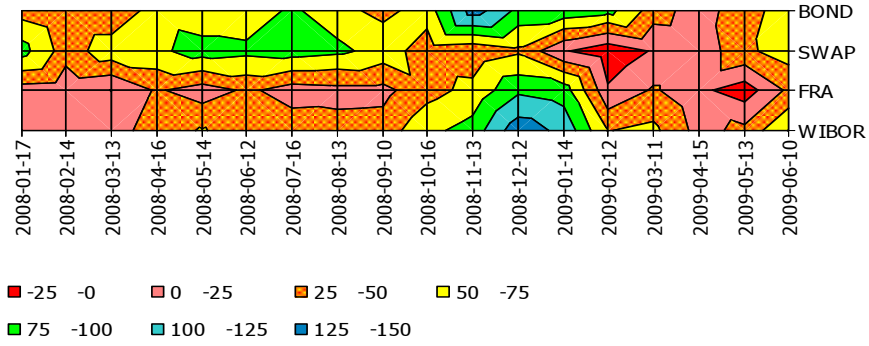

Source: own computations

The results shown in Chart 2 could be used as a leading indicator of market disturbances – since October 2008 the predicting power of all data (especially FRA) has become lower. The higher positive premium in a form of calculated differences (ranged from 4 to 140 basis points) reflect the investors and traders behavior, whose reaction (to new information – here about the financial crisis) is exaggerated. This could have caused the assets' price to change strongly, so they will not truly reflect the situation in the market. In January 2009 the reversal behavior could be noticed – in spite of the financial crisis the assets' prices showed the tendency to return back to its common value. It was probably the effect of messages sent by central bank's officials who wanted (like other central bankers around the world) to assure markets that they control the situation and do not let investors lose the mutual confidence.

In a whole analyzed period the implied forward rate curve overestimated future short rates. When the curve was upward sloping it was too upward sloping and if the curve was downward sloping it was not enough downward sloping. Such surprisingly results (meaningless which data were used to create the implied forward) give market's participants an easy possibility to make excess profits. For the central bank it is additional information which should be taken into account during an analysis of a monetary transmission mechanism.

5. Summary.

For several years central banks have focused on an extraction of market expectations from term structures, which helps to judge their influence on real economy (ECB 2006). In countries with well developed debt market parsimonious models play an important role in term structure building process. For research purposes, the most useful source of rates is the FRA market, which becomes an important segment of financial markets.

This paper takes data for several segments of Polish market: interbank deposits forward rate agreements (FRA), interest rate swaps, and coupon bonds and examines the quality of extracted market expectation during last 18 months. Parameters were compared every two weeks before a central bank decision-making meeting to examine if the market participants expected movements correctly.

According to the analysis the best source of data seems to be a derivative market whose construction minimizes the influence of biases even during turbulences. These results should be interpreted with caution, since they are specific to one particular Svensson model. A small open market, very sensitive for external shocks and speculators' attacks (like Polish one) is too changeable to take received results as typical. In such case it is better not to relay on one source of data but examine several types of assets to get a wider spectrum of the market's situation.

The useful supplementary information is that market participants overestimate (overreaction in a behavioral sense) future movements of the Polish central bank as an effect of bank transparency. It is an additional argument for the central bank's authorities to inform (officially and unofficially) about future movements of the key interest rates to keep the interbank rates as stable as possible.

SOURCES:

1. Anderson, N., Breedon, F., Deacon, M., Derry, A., Murphy, G., (1996) *Estimating and interpreting the yield curve*. Chichester: John Wiley & Sons, Inc.
2. Anderson, N., Sleath, J., (2001) New estimates of the UK real and nominal yield curves, *Bank of England Working Paper* no.126.

3. Audley D., R. Chin, and S. Ramamurthy, (2002) *Term Structure Modeling*. [in]: F.J. Fabozzi (ed), Interest Rate, Term Structure and valuation modeling. John Wiley & Sons Inc., Hoboken, New Jersey, pp. 93-136.
4. Bliss, R.R., (1996) Testing term structure estimation methods. *Federal Reserve Bank of Atlanta Working Paper* 96-12a.
5. Choudhry, M., (2002) An introductory guide to analyzing and interpreting the yield curve, in F.J. Fabozzi (ed): *Interest rate, term structure and valuation modelling*. Hoboken: John Wiley & Sons, Inc.: 73-92.
6. Choudhry, M., (2004) *Analysing and Interpreting the Yield Curve*, Singapore: John Wiley & Sons, Inc.
7. McCulloch, J. H. (1971) Measuring the term structure of interest rates, *Journal of Business*, 44: 19-31;
8. McCulloch, J. H. (1975) The tax-adjusted yield curve. *Journal of Finance*, 30: 811-830.
9. ECB, (2006) *Monthly Bulletin*, January.
10. Fama, E., (1976) Forward rates as predictors of future spot rates, *Journal of Financial Economics*, 4: 361-377.
11. Fisher, M., Nychka, D., Zervos, D., (1995) Fitting the term structure of interest rates with smoothing splines. Federal Reserve Board, *Finance and Economics Discussion Series,* Working Paper 95-1.
12. James, J., Webber, N. (2000) *Interest Rate Modelling*. Chichester: John Wiley & Sons, Inc.
13. de La Grandville, O., (2001) *Bond Pricing and Portfolio Analysis*. Cambridge and London: The MIT Press.
14. Lutz, F. (1940-41) The structure of interest rates, *Quarterly Journal of Economics*, 36-63.
15. Nawalkha, S.K., Soto, G.M., Beliaeva, N.A., (2005), *Interest Rate Risk Modeling*, Hoboken: John Wiley & Sons, Inc.
16. Nelson, C. R., Siegel, A. F. (1987) Parsimonious modelling of yield curves. *Journal of Business*, 60 no.4: 473-489.
17. Shiller, R.J., Campbell, J.Y., Schoenholtz, K.L., (1983) Forward rates and future policy: interpreting the term structure of interest rates. *Brookings Papers on Economic Activity*, Yale University, 1:173-223.
18. Shiller, R.J., McCulloch J.H., (1990) The term structure of interest rates, in B.M. Friedman, F.H. Hahn (ed), *Handbook of Monetary Economics*, Vol. 1, North Holland: Elsevier Science Publishers: 644-651.
19. Svensson, L.E.O., (1994) Estimating and interpreting forward interest rates: Sweden 1992-1994. NBER Working Paper Series No. 4871.
20. Tuckman, B., (2002) *Fixed Income Securities*, 2 ed., Hoboken: John Wiley & Sons, Inc.
21. Waggoner, D., (1997) Spline methods for extracting interest rates from coupon bond prices. Federal Reserve Bank of Atlanta, Working Paper 97-10.

RENDICONTI DEL CIRCOLO MATEMATICO DI PALERMO
Serie II, Suppl. 83 (2011), pp. 175-188

INVARIANT THEORY OF FOLIATIONS OF THE PROJECTIVE PLANE

EDUARDO ESTEVES AND MARINA MARCHISIO

Abstract. We study the invariant theory of singular foliations of the projective plane. Our first main result is that a foliation of degree $m > 1$ is not stable only if it has singularities in dimension 1 or contains an isolated singular point with multiplicity at least $(m^2 - 1)/(2m + 1)$. Our second main result is the construction of an invariant map from the space of foliations of degree m to that of curves of degree $m^2 + m - 2$. We describe this map explicitly in case $m = 2$.

1. Introduction

The study of (singular) foliations of the projective plane is an old one. It was central in works by Darboux [4] and Poincaré [11] in the XIX Century. More recently, the interest in the subject has been revived by Jouanolou [9]. It has been an active area of study ever since.

If we want to study foliations up to projective equivalence, we enter the realm of Invariant Theory. Though the motivation for this study is natural, and Invariant Theory is a classical subject, not much has been done so far in this direction. We can mention the work by Goméz-Mont and Kempf [8], who have shown that a foliation whose all singular points have Milnor number 1 is stable. (In fact, they showed the same result holds for singular foliations of higher dimension spaces as well.) Only recently, Alcántara [1], [2] has characterized the semi-stable foliations of degree 1 and 2, and studied their quotient spaces.

In these notes we propose to advance this study. Our first main result is Theorem 9, which says that a foliation of degree $m > 1$ is nonstable (resp. nonsemistable) only if it has singularities in dimension 1 or contains an isolated singular point of multiplicity at least (resp. greater than) $(m^2 - 1)/(2m + 1)$.

Our second main result is Theorem 10, which yields an invariant rational map Φ from the (projective) space of foliations of degree $m \geq 2$ to that of plane curves of degree $m^2 + m - 2$. Using this map, we can, in principle, produce invariants of foliations out of invariants of plane curves. However, though the invariants of plane curves can all be described by the symbolic method of the XIX Century, generators for the algebras of invariants are known only for very small degrees, not larger than 8. Since for $m \geq 3$, the curves have degree at least 10, the map Φ might be manageable only for $m = 2$, in which case we are dealing with quartics. In this case, we describe the map explicitly in Section 4.

These notes report on work partly done during a visiting professorhip of the first named author at the Università degli Studi di Torino. That author would like

to thank Regione Piemonte for financing his position. Also, he would like to thank the Dipartimento di Matematica of the Università, specially Prof. Alberto Conte, for the warm hospitality extended. Finally, he acknowledges support from CNPq, Proc. 303797/2007-0 and 473032/2008-2, and FAPERJ, Proc. E-26/102.769/2008 and E-26/110.556/2010.

2. Singular foliations

1. *Foliations.* Given a smooth algebraic variety X over an algebraically closed field k, a d-dimensional foliation of X is a rank-d subbundle of the tangent bundle of X. Typically though, these subbundles do not exist. For instance, take the projective plane $X := \mathbf{P}^2_k$. A subbundle of rank 1 of the tangent bundle would give rise to an exact sequence of locally free sheaves,

$$0 \to \mathcal{O}_{\mathbf{P}^2_k}(m) \to \Omega^1_{\mathbf{P}^2_k} \to \mathcal{O}_{\mathbf{P}^2_k}(n) \to 0$$

for certain integers m and n, and this sequence would split because

$$H^1(\mathbf{P}^2_k, \mathcal{O}_{\mathbf{P}^2_k}(m-n)) = 0.$$

Thus,

$$\Omega^1_{\mathbf{P}^2_k} \cong \mathcal{O}_{\mathbf{P}^2_k}(m) \oplus \mathcal{O}_{\mathbf{P}^2_k}(n).$$

Then it would follow that Euler sequence,

$$0 \to \Omega^1_{\mathbf{P}^2_k} \to \mathcal{O}_{\mathbf{P}^2_k}(-1)^{\oplus 3} \to \mathcal{O}_{\mathbf{P}^2_k} \to 0, \tag{1}$$

would split as well, as

$$H^1(\mathbf{P}^2_k, \mathcal{O}_{\mathbf{P}^2_k}(-m)) = H^1(\mathbf{P}^2_k, \mathcal{O}_{\mathbf{P}^2_k}(-n)) = 0,$$

giving rise to a nonzero global section of $\mathcal{O}_{\mathbf{P}^2_k}(-1)$, an absurd.

2. *Singular foliations.* One might ask however not for a subbundle, but for a subsheaf. This gives rise to a *singular foliation*. In other words, a singular foliation is a subsheaf of the tangent sheaf of X. Its dimension is the generic rank of the sheaf. For instance, take the projective plane $X := \mathbf{P}^2_k$. Given a singular foliation of dimension 1, we may replace the subsheaf by a possibly larger reflexive subsheaf. Since X is smooth of dimension 2, this means that the subsheaf is locally free by [10], Lemma 1.1.10, p. 149. So, a singular foliation of $\mathbf{P}^2_k$ is a nonzero (thus injective) map

$$\eta\colon \mathcal{O}_{\mathbf{P}^2_k}(1-m) \longrightarrow T_{\mathbf{P}^2_k}, \tag{2}$$

where $T_{\mathbf{P}^2_k}$ is the tangent sheaf of $\mathbf{P}^2_k$. We will deal only with one-dimensional singular foliations of $\mathbf{P}^2_k$ from now on, and will thus drop the adjective "singular."

Taking duals in the Euler sequence (1), we obtain the exact sequence

$$0 \longrightarrow \mathcal{O}_{\mathbf{P}^2_k} \to \mathcal{O}_{\mathbf{P}^2_k}(1)^{\oplus 3} \to T_{\mathbf{P}^2_k} \to 0. \tag{3}$$

Since $\operatorname{Ext}^1(\mathcal{O}_{\mathbf{P}^2_k}(1-m), \mathcal{O}_{\mathbf{P}^2_k}) = 0$, any map η as in (2) lifts to a map

$$\widetilde{\eta}\colon \mathcal{O}_{\mathbf{P}^2_k}(1-m) \to \mathcal{O}_{\mathbf{P}^2_k}(1)^{\oplus 3},$$

which corresponds to a choice of three homogeneous polynomials F, G and H of degree m. In other words, η induces a homogeneous vector field on the three-dimensional affine space $\mathbf{A}^3_k$:

$$D := F\frac{\partial}{\partial x} + G\frac{\partial}{\partial y} + H\frac{\partial}{\partial z}. \tag{4}$$

Here x, y and z are the coordinates of $\mathbf{A}^3_k$. This vector field is not unique, as the lifting $\widetilde{\eta}$ of η is not, but any other vector field is obtaining from the above one by summing a multiple of the Euler field:

$$P\Big(x\frac{\partial}{\partial x} + y\frac{\partial}{\partial y} + z\frac{\partial}{\partial z}\Big).$$

At any rate, we may harmlessly say that D, instead of η, is the foliation.

Conversely, given D as in (4), one can describe the foliation η in very concrete terms: the direction given by η at a point $(x : y : z) \in \mathbf{P}^2_k$ is that of the line passing through $(x : y : z)$ and $(F(x,y,z) : G(x,y,z) : H(x,y,z))$, whenever these two points are distinct.

3. *The space of foliations.* There are thus many (singular) foliations. In fact, identifying foliations that differ one from the other by multiplication by a nonzero constant, we obtain a projective space,

$$\mathbf{F}_m := \mathbf{P}(H^0(\mathbf{P}^2_k, T_{\mathbf{P}^2_k} \otimes \mathcal{O}_{\mathbf{P}^2_k}(m-1))).$$

It follows from the long exact sequence in cohomology associated to (3) that

$$\begin{aligned}\dim \mathbf{F}_m &= 3h^0(\mathbf{P}^2_k, \mathcal{O}_{\mathbf{P}^2_k}(m)) - h^0(\mathbf{P}^2_k, \mathcal{O}_{\mathbf{P}^2_k}(m-1)) - 1\\ &= 3\binom{m+2}{2} - \binom{m+1}{2} - 1\\ &= m^2 + 4m + 2.\end{aligned}$$

4. *Singular points.* The map η in (2), though injective, does not give rise to a subbundle. In other words, the degeneracy scheme of the map is nonempty. The degeneracy scheme is called the *singular locus* of the foliation, and its points the *singular points* or *singularities* of the foliation. Since $\eta \neq 0$, the dimension of this locus is at most 1. If the dimension is 1, then η decomposes in a unique way as

$$\mathcal{O}_{\mathbf{P}^2_k}(1-m) \longrightarrow \mathcal{O}_{\mathbf{P}^2_k}(1-n) \longrightarrow T_{\mathbf{P}^2_k},$$

where the first map is multiplication by a homogeneous polynomial of degree $m-n$, for a certain $n < m$, and the second is a foliation with finite singular locus. In this case, we say that η has singularities in dimension 1.

If the dimension is zero each singularity appears with a certain length in the singular locus, called its *Milnor number*. Then we can use Porteous Formula (see

[7], Thm. 14.4, p. 254) to compute the sum δ of the Milnor numbers:

$$\begin{aligned}
\delta &= \int_{\mathbf{P}^2_k} c_2(T_{\mathbf{P}^2_k} \otimes \mathcal{O}_{\mathbf{P}^2_k}(m-1)) \cap [\mathbf{P}^2_k] \\
&= \int_{\mathbf{P}^2_k} \left[\frac{c(\mathcal{O}_{\mathbf{P}^2_k}(m))^3}{c(\mathcal{O}_{\mathbf{P}^2_k}(m-1))} \right]_2 \cap [\mathbf{P}^2_k] \quad \text{(Sequence (3) and Whitney Formula)} \\
&= \int_{\mathbf{P}^2_k} \left[\frac{(1+mh)^3}{1+(m-1)h} \right]_2 \cap [\mathbf{P}^2_k] \quad \text{(where } h := c_1(\mathcal{O}_{\mathbf{P}^2_k}(1))\text{)} \\
&= \int_{\mathbf{P}^2_k} [(1+3mh+3m^2h^2)(1-(m-1)h+(m-1)^2h^2)]_2 \cap [\mathbf{P}^2_k] \\
&= (m-1)^2 - 3m(m-1) + 3m^2 \\
&= m^2 + m + 1.
\end{aligned}$$

Another important invariant of a singular point of the foliation is its *multiplicity*, the maximum power of the maximal ideal of the local ring of $\mathbb{P}^2$ at the point containing the ideal of the singular locus of the foliation.

5. *The degree.* Given a singular foliation η as in (2), the integer m, clearly non-negative, has a geometric interpretation. Indeed, m is the number of tangencies of η to a general line. More precisely, given a line L on $\mathbf{P}^2_k$, we may look at the set of points where η is either singular or assigns a line equal to L. Given a general line, this is a finite set. (Just pick a nonsingular point P of η, and choose L transversal to the line at P given by η.) The number of points s of this set, counted with the appropriate weights, is given by Porteous Formula, as the length of the degeneracy scheme of the map of vector bundles

$$\mathcal{O}_{\mathbf{P}^2_k}(1-m)|_L \oplus T_L \xrightarrow{(\eta|_L, \beta)} T_{\mathbf{P}^2_k}|_L,$$

where β is the natural inclusion between tangent bundles. Thus

$$\begin{aligned}
s &= \int_L \big(c_1(T_{\mathbf{P}^2_k}|_L) - c_1(\mathcal{O}_{\mathbf{P}^2_k}(1-m)|_L) - c_1(T_L)\big) \cap [L] \\
&= \int_L \big(3h - (1-m)h - 2h\big) \quad \text{(where } h \text{ is the class of a point)} \\
&= m.
\end{aligned}$$

6. *The dual point of view.* Let

$$\omega := \bigwedge^2 \Omega^1_{\mathbf{P}^2_k} \cong \mathcal{O}_{\mathbf{P}^2_k}(-3).$$

The natural product map

$$\Omega^1_{\mathbf{P}^2_k} \otimes \Omega^1_{\mathbf{P}^2_k} \longrightarrow \omega$$

gives rise to an isomorphism

$$\Omega^1_{\mathbf{P}^2_k} \longrightarrow T_{\mathbf{P}^2_k} \otimes \omega.$$

Under this isomorphism, a map η as in (2), which corresponds to a section of $T_{\mathbf{P}_k^2} \otimes \mathcal{O}_{\mathbf{P}_k^2}(m-1)$, corresponds to a section

$$\tau \in H^0(\mathbf{P}_k^2, \Omega^1_{\mathbf{P}_k^2} \otimes \mathcal{O}_{\mathbf{P}_k^2}(m+2)). \tag{5}$$

Because of (1), this section corresponds to three homogeneous polynomials A, B and C of degree $m+1$ satisfying the relation

$$xA + yB + zC = 0. \tag{6}$$

We may view the polynomials as giving a homogeneous form on $\mathbf{A}_k^3$:

$$w := Adx + Bdy + Cdz. \tag{7}$$

If η is given by D as in (4), then w is obtained from the determinant:

$$\begin{vmatrix} x & y & z \\ F & G & H \\ dx & dy & dz \end{vmatrix}$$

In other words, $A = yH - zG$, $B = zF - xH$ and $C = xG - yF$. Of course, the assignment $\eta \mapsto \tau$ gives rise to a (linear) isomorphism:

$$\mathbf{P}(H^0(\mathbf{P}_k^2, T_{\mathbf{P}_k^2} \otimes \mathcal{O}_{\mathbf{P}_k^2}(m-1))) \longrightarrow \mathbf{P}(H^0(\mathbf{P}_k^2, \Omega^1_{\mathbf{P}_k^2} \otimes \mathcal{O}_{\mathbf{P}_k^2}(m+2))).$$

We may view $\mathbf{F}_m$ as the space on the left-hand side or that on the right-hand side, at our convenience. And we may harmlessly say that τ or w is the foliation.

Geometrically, for each point $(a : b : c)$ of $\mathbf{P}_k^2$ the direction at the point given by η is that of the line with equation:

$$A(a,b,c)x + B(a,b,c)y + C(a,b,c)z = 0.$$

And the singular locus of the foliation is given by $A = B = C = 0$.

Notice that, because of (6), the singular locus is locally given by two equations. So the following inequality holds relating the Milnor number μ_P and the multiplicity e_P of a singularity P of the foliation:

$$\mu_P \geq \frac{(e_P+1)e_P}{2} + e_P - 1 = \frac{e_P^2 + 3e_P - 2}{2}.$$

3. The action

7. *The action.* The group of automorphisms of $\mathbf{P}_k^2$, namely PGL(3), acts in a natural way on the space of foliations. The action can be described very simply in geometric terms: Let ϕ be an automorphism of $\mathbf{P}_k^2$; given a foliation η, the new foliation $\phi \cdot \eta$ assigns to every point $P \in \mathbf{P}_k^2$ the line $\phi(L)$, where L is the line given by η at $\phi^{-1}(P)$. Algebraically, let g be a 3-by-3 matrix corresponding to ϕ, and let w as in (7) correspond to η. Then $\phi \cdot \eta$ corresponds to $g \cdot w$, where

$$g \cdot w = \begin{bmatrix} A^g & B^g & C^g \end{bmatrix} g^{-1} \begin{bmatrix} dx \\ dy \\ dz \end{bmatrix}.$$

(Given any polynomial $P \in k[x,y,z]$, we denote by P^g the polynomial which, viewed as a function on $\mathbf{A}^3_k$, interpreted as the space of column vectors of dimension 3, satisfies

$$P^g(v) = P(g^{-1}v) \quad \text{for each } v \in \mathbf{A}^3_k.)$$

8. *Stable points.* The action of PGL(3) produces the same orbits as the action by SL(3), the special linear group, that of 3-by-3 matrices with determinant 1, induced by the natural surjection $\mathrm{SL}(3) \to \mathrm{PGL}(3)$. So we will consider this induced action.

Geometric Invariant Theory tells us that there is a categorical quotient of a certain open subset of $\mathbf{F}_m$, that of *semi-stable* points. The semi-stable points are those for which there is an invariant homogeneous polynomial on the coordinates of $\mathbf{F}_m$ not vanishing at the point. And the quotient is simply the projective scheme associated to the (graded) algebra of invariants. Furthermore, a smaller open subset of $\mathbf{F}_m$, consisting of *stable* points, whose orbits in the semi-stable locus are closed, admits even a geometric quotient, which is thus an orbit space; see [6].

To understand the quotient, it is crucial to describe the semi-stable points. However, it is not easy to determine them from the definition. A lot more manageable than the definition is the Hilbert–Mumford Numerical Criterion, by means of one-parameter subgroups.

It was using this criterion that Goméz-Mont and Kempf [8] have shown that a foliation whose all singular points have Milnor number 1 is stable, that is, corresponds to a stable point of $\mathbf{F}_m$. And Alcántara [1], [2] has characterized the semi-stable foliations of degrees 1 and 2.

In our case, a one-parameter subgroup is a nontrivial homomorphism of algebraic groups $\lambda\colon \mathbb{G}_m \to \mathrm{SL}(3)$, where $\mathbb{G}_m$ is the multiplicative group of the field k. Every such homomorphism is diagonalizable: there is $g \in \mathrm{SL}(3)$ such that

$$g^{-1}\lambda(t)g = \lambda_{r_1,r_2,r_3}(t), \quad \text{where } \lambda_{r_1,r_2,r_3}(t) = \begin{bmatrix} t^{r_1} & 0 & 0 \\ 0 & t^{r_2} & 0 \\ 0 & 0 & t^{r_3} \end{bmatrix}$$

for each $t \in \mathbb{G}_m$. Since $\det \lambda(t) = 1$ for every t, the r_i are integers such that

$$r_0 + r_1 + r_2 = 0.$$

We may also assume that $r_1 \geq r_2 \geq r_3$. Since λ is nontrivial, $r_1 > 0 > r_3$.

Now, the space of forms w as in (7), satisfying (6), has a basis of the form:

$$\begin{aligned} w^1_\alpha &:= x^{\alpha_1}y^{\alpha_2}z^{\alpha_3}(-ydx + xdy), \\ w^2_\beta &:= x^{\beta_1}y^{\beta_2}z^{\beta_3}(-zdx + xdz), \\ w^3_\gamma &:= y^{\gamma_2}z^{\gamma_3}(-zdy + ydz), \end{aligned} \tag{8}$$

where $\alpha := (\alpha_1,\alpha_2,\alpha_3)$ and $\beta := (\beta_1,\beta_2,\beta_3)$ (resp. $\gamma := (\gamma_2,\gamma_3)$) run through all triples (resp. pairs) of nonnegative integers summing up to m. This basis

diagonalizes the action of λ_{r_1,r_2,r_3}. More precisely,

$$\begin{aligned}\lambda_{r_1,r_2,r_3}(t)\cdot w^1_\alpha &= t^{-r_1(\alpha_1+1)-r_2(\alpha_2+1)-r_3\alpha_3}w^1_\alpha,\\ \lambda_{r_1,r_2,r_3}(t)\cdot w^2_\beta &= t^{-r_1(\beta_1+1)-r_2\beta_2-r_3(\beta_3+1)}w^2_\beta,\\ \lambda_{r_1,r_2,r_3}(t)\cdot w^3_\gamma &= t^{-r_2(\gamma_2+1)-r_3(\gamma_3+1)}w^3_\gamma.\end{aligned}$$

Finally, consider a point of $\mathbf{F}_m$, corresponding to w as in (7). Then, for each $g\in \mathrm{SL}(3)$,

$$g\cdot w=\sum_\alpha a_\alpha(g)w^1_\alpha+\sum_\beta b_\beta(g)w^2_\beta+\sum_\gamma c_\gamma(g)w^3_\gamma, \tag{9}$$

for unique $a_\alpha(g)$, $b_\beta(g)$ and $c_\gamma(g)$ in k. Then the Hilbert–Mumford Numerical Criterion says that w is not stable, that is, the corresponding point on $\mathbf{F}_m$ is not stable, if and only if there are $g\in\mathrm{SL}(3)$ and integers r_1,r_2,r_3 satisfying $r_1+r_2+r_3=0$ and $0<r_1\geq r_2\geq r_3<0$ such that all of the following conditions hold:

$$\begin{aligned} r_1(\alpha_1+1)+r_2(\alpha_2+1)+r_3\alpha_3 &\leq 0 \quad \text{if } a_\alpha(g)\neq 0,\\ r_1(\beta_1+1)+r_2\beta_2+r_3(\beta_3+1) &\leq 0 \quad \text{if } b_\beta(g)\neq 0,\\ r_2(\gamma_2+1)+r_3(\gamma_3+1) &\leq 0 \quad \text{if } c_\gamma(g)\neq 0.\end{aligned} \tag{10}$$

Furthermore, w is nonsemi-stable if in addition all the inequalities above are strict.

Theorem 9. *A foliation of degree $m>1$ is nonstable (resp. nonsemi-stable) only if it has singularities in dimension 1 or contains an isolated singular point with multiplicity at least (resp. greater than) $(m^2-1)/(2m+1)$.*

Proof. Let w as in (7) correspond to the foliation. Assume first that w is nonstable. Then there are $g\in\mathrm{SL}(3)$ and integers r_1,r_2,r_3 satisfying

$$r_1+r_2+r_3=0 \quad\text{and}\quad 0<r_1\geq r_2\geq r_3<0 \tag{11}$$

such that (10) holds. Since w is stable if and only $g\cdot w$ is, and the foliation w has singularities in dimension 1 or contains an isolated singular point with a certain multiplicity if and only if the same holds for $g\cdot w$, we may assume that $g=1$, and simplify the notation:

$$a_\alpha:=a_\alpha(1),\quad b_\beta:=b_\beta(1),\quad c_\gamma:=c_\gamma(1).$$

We claim that either the foliation has singularities in dimension 1 or

$$r_2\leq\frac{-r_3}{m+1}. \tag{12}$$

Indeed, suppose (12) does not hold. Let $\alpha=(\alpha_1,\alpha_2,\alpha_3)$ be a triple of nonnegative integers with $\alpha_3=0$ and $\alpha_1+\alpha_2=m$. Then, since $\alpha_1, r_1-r_2\geq 0$ and $-r_3, r_2>0$,

$$\begin{aligned}0<(r_1-r_2)\alpha_1+r_2m-r_3&=(r_1-r_2)\alpha_1+r_2(\alpha_1+\alpha_2)-r_3\\ &=r_1(\alpha_1+1)+r_2(\alpha_2+1)+r_3\alpha_3.\end{aligned}$$

Thus (10) yields $a_\alpha = 0$.

Also, let $\beta = (\beta_1, \beta_2, \beta_3)$ be a triple of nonnegative integers with $\beta_3 = 0$ and $\beta_1 + \beta_2 = m$. Then, since $\beta_1, r_1 - r_2 \geq 0$ and $r_2, m - 1 > 0$,

$$\begin{aligned} 0 < (r_1 - r_2)\beta_1 + r_2(m-1) &= (r_1 - r_2)\beta_1 + r_2(\beta_1 + \beta_2) - r_2 \\ &= r_1(\beta_1 + 1) + r_2\beta_2 + r_3(\beta_3 + 1). \end{aligned}$$

Thus (10) yields $b_\beta = 0$.

Finally, since $r_2(m+1) + r_3 > 0$, we have that $c_{(m,0)} = 0$. But then it follows from (9) that $z|w$, and thus the singular locus of the foliation contains a line.

Assume now that the singular locus of the foliation is finite. Then (12) holds, from which we obtain

$$r_1 - r_3 = -r_2 - 2r_3 \geq \frac{r_3}{m+1} - 2r_3 = -r_3\frac{2m+1}{m+1}. \tag{13}$$

Let $\alpha = (\alpha_1, \alpha_2, \alpha_3)$ be a triple of nonnegative integers summing up to m. We claim:

$$\text{If } \alpha_1 > \frac{m^2-1}{2m+1} \text{ then } a_\alpha = 0. \tag{14}$$

Indeed, if $\alpha_1 > (m^2-1)/(2m+1)$ then

$$\begin{aligned} r_1(\alpha_1 + 1) + r_2(\alpha_2 + 1) + r_3\alpha_3 &= (r_1 - r_3)\alpha_1 + (r_2 - r_3)\alpha_2 + r_3(m-1) \\ &\geq -r_3\frac{2m+1}{m+1}\alpha_1 + r_3(m-1) \\ &> 0, \end{aligned}$$

where for the equality above we used that $\alpha_3 = m - \alpha_1 - \alpha_2$ and $r_3 = -r_1 - r_2$, and for the first inequality we used (13), $\alpha_2 \geq 0$ and $r_2 \geq r_3$. Thus $a_\alpha = 0$ from (10).

Similarly:

$$\text{If } \beta_1 > \frac{m^2+m+1}{2m+1} \text{ then } b_\beta = 0. \tag{15}$$

Indeed, if $\beta_1 > (m^2+m+1)/(2m+1)$ then

$$\begin{aligned} r_1(\beta_1 + 1) + r_2\beta_2 + r_3(\beta_3 + 1) &= (r_1 - r_3)\beta_1 + (r_2 - r_3)\beta_2 + r_3m - r_2 \\ &\geq -r_3\frac{2m+1}{m+1}\beta_1 + r_3\Big(m + \frac{1}{m+1}\Big) \\ &> 0, \end{aligned}$$

where for the first inequality above we used (12). Thus $b_\beta = 0$ from (10).

Now, using (8) to expand (9), we get $w = Adx + Bdy + Cdz$, where

$$\begin{aligned} B &= \sum_\alpha a_\alpha x^{\alpha_1+1}y^{\alpha_2}z^{\alpha_3} - \sum_\gamma c_\gamma y^{\gamma_2}z^{\gamma_3+1}, \\ C &= \sum_\beta b_\beta x^{\beta_1+1}y^{\beta_2}z^{\beta_3} + \sum_\gamma c_\gamma y^{\gamma_2+1}z^{\gamma_3}. \end{aligned}$$

Let $P := (1:0:0)$. Since $xA + yB + zC = 0$, the ideal of the singular locus of the foliation at P is generated by $B(1, y/x, z/x)$ and $C(1, y/x, z/x)$. Since $\gamma_2 + \gamma_3 = m$, it follows that the multiplicity of the foliation at P is $\min(m+1, \xi)$ where

$$\begin{aligned}\xi :=& \min\big(\min(\alpha_2+\alpha_3 \,|\, a_\alpha \neq 0), \min(\beta_2+\beta_3 \,|\, b_\beta \neq 0)\big)\\ =& \min\big(\min(m-\alpha_1 \,|\, a_\alpha \neq 0), \min(m-\beta_1 \,|\, b_\beta \neq 0)\big)\\ =& m - \max\big(\max(\alpha_1 \,|\, a_\alpha \neq 0), \max(\beta_1 \,|\, b_\beta \neq 0)\big).\end{aligned}$$

(The minimum (resp. maximum) of the empty set is $+\infty$ (resp. $-\infty$) by convention.) Thus, it follows from (14) and (15) that

$$\xi \geq m - \max\Big(\frac{m^2-1}{2m+1}, \frac{m^2+m+1}{2m+1}\Big) = m - \frac{m^2+m+1}{2m+1} = \frac{m^2-1}{2m+1}. \tag{16}$$

If w is nonsemi-stable then the same proof works with the following modifications: the inequality in (12) is strict while those in (13), (14), (15) and (16) are not. □

4. The dual discriminant curve

Theorem 10. *Given a foliation of $\mathbf{P}^2_k$ of degree $m \geq 2$ whose singular locus does not contain a double curve, the lines tangent to the foliation with multiplicity at least 2 are parameterized by a curve on the dual plane $\check{\mathbf{P}}^2_k$ of degree m^2+m-2.*

Proof. Let $\check{x}$, $\check{y}$ and $\check{z}$ be coordinates of $\check{\mathbf{P}}^2_k$ dual to x, y and z. The incidence variety $I \subset \mathbf{P}^2_k \times \check{\mathbf{P}}^2_k$ is thus given by

$$\check{x}x + \check{y}y + \check{z}z = 0.$$

Let D as in (4) correspond to the foliation. Requiring the above line to be tangent to the foliation at $(x:y:z)$ is to impose that

$$\check{x}F + \check{y}G + \check{z}H = 0.$$

Let $V \subseteq I$ be the subscheme of I given by the above equation. It parameterizes the pairs (P, L) where L is a line on $\mathbf{P}^2_k$ and P is a point on L where the foliation is singular or tangent to L. Let $\pi\colon V \to \check{\mathbf{P}}^2_k$ denote the projection, and let $D \subseteq V$ be the degeneracy locus of the natural map $\pi^*\Omega^1_{\check{\mathbf{P}}^2_k} \to \Omega^1_V$. Since the singular locus of the foliation contains no double curve, $\pi(D) \neq \check{\mathbf{P}}^2_k$. Let $C \subseteq \check{\mathbf{P}}^2_k$ be the curve such that $\pi_*[D] = [C]$ as cycles. This is the curve parameterizing lines tangent to the foliation with multiplicity at least 2.

We claim that $\deg C = m^2+m-2$. Indeed, let h_1 (resp. h_2) be the pullback to $\mathbf{P}^2_k \times \check{\mathbf{P}}^2_k$ of the hyperplane class h on $\mathbf{P}^2_k$ (resp. $\check{h}$ on $\check{\mathbf{P}}^2_k$). Then

$$[I] = h_1 + h_2 \quad \text{and} \quad [V] = (h_1+h_2)(mh_1+h_2)$$

in the Chow ring of $\mathbf{P}^2_k \times \check{\mathbf{P}}^2_k$. Now,

$$[D] = c_1(\Omega^1_V) \cap [V] - c_1(\pi^*\Omega^1_{\check{\mathbf{P}}^2_k}) \cap [V].$$

It follows from the Whitney Sum Formula ([7], Thm. 3.2(e), p. 50) and the Euler exact sequence that

$$\pi^* c_1(\Omega^1_{\check{\mathbf{P}}^2_k}) \cap [\mathbf{P}^2_k \times \check{\mathbf{P}}^2_k] = -3h_2.$$

In addition, Ω^1_V sits in the natural exact sequence,

$$0 \longrightarrow \mathcal{O}_V(-1,-1) \oplus \mathcal{O}_V(-m,-1) \longrightarrow \Omega^1_{\mathbf{P}^2_k \times \check{\mathbf{P}}^2_k}|_V \longrightarrow \Omega^1_V \longrightarrow 0.$$

Thus, applying the Whitney Sum Formula again,

$$\begin{aligned} c_1(\Omega^1_V) \cap [V] =& (-3(h_1+h_2) + (h_1+h_2) + (mh_1+h_2))[V] \\ =& ((m-2)h_1 - h_2)[V]. \end{aligned}$$

So,

$$[D] = ((m-2)h_1 + 2h_2)[V] = ((m-2)h_1 + 2h_2)(h_1+h_2)(mh_1+h_2).$$

Since $h_1^3 = h_2^3 = 0$, we get

$$\begin{aligned} [D] =& (2m + m(m-2) + (m-2))h_1^2 h_2 + ((m-2) + 2 + 2m)h_1 h_2^2 \\ =& (m^2 + m - 2)h_1^2 h_2 + 3m h_1 h_2^2, \end{aligned}$$

and thus $\pi_*[D] = (m^2 + m - 2)h$. □

11. *Degree* 2. Let

$$\mathbf{C}_d := \mathbf{P}(H^0(\mathbf{P}^2_k, \mathcal{O}_{\mathbf{P}^2_k}(d))),$$

the projective space parameterizing plane curves of degree d. It has dimension $(d^2+3d)/2$. By Theorem 10, there is a rational map

$$\Phi \colon \mathbf{F}_m \dashrightarrow \mathbf{C}_{m^2+m-2}.$$

In case $m = 2$, both the target and the source of Φ have the same dimension, as

$$m^2 + 4m + 2 = \frac{(m^2+m-2)^2 + 3(m^2+m-2)}{2} = 14.$$

In this case, the dimensions are small enough that Φ can be explicitly described, using CoCoA[3] (assuming the ground field k has characteristic 0).

Consider a point of $\mathbf{F}_2$ given by w as in (7). As in Section 3 we may write

$$w = \sum_\alpha a_\alpha w^1_\alpha + \sum_\beta b_\beta w^2_\beta + \sum_\gamma c_\gamma w^3_\gamma,$$

for unique a_α, b_β and c_γ in k, where $\alpha := (\alpha_1, \alpha_2, \alpha_3)$ and $\beta := (\beta_1, \beta_2, \beta_3)$ (resp. $\gamma := (\gamma_2, \gamma_3)$) run through all triples (resp. pairs) of nonnegative integers summing up to 2, and the w^1_α, w^2_β and w^3_γ are given in (8).

The coefficients a_α, b_β and c_γ can be seen as coordinates of $\mathbf{F}_2 \cong \mathbf{P}_k^{14}$. Then the associated quartic to w is given by:

$$
\begin{aligned}
&\Big(c_{(2,0)}c_{(0,2)} - \frac{c_{(1,1)}^2}{4}\Big)\check{x}^4 + \Big(\frac{c_{(1,1)}b_{(0,1,1)}}{2} - c_{(0,2)}b_{(0,2,0)} - c_{(2,0)}b_{(0,0,2)}\Big)\check{x}^3\check{y}\\
&+\Big(b_{(0,2,0)}b_{(0,0,2)} + c_{(0,2)}b_{(1,1,0)} - \frac{b_{(0,1,1)}^2}{4} - \frac{c_{(1,1)}b_{(1,0,1)}}{2}\Big)\check{x}^2\check{y}^2\\
&+\Big(\frac{b_{(1,0,1)}b_{(0,1,1)}}{2} - c_{(0,2)}b_{(2,0,0)} - b_{(0,0,2)}b_{(1,1,0)}\Big)\check{x}\check{y}^3 + \Big(b_{(2,0,0)}b_{(0,0,2)} - \frac{b_{(1,0,1)}^2}{4}\Big)\check{y}^4\\
&+\Big(c_{(0,2)}a_{(0,2,0)} + c_{(2,0)}a_{(0,0,2)} - \frac{c_{(1,1)}a_{(0,1,1)}}{2}\Big)\check{x}^3\check{z}\\
&+\Big(\frac{c_{(1,1)}a_{(1,0,1)}}{2} + \frac{b_{(0,1,1)}a_{(0,1,1)}}{2} + c_{(2,0)}b_{(1,0,1)} - \frac{c_{(1,1)}b_{(1,1,0)}}{2} - b_{(0,0,2)}a_{(0,2,0)}\\
&\quad - b_{(0,2,0)}a_{(0,0,2)} - c_{(0,2)}a_{(1,1,0)}\Big)\check{x}^2\check{y}\check{z}\\
&+\Big(\frac{b_{(1,1,0)}b_{(0,1,1)}}{2} + c_{(0,2)}a_{(2,0,0)} + b_{(1,1,0)}a_{(0,0,2)} + b_{(0,0,2)}a_{(1,1,0)} + c_{(1,1)}b_{(2,0,0)}\\
&\quad - \frac{b_{(0,1,1)}a_{(1,0,1)}}{2} - \frac{b_{(1,0,1)}a_{(0,1,1)}}{2} - b_{(0,2,0)}b_{(1,0,1)}\Big)\check{x}\check{y}^2\check{z}\\
&+\Big(\frac{b_{(1,1,0)}b_{(1,0,1)}}{2} + \frac{b_{(1,0,1)}a_{(1,0,1)}}{2}\\
&\quad - b_{(2,0,0)}b_{(0,1,1)} - b_{(0,0,2)}a_{(2,0,0)} - b_{(2,0,0)}a_{(0,0,2)}\Big)\check{y}^3\check{z}\\
&+\Big(a_{(0,2,0)}a_{(0,0,2)} + \frac{c_{(1,1)}a_{(1,1,0)}}{2} - \frac{a_{(0,1,1)}^2}{4} - c_{(2,0)}a_{(1,0,1)}\Big)\check{x}^2\check{z}^2\\
&+\Big(\frac{a_{(1,0,1)}a_{(0,1,1)}}{2} + b_{(1,0,1)}a_{(0,2,0)} + b_{(0,2,0)}a_{(1,0,1)} - \frac{b_{(0,1,1)}a_{(1,1,0)}}{2} - \frac{b_{(1,1,0)}a_{(0,1,1)}}{2}\\
&\quad - c_{(2,0)}b_{(2,0,0)} - c_{(1,1)}a_{(2,0,0)} - a_{(0,0,2)}a_{(1,1,0)}\Big)\check{x}\check{y}\check{z}^2\\
&+\Big(b_{(2,0,0)}b_{(0,2,0)} + b_{(0,1,1)}a_{(2,0,0)} + a_{(2,0,0)}a_{(0,0,2)} + b_{(2,0,0)}a_{(0,1,1)} - \frac{b_{(1,1,0)}^2}{4} - \frac{a_{(1,0,1)}^2}{4}\\
&\quad - \frac{b_{(1,0,1)}a_{(1,1,0)}}{2} - \frac{b_{(1,1,0)}a_{(1,0,1)}}{2}\Big)\check{y}^2\check{z}^2\\
&+\Big(\frac{a_{(1,1,0)}a_{(0,1,1)}}{2} + c_{(2,0)}a_{(2,0,0)} - a_{(0,2,0)}a_{(1,0,1)}\Big)\check{x}\check{z}^3\\
&+\Big(\frac{b_{(1,1,0)}a_{(1,1,0)}}{2} + \frac{a_{(1,1,0)}a_{(1,0,1)}}{2}\\
&\quad - b_{(0,2,0)}a_{(2,0,0)} - b_{(2,0,0)}a_{(0,2,0)} - a_{(2,0,0)}a_{(0,1,1)}\Big)\check{y}\check{z}^3\\
&+\Big(a_{(2,0,0)}a_{(0,2,0)} - \frac{a_{(1,1,0)}^2}{4}\Big)\check{z}^4 = 0,
\end{aligned}
$$

where $\check{x}$, $\check{y}$ and $\check{z}$ are the coordinates of $\check{\mathbf{P}}_k^2$ dual to x, y and z.

12. *Invariants and instability.* Invariants for degree-2 foliations can thus be obtained from invariants for plane quartics by composition. However, the latter invariants are not completely known. In [5], Thm. 3.2, p. 286, assuming k is the field of complex numbers, Dixmier produced a homogeneous system of parameters for the algebra of invariants of the quartics: seven homogeneous invariants of degrees 3, 6, 9, 12, 15, 18 and 27. More invariants should be necessary. According to [5], p. 280, the algebra of invariants can be generated by 56 invariants, though Shioda [12], p. 1046, conjectured that 13 should be enough.

At any rate, if the foliation is not semi-stable, neither is the corresponding quartic. This can be seen directly from our explicit description of the associated quartic, as follows. If w is not semi-stable, there are $g \in \mathrm{SL}(3)$ and integers r_1, r_2, r_3 satisfying

$$r_1 + r_2 + r_3 = 0 \quad \text{and} \quad 0 < r_1 \geq r_2 \geq r_3 < 0$$

such that (10) holds and the inequalities are strict. As in the proof of Theorem 9, assume $g = 1$. Then, reasoning as in the proof of that theorem, we can show that

$$a_{(2,0,0)} = a_{(1,1,0)} = a_{(1,0,1)} = b_{(2,0,0)} = b_{(1,1,0)} = 0. \tag{17}$$

Furthermore, either $b_{(1,0,1)} = 0$ or

$$a_{(0,2,0)} = a_{(0,1,1)} = b_{(0,2,0)} = 0. \tag{18}$$

Thus, using (17) to simplify the equation of the quartic, we get:

(19)

$$\begin{aligned}
&\Big(c_{(2,0)}c_{(0,2)} - \frac{c_{(1,1)}^2}{4}\Big)\check{x}^4 + \Big(\frac{c_{(1,1)}b_{(0,1,1)}}{2} - c_{(0,2)}b_{(0,2,0)} - c_{(2,0)}b_{(0,0,2)} = 0\Big)\check{x}^3\check{y}\\
&+\Big(b_{(0,2,0)}b_{(0,0,2)} - \frac{b_{(0,1,1)}^2}{4} - \frac{c_{(1,1)}b_{(1,0,1)}}{2}\Big)\check{x}^2\check{y}^2 + \Big(\frac{b_{(1,0,1)}b_{(0,1,1)}}{2}\Big)\check{x}\check{y}^3\\
&-\Big(\frac{b_{(1,0,1)}^2}{4}\Big)\check{y}^4 + \Big(c_{(0,2)}a_{(0,2,0)} + c_{(2,0)}a_{(0,0,2)} - \frac{c_{(1,1)}a_{(0,1,1)}}{2}\Big)\check{x}^3\check{z}\\
&+\Big(\frac{b_{(0,1,1)}a_{(0,1,1)}}{2} + c_{(2,0)}b_{(1,0,1)} - b_{(0,0,2)}a_{(0,2,0)} - b_{(0,2,0)}a_{(0,0,2)}\Big)\check{x}^2\check{y}\check{z}\\
&-\Big(b_{(0,2,0)}b_{(1,0,1)} + \frac{b_{(1,0,1)}a_{(0,1,1)}}{2}\Big)\check{x}\check{y}^2\check{z} + \Big(a_{(0,2,0)}a_{(0,0,2)} - \frac{a_{(0,1,1)}^2}{4}\Big)\check{x}^2\check{z}^2\\
&+\Big(b_{(1,0,1)}a_{(0,2,0)}\Big)\check{x}\check{y}\check{z}^2 = 0.
\end{aligned}$$

Then $(0:0:1)$ is a singular point of the quartic. Furthermore, if $b_{(1,0,1)} \neq 0$, then (18) holds, and the equation becomes:

$$\begin{aligned}
&\Big(c_{(2,0)}c_{(0,2)} - \frac{c_{(1,1)}^2}{4}\Big)\check{x}^4 + \Big(\frac{c_{(1,1)}b_{(0,1,1)}}{2} - c_{(2,0)}b_{(0,0,2)}\Big)\check{x}^3\check{y}\\
&-\Big(\frac{b_{(0,1,1)}^2}{4} + \frac{c_{(1,1)}b_{(1,0,1)}}{2}\Big)\check{x}^2\check{y}^2 + \Big(\frac{b_{(1,0,1)}b_{(0,1,1)}}{2}\Big)\check{x}\check{y}^3 - \Big(\frac{b_{(1,0,1)}^2}{4}\Big)\check{y}^4\\
&+\Big(c_{(2,0)}a_{(0,0,2)}\Big)\check{x}^3\check{z} + \Big(c_{(2,0)}b_{(1,0,1)}\Big)\check{x}^2\check{y}\check{z} = 0.
\end{aligned}$$

In this case, the quartic has a triple point at $(0:0:1)$ with two equal tangent lines, or a quadruple point, whence is not semi-stable, according to [6], p. 80. On the other hand, if $b_{(1,0,1)}=0$, then the equation of the quartic becomes

$$\begin{aligned}
&\Big(c_{(2,0)}c_{(0,2)}-\frac{c_{(1,1)}^2}{4}\Big)\check{x}^4+\Big(\frac{c_{(1,1)}b_{(0,1,1)}}{2}-c_{(0,2)}b_{(0,2,0)}-c_{(2,0)}b_{(0,0,2)}\Big)\check{x}^3\check{y}\\
&+\Big(b_{(0,2,0)}b_{(0,0,2)}-\frac{b_{(0,1,1)}^2}{4}\Big)\check{x}^2\check{y}^2+\Big(c_{(0,2)}a_{(0,2,0)}+c_{(2,0)}a_{(0,0,2)}-\frac{c_{(1,1)}a_{(0,1,1)}}{2}\Big)\check{x}^3\check{z}\\
&+\Big(\frac{b_{(0,1,1)}a_{(0,1,1)}}{2}-b_{(0,0,2)}a_{(0,2,0)}-b_{(0,2,0)}a_{(0,0,2)}\Big)\check{x}^2\check{y}\check{z}\\
&+\Big(a_{(0,2,0)}a_{(0,0,2)}-\frac{a_{(0,1,1)}^2}{4}\Big)\check{x}^2\check{z}^2=0,
\end{aligned}$$

whence the union of a double line, $\check{x}=0$, and a conic, thus again not semi-stable, according to loc. cit..

However, there are nonsemi-stable quartics with milder singularities that do not correspond to nonsemi-stable foliations. For instance, if we set (17), we end up with Equation (19) for the quartic. If we further set $a_{(0,2,0)}=a_{(0,1,1)}=0$, we get

$$\begin{aligned}
&\Big(c_{(2,0)}c_{(0,2)}-\frac{c_{(1,1)}^2}{4}\Big)\check{x}^4+\Big(\frac{c_{(1,1)}b_{(0,1,1)}}{2}-c_{(0,2)}b_{(0,2,0)}-c_{(2,0)}b_{(0,0,2)}\Big)\check{x}^3\check{y}\\
&+\Big(b_{(0,2,0)}b_{(0,0,2)}-\frac{b_{(0,1,1)}^2}{4}-\frac{c_{(1,1)}b_{(1,0,1)}}{2}\Big)\check{x}^2\check{y}^2+\Big(\frac{b_{(1,0,1)}b_{(0,1,1)}}{2}\Big)\check{x}\check{y}^3\\
&-\Big(\frac{b_{(1,0,1)}^2}{4}\Big)\check{y}^4+\Big(c_{(2,0)}a_{(0,0,2)}\Big)\check{x}^3\check{z}+\Big(c_{(2,0)}b_{(1,0,1)}-b_{(0,2,0)}a_{(0,0,2)}\Big)\check{x}^2\check{y}\check{z}\\
&-\Big(b_{(0,2,0)}b_{(1,0,1)}\Big)\check{x}\check{y}^2\check{z}=0.
\end{aligned}\tag{20}$$

This quartic has a triple or quadruple point, and is thus nonsemi-stable. If we choose the remaining coordinates of $\mathbf{F}_2$ such that

$$b_{(1,0,1)}b_{(0,2,0)}\neq 0 \quad\text{and}\quad b_{(1,0,1)}c_{(2,0)}+a_{(0,0,2)}b_{(0,2,0)}\neq 0,$$

then the triple point has distinct tangent lines. If we now let none of these lines be contained in the quartic, which is an open condition on the parameters that can be satisfied, as it can be easily verified with CoCoA[3], then $(0:0:1)$ is the unique singular point of the quartic. Thus, the quartic arises from a semi-stable foliation. The above simple example shows that there are invariants of degree-2 foliations that do not arise from invariants of quartics.

References

[1] C. Alcántara, *The good quotient of the semi-stable foliations of* $\mathbb{CP}^2$ *of degree* 1, Results Math. **53** (2009), 1–7.

[2] C. Alcántara, *Geometric invariant theory for holomorphic foliations on* $\mathbb{CP}^2$ *of degree* 2, Glasgow Math. J. **53** (2011), 153–168.

[3] CoCoATeam, CoCoA*: a system for doing Computations in Commutative Algebra*. Available at http://cocoa.dima.unige.it.

[4] G. Darboux, *Mémoire sur les équations différentielles algébriques du premier ordre e du premier degré (Mélanges)*, Bull. Sci. Mathèmatiques 2ème série **2** (1878), 60–96; 123–144; 151–200.
[5] J. Dixmier, *On the projective invariants of quartic plane curves*, Adv. in Math. **64** (1987), 279–304.
[6] J. Fogarty, F. Kirwan and D. Mumford, *Geometric Invariant Theory*, Ergebnisse der Mathematik und ihrer Grenzgebiete (2), vol. 34, Springer-Verlag, Berlin, 1994.
[7] W. Fulton, *Intersection Theory*, Ergebnisse der Mathematik und ihrer Grenzgebiete (3), vol. 2, Springer-Verlag, Berlin, 1984.
[8] X. Goméz-Mont and G. Kempf, *Stability of meromorphic vector fields in projective spaces*, Comment. Math. Helv. **64** (1989), 462–473.
[9] J.-P. Jouanolou, *Équations de Pfaff algébriques*, Lecture Notes in Mathematics, vol. 708, Springer-Verlag, Berlin, 1979.
[10] C. Okonek, M. Schneider and H. Spindler, *Vector bundles on complex projective spaces*, Progress in Mathematics, vol. 3, Birkhäuser, Boston, 1980.
[11] H. Poincaré, *Sur l'intégration algébrique des équations différentielles du premier ordre et du premier degré*, I and II, R. Circ. Mat. Palermo **5** (1891), 161–191; **11** (1897), 193–239.
[12] T. Shioda, *On the graded ring of invariants of binary octavics*, Amer. J. Math. **89** (1967), 1022–1046.

Instituto de Matemática Pura e Aplicada, Estrada Dona Castorina 110, 22460-320 Rio de Janeiro RJ, Brazil
E-mail address: esteves@impa.br

Università degli Studi di Torino, Via Carlo Alberto 10, 10123 Torino, Italy
E-mail address: marina.marchisio@unito.it

RENDICONTI DEL CIRCOLO MATEMATICO DI PALERMO
Serie II, Suppl. 83 (2011), pp. 189-198

A problem of Buffon type for regular lattices with regular obstacles

Gioia Failla
University of Reggio Calabria,
Faculty of Engineering, DIMET
E-mail: gioiafailla@hotmail.it

Abstract

In this paper we solve problems of Buffon type for a regular lattice with fundamental cell an equilateral triangle with equilateral triangles (Fig.1) or circular sectors (Fig.8) as obstacles.

Introduction

A problem of Buffon type for triangular lattices with triangular obstacles was previously studied by Stoka and Duma in [1], where they considered as test bodies rectangles of constant sides, circles of constant radius, equilateral triangles of constant side or segments of non-small constant length. In particular the barycenters of the triangular obstacles were in the vertices of the triangles of the lattice. In this paper we consider first triangular lattices with equilateral triangular obstacles, whose one of the vertices coincides with one of the vertices of the equilateral triangle, fundamental cell in the lattice (see Fig.1). After we consider as obstacles circular sectors (as appears in Fig.8). As test bodies we take a line segment of constant length.

1

Let $\mathcal{R}_1(a, b)$ be a regular lattice whose fundamental cell is a equilateral triangle, with edge a, with equilateral obstacles, with edge b, $b < \frac{a}{2}$, $(Fig.1)$:

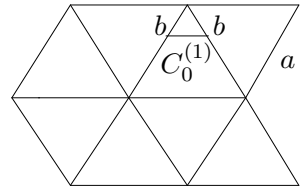

Fig.1

Denoting by $C_0^{(1)}$ this cell, we have

$$\text{area } C_0^{(1)} = \frac{\sqrt{3}a^2}{4} - 3\frac{\sqrt{3}b^2}{4}.$$

We want to determine the probability that a line segment s of constant length l (with $b < l < \frac{a}{2}$) and of random position intersects an edge of the lattice $\mathcal{R}_1$; obviously this probability is equal to the probability $P_{int}^{(1)}$ that the line segment s intersects an edge of the fundamental cell.
Consider now a position of the line segment s of midpoint p that shapes an angle φ with the coordinate axis x. Moreover, consider the limit positions of the line segment s and let $\hat{C}_0^{(1)}(\varphi)$ be the figure determined by these positions for a fixed value of φ, (Fig.2):

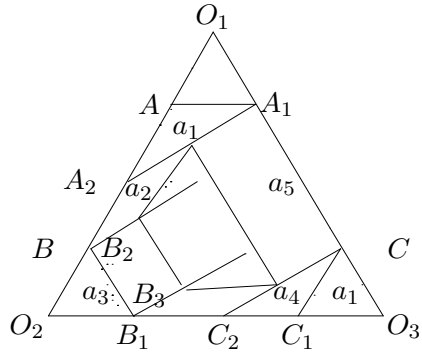

Fig.2

With the notations of the previous figure, it follows area $\hat{C}_0^{(1)}(\varphi) =$

area $C_0^{(1)}$−[2 area $a_1(\varphi)$+ area $a_2(\varphi)$+ area $a_3(\varphi)$ area $a_4(\varphi)$+ area $a_5(\varphi)$]. (1.1)

To compute the area $a_1(\varphi)$, consider the figure

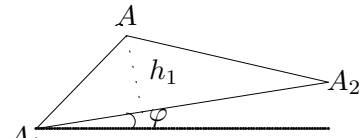

Fig.3

We have

$$| A_1A_2 |= l, | AA_1 |= b, \widehat{AA_1A_2} = \varphi, \widehat{A_2AA_1} = \frac{2\pi}{3}, \widehat{AA_2A_1} = \frac{\pi}{3} - \varphi, \quad (1.2)$$

then

$$h_1 = bsin\varphi$$

and

$$\text{area } a_1(\varphi) = \frac{lh_1}{2}$$

that is

$$\text{area } a_1(\varphi) = \frac{bl\sin\varphi}{2}.$$

Moreover, by the triangle AA_1A_2 it follows

$$\frac{| AA_2 |}{\sin\varphi} = \frac{l}{\sin\frac{2\pi}{3}} = \frac{b}{\sin(\frac{\pi}{3} - \varphi)}, \quad (1.3)$$

then

$$| AA_2 |= \frac{2\sqrt{3}l\sin\varphi}{3}. \quad (1.4)$$

To compute area $a_2(\varphi)$, consider the figure

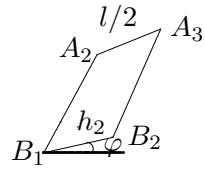

Fig.4

Taking in account the relation (1.4), one has

$$| A_2B_1 |= a - 2b - | AA_2 |= a - 2b - \frac{2\sqrt{3}l\sin\varphi}{3}. \tag{1.5}$$

Since $\widehat{A_2B_1B_2} = \frac{\pi}{3} - \varphi$, it follows

$$h_2 = \frac{l}{2}\sin(\frac{\pi}{3} - \varphi) = \frac{l}{4}(\sqrt{3}\cos\varphi - \sin\varphi).$$

Then

$$\text{area } a_2(\varphi) = \left(a - 2b - \frac{2\sqrt{3}l\sin\varphi}{3}\right)(\sqrt{3}\cos\varphi - \sin\varphi)\frac{l}{4}. \tag{1.6}$$

The figure

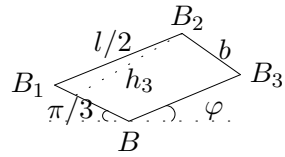

Fig.5

allow us to compute the area a_5.

We have

$$\widehat{BB_1B_2} = \frac{2\pi}{3} - \varphi, \widehat{B_1BB_3} = \frac{\pi}{3} + \varphi,$$

then

$$h_3 = \frac{l}{2}\sin(\frac{\pi}{3} + \varphi) = \frac{l}{4}(\sqrt{3}\cos\varphi + \sin\varphi)$$

and

$$\text{area } a_3(\varphi) = \frac{bl}{4}(\sqrt{3}\cos\varphi + \sin\varphi). \tag{1.7}$$

To compute area $a_4(\varphi)$, consider the figure

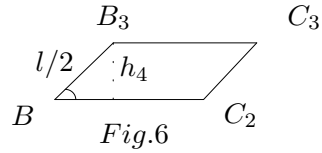

$Fig.6$

that provides

$$h_4 = \frac{l}{2}\sin\varphi.$$

We have $\Delta AA_1A_2 = \Delta CC_1C_2$, then $\mid C_1C_2 \mid = \mid AA_2$ and with 1.4,

$$\mid C_1C_2 \mid = \frac{2\sqrt{3}l\sin\varphi}{3}.$$

Then

$\mid BC_2 \mid = a - 2b - \mid C_1C_2 \mid = a - 2b - \dfrac{2\sqrt{3}l\sin\varphi}{3}\dfrac{l}{2}\sin\varphi$. The figure

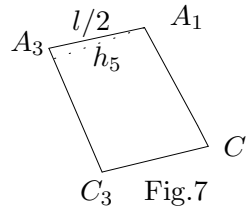

Fig.7

gives us $\mid CA_1 \mid = a - 2b$. Since $\widehat{A_1A_3C_3} = \frac{2\pi}{3} - \varphi$, we have

$$h_5 = \frac{l}{2}\sin(\frac{\pi}{3} + \varphi) = \frac{l}{4}(\sqrt{3}\cos\varphi + \sin\varphi)$$

and

$$\text{area } a_5(\varphi) = \mid A_3C_3 \mid h_5 = \frac{(a-2b)l}{a}(\sqrt{3}\cos\varphi + \sin\varphi). \qquad (1.8)$$

Replacing in (1.1) the relation (1.3), (1.5), (1.6), (1.7), (1.8) we obtain

$$\text{area } \widehat{C}_0^{(1)}(\varphi) = \text{ area } C_0^{(1)} - [bl\sin\varphi + (a-2b-\frac{2\sqrt{3}\sin\varphi}{3})](\sqrt{3}\cos\varphi - \sin\varphi)\frac{l}{4} +$$
$$\frac{bl}{4}(\sqrt{3}\cos\varphi + \sin\varphi) + (a-2b-\frac{2\sqrt{3}}{3}l\sin\varphi)\frac{l}{2}\sin\varphi) + \frac{a-2b}{4}(\sqrt{3}\cos\varphi + \sin\varphi)l =$$
$$\text{area } C_0^{(1)} + -\frac{1}{4}[\sqrt{3}(2a-3b)l\cos\varphi + (b-a)l\sin\varphi - l^2(\sin 2\varphi + \frac{\sqrt{3}}{3}\cos 2\varphi - \frac{\sqrt{3}}{3}] \quad (1.9)$$

Denoting by $\mathcal{M}_1$ the set of the line segments s that have the midpoint in $C_0^{(1)}$ and with $\mathcal{N}_1$ the set of the segments s entirely contained in $C_0^{(1)}$, we have [2]:

$$P_{int}^{(1)} = 1 - \frac{\mu(\mathcal{N}_1)}{\mu(\mathcal{M}_1)}, \quad (1.10)$$

where μ is the Lesbegue measure in the euclidian plane. The measures $\mu(\mathcal{M}_1)$ and $\mu(\mathcal{N}_1)$ are computed using the cinematic measure of Poincarè [1]

$$dK = dx \wedge dy \wedge d\varphi,$$

where x, y are the coordinates of the midpoint p of the segment s and φ is the angle already defined.
Since $\varphi \in [0, \frac{\pi}{3}]$, we have:

$$\mu(\mathcal{M}_1) = \int_0^{\frac{\pi}{3}} d\varphi \int\int_{\{(x,y)\in C_0^{(1)}\}} = \int_0^{\frac{\pi}{3}} \text{area} C_0^{(1)} d\varphi = \frac{\pi}{3} \text{ area } C_0^{(1)} \quad (1.11)$$

and taking in account the relation (1.9),

$$\mu(\mathcal{N}_1) = \int_0^{\frac{\pi}{3}} d\varphi \int\int_{\{(x,y)\in \widehat{C}_0^{(1)}\}} = \int_0^{\frac{\pi}{3}} \text{ area } \widehat{C}_0^{(1)} d\varphi = \frac{\pi}{3}\text{area } C_0^{(1)} +$$
$$-\frac{1}{4}\int_0^{\frac{\pi}{3}} \left[(2a-3b)\sqrt{3}l\cos\varphi + (b-a)l\sin\varphi - l^2\left(\sin 2\varphi + \frac{\sqrt{3}}{3}\cos 2\varphi - \frac{\sqrt{3}}{3}\right)\right] d\varphi =$$
$$\frac{\pi}{3}\text{area } C_0^{(1)} - \frac{1}{4}[(a-4b)l - (\frac{9}{4} - \frac{\pi\sqrt{3}}{9}l^2)]. \quad (1.12)$$

The relations (1.10), (1.11), (1.12) give us

$$P_{int}^{(1)} = \frac{3[(a-4b)l - (\frac{9}{4} - \frac{\pi\sqrt{3}}{9})l^2]}{\pi\sqrt{3}(a^2-3b^2)}. \quad (1.13)$$

2

Let $\mathcal{R}_2(a,b)$ be the regular lattice with fundamental cell an equilateral triangle with circular sector as obstacles (Fig. 8)

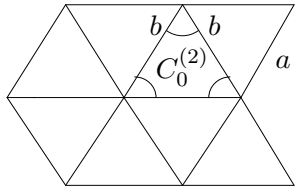

Fig.8

Denoting by $C_0^{(2)}$ this cell, we have

$$\text{area}C_0^{(2)} = \frac{\sqrt{3}a^2}{4} - 3\frac{\pi b^2}{6}.$$

As in the previous Section, we want to compute the probability that a line segment s of constant length l (with $b < l < \frac{a}{2}$) and of random position intersects an edge of the lattice $\mathcal{R}_2$, that is the probability $P_{int}^{(2)}$ that the line segment s intersects an edge of the fundamental cell. Consider a position of the line segment s of midpoint p that shapes an angle φ with the coordinate axis x. Denote by $\widehat{C}_0^{(2)}$ the figure determined by the limit positions of the line segment s for a fixed value of φ (Fig.9)

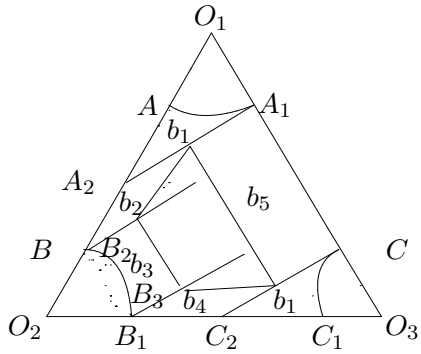

Fig.9

From the notations of the previous figure, it follows area $\widehat{C}_0^{(2)}(\varphi) =$

$$\text{area } C_0^{(2)} - [2 \text{ area} b_1(\varphi) + \text{ area} b_2(\varphi) + \text{ area} b_3(\varphi) + \text{ area} b_4(\varphi) + \text{ area} b_5(\varphi)]. \tag{2.1}$$

The figure 2 and 9 and the relations (1.5), (1.7), (1.8) give us

$$\text{area } b_2(\varphi) = \text{ area } a_2(\varphi) = \left(a - 2b - \frac{2\sqrt{3}l\sin\varphi}{3}\right)\left(\sqrt{3}\cos\varphi - \sin\varphi\right)\frac{l}{4},$$

$$\text{area } b_4(\varphi) = \text{ area} a_4(\varphi) = \left(a - 2b - \frac{2\sqrt{3}l\sin\varphi}{3}\right)\frac{l}{2}\sin\varphi,$$

$$\text{area } b_5(\varphi) = \text{ area } a_5(\varphi) = \left(\frac{a-2b}{4}\right)\left(\sqrt{3}\cos\varphi + \sin\varphi\right) \tag{2.2}$$

Then, the relations (1.3), (1.6) give

$$\text{area } b_1(\varphi) = \text{ area } a_1(\varphi) - \frac{b^2}{4}(2\pi - \sqrt{3}) = \frac{bl\sin\varphi}{2} - \frac{b^2}{4}(2\pi - \sqrt{3}), \text{ area} b_3(\varphi) =$$

$$\text{area} a_3(\varphi) - \frac{b^2}{4}(2\pi - \sqrt{3}) = \frac{bl}{4}(\sqrt{3}\cos\varphi + \sin\varphi) - \frac{b^2}{4}(2\pi - \sqrt{3}) \tag{2.3}$$

Replacing the expressions (2.2) and (2.3) in (2.1), we obtain

$$\text{area } \widehat{C}_0^{(2)}(\varphi) = \text{ area } C_0^{(2)} - [bl\sin\varphi + \left(a - 2b - \frac{2\sqrt{3}l\sin\varphi}{3}\right)\left(\sqrt{3}\cos\varphi - \sin\varphi\right)\frac{l}{4} +$$

$$+ \frac{bl}{4}(\sqrt{3}\cos\varphi - \sin\varphi) + \left(a - 2b - \frac{2\sqrt{3}l\sin\varphi}{3}\right)\frac{l}{2}\sin\varphi + \frac{a-2b}{4}(\sqrt{3}\cos\varphi + \sin\varphi) +$$

$$- \frac{3b^2}{4}(2\sqrt{\pi} - \sqrt{3})].$$

Taking in account the relation (1.9), we have

$$\text{area } \widehat{C}_0^{(2)}(\varphi) = \text{ area } \widehat{C}_0^{(1)}(\varphi) + \text{ area } C_0^{(2)}(\varphi) + \text{ area } C_0^{(1)}(\varphi) + \frac{3b^2}{4}(2\pi - \sqrt{3}),$$

that is

$$\text{area } \widehat{C}_0^{(2)}(\varphi) = \text{ area } \widehat{C}_0^{(1)}(\varphi) + \pi b^2 \tag{2.4}$$

Denoting by $\mathcal{M}_2$ the set of the line segments s that have midpoint in $\mathcal{C}_0^2$ and with $\mathcal{N}_2$ the set of line segments s totally contained in $\mathcal{C}_0^2$, one has:

$$P_{int}^{(2)} = 1 - \frac{\mu(\mathcal{N}_2)}{\mu(\mathcal{M}_2)}. \tag{2.5}$$

$$\mu(\mathcal{M}_2) = \int_0^{\frac{\pi}{3}} d\varphi \int\int_{\{(x,y)\in \widehat{C}_0^{(2)}\}} = \int_0^{\frac{\pi}{3}} \text{ area } \widehat{C}_0^{(2)} d\varphi =$$

$$\frac{\pi}{3}\text{area } C_0^{(2)} = \frac{\pi}{3}(\frac{\sqrt{3}a^2}{4} - \frac{\pi b^2}{2}) \tag{2.6}$$

and, taking in account of the relations (2.4)

$$\mu(\mathcal{N}_2) = \int_0^{\frac{\pi}{3}} d\varphi \int\int_{\{(x,y)\in \widehat{C}_0^{(2)}\}} dxdy = \int_0^{\frac{\pi}{3}} \text{ area } \widehat{C}_0^{(2)}(\varphi)d\varphi = \int_0^{\frac{\pi}{3}} \text{ area } \widehat{C}_0^{(1)}(\varphi)d\varphi + \frac{\pi b^2}{3}.$$

The relations (1.12) give us

$$\int_0^{\frac{\pi}{3}} \text{ area } \widehat{C}_0^{(1)}(\varphi)d\varphi = \frac{\pi}{3}(\frac{\sqrt{3}}{a}^2 4 - 3\frac{\sqrt{3}}{a}^2 4) - \frac{1}{4}[(a-4b)l - (\frac{9}{4} - \frac{\pi\sqrt{3}}{9})l^2] =$$

$$= \frac{\sqrt{3}\pi}{12}(a^2 - 3b^2) - \frac{1}{4}[(a-4b)l - \left(\frac{9}{4} - \frac{\pi\sqrt{3}}{9}\right) l^2],$$

then

$$\mu(\mathcal{N}_2) = \sqrt{3}\pi(a^2 - 3b^2) + \frac{\pi^2 b^2}{3} - \frac{1}{4}[(a-4b)l - \left(\frac{9}{4} - \frac{\pi\sqrt{3}}{9}\right) l^2] \tag{2.7}$$

The relations (2.5), (2.6), (2.7) give us

$$P_{int}^{(2)} = \frac{(a-3b)l - \left(\frac{9}{4} - \frac{\pi\sqrt{3}}{9}\right) l^2 - \frac{4\pi^2 b^2}{3}}{\pi\sqrt{3}(a^2 - 3b^2)} \tag{2.8}$$

For $b \to 0$, by relations 1.13 and 2.8, it follows:

$$P_{int}^{(1)} = P_{int}^{(2)}.$$

References

[1] Duma A.,Stoka M. I., Pub. Inst. Stat.Univ. Paris, XLIX, fasc. 2-3, 2005,57-72

[2] Poincaré H., Calcul des probabilités, ed. 2, Carré, Paris, 1912

[3] Stoka M. I., probabilités géometriques de type Buffon dans le plan euclidien, Atti Acc. sci. Torino,T. 110, pp 51-59.

RENDICONTI DEL CIRCOLO MATEMATICO DI PALERMO
Serie II, Suppl. 83 (2011), pp. 199-208

VALUE AT RISK – SECURITIES OF PORTFOLIO OPTIMIZATION. A GEOMETRIC BROWNIAN MOTION CASE

DANIEL ISKRA
Department of Applied Mathematics
University of Economics in Katowice

Abstract. This paper presents the optimization of securities portfolio. Taking into account the Value at Risk the optimization concerns the portfolio's structure. Value at Risk (VaR) is one of the modern risk measures. The Value at Risk is defined as follows:

$$P(S_0 - S_t < VaR(\alpha, t)) = 1 - \alpha,$$

S_0, S_t - the initial and final instrument price or portfolio value,

$VaR(\alpha, t)$ -Value at Risk on the time horizon t and the level of acceptance α.

The author considers the strategy in which VaR of portfolio is minimized for fixed probability level α. The portfolio contains shares. Dynamics of shares' prices are described by Geometric Brownian Motion. The model is tested using empirical data. The results of empirical research are presented in the article.

Keywords: Value at Risk, Geometric Brownian Motion, portfolio

Introduction

Risk management is an important aspect of modern finance [1, 4, 8]. Intensive research work in this field of science has brought us many tools to risk management [1, 2, 3, 4, 6, 7]. One of the measures of risk, which has become very popular is Value at Risk.

The Value at Risk is defined as follows [12]:

$$P(S_0 - S_t < VaR) = 1 - \alpha, \tag{1}$$

S_0, S_t - the initial and final instrument price or portfolio value,

VaR - Value at Risk on the time horizon t and the level of acceptance α.

Value at Risk is the value where decrease of portfolio value can be bigger then VaR with α probability for set time t. As we can see from definition, Value at Risk is a difference between initial value of the portfolio and proper quintile of distribution of probability, that means, the Value at Risk depends on distribution of probability [1, 4, 5, 8].

This paper presents the optimization of securities portfolio. Taking into account the Value at Risk the optimization concerns the portfolio's structure.

The author considered the strategy in which VaR of portfolio is minimized for fixed probability level α. The portfolio used in the research contained shares. Dynamics of shares' prices were described by Geometric Brownian Motion. The model was tested by using empirical data. The results of empirical research are presented in the article.

Probability distribution of portfolio

Let the initial value of portfolio be greater then zero and dynamics of share is described by Geometric Brownian Motion with constant parameters [9, 12]:

$$\frac{dS_t}{S_t} = \mu dt + \sigma dW_t, \tag{2}$$

where:

S_t - price of share,

μ - drift,

σ - volatility,

W_t - Wiener process.

Let the portfolio consists of n different types of shares. If dynamics of shares is described by Geometric Brownian Motion (see formula nr (2)), then value of portfolio with its constant structure of the valuable ($w_i = const$, $\sum_{i=1}^{n} w_i = 1$, $i \in \{1,2,...,n\}$) is also to be described by Geometric Brownian Motion:

$$\frac{d\Pi_t}{\Pi_t} = \mu_\Pi dt + \sigma_\Pi dW_t \tag{3}$$

where:

$$\mu_\Pi = \sum_{i=1}^{n} w_i \mu_i \ , \tag{4}$$

$$\sigma_\Pi = \sqrt{\left(\sum_{i=1}^{n} w_i^2 \sigma_i^2 + 2 \sum_{i=1}^{n} \sum_{j>i}^{n} w_i w_j \sigma_i \sigma_j \rho_{ij} \right)} , \tag{5}$$

where:

Π_t - price of portfolio,

μ_Π - drift of portfolio,

σ_Π - volatility of portfolio,

ρ_{ij} - correlation coefficient,

W_t - Wiener process.

As we assumed, μ and σ are constant for each instrument ($\mu_i = const$ and $\sigma_i = const$, $i \in \{1,2,...,n\}$) so parameters μ_Π and σ_Π are constant, too.

We can find probability distribution of the value of portfolio by solving Kolmogorov equation [10]. Next we can calculate the probability that the value of portfolio is not bigger than fixed value - π^* for fixed time. This probability can be described by formula:

$$P(\Pi_t \le \pi^*, t) = P(X_t \le x^*, t) =$$

$$= \frac{1}{\sqrt{2\pi\sigma_\Pi^2 t}} \int_{-\infty}^{x^*} \exp\left(\frac{-[x - (\mu_\Pi - \frac{1}{2}\sigma_\Pi^2)t]^2}{2\sigma_\Pi^2 t}\right) dx \tag{6}$$

where random variable:

$$X_t = \ln(\frac{\Pi_t}{\pi_0}), \tag{7}$$

describes logarihtmic rate of return. As it follows from the formula nr (6) random variable X_t has normal distribution $\mathrm{N}((\mu_\Pi - \frac{1}{2}\sigma_\Pi^2)t, \sigma_\Pi\sqrt{t})$.

We can transform the formula nr (6) into cumulative distribution function of standard normal distribution:

$$N(z) = \frac{1}{\sqrt{2\pi}} \int_{-\infty}^{z} e^{-\frac{x^2}{2}} dx, \tag{8}$$

where:

$$z = \frac{\ln(\frac{\pi_t}{\pi_0}) - (\mu_\Pi - \frac{1}{2}\sigma_\Pi^2)t}{\sigma_\Pi\sqrt{t}}. \tag{9}$$

For $\pi_t = \pi_0 - \Delta\pi_t$ ($\Delta\pi_t$ represents the *VaR* – positive value means the fall down of the value of portfolio with relation to initial value of the portfolio, negative value - increase) formula nr (9) can be written as:

$$z = \frac{\ln(1 - \frac{\Delta\pi_t}{\pi_0}) - (\mu_\Pi - \frac{1}{2}\sigma_\Pi^2)t}{\sigma_\Pi\sqrt{t}}, \tag{10}$$

where $\frac{\Delta\pi_t}{\pi_0}$ represents relativity value of the *VaR*.

Value at Risk - portfolio optimization.

In optimization of the portfolio strategy, taking into account the Value at Risk we have to select weight (w_i, i={1,…,n}) so that the value $\frac{\Delta\pi_t}{\pi_0}$ was minimal for fixed probability α. In this case

we have to set the value z for which distribution function of normal distribution is equal α:

$$z = N^{-1}(\alpha). \tag{11}$$

If we transform the equation (10) we will get the formula:

$$\frac{\Delta\pi_t}{\pi_0} = 1 - e^{z\sigma_\Pi\sqrt{t}+(\mu_\Pi-\frac{1}{2}\sigma_\Pi^2)t}, \tag{12}$$

were μ_Π i σ_Π are described by the formulas nr (4) and (5).

In the formula (12) the expressions μ_Π and σ_Π depend on the weights (w_i i={1,…,n}) so expression $\frac{\Delta\pi_t}{\pi_0}$ depends on the weights, too. In next part of the article notation the expressions μ_Π and σ_Π will be the same. Only notation of the expression $\frac{\Delta\pi_t}{\pi_0}$ will be changed, so the formula (12) is:

$$\frac{\Delta\pi_t}{\pi_0}(w_1,\ldots,w_n) = 1 - e^{z\sigma_\Pi\sqrt{t}+(\mu_\Pi-\frac{1}{2}\sigma_\Pi^2)t}, \tag{13}$$

Calculating the weights for which the formula (13) is minimal, we can get the variable structure of the portfolio where the Value at Risk is also minimal for the fixed level of probability α (significance level).

Estimation of parameters

In the work, the estimation of parameters of the model was proposed by logarithmic rate of return.

If dynamics of share is described by Geometric Brownian Motion (2), then dynamics of logarithmic rate of return of share can be determined by Ito lema [9, 11]:

$$d\ln(\frac{S_t}{S_0}) = (\mu - \frac{1}{2}\sigma^2)dt + \sigma dW_t. \tag{14}$$

Because:

$$d\ln(\frac{S_t}{S_0}) = \ln(\frac{S_{t+dt}}{S_0}) - \ln(\frac{S_t}{S_0}) = \ln(\frac{S_{t+dt}}{S_t}), \tag{15}$$

therefore:

$$\ln(\frac{S_{t+dt}}{S_t}) = (\mu - \frac{1}{2}\sigma^2)dt + \sigma dW_t. \tag{16}$$

So, according to the above formula, logarithmic returns about period of time dt have normal probability:

$$N((\mu - \frac{1}{2}\sigma^2)dt, \sigma\sqrt{dt}) \tag{17}$$

In this case, the estimators μ and σ (determined by the methods of moments) are:

$$\mu = E(\ln(\frac{S_{t+dt}}{S_t}))\frac{1}{dt} + \frac{1}{2}\sigma^2, \tag{18}$$

$$\sigma = D(\ln(\frac{S_{t+dt}}{S_t}))\frac{1}{\sqrt{dt}}, \tag{19}$$

where:

$E(\bullet)$ - expected value of the logarithmic rate of return of share,

$D(\bullet)$ - standard deviation of the logarithmic rate of return of share.

The estimator correlation coefficient is:

$$\rho_{ij} = \frac{\operatorname{cov}(\ln(\frac{S_{i,t+dt}}{S_{i,t}}), \ln(\frac{S_{j,t+dt}}{S_{j,t}}))}{\sigma_i \sigma_j dt} \tag{20}$$

i, j – numbers of shares.

Simulations

In the empirical research, short selling of the instruments was not taken into consideration by the author. This fact means that the weights of structure of the portfolio have to be positive:

$$\forall_{i=\{1,\ldots,n\}} w_i \geq 0 \tag{21}$$

To research the author selected shares which were included in Standard&Poor 100 Index and the stock quotes of shares were from 1990 to 2010. Shares included in the research are presented below (shortcuts used in the stock market)

AA	CVS	JNJ	SLB
AAPL	CVX	JPM	SLE
ABT	DD	KO	SO
AEP	DELL	LMT	T
AMGN	DIS	LOW	TXN
AVP	DOW	MCD	USB
AXP	EMC	MDT	UTX
BA	ETR	MMM	VZ
BAC	EXC	MO	WAG
BAX	F	MRK	WFC
BHI	FDX	MSFT	WMB
BK	GD	NKE	WMT
BMY	GE	NSC	WY
C	HAL	ORCL	XOM
CAT	HD	OXY	XRX
CL	HNZ	PEP	
CMCSA	HON	PFE	
COP	HPQ	PG	
COST	IBM	RTN	
CPB	INTC	S	

Table nr 1. Shares included in the research (shortcut).

Next the author has constructed one hundred portfolios which consisted of two random chosen shares each.

In every single portfolio the variable structure was calculated so that one day Value at Risk was minimal (by formula (13)). The Value at Risk was predicted for probability $\alpha = 0.05$. As a unit of time the author assumed one session year (exactly 250 trading session days) so it means that $dt = 1/250$.

Parameters of the model were estimated by 70, 100, 150 and 200 daily logarithmic rates of return for each share by formulas (18) and (19). Next, the author checked if these logarithmic rates of return used to estimate had a normal probability with estimated parameters by Lilliefors test. In each case it was checked if the assumptions of the model were fulfilled (it means that both shares included in the portfolio have had a normal probability at the same time). If yes, the forecast of *VaR* for next day was numbered among the set of the samples used for *VaR* test. If not, the forecast was not considered. Next to the time series with rates of return of shares there was a new rate of return added, and the oldest one was deleted. The whole procedure was repeated again and again.

In work, there was Kupiec test [1] and structure test used to verify the *Value at Risk* with level of significance equal to 5% . The author assumed that predicted Value at Risk was correct if both tests did not reject null hypothesis.

Percentage of the portfolios (in which the forecast *VaR* was verified positively by *VaR* tests) is presented in table nr 2. As we remember, there were one hundred of all the portfolios. Forecasts of *VaR* (on average more than one thousand) were calculated for one day and level of significance equal to 5% for each portfolio.

Significant level used in the Lilliefors test	Number of rates of return used to estimate the parameters			
	70	**100**	**150**	**200**
α=0,05	**56%**	**87%**	**94%**	**87%**
α=0,1	**76%**	**88%**	**88%**	**86%**

Table nr 2. Percentage of portfolios in which the forecasted *VaR* was verified positively by VaR tests.

As we can see in the table, the best result was in the case where parameters of the model were estimated by 150 logarithmic rates of return. In this case, the percentage of the portfolios, in which *VaR* was calculated correctly, was about 90%. The results were similar when parameters of the model were estimated by 100 and 200 logarithmic rates of return. The worst result was obtained in the case when parameters were estimated by 70 ones.

Conclusions

This paper presents the optimization of the securities of portfolio. Taking into account the *VaR*, the optimization concerns the valuable structure of the portfolio. Each portfolio contained two types of shares. Dynamics of shares' prices were described by Geometric Brownian Motion. The model was tested by using empirical data. Parameters of the model were estimated by 70, 100, 150 and 200 daily logarithmic rates of return.

The key finding of the analysis is that proposed model of optimizing the portfolio (due to the value at risk) worked well, if parameters of the model were estimated by the data from the last six months (about six months). The Value at Risk was consistent with the real loss (no significant difference) in about 90% of the portfolios. Estimation of the parameters of the model for shorter period gave worse results and for longer period the number of days in which the model could be used to predict *VaR* was smaller.

References

1. Alexander C.: Market Risk Analysis: Value at Risk Models. Vol. IV, John Wiley & Sons, England, 2008,
2. Czernik T., Optymalizacja pewnej strategii inwestycyjnej z punktu widzenia maksymalnej straty [w:] Rynek kapitałowy. Skuteczne inwestowanie. Wyd. Naukowe Uniwersytetu Szczecińskiego, Szczecin, 2004,
3. Czernik T.: Miary ryzyka z rodziny ML, [w] Prace Naukowe nr 991, Wyd. AE we Wrocławiu, Wrocław 2003,

4. Grinold R. C., Kahn R. N.: Active Portfolio Management, McGrawHill, 2000,
5. Holton G. A.: Value at Risk. Theory and Practice. Academic Press, USA, 2003,
6. Iskra D.. Optymalizacja portfela inwestycyjnego ze względu na warunkowy VaR, [w:] Matematyczne i ekonometryczne metody oceny ryzyka finansowego., Wyd. Akademii Ekonomicznej w Katowicach, Katowice, 2007,
6. Iskra D.: VaR - optymalny liniowy portfel inwestycyjny z ograniczeniami [w:] Inwestycje finansowe i ubezpieczenia - tendencje światowe a polski rynek, Wyd. Akademii Ekonomicznej we Wrocławiu, Wrocław 2005,
7. Jorion P.: Value at risk: the new benchmark for managing financial risk. 2nd edition, McGraw-Hill, 2001,
8. Oksendal B.: Stochastic Differentia Equations, Springer, New York, 2003,
9. Papoulis A.: Probability, Random Variables and Stochastic Processes., McGraw Hill Higher Education, 2002,
11. Shreve S.E.: Stochastic Calculus for Finance II. Continues-Time Models, Springer, New York, 2004,
12. Wilmot P.: Paul Wilmot On Quantitive Finance, John Wiley & Sons, England, 2006.

RENDICONTI DEL CIRCOLO MATEMATICO DI PALERMO
Serie II, Suppl. 83 (2011), pp. 209-217

EVALUATION OF GLOBAL COMFORT FOR TRAIN PASSENGERS

Giovanni Leonardi – Riccardo Ferrara

Abstract. The aim of this study is to propose a method for the evaluation of railway passengers' comfort in relationship to temperature, noise, and vibration. Estimated the single comfort for every sensation considered, the global comfort is evaluated with the Hyper-Sphere Method proposed by Corriere & Lo Bosco [1]. The human-vehicle-infrastructure-environment variables which influence comfort are individuated. Thus their value and correspondent global comfort could be evaluated in management strategy or predicted in design problem. The results show how to construct the hyper-sphere in which the surface is representative of best possible condition for human comfort and the centre represents the minimum.

Keywords: thermal comfort, vibration, noise, global comfort, hyper sphere, train passengers, railway.

1. Introduction

The principal goal of this paper is to define an index representative of passenger satisfaction in relation to comfort. The proposed model considers the following three variables: temperature, noise and vibration. These three aspects of comfort have been well documented and analysed in numerous studies.

American Society of Heating, Refrigerating and Air-Conditioning Engineers [2, 3] studied the effects of environmental variables on thermal comfort.

Yang & Kang [4] investigated the acoustic comfort in urban open public spaces, but without finding a good Leq/Comfort-Index correlation coefficient.

Huston, Zhao and Johnson [5] studied the dependency between comfort and vibration frequency/amplitude but they didn't give a method to relate comfort with design variables.

The present study examines how human-vehicle-infrastructure-environment variables produce noise, vibration and condition temperature influencing passenger comfort.

2. Method

Human-vehicle-infrastructure-environment variables are split into two different sets: the "Environment Set (E)" (including vehicle-infrastructure-environment variables) and the "Human Set (H)" (Fig. 1).

The threshold between these sets represents the perceptive organs.

Firstly design variables must be individuated for the chosen parameters aspects of comfort: thermal, noise and vibration.

Then, the relationship functions: temperature/comfort-index, noise/comfort-index and vibration/comfort-index are constructed. For every function and every variable, fixing all variables except one, it's possible to define the superior threshold in relation with maximum comfort while all other variables are fixed at an inferior threshold and vice versa. The $n+m$ variables represent $n+m$ axes of the $\mathbb{R}^{n+m}$ space.

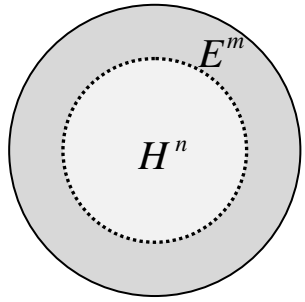

Subsequently all coordinates have been normalised with maximum and minimum threshold calculated by eq. (2).

$$\begin{cases} \varsigma_1 = \frac{\alpha_1 - \alpha_1^i}{\alpha_\Delta}, \dots, \tau_m = \frac{\alpha_m - \alpha_m^i}{\alpha_\Delta} & \alpha_\Delta = (\alpha^s - \alpha^i) \\ \tau_1 = \frac{Z_1 - Z_1^i}{Z_\Delta}, \dots, \tau_n = \frac{Z_n - Z_n^i}{Z_\Delta} & Z_\Delta = (Z^s - Z^i) \end{cases} \tag{2}$$

After this transformation of coordinate, a hyper-sphere (3), in which the surface is representative of best possible condition for human comfort and the centre represents the minimum, is defined:

$$\tau_1^2 + \dots + \tau_n^2 + \varsigma_1^2 + \dots + \varsigma_m^2 \leq 1 \tag{3}$$

Hyper vectors satisfying equation (2) are inside the hyper-sphere and their module represents the Global Comfort Index – $CI \in [0; 1]$. Once the global comfort vector is defined, it's possible to evaluate the comfort index to optimize the best management strategy or, in design case, to chose between different planning alternatives. The best solution is the one that maximizes the global comfort vector module.

3. Thermal comfort

The thermal comfort is established by a man-environment energy balance [6] and the equation, for surface area unit, is the following:

$$S = M - W_k - E_{sk} - E_r - C - R - C_k \tag{4}$$

Where S is the instantaneous energy balance of human body (Table 1).

Table 1

Variables introduced in eq. (4)		*Variables introduced in eq. (5)*	
M	metabolic rate	E_{sw}	sweating heat loss
W_k	external work	rh	air relative humidity
E_{sk}	heat loss by evaporation from the skin	t_{mr}	mean radiant temperature
E_r	respiration heat loss, latent and dry	t_{sk}	skin temperature
C	the heat loss by convection from outer surface of the clothed body to air	I_{cl}	clothing, including thermal resistance and vapour permeability
R	the heat loss by radiation from outer surface of the clothed body to its environment		
C_k	heat loss by conduction due to the contact skin/solid object		

For equilibrium and for comfort, S has to result zero. If S results less than zero, the body is releasing more energy than it is producing, consequentially body temperature tends to decrease. Some human-variables in eq. (4) could be written as function of environmental-variables, thus there is equilibrium if (5) is satisfied.

$$f(M, W, I_{cl}, rh, t_{mr}, t_{sk}, E_{sw}) = 0 \tag{5}$$

Furthermore, this equation it's in accordance with Corriere & Lo Bosco [1] theory of comfort-equilibrium (1). Fanger [7] studied a correlation between the mean value of votes given, on a seven-point thermal sensation scale (Table 2), by a large group of people and some environmental and human parameters. Thus he proposed a comfort index called Predicted Mean Vote (6).

$$PMV = (0.303 \cdot e^{-0.036M} + 0.028) \cdot \{(M - W) - 3.05 \cdot 10^{-3}[5733 - 6.99 \cdot (M - W) - p_a] - 0.42[(M - W) - 58.15] - 1.7 \cdot 10^{-5} M \cdot (5867 - p_a) - 0.0014 \cdot M \cdot (34 - t_a) - 3.96 \cdot 10^{-8} f_{cl} \cdot [(t_{cl} + 273)^4 - (t_{mr} + 273)^4] - f_{cl} h_c \cdot (t_{cl} - t_a)\} \tag{6}$$

Table 2

Variables introduced in eq. (10)		*Thermal sensation scale*		
p_a	partial vapour pressure	+	*3*	Hot
f_{cl}	ratio of man's surface area clothed/nude	+	*2*	Warm
t_a	air temperature	+	*1*	Slightly warm
t_{cl}	surface temperature of clothing		*0*	Neutral
h_c	average skin air convective heat transfer coefficient	-	*1*	Slightly cool
		-	*2*	Cool
		-	*3*	Cold

Normally in a train, during travel, people are seated, so the metabolic rate could be fixed as $M = 58{,}15\ W/m^2$ [6]. Even the external work it's null, so $W_k = 0$. The partial vapour pressure could be calculated with an empiric equation [7]:

$$\begin{cases} P_a = rh \cdot P_s \\ \ln(P_s) = \frac{\alpha_1}{T} + \alpha_2 + \alpha_3 T + \alpha_4 T^2 + \alpha_5 T^3 + \alpha_6 T^4 + \alpha_4 \ln(T) \end{cases} \tag{7}$$

The ratio body surface/clothing can be calculated as follows:

$$f_{cl} = \begin{cases} 1.00 + 1.290 I_{cl} & for\ I_{cl} < 0.078\ m^2\ ^\circ C/W \\ 1.05 + 0.645 I_{cl} & for\ I_{cl} > 0.078\ m^2\ ^\circ C/W \end{cases} \tag{8}$$

where I_{cl} depends on passenger's clothing, and thus, on season and on external temperature. The average skin air convective heat transfer coefficient:

$$h_c = \begin{cases} 2.38(t_{cl} - t_a)^{0.25} & for\ 2.38(t_{cl} - t_a)^{0.25} > 12.1\sqrt{v_{ar}} \\ 12.1\sqrt{v_{ar}} & for\ 2.38(t_{cl} - t_a)^{0.25} < 12.1\sqrt{v_{ar}} \end{cases} \tag{9}$$

with:

$$v_{ar} = v_a + 0.005\left(\frac{M}{A_{DU}} - 58.15\right) \qquad A_{DU} = 2.02(w_b)^{0.425}(h_b)^{0.725}$$

where V_{ar} is the passenger relative air velocity, V_a is the air velocity, A_{DU} is the body surface calculated by the *Dubois Area* empiric equation. As height and weight of passengers tend to vary on a large range, reference is made to average values (e.g., in Italy, $\overline{h_m} = 1.75\ m$; $\overline{h_w} = 1.65\ m$; $\Longrightarrow \bar{h} = 1.70\ m$; $\overline{w} = 75\ kg \Longrightarrow A_{DU} = 1.86\ m^2$);
The surface temperature of clothing:

$$t_{cl} = 35.7 - 0.028(M - W) - I_{cl}\{3.96 \cdot 10^{-8} f_{cl}[(t_{cl} + 273)^4 + \\ -(t_{mr} + 273)^4 f_{cl} h_c (t_{cl} - t_a) \tag{10}$$

Air temperature is given by the value set by the regulation of the air conditioning system.
The mean radiant temperature is:

$$t_{mr} = \sum t_i F_{P,i} \tag{11}$$

where t_i is the temperature of the generic isothermal surface-i seeing the subject (a wall, a window, a piece of furniture, another person, etc.); $F_{p,i}$ is the view (or angle) factor between the subject-p and the surface-i.

Once all variables are calculated it is possible to estimate the *Predicted Mean Value* (6).

Finally the aim is to individuate the independent variables which could be controlled or varied in a train design/management problem. Looking at Table 3, these variables are identified with an asterisk (*):

α_1: thermal isolation;
α_2: air conditioning system power (capability to adjust air temperature and relative humidity);
α_3: air velocity;
α_4: mean radiant temperature.

Comfort thresholds recommended by ISO Standard 77302 [8] are $PMV = [-0.5;\ +0.5]$. It's also possible to predict percentage of dissatisfied passengers (*PPD)* with the equation (12).

$$PPD = 100 - 95e^{-(0.03353PMV^4 + 0.21PMV^2)} \tag{12}$$

In *PMV* range between -0.5 and +0.5 the *PPD* varies from 0% to 10%

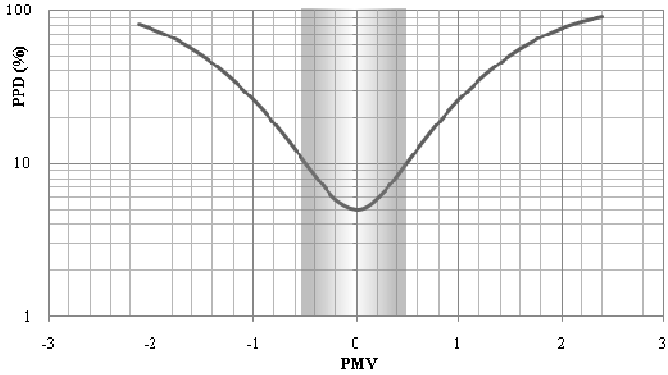

Fig. 1 – Relation "predicted percentage of dissatisfied – predicted mean value".

Last step it's to evaluate $\alpha_\Delta = \alpha^s - \alpha^i$ as viewed in first paragraph.

Table 3

PMV - Predicted Mean Vote

depends by												
M	W	t_a*	t_{mr}*	p_a		f_{cl}	h_c			t_{cl}		
fixed	fixed	adjustable	adjustable	depends by:	depends by:	depends by:	depends by:			depends by:		
0 [W/m^2]	0 [W/m^2]	thermal, isolation; air conditioning system	windows, places disposition	T	rh*	I_{cl}	v_{ar}		t_a	M,W	I_{cl}, f_{cl}, t_a	
				not adjustable	adjustable	not adjustable	depends by	depends by	adjustable	fixed	←	
				(Design Data)	e.g. air conditioning system	(Design Data)			←	←		
							v_a*	A_{DU}				
							adjustable	fixed				
							direction and velocity of air conditioned	e.g. 1.86 [m^2] (in average in Italy)				

4. Noise comfort

In a train, noises and mechanical vibrations are generated by the same source but the propagation is different. Noise is transmitted by air, while mechanical vibrations propagate through solid structures. Both are characterised by frequency and amplitude. Normally our ears work like a weighting filter, so the equivalent psychological impression induced by pure tones depends on the frequency. In this study, results of experiment conducted by Yamaguchi, Kato, Oimatsu & Saeki [9] have been revised to verify if a relationship between noise level and Comfort Index exists, while noise frequency are random.
During the experiment a group of people, everyone placed at the same distance from the noise source, was invited to indicate in a questionnaire their physiological impression in a scale from 1 to 7 (Table 4). Each five seconds the source produced a random frequency noise with a fixed level of decibels.

Table 4 - Psychological noise scale.

F_i	Impressions
1	very calm
2	quite calm
3	slightly calm
4	medium
5	slightly noisy
6	quite noisy
7	very noisy

The results was the frequency of index value (F_i) connected to noise level L(dB). So Yamaguchi, Kato, Oimatsu & Saeki drew seven statistic distributions (one for every index value). But if it draws a single graph taking into account the noise level connected at the peak frequency of index value the result is in Fig. 2.

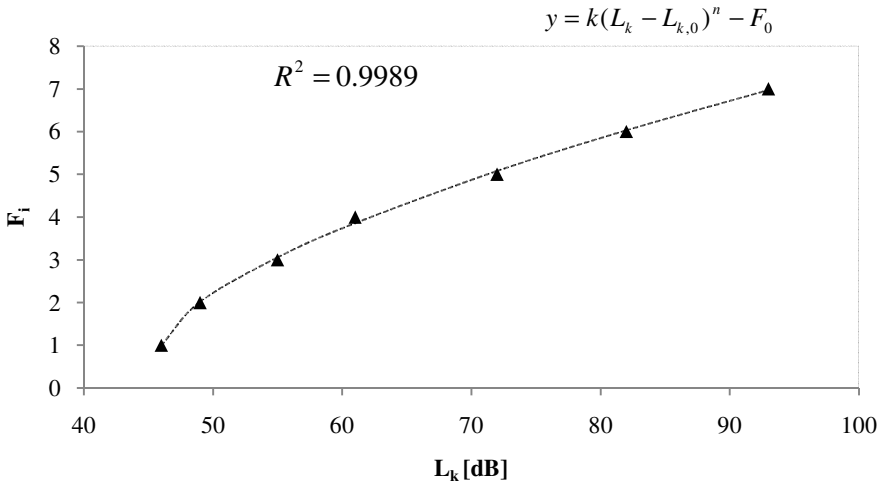

Fig. 2 – Relation "comfort index – noise level".

Applying the Stevens' Power Law [10], it's possible to hypothesize a relationship between the magnitude of a physical stimulus and its perceived intensity or strength.

$$\psi = k\varphi^n \tag{13}$$

Modifying the equation, adding the minimum threshold (46 dB) and the minimum index value ($F_i = 1$), the regression has a very good coefficient of correlation $R^2 = 0.9989$ (eq. 14; Fig. 2).

$$\begin{cases} F_i = k\left(L_k - L_{k,0}\right)^n - F_0 \\ k = 0.50; n = 0.64;\ L_{k,0} = 64\ dB;\ F_0 = 1 \end{cases} \tag{14}$$

At the end it's possible to estimate the management/design variables connected to the noise level, and evaluate the relative threshold as seen before. The variables identified are:

α_5: acoustic isolation;
α_6: train speed;
α_7: wheel defects;
α_8: rail defects;
α_9: twist index.

5. Vibration comfort

Many comfort indexes for vibration discomfort have been developed and proposed in scientific literature. Most of these usually connect physic stimulus with the acceleration transmitted to passengers' body. Also in this case, as in noise comfort, our sensations depend on amplitude and frequency. The acceleration has to be measured by accelerometers or predicted with a simulation analysis in three directions: along train motion (x-axis), vertical (z-axis) and transversal (y-axis). Then it's possible to evaluate comfort index using ISO 2631 [11] method. The three accelerations revealed, or predicted has to be weighted by a filter, then the root mean square values can be calculated as follows:

$$a_w^{r.m.s.} = \sqrt{\frac{1}{T_2 - T_1} \int_{T_1}^{T_2} a_w^2 \, dt} \tag{15}$$

Then comfort index can be calculated as follows:

$$a = \sqrt{k_x a_{xw}^{r.m.s.2} + k_y a_{yw}^{r.m.s.2} + k_z a_{zw}^{r.m.s.2}} \tag{16}$$

Comfort Index thresholds, which has the dimension of an acceleration $[m/s^2]$, are: $a = [0; 0.53]$.
In this case many variables which influence acceleration are the same of noise vibration case, just because the source of vibration is the same. Variables individuated are:

α_{10}: dissipation system;
α_{11}: train speed;
α_{12}: wheel defects;
α_{13}: rail defects;
α_{14}: twist index.

The last step is to evaluate $\alpha_\Delta = \alpha^s - \alpha^i$ as viewed in the first paragraph.

6. Conclusions

Once all the variables and their respective thresholds are individuated, it's possible to define the hyper sphere in the $\mathbb{R}^{n+m}$ space and the global comfort vector associated to design or management problems. A consideration has to be done concerning human variables. Even if these variables have correlation with comfort, especially in case of thermal comfort, they are not considered as

dimension of the hyper-sphere because they cannot be regulated (as seen in [3]). So these variables are considered as boundary conditions in thresholds computation, i.e. threshold have to be recalculated in every problem in dependency of: season, external temperature, external humidity; conditions which influences passengers' wearing apparel. Concerning noise comfort, even if the noise frequency is relevant in determination of passenger perception, experimental data demonstrates that it's possible to define a direct relationship between the comfort index and the waves' amplitude, if wave frequency varies randomly. Vibration comfort index and noise comfort index are not influenced by human factors. An exception has to be done in case of night sleeper trains; in which passengers lie in horizontal position therefore the vibration comfort index is modified.

REFERENCES

[1] F. Corriere, D. Lo Bosco. Comfort Globale e Sicurezza d'Esercizio nelle Infrastrutture Viarie: Un Modello Matematico per l'analisi delle relazioni uomo-veicolo-infrastruttura-ambiente. S.I.I.V. 2001 – XI Convegno Nazionale.
[2] ASHRAE. Thermal Environmental Conditions for Human Occupancy. ASHRAE Standard 55-1992.
[3] ASHRAE. Thermal Comfort. ASHRAE Handbook: Fundamentals, 2001.
[4] W. Yang, J. Kang. Acoustic comfort evaluation in urban open spaces. Applied Acoustics 66, 2005.
[5] D. Huston, X. Zhao, C. Johnson. Whole-Body shock and vibrations: Frequency and Amplitude dependence of comfort. Journal of Sound and Vibration, 2000.
[6] F.M. Butera. Principles of Thermal Comfort. Renewable & sustainable energy reviews, 1998.
[7] ASHRAE. Fundamentals, 1989.
[8] International Standard ISO 7730. Moderate thermal environments – Determination of the *PMV* and *PPD* indices and Specifications of the conditions of thermal comfort, 1984.
[9] Shizuma Yamaguchi, Yuichi Kato, Kensei Oimatsu & Tetsuro Saeki. A Psychological Evaluation Method for Fluctuating Random Noise Base on Fuzzy Set Theory. Applied Acoustics 45 - 1995.
[10] S.S. Stevens, Psychophysics, Introduction to its Perceptual, Neural and Social Prospects, Wiley, New York, 1975.
[11] ISO 2631, Guide to evaluation of human exposure to whole-body mechanical vibrations, 1985.

Giovanni Leonardi
DIMET - University of Reggio Calabria – giovanni.leonardi@unirc.it

Riccardo Ferrara
MECMAT - University of Reggio Calabria – riccardo.ferrara@unirc.it

RENDICONTI DEL CIRCOLO MATEMATICO DI PALERMO
Serie II, Suppl. 83 (2011), pp. 219-227

Laplace problems for regular lattices with asymmetric cell and different obstacles

Maria Pettineo
Department of Mathematics
University of Palermo
via Archirafi, 34
90123 - Palermo

Abstract

In this paper we consider two regular lattices with asymmetric cell and different obstacles and we compute the probability that a segment of random position and of costant lenght intersects a side of lattice. In particular we obtain the Laplace probability.Laplace probability.

Keywords: Geometric Probability, stochastic geometry, random sets, random convex sets and integral geometry.
AMS Classification:60D05, 52A22.

1 Section

Let $\Re_1\,(a,b,c,d;\alpha,\beta,)$ be the regular lattice with fundamental cell $C_0^{(1)}$ asymmetric trapezium is as in fig. 1, where α and β are two angles with $0 < \beta \leq \alpha \leq \frac{\pi}{2}$ and with four obstacles that are isosceles triangles different each other.

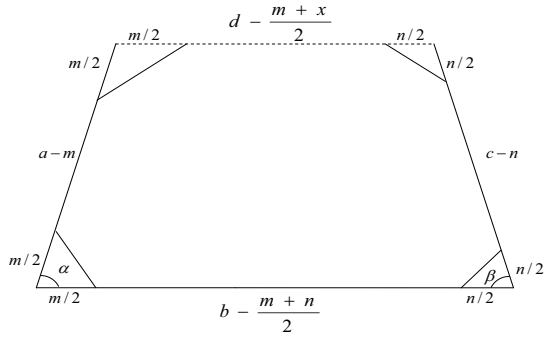

fig.1

From this figure result the condition

$$a \sin \alpha = c \sin \beta \tag{1}$$

We have

$$areaC_0^{(1)} = \frac{a\,(b+d)\sin\alpha}{2} - \frac{m^2}{4}\sin\alpha - \frac{n^2}{4}\sin\beta \tag{2}$$

Considering a segment s of random position and of constant length l with $l < \min(a, b, c, d)$, we want compute the probability that this segment intersects a side of lattice; obviously this probability is equal to probability $P_{int}^{(1)}$ that the segment s intersects the bounderay of the fundamental cell.

The position of the segment s is determinated by the middle point 0 and by the angle that the segment φforms with the axis x

We consider the limit positions of the segment s, and let $\widehat{C}_0^{(1)}(\varphi)$ be the determinated figure from these positions for a assigned value of φ, (fig. 2):

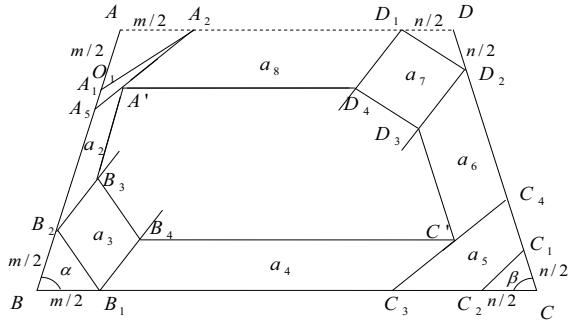

fig.2

From this figure we can write:

$$area\widehat{C}_0^{(1)}(\varphi) = areaC_0^{(1)} -$$

$$[areaa_1(\varphi) + areaa_2(\varphi) + ... + areaa_8(\varphi)]\,. \tag{3}$$

Considering the figure:

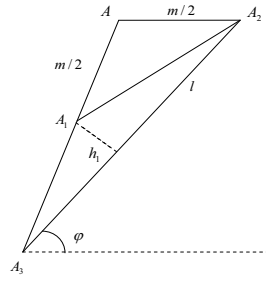

fig.3

We have:

$$\widehat{A_1AA_2} = \pi - \alpha, \quad \widehat{AA_1A_2} = \frac{\alpha}{2}, \quad \widehat{A_1A_3A_2} = \alpha - \varphi,$$
$$\widehat{A_3A_1A_2} = \pi - \frac{\alpha}{2}, \quad \widehat{A_3A_2A_1} = \varphi - \frac{\alpha}{2}.$$

The triangle $\widehat{AA_2A_3}$ give us:

$$\frac{m/2}{\sin(\alpha - \varphi)} = \frac{l}{\sin(\pi - \alpha)} = \frac{|AA_3|}{\sin\varphi}$$

From here follow the relation:

$$m \sin\alpha = 2l \sin(\alpha - \varphi) \tag{4}$$

and similarly

$$|AA_3| = \frac{l \sin\varphi}{\sin\alpha}$$

then

$$|A_1A_3| = \frac{l \sin\varphi}{\sin\alpha} - \frac{m}{2}$$

and

$$h_1 = |A_1A_3| \sin(\alpha - \varphi) = \left(\frac{l \sin\varphi}{\sin\alpha} - \frac{m}{2}\right) \sin(\alpha - \varphi),$$

hence

$$areaa_1(\varphi) = \left(\frac{l \sin\varphi}{\sin\alpha} - \frac{m}{2}\right) \frac{l}{2} \sin(\alpha - \varphi)$$

The figure:

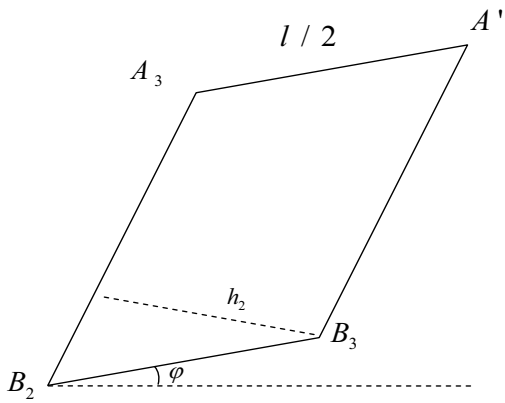

fig.4

give us

$$\widehat{A_3B_2B_3} = \alpha - \varphi, \qquad h_2 = \frac{l}{2}\sin(\alpha - \varphi)$$

and

$$|A_3B_2| = a - |AA_3| - \frac{m}{2} = a - \frac{m}{2} - \frac{l\sin\varphi}{\sin\alpha}$$

hence

$$areaa_2(\varphi) = .\left(a - \frac{m}{2} - \frac{l\sin\varphi}{\sin\alpha}\right)\frac{l}{2}\sin(\alpha - \varphi) \tag{5}$$

Considering the figure:

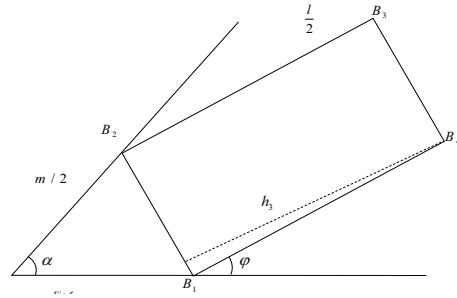

fig.5

From here follow that:

$$\widehat{BB_1B_2} = \frac{\pi}{2} - \frac{\alpha}{2}, \qquad \widehat{B_2B_1B_4} = \pi - \left(\varphi + \frac{\pi}{2} - \frac{\alpha}{2}\right) = \frac{\pi}{2} - \varphi + \frac{\alpha}{2},$$

$$h_3 = \frac{l}{2}\sin\left(\frac{\pi}{2} - \varphi + \frac{\alpha}{2}\right) = \frac{l}{2}\cos\left(\varphi - \frac{\alpha}{2}\right)$$

and hence:

$$|B_1B_2| = m\sin\frac{\alpha}{2},$$

we have

$$areaa_3(\varphi) = \frac{ml}{2}\cos\left(\varphi - \frac{\alpha}{2}\right)\sin\frac{\alpha}{2}. \tag{6}$$

For $m \to n$ and $\alpha \to \pi - \beta$ we have the area $areaa_3(\varphi) \to areaa_2(\varphi)$, hence

$$areaa_7(\varphi) = \frac{nl}{2}\cos\left(\varphi - \frac{\pi-\beta}{2}\right)\sin\frac{\pi-\beta}{2},$$

therefore

$$areaa_7(\varphi) = \frac{nl}{2}\sin\left(\varphi + \frac{\beta}{2}\right)\cos\frac{\beta}{2}. \tag{7}$$

The figure:

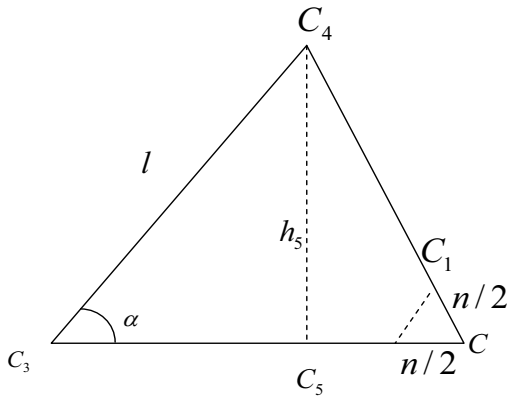

fig.6

give us:

$$\widehat{CC_4C_3} = \pi - \varphi - \beta, \qquad h_5 = l\sin\varphi, \qquad |C_3C_5| = l\cos\varphi,$$

On the other hand, therefore

$$|CC_5| = h_5\cot\beta = l\cot\beta\sin\varphi,$$

we have

$$|CC_3| = l\left(\cos\varphi + \cot\beta\sin\varphi\right), \tag{8}$$

hence

$$areaCC_3C_4 = \frac{l^2}{2}\left(\cos\varphi + \cot\beta\sin\varphi\right)\sin\varphi = \frac{l^2}{4}\left[\sin 2\varphi + \cot\beta\left(1-\cos 2\varphi\right)\right]$$

and considering that:

$$areaCC_1C_2 = \frac{n^2}{8}\sin\beta,$$

follow that

$$areaa_5(\varphi) = \frac{l^2}{4}\left[\sin 2\varphi + \cot\beta\,(1-\cos 2\varphi)\right] - \frac{n^2}{8}\sin\beta. \tag{9}$$

Considering the figure:

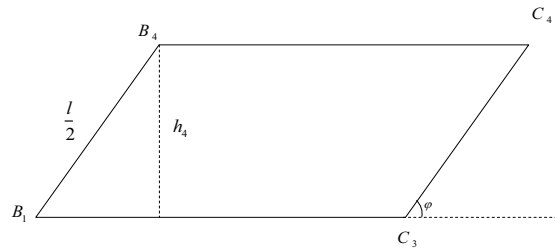

fig.7

and the relations (9) follow that:

$$|B_1C_3| = b - \frac{m}{2} - |CC_3| = b - \frac{m}{2} - l\,(\cos\varphi + \cot\beta\sin\varphi)\,.$$

then

$$h_4 = \frac{l}{2}\sin\varphi,$$

hence

$$areaa_4(\varphi) = \left[b - \frac{m}{2} - l\,(\cos\varphi + \cot\beta\sin\varphi)\right]\frac{l}{2}\sin\varphi \tag{10}$$

For $m \to n$ and $\alpha \to \pi - \beta$, from the relation (1) follow that $a = c$ and we have $areaa_2(\varphi) \to areaa_6(\varphi)$, hence

$$areaa_6(\varphi) = \left(c - \frac{n}{2} - \frac{l\sin\varphi}{\sin\beta}\right)\frac{l}{2}\sin(\varphi+\beta) =$$

$$\left(c - \frac{n}{2}\right)\frac{l}{2}\left(\sin\varphi\cos\beta + \sin\beta\cos\varphi\right) - \frac{l^2}{4}\left[\sin 2\varphi + \cot\beta\,(1-\cos 2\varphi)\right]. \tag{11}$$

and, then $h_5 = \frac{l}{2}\sin\varphi$, follow that:

$$areaa_5(\varphi) = (b - c\cos\alpha - l\cos\varphi)\,\frac{l}{2}\sin\varphi. \tag{12}$$

The figure:

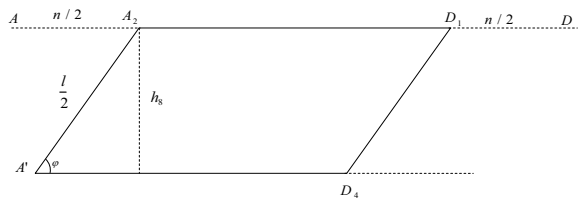

fig. 8

give us

$$|A_2A_1| = d - \frac{m+n}{2}, \qquad h_8 = \frac{l}{2}\sin\varphi,$$

hence:

$$areaa_8(\varphi) = \left(d - \frac{m+n}{2}\right)\frac{l}{2}\sin\varphi = \left(d - \frac{n}{2}\right)\frac{l}{2}\sin\varphi - \frac{ml}{4}\sin\varphi,$$

Considering of (4),

$$areaa_8(\varphi) = \left(d - \frac{n}{2}\right)\frac{l}{2}\sin\varphi - \frac{l}{2}\left[\sin 2\varphi - \cot\alpha\,(1-\cos 2\varphi)\right]$$

Replacing in the (3) the expressions (5), (6), (7), (8), (10), (11), (12) and (13), we obtain:

$$\begin{aligned} area\widehat{C}_0^{(1)}(\varphi) = areaC_0^{(1)} - \\ \left\{\left(\frac{l\sin\varphi}{\sin\alpha} - \frac{m}{2}\right)\frac{l}{2}\sin(\alpha-\varphi) + \left(a - \frac{m}{2} - \frac{l\sin\varphi}{\sin\alpha}\right)\frac{l}{2}\sin(\alpha-\varphi) + \right. \\ \frac{ml}{2}\cos\left(\varphi - \frac{\alpha}{2}\right)\sin\frac{\alpha}{2} + \frac{nl}{2}\sin\left(\varphi + \frac{\beta}{2}\right)\cos\frac{\beta}{2} + \frac{l^2}{4}\left[\sin 2\varphi + \right. \\ \cot\beta\,(1-\cos 2\varphi)] - \frac{n^2}{8}\sin\beta + \left[b - \frac{m}{2} - l\,(\cos\varphi + \cot\beta\sin\varphi)\right]\frac{l}{2}\sin\varphi + \\ \left(c - \frac{n}{2} - \frac{l\sin\varphi}{\sin\beta}\right)\frac{l}{2}\sin(\varphi+\beta) + \left(d - \frac{n}{2}\right)\frac{l}{2}\sin\varphi - \\ \left.\left.\frac{l^2}{4}\left[\sin 2\varphi - \cot\alpha\,(1-\cos 2\varphi)\right]\right\} = \end{aligned} \tag{13}$$

$$areaC_0^{(1)} - \left\{\left(2a - \frac{m}{2}\right)\frac{l}{2}\cos\varphi + \left(b + d + \frac{m}{2}\cos\alpha - \frac{n}{2}\cos\beta\right)\frac{l}{2}\sin\varphi - \right.$$

$$\left.\frac{l^2}{4}\left[2\sin 2\varphi + (\cot\beta - \cot\alpha)\,\frac{1-\cos 2\varphi}{2}\right] - \frac{n^2}{8}\sin\beta\right\}.$$

Denoting with M_1 the set of segments s that intersects a side of the fundamental cell and with N_1 the set of segments s whose the middle point are in $\widehat{C}_0(\varphi)$ and with N the set of segments s completely contained in the fundamental cell we have:

$$P_{int}^{(1)} = 1 - \frac{\mu(N_1)}{\mu(M_1)}, \tag{14}$$

where μ is the Lebesgue measure in Euclidean plane.

The measures $\mu(M_1)$ and $\mu(N_1)$ we compute using the Poincaré kinematic measure [1]

$$dK = dx \wedge dy \wedge d\varphi,$$

where x, y are the coordinates of middle point 0 of the segment s and y the defined angle.

Since $\varphi \in [0,\ \alpha]$, we have:

$$\mu(M_1) = \int_0^{\alpha} d\varphi \iint\limits_{\left\{(x,y)\in C_0^{(1)}\right\}} dxdy = \int_0^{\alpha} \left[area C_0^{(1)}\right] d\varphi = \alpha area C_0^{(1)}. \tag{15}$$

and, considering the (14),

$$\mu(N_1) = \int_0^{\alpha} d\varphi \iint\limits_{\left\{(x,y)\in \widehat{C}_0^{(2)}(\varphi)\right\}} dxdy = \int_0^{\alpha} \left[area \widehat{C}_0^{(1)}(\varphi)\right] d\varphi =$$

$$\alpha area C_0^{(1)} - \left\{\left(2a + \frac{m}{2}\right)\frac{l}{2}\sin\varphi - \left(b + d + \frac{m}{2}\cos\alpha - \frac{n}{2}\cos\beta\right)\frac{l}{2}\cos\varphi - \right.$$

$$\left. \frac{l^2}{4}\left[-\cos 2\varphi + (\cot\beta - \cot\alpha)\frac{\varphi - \frac{\sin 2\varphi}{2}}{2}\right] - \frac{n^2\varphi}{8}\sin\beta\right\} =$$

$$\alpha\cos C_0^{(1)} - \left\{\left(2a - \frac{m}{2}\right)\frac{l}{2}\sin\alpha + \left(b + d + \frac{m}{2}\cos\alpha - \frac{n}{2}\cos\beta\right)\frac{l}{2}(1 - \cos\alpha) - \right.$$

$$\left. \frac{l^2}{4}\left[1 - \cos 2\varphi + \frac{\cot\beta - \cot\alpha}{4}(2\alpha - \sin 2\alpha)\right]\right\}. \tag{16}$$

The formulas (15), (16) and (17) give us that:

$$P_{int}^{(1)} = \frac{1}{\alpha\left[\frac{a(b+d)\sin\alpha}{2} - \frac{m^2}{4}\sin\alpha - \frac{n^2}{4}\sin\beta\right]}\left\{\left(2a - \frac{m}{2}\right)\frac{l}{2}\sin\alpha + \right.$$

$$\left(b + d + \frac{m}{2}\cos\alpha - \frac{n}{2}\cos\beta\right)\frac{l}{2}(1 - \cos\alpha) -$$

$$\left. \frac{l^2}{4}\left[1 - \cos 2\varphi + \frac{\cot\beta - \cot\alpha}{4}(2\alpha - \sin 2\alpha)\right]\right\}. \tag{17}$$

When $\alpha \to \frac{\pi}{2}$ and $\beta \to \frac{\pi}{2}$, $m \to 0$, $n \to 0$ we $c = a$, $d = b$, the cell $C_0^{(1)}$ becames a rectangle with side a and b and the probability (18) becomes the Laplace probability:

$$P = \frac{2(2a + b)l - l^2}{2\pi ab}.$$

References

[1] Poincaré H., Calcul des probabilitiés, ed. 2, Carré, Paris, 1912.

[2] Stoka M., Probabilités géométriques de type Buffon dans le plan euclidean, Atti Acc. Sci. Torino, T. 110, pp. 53-59, 1975-1976.

RENDICONTI DEL CIRCOLO MATEMATICO DI PALERMO
Serie II, Suppl. 83 (2011), pp. 229-236

EXPLORING BREAST CANCER DIAGNOSIS WITH FRACTAL ANALYSIS AND CLASSIFICATION METHODS

GRAZIA RAGUSO1* - ANTONIETTA ANCONA[2] - LOREDANA CHIEPPA[1]
SAMUELA L'ABBATE[3] - MARIA LUISA PEPE[4]
FRANCESCO D. D'OVIDIO[3].
[1]Department of Mathematics, University of Bari, Bari, Italy.
[2]Radiology Unit, San Paolo Hospital of Bari, Bari, Italy.
[3]Department of Statistics, University of Bari, Bari, Italy.
[4]Department of Radiology, University Hospital - Policlinico of Bari, Bari, Italy.
[*]To whom all correspondence should be addressed
e-mail: raguso@dm.uniba.it
Phone: +39 – 080 – 544 – 2682
Fax: +39 – 080 – 544 – 3610

Abstract. Screening and diagnostic mammography are the most effective tools available for detection and diagnosis of breast cancer. In the last decade many techniques based upon measures of the shape of the contours of breast masses are been developed to investigate the nature of lesions between malignant tumours and benign masses. This paper presents methods for statistical analysis on a data set of 192 contours of breast masses. Results of these analysis lead to levels of accurate prediction in 90% of the cases, overcoming 98% for the diagnosis of malignant lesions. In this study we applied multivariate statistical techniques for examining relationships among more variables at the same time. We used in addition to the shape factors of contour masses also the age of the patients at the time of mammography, using both ROC analysis and segmentation analysis through Classification and Regression Tree.

1 Introduction.

Recent studies have shown that early detection through mammographic screening of asymptomatic women reduce breast cancer mortality. The true-positive and false-positive rates of

mammography vary in different age groups; the sensitivity of mammography is higher in women older than 50 years [1]. Mammography is the best method available for early detection of breast cancer. In order to assess a contour mass on mammograms, shape parameter are taken into consideration. On the basis of the notable shape differences we can distinguish between benign masses and malignant tumours. These observations have led to the idea of applying the concept of fractal dimension (FD) to analyze the contours of breast lesions [2]. Fractal analysis can characterize the degree of complexity of a contour or shape, and can provide parameters to discriminate between benign masses and malignant tumours [3].

In [3] we studied a data set of 192 mammograms were obtained from 192 patients at the Senology Unit, San Paolo Hospital, Bari, Italy, ASL Ba/4. The patients were diagnosed to have breast disease via screen-film mammography and confirmed from histological data; 163 of the cases were malignant and 29 were benign. The most useful mammographic projections were selected to analyze the contours of lesions. During an initial phase, contours of the present mammary lesions on the film images were traced by a team of radiologists specialized in mammography and successively, by a graphic tablet, we obtained a digital representation of the contour using Matlab software. Furthermore, we reported on a morphological study of 192 contours, with the aim of discriminating between benign masses and malignant tumours. From the contour of each mass, we computed the fractal dimension (FD) and a few shape factors, including compactness, 3 fractional concavity, and spiculation index. We calculated FD by using four different methods: the ruler and box-counting methods applied to each 2-dimensional (2D) contour and its 1-dimensional signature. Analysis using receiver operating characteristics (ROC) was performed with each shape feature to determine the diagnostic accuracy achievable in order to discriminate between benign masses and malignant tumours. ROC analysis indicated the area under the curve, A_z, of up to 0.92, having the individual shape features. The combination of compactness, FD with the 2D ruler method, and the spiculation index had as result in the highest A_z value of 0.93.

The data set, the shape features calculated for all data and the results obtained in the previous work [3], are used in this paper to

implement a different algorithm called CRT to have binary statistical classification of the variables (shape features). In addition to the shape factors of mass contours we introduced also the age of the patients at the time of mammography.

1.1 Fractal dimension and shape factors.

Fractals are irregular figures, and can be generated by the iteration of linear or nonlinear functions [4, 5]. Sometimes they are self-similar, and have a fine structure which reveals new details at every level of magnification [4]. In order to measure the degree of complexity or irregularity of a fractal, the concept of FD was introduced; this concept is derived from the more general notion of the Hausdorff dimension [6]. Cancerous tumours exhibit a certain degree of randomness associated with their growth, and are typically irregular and complex in shape. The degree of irregularity of the contour of a mass is the first parameter assessed: benign masses are often smooth, rounded, well-circumscribed, whereas a malig- 4 nant tumour is often characterized by an irregular contour with the spicules, that could be considered as a fractal pattern. Therefore, fractal analysis can provide a better measure of complex patterns. The Hausdorff dimension generalizes the concept of the self-similarity dimension in the sense that it is applicable to any set of the plane, and therefore, to a fractal set that is not strictly self-similar. The difficulties involved in defining the Hausdorff dimension have led many authors to find alternative methods for estimating FD. The common numerical methods are the box-counting and the ruler methods, which have been extensively described in the literature [6, 2].

On the basis of the differences in shape between benign masses and malignant tumours, various measures can be associated with a contour or curve: these are the so-called shape factors, which have proven to be effective in describing shapes in many research fields, in particular in the medical field [2, 7]. The shape factors used are compactness *cf*, fractional concavity f_{cc}, spiculation index SI; these measures have been proven to be effective in the classification of breast masses [8, 2, 9, 7]. See Rangayyan and Nguyen [2] and Rangayyan [7] for details on the shape factors.

Compactness is defined as [7]

$$cf = 1 - \frac{4\pi}{P^2}, \tag{1}$$

where P and A are the perimeter and the area of the contour, respectively. A high compactness value indicates a long perimeter enclosing a small area. Fractional concavity is defined as [8, 7]

$$f \propto = 1 - \frac{CC}{L}, \tag{2}$$

where CC represents sum of the lengths of the concave segments of the contour and L is the total length of the contour. Spiculation index is defined as

$$SI = 1 - \frac{\sum_{n=1}^{N} (1 + \cos\theta_n) S_n}{\sum_{n=1}^{N} S_n}, \tag{3}$$

where θ_n and S_n are the narrowness angle and the spicule length, respectively.

1.2 Statistics method: CRT algorithm.

The segmentation analysis allows researchers to determine (starting from a learning sample [10] of n independent units whose determinations are known in both dependent and explanatory variables) a classification rule able to divide the population in groups as homogeneous as possible inside them. Such rule will also be able to estimate the probability to detect a specific response, for other cases with unknown values of dependent variable but predictors with known determinations [11, 12]: in our case, the distribution of patients with unknown type of lesion (benign / malignant), based on some combinations of predictors. The segmentation analysis, in itself, is a recursive computing method which has some conceptual similarity with the cluster analysis: in both the methods will define some groups of observations which are homogeneous within the group and different from those of

other groups. Their basic principles, however, are different: the cluster analysis joins together the individual units sampled in groups according to all the considered variables, with the constraint of minimum variability "within" and maximum variability "between", without any constraints of hierar- 6 chy or dependence [13, 14]. The segmentation analysis, instead, divides a sample in aggregates which are more and more internally homogeneous with respect to a dependent variable, based on the values assumed by other variables, taken as explanatory, and on the relations between such variables and the dependent ones [13]. The best segmentation among all possible ones, based on the combination of different predictors, is that one that best meets the criteria of internal homogeneity of the groups generated (also known as "purity" [10]). Ideally, all cases of an final node should have the same value as the dependent variable (maximum purity). There are several methods of segmentation, but currently the most used are, among the algorithms of binary division, the CRT method [10, 15], and the CHAID type [16] among ternary or multiple algorithms.

2 Results and discussion.

The combined use of the shape parameters in [3] led to slight improvements in terms of accuracy: the combination of FD calculated using the 2D ruler method with *cf* and *SI* gave the highest A_z of 0.927. However, the combinations do not have a significant difference between one another. Nevertheless, in this work, we show that the conditioned combination of such factors can give us further information. Applying a segmentation analysis to data set (through CRT algorithm), we obtain classification trees that analyze the phenomena in the best way. The best result involves, in various combinations, (see Figure 1), both FD-2D calculated with ruler method and *SI*, as well as FD-1D calculated with the same method and age at diagnosis: i.e., women with *SI*>0.232 and age > 45, 5 years in the 98, 6% of analyzed cases have malignant lesions, but the disease probability is clearly lower (<52%) in women which *SI* is < 0.232 (none of those aged 7 < 50.5 years presents malignant lesions). Stopping the algorithm to first levels, the correct classification is near 91%, but further levels of

the analysis drive us to predict true positives and true negatives in 96% of the cases, with most capability in the analysis of the malignant disease (98%) than of benign masses (83%) (see Table 1, Table 2). Robustness of the algorithm showed in figure (classification tree) is sufficient: the jackknife re-sampling method (100 different sub-samples with half number of cases) give a maximal error risk < 0.12.

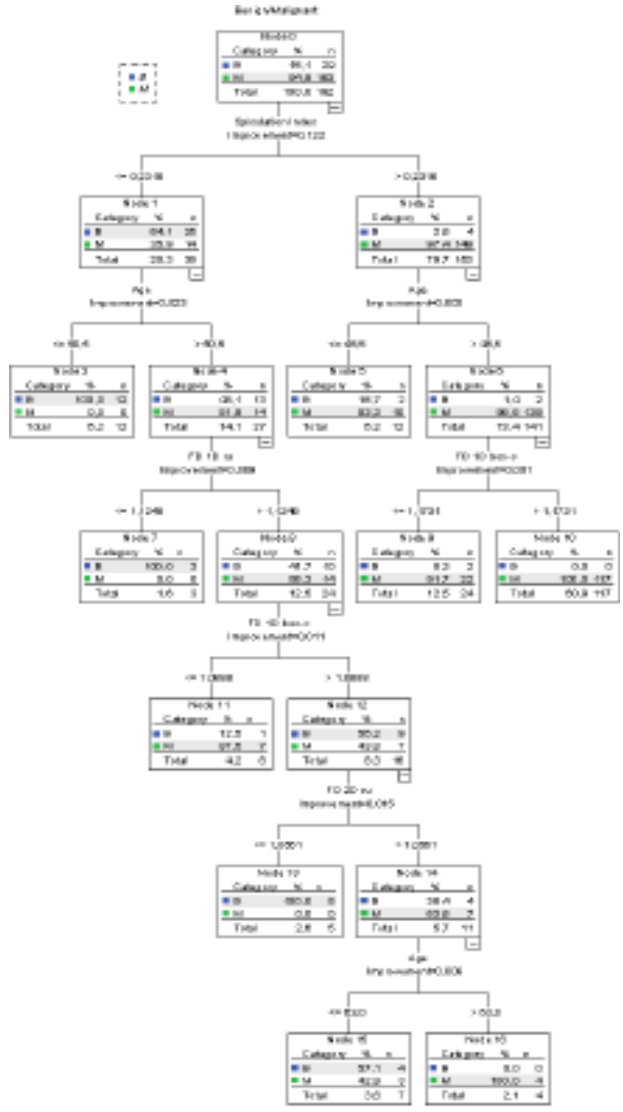

Figure 1: Segmentation Tree.

Table 1: Growing Method: CRT. Dependent Variable: Benign/Malignant.

Indipendent Variable	Importance	Normalized Importance
Spiculation Index	0.138	100.0%
FD-ruler 2D	0.137	99.3%
Compactness	0.125	90.6%
FD-ruler 1D	0.100	72.5%
FD-box 1D 0.	082	59.5%
FD-box 2D	0.081	58.7%
Fractional Concavity	0.055	39.8%
Age	0.047	34.1%

Table 2: Growing Method: CRT. Dependent Variable: Benign/Malignant.

Observed	Predicted		
	B	N	Percent Correct
B	24	5	82.8%
M	3	160	98.2%
Overall Percentage	14.1%	85.9%	95.8%

Acknowledgments

This work was supported by Fondazione Cassa di Risparmio di Puglia, Italy. We thank Rangayyan R.M., Thanh M. Nguyen and Naga R. Mudigonda for their contribution and discussion on the topic of this work.

REFERENCES

[1] R. W. Koudies A. I. Mushlin and D. E. Shapiro. Estimating the accuracy of screening maxnmography: a metaanalysis. *American Journal of Preventive Medicine,* 14:143–153, 1998.

[2] R. M. Rangayyan and T. M. Nguyen. Fractal analysis of contours of breast masses in mammograms. *Journal of Digital Imaging,* 20(3):223–237, 2007.

[3] G. Raguso, A. Ancona, L. Chieppa, S. L'Abbate, M. L. Pepe, F. Mangieri, M. De Palo, and R. M. Rangayyan. Application of fractal analysis to mammography. In *Proceedings of the 32nd Annual International Conference of the IEEE Engineering in Medicine and Biology Society 2010,* Buenos Aires, Argentina, August 31-September 4, 2010.

[4] B. B. Mandelbrot. *The Fractal Geometry of Nature.* W. H. Freeman, San Francisco, CA, 1983.

[5] H. O. Peitgen and P. H. Richter. *The Beauty of Fractals - Images of Complex Dynamical Systems.* Springer - Verlag, Berlin Heidelberg, Germany, 1986.

[6] H. O. Peitgen, H. Jurgens, and D. Saupe. *Chaos and Fractals: New Frontiers of Science.* Springer, New York, NY, 2004.

[7] R. M. Rangayyan. *Biomedical Image Analysis.* CRC Press, Boca Raton, FL, 2005. 10

[8] R. M. Rangayyan, N. R. Mudigonda, and J. E. L. Desautels. Boundary modelling and shape analysis methods for classification of mammographic masses. *Medical and Biological Engineering and Computing,* 38:487–496, 2000.

[9] R. M. Rangayyan, N. M. El-Faramawy, J. E. L. Desautels, and O. A. Alim. Measures of acutance and shape for classification of breast tumors. *IEEE Transactions on Medical Imaging,* 16(6):799–810, 1997.

[10] L. Breiman, J. H. Friedman, R. A. Olshen, and C. J. Stone. *Classification and Regression Trees.* Chapman and Hall, New York, NY, 1993.

[11] J. A. Sonquist and J. N. Morgan. *The Detection of Interaction Effects.* Institute for Social Research, The University of Michigan, Ann Arbor, MI, 1964.

[12] J. A. Sonquist. *Multivariate Model Building. The Validation of a Search Strategy.* Institute for Social Research, The University of Michigan, Ann Arbor, MI, 1970.

[13] L. Fabbris. *Statistica multivariata. Analisi esplorativa dei dati.* McGraw-Hill, Milano, IT, 1997.

[14] F. Delvecchio. *Statistica per l'analisi di dati multidimensionali.* Cleup, Padova, IT, 2010.

[15] D. Biggs, B. De Ville, and E. Suen. A method of choosing multiway partitions for classification and decision trees. *Journal of Applied Statistics,* 18:49–62, 1991. 11

[16] G. Kass. An exploratory technique for investigating large quantities of categorical data. *Applied Statistics,* 29(2):119–127, 1980.

RENDICONTI DEL CIRCOLO MATEMATICO DI PALERMO
Serie II, Suppl. 83 (2011), pp. 237-248

UN PROBLEMA DI TIPO BUFFON PER UN RETICOLO IRREGOLARE

ALESSANDRA ROMOLO

SUNTO. In questo lavoro si considera un reticolo irregolare la cui cella fondamentale è rappresentata nella figura 2 e si calcola la probabilità che un segmento di posizione aleatoria e di lunghezza costante intersechi un lato del reticolo.

1 Trattazione

Consideriamo la figura

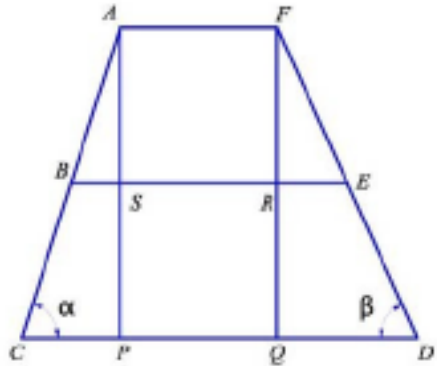

Fig. 1.

Posto

$$|AF| = a, \quad |CD| = 2a, \quad |AS| = |SP| = |FR| = |RQ| = h \tag{1}$$

risulta

$$|BE| = \frac{3a}{2}, \quad |AB| = |BC| = \frac{h}{\sin\alpha}, \quad |DE| = |EF| = \frac{h}{\sin\beta}, \tag{2}$$
$$|CP| = 2h\mathrm{ctg}\alpha, \quad |DQ| = 2h\mathrm{ctg}\beta.$$

Con questi valori, possiamo scrivere

$$2a = a + h\,(\mathrm{ctg}\alpha + \mathrm{ctg}\beta),$$

quindi

$$h = \frac{a\sin\alpha\sin\beta}{2\sin(\alpha+\beta)}. \tag{3}$$

Allora

(4) $$|AB| = |BC| = \frac{a\sin\beta}{2\sin(\alpha+\beta)}, \quad |EF| = |ED| = \frac{a\sin\alpha}{2\sin(\alpha+\beta)}.$$

Consideriamo ora il reticolo $R(a;\alpha,\beta)$ con $\beta \le \alpha$, la cui cella fondamentale C_0 è rappresentata nella figura

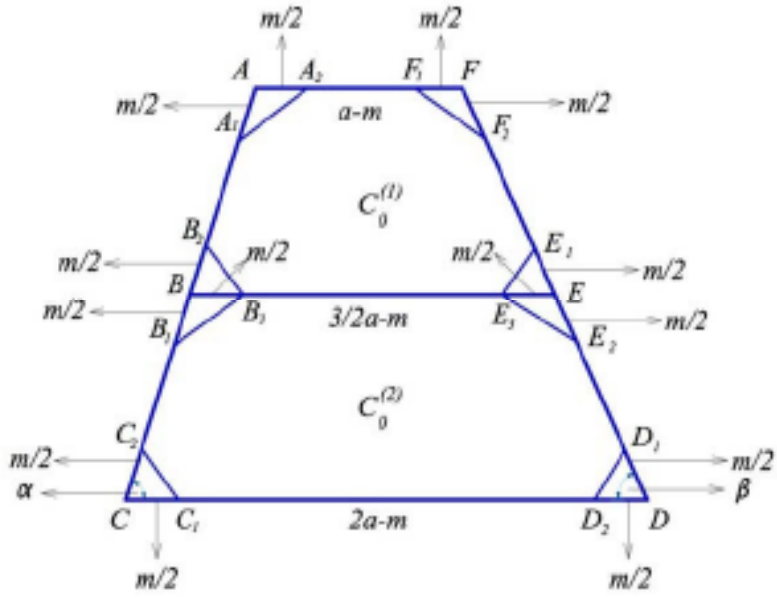

Fig. 2.

Gli otto ostacoli sono triangoli isosceli di lati $m/2$.

Indicando con O_1 l'ostacolo A A_1 A_3, con O_2 l'ostacolo B B_2 B_3, con O_3 l'ostacolo F F_1 F_2 e con O_4 l'ostacolo E E_1 E_5, abbiamo

(5) $$\text{area } O_1 = \text{area } O_2 = \frac{m^2}{8}\sin\alpha, \quad \text{area } O_3 = \text{area } O_4 = \frac{m^2}{8}\sin\beta.$$

Ugualmente si ha

(6) $$|A_1A_2| = |B_1B_3| = m\cos\frac{\alpha}{2}, \quad |B_2B_3| = |C_1C_2| = m\sin\frac{\alpha}{2},$$

$$|F_1F_2| = |E_2E_3| = m\cos\frac{\beta}{2}, \quad |E_1E_3| = |D_1D_2| = m\sin\frac{\beta}{2}.$$

Dalla figura 2 e dalle relazioni (3) e (5), segue

(7) $$area\, C_0^{(1)} = \frac{5a^2\sin\alpha\sin\beta}{8\sin(\alpha+\beta)} - \frac{m^2}{4}(\sin\alpha+\sin\beta);$$

$$area\, C_0^{(2)} = \frac{7a^2 \sin\alpha \sin\beta}{8\sin(\alpha+\beta)} - \frac{m^2}{4}(\sin\alpha + \sin\beta);$$

quindi

$$area\, C_0 = \frac{3a^2 \sin\alpha \sin\beta}{2\sin(\alpha+\beta)} - \frac{m^2}{2}(\sin\alpha + \sin\beta)\,. \tag{8}$$

Consideriamo ora un segmento s di posizione aleatoria e di lunghezza costante $l < \frac{a}{2} - m;$ vogliamo determinare la probabilità che il segmento s intersechi un lato del reticolo, cioè la probabilità P_{int} che il segmento s intersechi un lato della cella fondamentale C_0.

La posizione del segmento s è determinata dal suo punto medio O e dall'angolo che esso forma con il lato CD (o BE) della cella C_0.

Per calcolare la probabilità P_{int} consideriamo dapprima le posizioni limite del segmento s per un valore prefissato di φ situate in $C_0^{(1)}$ e poi le posizioni limite di s per lo stesso valore di φ, situate in $C_0^{(2)}$ (*fig.3*).

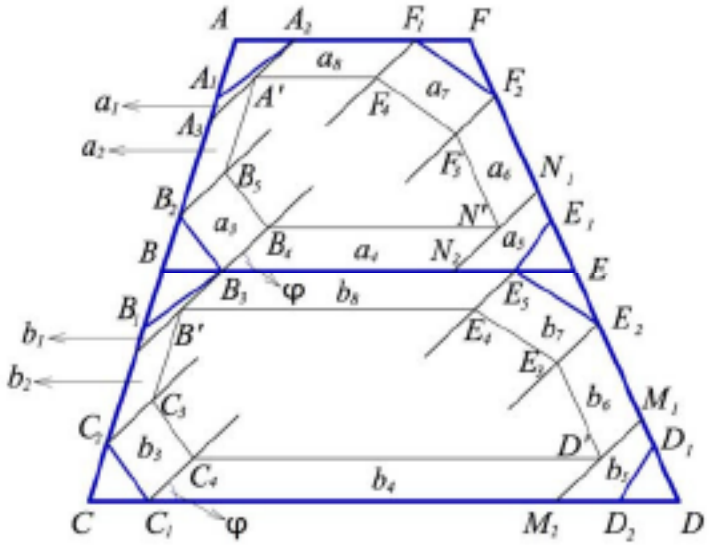

Fig. 3.

Indicando con $\hat{C}_0^{(1)}(\varphi)$ il poligono determinato dalle posizioni limite di s nel primo caso e con $\hat{C}_0^{(2)}(\varphi)$ il poligono determinato dalle posizioni limite di s nel secondo caso, la figura 3 ci dà

$$\text{area}\,\hat{C}_0^{(1)}(\varphi) = a\text{area}\,C_0^{(1)} - \left[a\text{area}\,a_1(\varphi) + \text{area}\,a_2(\varphi) + \ldots\ldots\ldots + \text{area}\,a_8(\varphi)\right] \tag{9}$$

e

$$\text{area}\,\widetilde{C}_0^{(2)}(\varphi) = \text{area}\,C_0^{(2)} - \left[\text{area}\,b_1(\varphi) + \text{area}\,b_2(\varphi) + \ldots\ldots\ldots + \text{area}\,b_8(\varphi)\right] \tag{10}$$

Per calcolare $\text{area}\,a_1(\varphi)$, consideriamo la figura

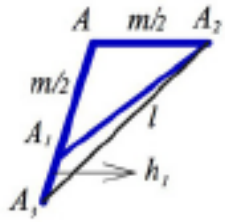

Fig. 4.

Abbiamo

$$A\hat{A}_2A_1 = A\hat{A}_1A_2 = \frac{\alpha}{2}, \quad A_3\hat{A}_2A = \varphi, \quad A\hat{A}_3A_2 = \pi - (\pi - \alpha + \varphi) = \alpha - \varphi.$$

Il triangolo $A_1A_2A_3$ ci dà

$$\frac{|A_1A_3|}{\sin\left(\varphi - \frac{\alpha}{2}\right)} = \frac{l}{\sin\left(\frac{\alpha}{2}\right)} = \frac{m\cos\left(\frac{\alpha}{2}\right)}{\sin(\alpha - \varphi)}.$$

Da qui segue

$$|A_1A_3| = l\sin\left(\varphi - \frac{\alpha}{2}\right) \tag{11}$$

e la condizione

$$2l\sin(\alpha - \varphi) = m\sin\alpha. \tag{12}$$

Poi si ha

$$h_1 = |A_1A_2|\sin A_1\hat{A}_2A_3 = m\cos\frac{\alpha}{2}\sin\left(\varphi - \frac{\alpha}{2}\right).$$

Allora

$$\text{area}\,a_1(\varphi) = \frac{ml}{2}\cos\frac{\alpha}{2}\sin\left(\varphi - \frac{\alpha}{2}\right). \tag{13}$$

La figura

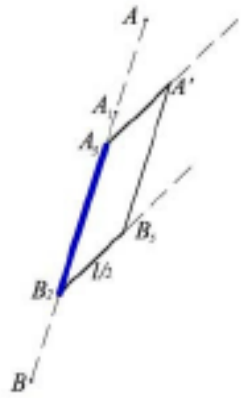

Fig. 5

e le relazioni (4) e (11) ci danno :

$$|A_3B_2| = |AB| - |AA_1| - |A_1A_3| - |BB_2|,$$

cioè

$$|A_3A_2| = \frac{a\sin\beta}{2\sin(\alpha+\beta)} - m - \frac{l\sin\left(\varphi-\frac{\alpha}{2}\right)}{\sin\frac{\alpha}{2}}.$$

Poichè $A\hat{B}_2B_5 = A_1\hat{A}_3A_2 = \alpha - \varphi,$ abbiamo

$$h_2 = \frac{l}{2}\sin(\alpha-\varphi),$$

quindi $$\text{area } a_2(\varphi) = \left[\frac{a\sin\beta}{2\sin(\alpha+\beta)} - m - \frac{l\sin\left(\varphi-\frac{\alpha}{2}\right)}{\sin\frac{\alpha}{2}}\right]\frac{l}{2}\sin(\alpha-\varphi).$$

Tenendo conto qui della relazione (12), otteniamo

(14) $$\text{area } a_2(\varphi) = \frac{al\sin\beta}{4\sin(\alpha+\beta)}\sin(\alpha-\varphi) - \frac{ml}{2}[3\sin(\alpha-\varphi) - \sin\varphi].$$

Consideriamo ora la figura

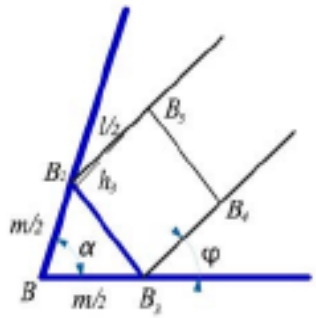

Fig. 6.

Abbiamo

$$B_2\hat{B}_3B_4 = \pi - \left(\frac{\pi}{2} - \frac{\alpha}{2} + \varphi\right) = \frac{\pi}{2} - \varphi + \frac{\alpha}{2}, \quad \mathrm{B_3\hat{B}_2B_5} = \frac{\pi}{2} - \frac{\alpha}{2} + \varphi,$$

$$h_3 = \frac{l}{2}\sin\left(\frac{\pi}{2} - \frac{\alpha}{2} + \varphi\right) = \frac{l}{2}\cos\left(\varphi - \frac{\alpha}{2}\right).$$

e, poichè $|B_1B_2| = m\,sin\frac{\alpha}{2}$, segue

(15) $$\text{area}\, a_3(\varphi) = \frac{ml}{2}\sin\frac{\alpha}{2}\cos\left(\varphi - \frac{\alpha}{2}\right).$$

La figura

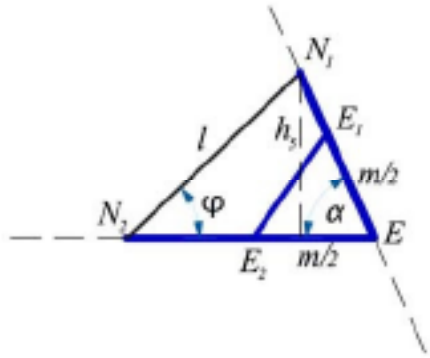

Fig. 7

ci dà

$$\frac{l}{\sin\beta} = \frac{|E_1N_1|}{\sin\varphi} = \frac{|EN_2|}{\sin(\beta+\varphi)},$$

quindi

(16) $$|EN_1| = \frac{l\sin\varphi}{\sin\beta}, \quad |EN_2| = \frac{l\sin(\beta+\varphi)}{\sin\beta}.$$

Inoltre, poiché $h_5 = l\sin\varphi,$ si ha

$$\text{area } EN_1E_2 = \frac{h_5|EN_2|}{2} = \frac{l^2\sin(\beta+\varphi)\sin\varphi}{2\sin\beta}.$$

Allora, con la (5),

(17) $$\text{area } a_5(\varphi) = \frac{l^2\sin(\beta+\varphi)\sin\varphi}{2\sin\beta} - \frac{m^2}{8}\sin\alpha.$$

Dalla figura

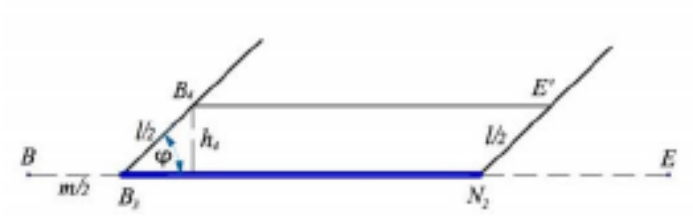

Fig. 8

e con la (16) segue

$$|B_3N_2| = |BE| - |BB_3| - |EN_2| = \frac{3a}{2} - \frac{m}{2} - \frac{l\sin(\beta+\varphi)}{\sin\beta}, \qquad h_4 = \frac{l}{2}\sin\varphi,$$

dunque

(18) $$\text{area } a_4(\varphi) = \left[3a - m - \frac{2l\sin(\beta+\varphi)}{\sin\beta}\right]\frac{l}{4}\sin\varphi.$$

Per calcolare $\text{area } a_6(\varphi)$, consideriamo la figura

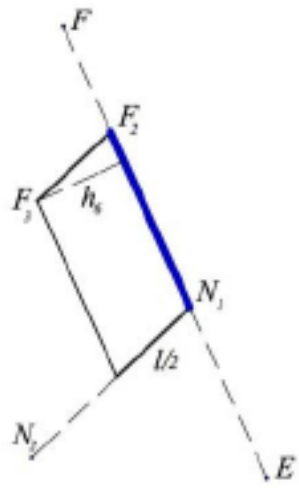

Fig. 9.

Abbiamo

$$F_3\hat{F}_2N_1 = N_2\hat{N}_1E = \pi - (\beta + \varphi),$$

quindi

$$h_6 = \frac{l}{2}\sin(\beta + \varphi).$$

Poi, tenendo conto delle relazioni (4) e (15), si ha

$$\left|F_2N_1\right| = \frac{a\sin\alpha}{2\sin(\alpha+\beta)} - \frac{m}{2} - \frac{l\sin\varphi}{\sin\beta}.$$

Allora

$$\text{area } a_6(\varphi) = \left[\frac{a\sin\alpha}{\sin(\alpha+\beta)} - m - \frac{2l\sin\varphi}{\sin\beta}\right]\frac{l}{4}\sin(\beta+\varphi). \tag{19}$$

Osserviamo che, se sostituiamo α con $\pi - \beta$, il parallelogramma $a_3(\varphi)$ diventa il parallelogramma $a_7(\varphi)$. Pertanto

$$\text{area } a_7(\varphi) = \frac{ml}{2}\cos\frac{\beta}{2}\sin\left(\varphi + \frac{\beta}{2}\right). \tag{20}$$

Infine consideriamo la figura

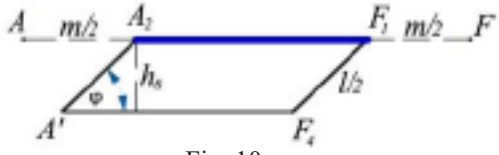

Fig. 10

Abbiamo

$$\left|A_2F_1\right| = \left|AF\right| - \left|AA_2\right| - \left|FF_1\right| = a - m$$

e

$$h_8 = \frac{l}{2}\sin\varphi,$$

dunque

$$\text{area } a_8(\varphi) = \frac{(a-m)l}{2}\sin\varphi. \tag{21}$$

Sostituendo nella (9) le espressioni (13), (14), (15), (17), (18), (19), (20) e (21) otteniamo

$$\begin{aligned}\text{area } \hat{C}_0^{(1)}(\varphi) = \text{area } C_0^{(1)} - \left\{\left[\frac{a\sin\alpha\sin\beta}{\sin(\alpha+\beta)} - \frac{3a}{2}\sin\alpha\right]\frac{l}{2}\cos\varphi + \left[4a - \frac{3m}{8} + \right.\right. \\ \left.\left. + \frac{a\sin(\alpha-\beta)}{2\sin(\alpha+\beta)} - \frac{3a\cos\alpha}{2}\right]\frac{l}{2}\sin\varphi - \frac{l^2}{2}(\sin 2\varphi - \operatorname{ctg}\beta\cos 2\varphi + \operatorname{ctg}\beta) - \frac{m^2}{8}\sin\alpha\right\}\end{aligned} \tag{22}$$

Dalla figura 3 segue

$$\text{area } b_1(\varphi) = \text{area } a_1(\varphi) = \frac{ml}{2}\cos\frac{\alpha}{2}\sin\left(\varphi - \frac{\alpha}{2}\right), \tag{23}$$

$$\text{area } b_2(\varphi) = \text{area } a_2(\varphi) = \frac{al\sin\beta}{4\sin(\alpha+\beta)}\sin(\alpha-\beta) - \frac{ml}{4}[3\sin(\alpha-\beta) - \sin\varphi],$$

$$\text{area } b_3(\varphi) = \text{area } a_3(\varphi) = \frac{ml}{2}\sin\frac{\alpha}{2}\cos\left(\varphi - \frac{\alpha}{2}\right),$$

$$\text{area } b_5(\varphi) = \text{area } a_5(\varphi) = \frac{l^2\sin(\beta+\varphi)\sin\varphi}{2\sin\beta} - \frac{m^2}{8}\sin\alpha,$$

$$\text{area } b_6(\varphi) = \text{area } a_6(\varphi) = \left[\frac{a\sin\alpha}{\sin(\alpha+\beta)} - m - \frac{2l\sin\varphi}{\sin\beta}\right]\frac{l}{4}\sin(\beta+\varphi),$$

$$\text{area } b_7(\varphi) = \text{area } a_7(\varphi) = \frac{ml}{2}\cos\frac{\beta}{2}\sin\left(\varphi + \frac{\beta}{2}\right).$$

Ci resta da calcolare l' area $b_4(\varphi)$ e l' area $b_8(\varphi)$.

La figura

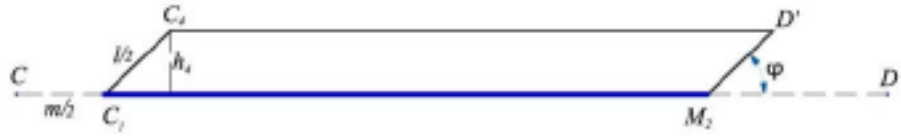

Fig. 11

ci dà

$$h_4 = \frac{l}{2}\sin\varphi.$$

D'altra parte, dall'uguaglianza dei triangoli DM_1M_2 ed EN_1N_2 e dalla formula (16), risulta

$$\left|DM_2\right| = \left|EN_2\right| = \frac{l\sin(\varphi+\beta)}{\sin\beta}.$$

Allora

$$\left|C_1M_2\right| = 2a - \frac{m}{2} - \frac{l\sin(\varphi+\beta)}{\sin\beta},$$

quindi

$$\text{area } b_4(\varphi) = \left[2a - \frac{m}{2} - \frac{l\sin(\varphi+\beta)}{\sin\beta}\right]\frac{l}{2}\sin\varphi. \tag{24}$$

Poi, dalla figura

Fig. 12

segue

$$\left|B_3E_5\right| = \frac{3a}{2} - m, \quad h_8 = \frac{l}{2}\sin\varphi,$$

dunque

$$\text{area } b_8(\varphi) = \frac{3a-2m}{4}\frac{l}{2}\sin\varphi. \tag{25}$$

$$\text{area}\,\hat{C}_0^{(2)}(\varphi) = \text{area}\,C_0^{(2)} - \left\{\left[\frac{a\sin\alpha\sin\beta}{\sin(\alpha+\beta)} - \frac{3m}{2}\sin\alpha\right]\frac{l}{2}\cos\varphi + \left[\frac{7a}{2} + \frac{m}{2} + \right.\right.$$

(26)

$$\left.\left. + \frac{3m\cos\alpha}{2} - \frac{a\sin(\alpha-\beta)}{2\sin(\alpha+\beta)}\right]\frac{l}{2}\sin\varphi - \frac{l^2}{4}[\sin 2\varphi + (1-\cos 2\varphi)\text{ctg}\beta] - \frac{m^2}{8}\sin\alpha\right\}.$$

Indichiamo con $\mathcal{M}_1$ l'insieme dei segmenti *s* che hanno il punto medio in $C_0^{(1)}$, con $\mathcal{M}_2$ l'insieme dei segmenti *s* che hanno il punto medio in $C_0^{(2)}$, con $\mathcal{N}_1$ l'insieme dei segmenti *s* interamente contenuti in $C_0^{(1)}$ e con $\mathcal{N}_2$ l'insieme dei segmenti *s* interamente contenuti in $C_0^{(2)}$. Allora abbiamo [2]

$$P_{\text{int}} = 1 - \frac{\mu(\mathcal{N}_1) + \mu(\mathcal{N}_2)}{\mu(\mathcal{M}_1) + \mu(\mathcal{M}_2)}, \tag{27}$$

dove μ è la misura di Lebesgue nel piano euclideo.

Le misure $\mu(\mathcal{M}_1), \mu(\mathcal{M}_2), \mu(\mathcal{N}_1), \mu(\mathcal{N}_2),$ si calcolano usando la misura cinematica di Poincaré [1]

$$dK = dx \wedge dy \wedge d\varphi,$$

dove $x, y,$ sono le coordinate del punto O e φ l'angolo già definito.

Tenendo conto che $\varphi \in [0, \alpha],$ si ha :

$$\mu(\mathcal{M}_1) = \int_0^{\alpha} d\varphi \iint_{\{(x,y)\in C_0^{(1)}\}} dxdy = \int_0^{\alpha} [\text{area}\,C_0^{(1)}]\,d\varphi = \alpha\,\text{area}\,C_0^{(1)},$$

$$\mu(\mathcal{M}_2) = \int_0^{\alpha} d\varphi \iint_{\{(x,y)\in C_0^{(2)}\}} dxdy = \int_0^{\alpha} [\text{area}\,C_0^{(2)}]\,d\varphi = \alpha\,\text{area}\,C_0^{(2)},$$

Poi, tenendo conto della (22), rispettivamente (26),

$$\mu(\mathcal{N}_1) = \int_0^{\alpha} d\varphi \iint_{\{(x,y)\in \hat{C}_0^{(1)}(\varphi)\}} dxdy = \int_0^{\alpha} [\text{area}\,\hat{C}_0^{(1)}]\,d\varphi = \alpha\,\text{area}\,C_0^{(1)} - \left\{\left[\left(\frac{11a}{2} - \frac{3m}{8}\right)(\cos\alpha - 1) + \right.\right.$$

$$\left. + \frac{a}{\sin(\alpha+\beta)}(\sin^2\alpha\sin\beta + (\cos\alpha - 1)\sin(\alpha-\beta))\right]\frac{l}{2} - \frac{l^2}{4}(1 - \cos 2\alpha - \text{ctg}\beta\sin 2\alpha +$$

$$\left. + 2\alpha\,\text{ctg}\beta) - \frac{m^2\alpha\sin\alpha}{8}\right\},$$

$$\mu(\mathcal{N}_2)=\int_0^{\alpha} d\varphi \iint_{\{(x,y)\in\hat{C}_0^{(2)}(\varphi)\}} dxdy \;=\int_0^{\alpha}[\text{area }\hat{C}_0^{(2)}]\,d\varphi=\alpha\ \text{area}\ C_0^{(2)}-\left\{\frac{l}{2}\left[4a-\frac{3m}{8}+\right.\right.$$

$$-\left(\frac{11-3m}{2}\right)\cos\alpha+\frac{3a}{2}\cos 2\alpha+\frac{a}{2\sin(\alpha+\beta)}\Big(\ \sin\alpha\sin\beta\ (2\sin\alpha-\cos\alpha)+$$

$$\left.\left.-\cos^2\alpha\cos\beta+\sin(\alpha-\beta)\ \Big)\right]-\frac{l^2}{4}[\sin 2\alpha+\operatorname{ctg}\beta(1-\cos 2\alpha+2\alpha)]-\frac{m^2\alpha\sin\alpha}{8}\right\}.$$

Con questi valori, la (27) ci dà

$$P_{\text{int}}=\frac{2}{\alpha\left[\dfrac{3a^2\sin\alpha\sin\beta}{\sin(\alpha+\beta)}-m^2(\sin\alpha+\sin\beta)\right]}\left\{\frac{l}{2}\left[\left(\frac{11a}{2}-\frac{3m}{8}\right)\cos\alpha-3a\sin^2\alpha+\right.\right.$$

$$\text{(28)}\quad \frac{a}{2\sin(\alpha+\beta)}(4\sin^2\alpha\sin\beta+\sin\alpha\cos\alpha\cos\beta-\sin\alpha\sin\beta\cos\alpha-\cos^2\alpha\cos\beta)\ \Big]$$

$$\left.-\frac{l^2}{4}[\sin\alpha(\sin\alpha+\cos\alpha)+\operatorname{ctg}\beta\sin\alpha(\sin\alpha-\cos\alpha)+2\alpha\operatorname{ctg}\beta]-\frac{m^2\alpha\sin\alpha}{4}\right\}.$$

Per $m\to 0$ gli ostacoli diventano punti e la probabilità (28) si scrive

$$P_{\text{int}}=\frac{2\sin(\alpha+\beta)}{3a^2\alpha\sin\alpha\sin\beta}\left\{\frac{l}{2}\left[\frac{11a}{2}\cos\alpha-3a\sin^2\alpha+\frac{a}{2\sin(\alpha+\beta)}(4\sin^2\alpha\sin\beta+\right.\right.$$

$$+\sin\alpha\cos\alpha\cos\beta-\sin\alpha\sin\beta\cos\alpha-\cos^2\alpha\cos\beta)\ \Big]-\frac{\sin\alpha}{2}[\sin\alpha+\cos\alpha+$$

$$\left.+\operatorname{ctg}\beta(\sin\alpha-\cos\alpha)+2\alpha\operatorname{ctg}\beta]l^2\ \right\}$$

2 BIBLIOGRAFIA

[1] Poincarè H.: *Calcul des probabilités*, ed.2, Carrè, Paris, 1912.

[2] Stoka M.: *Probabilités géométriques de type Buffon dans le plan euclidien,* Atti Acc. Sci.Torino, T.110, pp.53-59, 1975-76.

RENDICONTI DEL CIRCOLO MATEMATICO DI PALERMO
Serie II, Suppl. 83 (2011), pp. 249-257

GEOMETRIC PROBABILITY OF THE LENGHT OF A CHORD FOR AN ARBITRARY REGULAR POLYGON

LOREDANA SORRENTI

Abstract: Let $\mathfrak{R}_a$ be the lattice of Buffon. For a "small" convex body $\mathcal{P}$ (a regular polygon with n edges) placed with random position in the Euclidean plane E_2, we give formulas for the probability p_s that $\mathcal{P}$ intercepts a line segment of length at least equal to s on a line of the lattice $\mathfrak{R}_a$. As an application we obtain the distribution of secants in $\mathcal{P}$, i.e. we determine the function F, which assigns to each real number s, the probability, that any secants in $\mathcal{P}$ has a length less or equal than s.

AMS 2000 Subject Classifications: Geometric probability, stochastic geometry, random sets and random convex sets.
AMS Classification: 60D05, 52A22.

1. Introduction

Let $\mathfrak{R}_a$ be the lattice of Buffon, s a real number. The Buffon problem of calculating the probability that a "small" convex polygon $\mathcal{P}$ in the Euclidean plane E_2 intercepts a line segment of length at least equal to s on a line of the lattice $\mathfrak{R}_a$ (strips of constant width a), has been studied for special classes of regular polygons. In particular the problem is solved if $\mathcal{P}$ is an equilateral triangle, a square, a pentagon or an hexagon, in [5], [8], [9] and [1] respectively. There exists some recent bibliography, in which, the problem is studied in case $\mathcal{P}$ is a non regular polygon, such as a non regular triangle, a rectangular trapezium or an isosceles trapezium (see [3], [4], [10]).
The purpose of this paper is to generalize the results of [5], [8], [9] and [1], considering an arbitrary "small" regular polygon of constant side placed at random on the Euclidean plane E_2 as test body.
In the Euclidean plane E_2 let $\mathfrak{R}_a$ be a lattice of parallel equidistant lines with distance a. Let $\mathcal{P}$ be a random regular polygon with constant side l, and number of edges equal to n. We say $\mathcal{P}$ is "small", in the sense given in [2], if $\frac{l}{\sin(\frac{\pi}{n})} < a$. For any fixed $0 \leq s \leq \frac{l}{\sin(\frac{\pi}{n})}$ we compute the probability p_s that $\mathcal{P}$ intercepts a line-segment of length at least equal to s on a line of the lattice $\mathfrak{R}_a$. As an application, we give a contribution to the problem

of determining the distribution function of a chord in a polygon $\mathcal{P}$, which is also studied in [6] and in [7].

2. Main Results

Let F be a strip with constant width $\frac{a}{2}$ such that one distinguished straight line g of the lattice $\mathfrak{R}_a$ is one of the two connected components of the border of F. We take F as the elementary tile of $\mathfrak{R}_a$. We assume

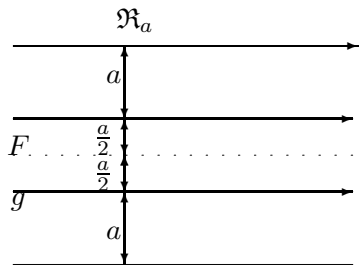

Figure 1

that the straight lines of $\mathfrak{R}_a$ and the polygon $\mathcal{P}$ to be oriented as shown in figure 2.

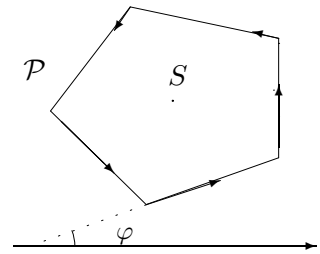

Figure 2

If the barycenter S of $\mathcal{P}$ is fixed, we obtain, for symmetry reasons, all positions of $\mathcal{P}$, with respect to $\mathcal{R}_a$, exactly once, if the angle φ between one distinguished oriented side of $\mathcal{P}$ and the direction of g varies between 0 and $\frac{\pi}{n}$. To simplify matters we call φ the angle of $\mathcal{P}$. Let from now on also $\varphi \in \left[0, \frac{\pi}{n}\right]$ be fixed. We denote by $x_s(\varphi)$ the distance between two parallel chords of $\mathcal{P}$, with length s. Obviously only the chords between these two chords have length greater or equal than s. We note that $x_s(\varphi) = 2h_s(\varphi)$, where $h_s(\varphi)$ is the distance between the barycenter S of $\mathcal{P}$ and the line g,

intercepting on $\mathcal{P}$ a chord with length s. In order to compute the desired probability p_s we use Stoka's [11] well known formula:

$$p_s = \frac{\int_0^{\pi} x_s(\varphi)\mathrm{d}\varphi}{\int_0^{\pi} a\mathrm{d}\varphi}. \tag{1}$$

Since we want to consider each possible position of $\mathcal{P}$ we should take $\varphi \in [0,\pi]$, but for the existing symmetries we can consider $\varphi \in \left[0,\frac{\pi}{n}\right]$. Then, instead of (1) we may use the following:

$$p_s = \frac{\int_0^{\frac{\pi}{n}} x_s(\varphi)\mathrm{d}\varphi}{\int_0^{\frac{\pi}{n}} a\mathrm{d}\varphi}. \tag{2}$$

In the following we compute the probability that a regular convex polygon with constant side l, and with number of edges equal to n, intersects one line segment with length at least s, where s is a real number $s \leq l$.

Theorem 1. *The probability that a random polygon $\mathcal{P}$ with constant side l and number of edges equal to n, uniformly distributed in a bounded region of the euclidian plane, intersects one line segment with length at least $s \leq l$ of the Buffon grid $\mathfrak{R}_a$ is:*

$$p_s = \frac{nl}{\pi a} - \frac{ns}{\pi a}\sin^2\frac{\pi}{n} - \frac{sn}{2\pi a}\cos\frac{2\pi}{n} + \frac{s}{a}\cot\frac{2\pi}{n}. \tag{3}$$

Proof. We note that, for $\varphi \in \left[0,\frac{\pi}{n}\right]$, $h_s(\varphi)$ is as in figure 3.

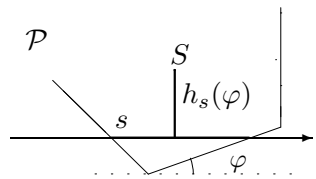

FIGURE 3

Then

$$x_s(\varphi) = 2l\sin\varphi + \frac{l}{\sin\frac{\pi}{n}}\cos\left(\frac{\pi}{n}+\varphi\right) - 2s\sin\varphi\cos\varphi + \tag{4}$$
$$+2s\sin^2\varphi\cot\frac{2\pi}{n}.$$

Therefore

$$\int_0^{\frac{\pi}{n}} x_s(\varphi)d\varphi = l - s\sin^2\frac{\pi}{n} - \frac{1}{2}\cos\frac{2\pi}{n} + \frac{s\pi}{n}\cot\frac{2\pi}{n}. \tag{5}$$

Finally, it follows from formulas (2) and (5), the desired probability (3). □

Remarks 2. **(a)** If $s = 0$ the probability p_s (that a random regular polygon of constant side l with the condition $\frac{l}{\sin\frac{\pi}{n}} < a$ intersects the lattice $\mathfrak{R}_a$) becomes $p_s = \frac{per(\mathcal{P})}{\pi a}$, where $per(\mathcal{P})$ is the perimeter of the polygon $\mathcal{P}$.

(b) If $n = 3$, then formula (3) returns Duma and Stoka's formula [5]

$$p_s = \frac{3l}{\pi a} - \frac{3s}{2\pi a} - \frac{3\sqrt{3}}{3a}, \tag{6}$$

which computes the probability that a regular triangle with side l, intersects on $\mathfrak{R}_a$ a segment with length at least s.

(c) If $n = 4$, then formula (3) returns Pettineo's formula [8]

$$p_s = \frac{4l}{\pi a} - \frac{2s}{\pi a}, \tag{7}$$

which computes the probability that a square with side l, intersects on $\mathfrak{R}_a$ a segment with length at least s, with $s \leq l$.

(d) If $n = 5$, then formula (3) returns the following formula, given by Theorem 3.1 in [9],

$$p_s = \frac{5l}{\pi a} - \frac{5s}{2\pi a} + \frac{s}{a}\frac{\sqrt{25 - 10\sqrt{5}}}{5}, \tag{8}$$

which computes the probability that a regular pentagon with side l, intersects on $\mathfrak{R}_a$ a segment with length at least s, with $s \leq l$.

(e) If $n = 6$, hen formula (3) returns Conserva and Duma's formula [1],

$$p_s = \frac{6l}{\pi a} - \frac{3s}{\pi a} + \frac{s}{a}\frac{\sqrt{3}}{3}, \tag{9}$$

which computes the probability that a regular hexagon with side l, intersects on $\mathfrak{R}_a$ a segment with length at least s, with $s \leq l$.

(f) We note that when $n \to \infty$, the side l of $\mathcal{P}$ tends to 0, $\mathcal{P}$ is a circle and $nl \to 2\pi r$, where r is the radius of $\mathcal{P}$. In such case, with the limitation given for s in Theorem 1, we obtain $s = 0$. Then

$$\begin{aligned} \lim_{n\to\infty} p_s &= \lim_{n\to\infty}\left(\frac{nl}{\pi a} - \frac{ns}{\pi a}\sin^2\frac{\pi}{n} - \frac{sn}{2\pi a}\cos\frac{2\pi}{n} + \frac{s}{a}\cot\frac{2\pi}{n}\right) = \\ &= \frac{2r}{a}, \end{aligned} \tag{10}$$

which is the probability that a circle with radius $r < \frac{a}{2}$ intersects one of the parallel lines of $\mathfrak{R}_a$.

Now we compute the probability that a regular convex polygon with constant side l, and with number of edges equal to n, intersects one line

segment with length at least s, where s is a real number $l \leq s \leq 2l\cos\frac{\pi}{n}$. If $l \leq s \leq 2l\cos\frac{\pi}{n}$, we denote by $\varphi_0 \in \left[0, \frac{\pi}{n}\right]$ the angle satisfying the following condition:

$$\sin\left(\frac{2\pi}{n} - \varphi_0\right) = \frac{l}{s}\sin\frac{2\pi}{n}. \tag{11}$$

With this notation, we obtain the following result.

Theorem 3. *The probability that a random polygon $\mathcal{P}$ with constant side l and number of edges equal to n, uniformly distributed in a bounded region of the euclidian plane, intersects one line segment with length at least $l \leq s \leq 2l\cos\frac{\pi}{n}$ of the Buffon grid $\mathfrak{R}_a$ is:*

$$\begin{aligned} p_s &= \frac{ns}{\pi a}\left(-\sin^2\frac{\pi}{n} - \frac{1}{2}\cos\frac{2\pi}{n} + \sin^2\varphi_0 + \frac{1}{2}\sin\varphi_0\cot\frac{2\pi}{n} + \right. \\ &\quad \left. -\varphi_0\cot\frac{2\pi}{n}\right) + \frac{s}{a}\cot\frac{2\pi}{n} + \frac{nl}{\pi a}\left(\cos\varphi_0 - \cot\frac{\pi}{n}\sin\varphi_0\right), \ \textit{if } \mathbf{n \leq 4}; \end{aligned} \tag{12}$$

$$\begin{aligned} p_s &= \frac{nl}{\pi a}\left(\cos\varphi_0 + \sin\varphi_0\tan\frac{2\pi}{n}\right) + \frac{sn}{\pi a}\left(\frac{1}{2}\cot\frac{4\pi}{n}\sin 2\varphi_0 + \right. \\ &\quad \left. -\sin^2\frac{\pi}{n} - \frac{1}{2}\cos\frac{2\pi}{n} + \frac{\pi}{n}\cot\frac{2\pi}{n} + \sin^2\varphi_0 - \varphi_0\csc\frac{4\pi}{n}\right), \textit{if } \mathbf{n > 4}. \end{aligned} \tag{13}$$

Proof. We first consider the case $\mathbf{n \leq 4}$.
We note that if $\varphi \in [0, \varphi_0]$, where φ_0 is the angle defined by (11), then $h_s(\varphi) = 0$. If $\varphi \in \left[\varphi_0, \frac{\pi}{n}\right]$, we have (see figure 4)

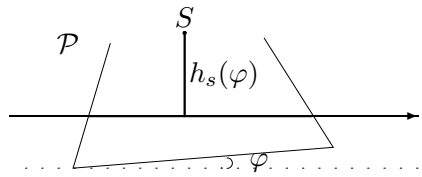

FIGURE 4

$$x_s(\varphi) = 2l\sin\varphi + \frac{l}{\sin\frac{2\pi}{n}}\cos\left(\frac{\pi}{n} + \varphi\right) 2s\sin\varphi\cos\varphi + 2s\sin^2\varphi\cot\frac{2\pi}{n}. \tag{14}$$

Thus

$$\begin{aligned}\int_0^{\frac{\pi}{n}} x_s(\varphi)\mathrm{d}\varphi &= \int_0^{\varphi_0} x_s(\varphi)\mathrm{d}\varphi + \int_{\varphi_0}^{\frac{\pi}{n}} x_s(\varphi)\mathrm{d}\varphi = \\ &= -s\sin^2\frac{\pi}{n} - \frac{1}{2}s\cos\frac{2\pi}{n} + \frac{\pi}{n}s\cot\frac{2\pi}{n} + 2l\cos\varphi_0 + s\sin^2\varphi_0 + \\ &\quad -\frac{l}{\sin\frac{\pi}{n}}\sin\left(\varphi_0+\frac{\pi}{n}\right) + \frac{1}{2}s\sin 2\varphi_0 - \varphi_0 s\cot\frac{2\pi}{n}. \qquad (15\end{aligned}$$

Then, by substituting (15) in (2), one can obtain formula (12).
Now, assume that $\mathbf{n \geq 4}$.
In this case we note that if $\varphi \in [0, \varphi_0]$, we have (see figure 5)

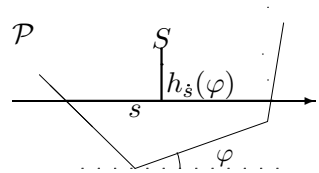

FIGURE 5

$$\begin{aligned}x_s(\varphi) &= l\cot\frac{\pi}{n}\cos\varphi + l\tan\frac{2\pi}{n}\cos\varphi - s\left(tan\frac{2\pi}{n}\cos^2\varphi + \right. \\ &\quad \left. -\cot\frac{2\pi}{n}\sin^2\varphi\right). \qquad (16)\end{aligned}$$

If $\varphi \in \left[\varphi_0, \frac{\pi}{n}\right]$, we obtain again formula (4) for $x_s(\varphi)$.
Thus

$$\begin{aligned}\int_0^{\frac{\pi}{n}} x_s(\varphi)\mathrm{d}\varphi &= \int_0^{\varphi_0} x_s(\varphi)\mathrm{d}\varphi + \int_{\varphi_0}^{\frac{\pi}{n}} x_s(\varphi)\mathrm{d}\varphi = \\ &= \frac{s}{2}\sin\varphi_0\cos\varphi_0\cot\left(\frac{2\pi}{n}\right) + \frac{s\pi}{n}\cot\left(\frac{2\pi}{n}\right) + \\ &- \frac{s\varphi_0}{2}\cot\left(\frac{2\pi}{n}\right) - \frac{s}{2}\sin\varphi_0\cos\varphi_0\tan\left(\frac{2\pi}{n}\right) + \\ &- \frac{s\varphi_0}{2}\tan\left(\frac{2\pi}{n}\right) - l\sin\varphi_0\tan\left(\frac{2\pi}{n}\right) + l\sin\varphi_0\cot\left(\frac{\pi}{n}\right) + \\ &+ l\cos\varphi_0 + s\sin^2(\varphi_0) - \frac{s}{2}. \qquad (17)\end{aligned}$$

Then, by substituting formula (17) in (2), one can obtain formula (13).
□

Remarks 4. **(a)** If $s = l$ then $\varphi_0 = 0$ and formulas (12), (13) and (2) coincide.

(b) If $n = 4$ then, it follows from formula 12 that $\varphi_0 = \arccos\left(\frac{l}{s}\right)$ and

$$p_s = \frac{2s}{\pi a} - \frac{4l\sin\varphi_0}{\pi a},$$

which is Pettineo's formula [8] which computes the probability that a square with side l, intersects on $\mathfrak{R}_a$ a segment with length at least s, with $l \leq s \leq l\sqrt{2}$.

(c) If $n = 6$ then formula 13 returns Conserva and Duma's formula [1],

$$p_s = \frac{12}{\pi a}\left[l\sin\left(\varphi_0 + \frac{\pi}{6}\right) + \frac{s}{2\sqrt{3}}\left(\frac{\pi}{6} - 2\varphi_0\right) - \frac{s}{2\sqrt{3}}\cos\left(\frac{\pi}{6} - 2\varphi_0\right)\right],$$

which computes the probability that a regular hexagon with side l, intersects on $\mathfrak{R}_a$ a segment with length at least s, with $l \leq s \leq l\sqrt{3}$.

(d) We note that when $n \to \infty$, the side l of $\mathcal{P}$ tends to 0, $\mathcal{P}$ is a circle and $nl \to 2\pi r$, where r is the radius of $\mathcal{P}$. In such case, with the limitation given for s in Theorem 3, we obtain $s = 0$. Then

$$\begin{aligned}\lim_{n\to\infty} p_s &= \lim_{n\to\infty}\left[\frac{nl}{\pi a}\left(\cos\varphi_0 + \sin\varphi_0\tan\frac{2\pi}{n}\right) + \right. \\ &\quad \frac{sn}{\pi a}\left(\frac{1}{2}\cot\frac{4\pi}{n}\sin 2\varphi_0 - \sin^2\frac{\pi}{n} - \frac{1}{2}\cos\frac{2\pi}{n} + \right. \\ &\quad \left.\left. + \frac{\pi}{n}\cot\frac{2\pi}{n} + \sin^2\varphi_0 - \varphi_0\csc\frac{4\pi}{n}\right)\right] \\ &= \frac{2r}{a}\end{aligned} \tag{18}$$

which is the probability that a circle with radius $r < \frac{a}{2}$ intersects one of the parallel lines of $\mathfrak{R}_a$.

3. The distribution of secants in $\mathcal{P}$

The distribution function F of the chord in the polygon $\mathcal{P}$, assigns to each $s \in [0, l]$ the probability that an arbitrary chord in $\mathcal{P}$ has a length less or equal than s and it is defined as follows:

$$F(s) = 1 - \frac{p_s}{p_0}. \tag{19}$$

As a consequence of Theorem 1 and Theorem 3 we obtain the following.

Corollary 5. *The distribution function of the chord of the polygon $\mathcal{P}$, which assigns to each $s \in \left[0, 2l\cos\frac{\pi}{n}\right]$ the probability that an arbitrary chord*

in $\mathcal{P}$ has a length less or equal than s is given by:

$$
\begin{aligned}
F(s) = \quad & \tfrac{s}{l}\sin^2\tfrac{\pi}{n} + \tfrac{s}{l}\cos\tfrac{2\pi}{n} - \tfrac{s\pi}{nl}\cot\tfrac{2\pi}{n}, && \text{if } s \le l;\\
F(s) = \quad & \tfrac{1}{4ln\cos\frac{\pi}{n}\sin\left(\varphi_0+\frac{\pi}{n}\right)}\left(ns\sin\tfrac{2\pi}{n}\cos 2\varphi_0 + \right.\\
& -(2n\varphi_0 - 2\pi)\cos\tfrac{2\pi}{n} + \\
& \left. +n\sin\varphi_0\cos\tfrac{2\pi}{n}\right), && \text{if } l \le s \le 2l\cos\frac{\pi}{n}, n \le 4;\\
F(s) = \quad & \tfrac{-s}{l\left(\cos\varphi_0+\sin\varphi_0\tan\frac{2\pi}{n}\right)}\left(\tfrac{1}{2}\cot\tfrac{4\pi}{n}\sin 2\varphi_0 + \right.\\
& -\sin^2\tfrac{\pi}{n} - \tfrac{1}{2}\cos\tfrac{2\pi}{n} + \tfrac{\pi}{n}\cot\tfrac{2\pi}{n} + \\
& \left. +\sin^2\varphi_0 - \varphi_0\csc\tfrac{4\pi}{n}\right), && \text{if } l \le s \le 2l\cos\frac{\pi}{n}, n > 4.
\end{aligned}
$$

Proof. The assertion follows from (19), Theorem 1 and Theorem 3. □

We note that the function F does not depend on the distance a between two lines of the lattice $\mathfrak{R}_a$ The density $f = F'$ of the distribution of the chord is a constant function in case $s \le l$ (Theorem 1), but it is not a constant function in case $l < s \le 2l\cos\frac{\pi}{n}$ (Theorem 3), since φ_0 is a non linear function of s.

References

[1] V. Conserva and A. Duma, *Intersections of a "small" convex body in a plane lattice*, Suppl. Rend. Circ. Mat. Palermo, Serie II, 80, 2008, pp. 75-82.

[2] A. Duma, *Problems of Buffon tye for "non small" needles*, Rend. Circ. Mat. Palermo, Serie II, Tomo XLVIII, 1999, pp. 23-40.

[3] A. Duma and S. Rizzo, *Chord lenght distribution function for an arbitrary triangle*, Suppl. Rend. Circ. Mat. Palermo, Serie II, 81, 2009, pp. 141-157.

[4] A.Duma and S. Rizzo, *La funzione di distribuzione di una corda su un trapezio rettangolo*, Preprint 2010.

[5] A. Duma and M. Stoka, *Schnitte eines "kleinen" gleichseitigen Dreiecks mit den Gittern von Buffon und Laplace*, Seminarberichte der Fernuniversität, pp. 13-22.

[6] H. S. Harutyunyan and V. K. Ohanyan, *The chord length distribution function for regular polygons*, Adv. in Appl. Probab., 41, 2 (2009), pp. 358-366.

[7] W. Gille, N. G. Aharonyan and H. S. Harutyunyan, *Chord length distribution of pentagonal and hexagonal rods: relation to small-angle scattering*, J. Appl. Cryst., 42,(2009), pp. 326-328.

[8] M. Pettineo, *Geometric probability problems for Buffon and Laplace grid*, Suppl. Rend. Circ. Mat. Palermo, Serie II, 80, 2008, pp. 267-274.

[9] L. Sorrenti, *On some geometric and algebraic models for image analysis*, Communications in Applied and Industrial Mathematics, DOI: 10.1685/2010CAIM484, ISSN 2038-0909, 1, 2010, pp. 225-236.

[10] L. Sorrenti, *Chord lenght distribution functions for an isosceles trapezium*, Preprint 2010.

[11] M. Stoka, *Probabilités géometriqués de type "Buffon" dans le plan euclidien*, Atti Acc. Sci. Torino, 110, pp. 53-59, 1975-76.

Università degli Studi Mediterranea di Reggio Calabria, DIMET, Facoltà di Ingegneria Via Graziella, Feo di Vito, 89100, Reggio Calabria, Italy, loredana.sorrenti@unirc.it

RENDICONTI DEL CIRCOLO MATEMATICO DI PALERMO
Serie II, Suppl. 83 (2011), pp. 259-267

ANALYSIS OF THE CPPI STRATEGY FOR INDEX PORTFOLIO AT THE WARSAW STOCK EXCHANGE

TOMASZ WĘGRZYN
University of Economics in Katowice
Department of Applied Mathematics

Abstract. The constant proportion portfolio insurance (CPPI) strategy is one of the strategies the main aim of which is to protect the minimum value of the investor's portfolio. That strategy is one of the active strategies – each changing in prices causes modifications in the portfolio structure. The CPPI strategy is used by some mutual funds that operate at the Polish stock market. It is important to check if that strategy is efficient in the Polish market in a long time. It will be checked after implementing the CPPI strategy to the portfolio of the WIG20 index.

Key words: CPPI strategy, Warsaw Stock Exchange, portfolio management, portfolio efficiency

1. The constant proportion portfolio insurance strategy.

The CPPI strategy is one of the portfolio insurance strategies. The main aim of the portfolio insurance strategies is to protect the minimum value of the investor's portfolio. Description of the CPPI strategy can be found in articles: F.Black, R.Jones (1987), F.Black, R.Jones (1988), A.F.Perold, W.F.Sharpe (1988), R.R.Trippi, R.B.Harriff (1991). The main aim of the CPPI strategy is to protect a value of the portfolio against the decrease under the floor value. The floor value of the portfolio is set by the manager and is less than the initial value of the portfolio. The floor value can increase at the interest rate over time.

In order to achieve the aim of the strategy, the portfolio is divided into two parts. One part is invested in active assets, while the second part is invested in reserve assets. The active assets, which are usually stocks, put risk into the portfolio. The reserve assets, which are usually T-bills or bonds, protect value of the portfolio at the level of the floor.

Definition of key concepts:

F - floor – the lowest value of the portfolio,

m - multiplier – set by investor, it determines the part of the portfolio invested in active assets,

c - cushion – a portfolio value minus the floor,

e - exposure – a part of the portfolio invested in active assets,

t - tolerance – a percentage change of the active assets that triggers the trade,

l - limit – a minimum part of the portfolio invested in active assets.

In order to calculate the exposure it is used as follows:

$$e = m \cdot c = m \cdot \left(portfolio - f \right) \tag{1}$$

If the value of active assets increases, the value of the portfolio also increases and it means that the cushion increases as well. As the result, the exposure grows (because of the multiplier) and more active assets are bought into the portfolio. The final result of the active assets' growth is a rise of the portfolio's risk.

If the value of active assets decreases, the value of the portfolio also falls, the difference between portfolio value and the floor declines and it means that the cushion also decreases. As the result, the exposure falls (because of the multiplier) and some active assets are sold. The final result of the active assets' fall is a decrease of the portfolio's risk. The lower value of cushion means the lower level of risk in portfolio. If the value of portfolio is less or equal to the floor then there is no active assets in portfolio and the risk of the portfolio is zero.

2. Portfolio management performance tools.

W.F. Sharpe (1966) introduced ratio in order to analyse the portfolio management performance. That ratio is usually commonly known as the Sharpe ratio. The Sharpe ratio measures the excess return compared to the total risk. It presents the return per unit of risk. It is defined as:

$$SR_P = \frac{E(R_P) - R_f}{D(R_P)} \tag{2}$$

R_F – risk-free rate,
$E(R_p)$ – average return rate on the portfolio,
$D(R_p)$ – standard deviation of return rate (volatility).

Implementing the CPPI strategy means that the exposure to the market risk of the portfolio is varying during the time. It is important to test hypothesis that the CPPI strategy allows to anticipate the stock market movements. In order to examine if an investor has an ability to implement market timing strategy, J.L.Treynor, K.K.Mazuy (1966) and R.C.Merton, R.D.Henriksson (1981) developed their models.

The Treynor-Mazuy model is defined as follows:

$$R_{pt} - R_{Ft} = \alpha + \beta_p (R_{Mt} - R_{Ft}) + \delta_p (R_{Mt} - R_{Ft})^2 + \varepsilon \tag{3}$$

α – intercept,
β_p – coefficient beta – denotes level of the systematic risk,
δ_p – coefficient delta – measures an ability to implement market timing strategy,
R_{Pt} – the portfolio return for the period studied,
R_{Mt} – market return for the period studied,
R_{Ft} – risk-free rate,
ε – disturbance term.

The α, β_p, δ_p coefficients are estimated by the least square method. The coefficient α measures the share of additional return that is due to

the manager's choices. The coefficient β_p denotes exposure to the market risk. The coefficient δ_p measures manager's ability to implement a market timing strategy. If δ_p is positive and significantly different from zero, then it can be concluded that the manager has successfully practised the market timing strategy.

The Hendriksson-Merton model is formulated as follows:

$$R_{pt} - R_{Ft} = \alpha + \beta_1 \cdot (R_{Mt} - R_{Ft}) + \beta_2 \cdot y \cdot (R_{Mt} - R_{Ft}) + \varepsilon \tag{4}$$

where

$$y = \begin{cases} 0 & if \quad R_{Mt} > R_{Ft} \\ -1 & if \quad R_{Mt} < R_{Ft} \end{cases} \tag{5}$$

α – intercept,
β_1 – coefficient beta 1,
β – coefficient beta 2,
R_{Pt} – the portfolio return for the period studied,
R_{Mt} – the market return for the period studied,
R_{Ft} – risk-free rate,
ε – disturbance term.

The α, β_1, β_2 coefficients are estimated by the least square method. The coefficient α measures the share of additional return that is due to the manager's choices. The coefficient β_1 denotes exposure to market risk when the market return is higher than the risk-free rate. The coefficient β_2 measures manager's ability to implement the market timing strategy. If β_2 is positive and significantly different from zero, then it can be concluded that the manager has successfully practised the market timing strategy.

3. Assumptions and data.

The study examines the implementation of the CPPI strategy to the portfolio of the WIG20 index during the period from 20th December 2004 to 31st August 2010. During that time, it can be

observed a bull market up to the end of the October 2007 and the fall in the market up to the end of February 2009.

The WIG20 index is the index from the Polish Stock Exchange in Warsaw. That index is dedicated for the biggest and the most liquid companies. The portfolio of the index is verified on the third Friday of March, June, September, December. It is assumed that one possesses the portfolio worth 4 mln PLN (about 1 mln €) invested in the WIG20 index and follows the CPPI strategy.

The parameters of the CPPI strategy:

f – floor – 90% of the portfolio value, established on the third Friday of each December[1], constant during the year,

m – multiplier – two,

t – tolerance – zero – trades each session,

l – limit – 0.

The most important parameter of the CPPI strategy is the floor. The floor is set at the 90% of the portfolio value on the third Friday of December. Next the floor is constant during the whole year, until the next third Friday of December.

Brokers commissions and fees: 0,40% of the transaction for each stock.

The risk-free rate is equal to the 90% of the WIBID ON[2]. The cash achieved from selling stocks is invested with the risk-free rate.

4. Performance analysis.

The figure 1 presents cumulated return rates achieved from such portfolios:

- the CPPI portfolio - portfolio that follows the CPPI strategy,
- the WIG20 portfolio - portfolio that contains stocks from index WIG20,
- the cash portfolio - portfolio that contains cash,
- the stock20% portfolio - portfolio that contains 80% cash and 20% stocks from index WIG20.

[1] That is the date of the WIG20 index verification.
[2] Warsaw Interbank Bid Rate Over Night

Figure 1. The cumulated return rates for the CPPI portfolio, the WIG20 portfolio, the cash portfolio and the stock20% portfolio.

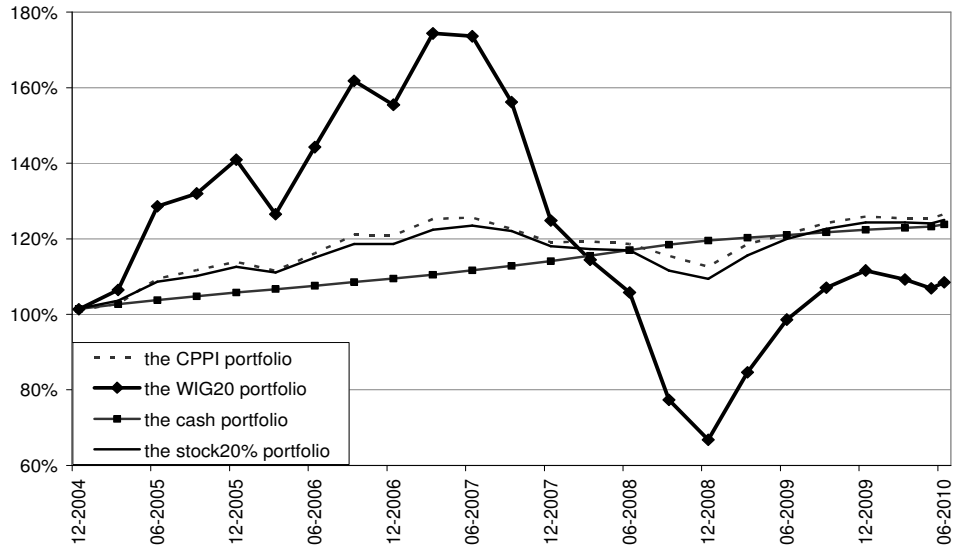

Source: own work.

As it can be noticed, until June 2007 the value of the WIG20 portfolio exceeds value of other portfolios. However, at the end of the analysed period, it is the WIG20 portfolio which is at the lowest value. Moreover, the CPPI portfolio and the stock20% portfolio behave very similar, but the cumulated return rate is always higher for the CPPI portfolio. During the whole period of the analysis, it can be seen that the CPPI portfolio and the stock20% portfolio usually outperform the cash portfolio with an exception of the period between September 2008 and September 2009.

In the table 1, the average daily rates, the standard deviations for daily rates and the Sharpe ratios for analysed portfolios are presented. As it can be noticed, the average daily rate is the highest for the WIG20 portfolio, while other portfolios have almost the same average daily rate. However, the average daily rate for the CPPI portfolio is higher than it is for the stock20% portfolio and it is significant under the null hypothesis. As the table 1 presents, standard deviation for daily rates is the highest for the WIG20 portfolio. The standard deviation for daily rates is almost the same for the CPPI portfolio and

the stock20% portfolio. However, it is lower for the CPPI portfolio than for the shares 20% portfolio and it is significant under the null hypothesis.

Table 1. Performances of analysed portfolios.

	Cumulated return rate	Average return rate	Standard deviation	Sharpe ratio
The CPPI portfolio	26,67%	0,017%	0,00337	0,62%
The WIG20 portfolio	8,46%	0,021%	0,01749	0,35%
The stock20% portfolio	25,00%	0,016%	0,00350	0,37%
The cash portfolio	23,23%	0,015%	0,00010	-

Source: own work.

In order to evaluate the achieved results, the Sharpe ratio was calculated. As the table 1 presents, it is the highest for the CPPI portfolio and almost equal for the WIG20 portfolio and the stock20% portfolio. Moreover, the Sharpe ratio is more than 50% higher for the CPPI portfolio than for any other analysed portfolios. It means that the CPPI portfolio is more efficient than any other analysed portfolio from that point of view. Furthermore, the cumulated rate of return is highest for the CPPI portfolio. The stock20 % portfolio gives almost the same cumulated rate of return as the cash portfolio. The WIG20 portfolio gives about 3 times lower cumulated rate of return than other analysed portfolios.

The coefficients of the Treynor-Mazuy model were estimated by the least square method and they are as follows:

$$\underset{}{R_{pt} - R_{Ft} =} \underset{(0,060)}{0,08} \underset{(0,002)}{+ 0,2 \cdot (R_{Mt} - R_{Ft})} \underset{(0,00004)}{- 0,000012 \cdot (R_{Mt} - R_{Ft})^2}$$

There are errors under each coefficient. It indicates, that δ_p is insufficiently different from zero. It means that under the CPPI strategy the market timing is not practised successfully. Moreover, β_p is sufficiently different from zero. It indicates that the average amount of stocks in the portfolio was about 20% during the whole analysed

period. It indicates that the stock20% portfolio is a good benchmark for the CPPI portfolio.

The coefficients of the Hendriksson-Merton model were estimated by the least square method and they are as follows:

$$\begin{array}{cccc} R_{pt} - R_{Ft} = & 0{,}01 & +0{,}2 \cdot \left(R_{Mt} - R_{Ft}\right) & -0{,}00003 \cdot y \cdot \left(R_{Mt} - R_{Ft}\right) \\ & (0{,}006) & (0{,}004) & (0{,}00005) \end{array}$$

There are errors under each coefficient. The coefficient β_1 is sufficiently different from zero. It indicates that the average amount of stocks in the portfolio was about 20% during the whole study. However, the coefficient β_2 is insufficiently different from zero. It means that under the CPPI strategy the market timing is not practised successfully.

Both the Treynor-Mazuy model and the Hendriksson-Merton model show that under the CPPI strategy the exposure to the market risk is not adapted in advance but after changes in the market prices. It means that under the CPPI strategy the market timing is not practised successfully. It indicates that there is no evidence that there are series in market return rates (plus or minus return rates).

5. Conclusions.

The CPPI strategy is analysed in this article. The analysis of the return rates indicates that implementing the CPPI strategy allows statistically significant reduction in the risk at the portfolio in comparison to the portfolio that contains constant mix of cash and stocks (the stock20% portfolio). The Sharpe ratio indicates that the CPPI portfolio is more efficient than other analysed portfolios.

Both the Treynor-Mazuy model and the Hendriksson-Merton model indicate that the average amount of stocks in the portfolio was about 20% during the whole analysed period. It means that the stock20% portfolio is a good benchmark for the CPPI portfolio. The models also indicate that under the CPPI strategy the market timing is not practiced successfully. It indicates that there is no evidence that there are series in market return rates (plus or minus return rates), because the exposure to the market risk is not adapted in advance but after changes in the market prices.

References.

1. Black F., Jones R.: Simplifying portfolio insurance, Journal of Portfolio Management, New York, Fall 1987, vol. 14, iss. 1, p 48
2. Black F., Jones R.: Simplifying portfolio insurance for corporate pension plans, Journal of Portfolio Management, New York, Summer 1988, vol. 14, iss. 4, p 33
3. Henriksson R.D., Merton R.C.: On market timing and investment performance II, Journal of Business, October 1981, vol. 54, iss. 4, p. 513
4. Perold A.F., Sharpe W.F.: Dynamic strategies for asset allocation, Financial Analysts Journal, January/February 1988, vol. 44, iss. 1, p 16
5. Treynor J.L., Mazuy K.K.: Can mutual funds outguess the market?, Harvard Business Review, July/August 1966, vol. 44, iss. 4, p. 131
6. Trippi R.R., Harriff R.B: Dynamic asset allocation rules: survey and synthesis, Journal of Portfolio Management, New York, Summer 1991, vol. 17, iss. 4, p 19
7. Sharpe W.F.: Mutual fund performance, Journal of Business, January 1966, vol. 39, iss. 1, p 119

RENDICONTI DEL CIRCOLO MATEMATICO DI PALERMO
Serie II, Suppl. 83 (2011), pp. 269-278

USE OF ALTERNATIVE LINK FUNCTIONS IN REGRESSION MODELS FOR ORDINAL RESPONSE VARIABLES: AN APPLICATION TO THE CUSTOMER SATISFACTION MEASUREMENT IN A SAMPLE OF FITNESS CENTERS IN MESSINA[1]

AGATA ZIRILLI - ANGELA ALIBRANDI

1. Introduction.

Customer satisfaction measurement can be defined as a methodology that relates the level of perception of a service (or product) with the level of expectations for that service (or product). The identification of customer satisfaction by business or government allows the relationship with users in order to understand their needs and expectations and, therefore, to redesign the policies and the system of service delivery. The measure of customer satisfaction is a relatively new concept for many companies whose interest, until recently, was addressed only to the data of income and assets. Now the global economy has changed some sceneries and the key to this change is just customer satisfaction. In this work the attention has been paid to customer satisfaction measurement in fitness centers, by virtue of the growing interest that people have toward their bodies. It is well known, in fact, that a regular physical activity of moderate intensity

[1] This note, though it is the result of a close collaboration, was specifically elaborated as follows: paragraphs 1, 2 and 5 by A. Zirilli and paragraphs 3 and 4 by A. Alibrandi

supports a healthy lifestyle, with remarkable health benefits of the whole person. In such context the statistical analysis aims to quantify the incidence of these factors, responsible of variations of the global satisfaction level and to verify, through the use of opportune models, the possible dependence from other variables.

Our goal is twofold: firstly, we propose to compare models with different link function to assess which of these lead to a better fit to data, on the other hand, we are interested into check the possible dependence of the customer satisfaction degree from some factors considered as potential predictors.

2. Modeling ordinal response.

The models for ordinal response variables were designed to analyze individual choices that led to high satisfaction levels; in fact, in social reality, the individual often must make the choice between alternatives and, in this approach, the individual sphere becomes more important than the temporal dimension in which the choices are employed.

In this class of models, the used categories are ordered and aimed to measure customer satisfaction (Lawson and Montgomery, 2006) or evaluation of services (Bogani, 2001; Giarelli , 2002).

The response variable is an ordinal variable with 4 categories; for this reason we estimated a regression model for ordinal data. The regression models for ordinal response variables are frequently used in the social sciences, in order to estimate the influence of one or more explanatory variables on the response probability (Agresti, 2002)

Let be Y an ordinal variable with J ordered categories $(y_1<y_2<\ldots<y_J)$ with $P(Y=j)=\pi_j$ and let be $\boldsymbol{x}$ a vector of K explicative variables.

Some regression models for ordinal variable don't require to assign scores to the categories; they use the ordering of Y variable modes, modeling the cumulative probabilities:

$$P(Y\leq j)=\Pi_j=\pi_1+\ldots+\pi_j$$

by a cumulative link model

$$\text{link}\,(\Pi_j)=\beta_{0j}+\boldsymbol{x}^T\boldsymbol{\beta}=\eta_j \qquad j=1,2,\ldots,J\text{-}1 \tag{1}$$

where link(·) is the known link function (Agresti, 1990). Often the researcher does not pay attention to the choice of link function to be used to specify the model; this choice becomes important to optimize the estimated model, instead. In this paper we estimated models with different link functions, to assess which among these better fit the data. The used link functions are the following:

$$\frac{\exp\{\eta\}}{1+\exp\{\eta\}} \tag{2}$$

$$\Phi\{\eta\} \tag{3}$$

$$1\text{-}\exp\{\text{-}\exp\{\eta\}\} \tag{4}$$

$$\int_{\eta} fCauchy(y)dy \tag{5}$$

where $f\,Cauchy(\cdot)$ is the Cauchy density.

We assumed that the observations $\{n_{kj}\}$ are organized in a $k \times J$ matrix, i.e. K conditioned multinomial distributions with J categories; the log-likelihood can be expressed as:

$$\ell(\theta) = \sum_{j}^{J}\sum_{k}^{K} n_{jk}\log(\pi_{jk}) \tag{6}$$

where $\boldsymbol{\theta}=(\alpha_{0j}, \beta^{T})^{T}$ is the parameters vector in the model, and

$$\pi_{j} = \Pi_{j} - \Pi_{j-1} \tag{7}$$

where $\Pi_j=\text{link}^{-1}(\eta_j)$ comes from the cumulative link model, with appropriate link function (Muggeo and Aiello, 2008). As is well known, the parameters are estimated by maximizing the likelihood, i.e.

$$\hat{\theta} = \arg\max \ell(\theta) \tag{8}$$

3. The data.

In this paper the data are derived from responses to a questionnaire. The sample consists of 138 subjects attending a gym in Messina city. The questionnaire was designed to measure the satisfaction level of these users towards the services provided by various gyms.

Each subject gave its agreement with reference to each item, on an ordinal scale consisting of four levels.

The survey was performed in the period June - July. Data were collected on the field by the administration of the questionnaire, distributed according to the technique of cluster sampling. Although this technique involves a higher sampling error than other techniques of randomization, its adoption is justified by the considerable savings in terms of time/ cost.

The questionnaire was structured into sections:

– an introductory registry section to obtain basic information on gender and age of the interviewee;

– a section where the respondent is asked to express a personal opinion about the indicators of interest (instructors professionalism, spaciousness and cleanliness of the fitness rooms, usability of the toilets, service cost, availability of equipment) according to an ordinal growing scale and, finally, an indication of the time taken to go to the gym;

– a section relative to the perceived inconvenience (expressed in presence or absence terms) in relation to noise, disorganization, waiting to use equipment, supportability of temperature within the fitness rooms and crowding of the halls;

– finally an overall judgment was required relatively to the services offered by the frequented gym, expressed, as already mentioned, in four satisfaction levels.

In Figure 1 we show the satisfaction mean levels of the examined subjects with reference to the six indicators.

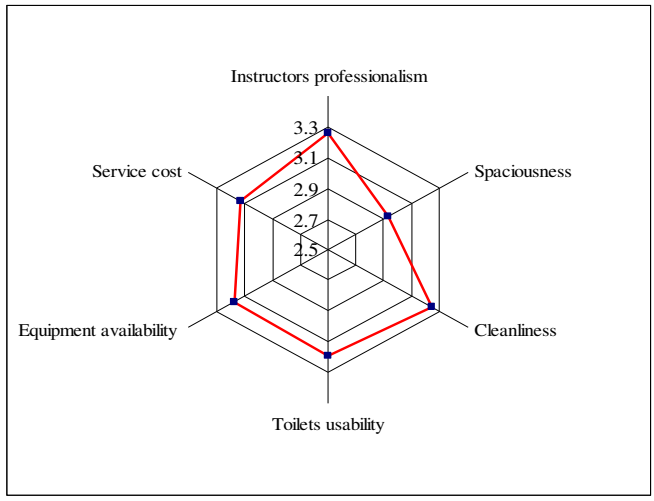

Figure 1 – Satisfaction mean level for indicators

Table 1: Frequencies of bivariate distributions of categorical variables for response levels

		Response Levels				
Factors		***1***	***2***	***3***	***4***	**Total**
Sex	M	10 (*7,2*)	18 (*13,0*)	38 (*27,5*)	24 (*17,4*)	**90 (*65,2*)**
	F	1 (*0,07*)	5 (*3,6*)	21 (*15,2*)	21 (*15,2*)	**48 (*34,8*)**
Age	≤25	6 (*4,3*)	11 (*8,0*)	26 (*18,8*)	16 (*11,6*)	**59 (*42,8*)**
	25-35	4 (*2,9*)	5 (*3,6*)	17 (*12,3*)	14 (*10,1*)	**40 (*29,0*)**
	>35	1 (*0,7*)	7 (*5,1*)	16 (*11,6*)	15 (*10,9*)	**39 (*28,2*)**
Weekly training	≤3	7 (*5,1*)	16 (*11,6*)	29 (*21,0*)	29 (*21,0*)	**81 (*58,7*)**
	>3	4 (*2,9*)	7 (*5,1*)	30 (*21,7*)	16 (*11,6*)	**57 (*41,3*)**
Course attendance	Yes	5 (*3,6*)	9 (*6,5*)	29 (*21,0*)	30 (*21,7*)	**73 (*52,9*)**
	No	6 (*4,3*)	14 (*10,1*)	30 (*21,7*)	15 (*10,9*)	**65 (*47,1*)**

As we can see, the highest mean levels of satisfaction are found for "instructors professionalism" and "cleanliness"; the lowest satisfaction, however, is referred to the "spaciousness".

Table 1 shows the observed frequencies of the bivariate distributions of answer variable for each categorical variables; the "age" has been categorized in classes.

In general, we note that the satisfaction assessments (3 and 4 response levels) are more numerous than the dissatisfaction assessments (1 and 2 response levels). In particular, the most satisfied subjects are male and aged less than 25 years.

4. Comparison among models with different link functions

We estimated models with different link functions to assess which of these is the best. Thus the description of the observed variability in ordinal responses also allowed to define the user's profile. Table 2 shows the parameter estimations (coefficient, standard error and relative p-value) obtained from models with different link functions. Moreover for each model we reported the Log-Likelihood value (ℓ) and the Log-likelihood ratio test (LR) with relative p-value.

We investigated the existence of possible interactions between the regressors, but in any case there were significant estimates of these effects, at the prefixed significance level (α=0.05).

By examining the results we can see that the *probit* is the link function that ensures a higher likelihood value (ℓ = -89.695), followed by *logit* (ℓ= - 90.267). This consideration allows the identification of this model as the best.

By the estimated models we can identify some statistically significant explanatory variables at the prefixed significance level. In particular we can see that customer satisfaction is significantly dependent on the spaciousness of the rooms, the service cost, the equipment availability and the toilets quality; also the low waiting times to use the equipment and the temperature tolerability appear to be significant factors on overall satisfaction; other factors result irrelevant.

Table 2: Parameter estimations obtained from models with different link functions

	Logit			***Probit***		
Factors	Est.	S.E	p	Est.	S.E.	p
Age	0.027	0.02	0.168	0.218	0.15	0.150
[Sex=M]*	-0.540	0.45	0.233	-0.280	0.25	0.259
Spaciousness	1.490	0.46	**0.001**	0.808	0.25	**0.001**
Toilets usability	0.972	0.36	**0.007**	0.597	0.20	**0.003**
Cleanliness	0.402	0.46	0.380	0.166	0.26	0.517
Equip. availab.	0.962	0.41	**0.018**	0.550	0.23	**0.015**
Service cost	1.907	0.39	**0.000**	1.071	0.21	**0.000**
Time to reach gym	0.100	0.25	0.685	0.048	0.14	0.731
[Noice =No]	1.407	1.32	0.287	0.713	0.76	0.349
[Disorganiz.=No]	1.800	1.40	0.199	0.950	0.79	0.228
[Waiting time=No]	1.965	0.79	**0.012**	1.220	0.47	**0.010**
[Temp. Supp.=No]	1.655	0.63	**0.008**	0.993	0.36	**0.006**
[Crowding=No]	0.353	0.61	0.561	0.211	0.34	0.534
LR test	158.652		**0.000**	159.797		**0.000**
ℓ	-90.267			-89.695		
	C-log-log			***Cauchy***		
Age	0.017	0.02	0.201	0.027	0.20	0.173
[Sex=M]	-0.573	0.29	0.051	-0.540	0.46	0.235
Spaciousness	1.205	0.32	**0.000**	1.490	0.47	**0.001**
Toilets usability	0.741	0.23	**0.001**	0.971	0.36	**0.008**
Cleanliness	0.162	0.30	0.586	0.402	0.46	0.380
Equip. availab.	0.653	0.26	**0.013**	0.962	0.41	**0.018**
Service cost	1.480	0.27	**0.000**	1.907	0.39	**0.000**
Time to reach gym	0.070	0.17	0.672	0.100	0.25	0.691
[Noice =No]	1.153	0.86	0.180	1.407	1.37	0.303
[Disorganiz.=No]	1.460	0.93	0.114	1.800	1.40	0.200
[Waiting time=No]	1.507	0.53	**0.004**	1.965	0.81	**0.016**
[Temp. Supp.=No]	1.320	0.40	**0.001**	1.655	0.64	**0.010**
[Crowding=No]	0.243	0.38	0.526	0.353	0.61	0.563
LR test	156.109		**0.000**	158.625		**0.000**
ℓ	-91.539			-90.287		

In brackets [ ] we reported the categorical variables; as it is known, for this kind of variable the model estimates only the coefficients associated with n-1 modes.

Finally, for only the "best" model, i.e. *probit model*, for the each variable we reported the exponential parameters estimation (OR) and related confidence interval (C.I.) at 95% significance level (Table 3).

Table 3 - Exponential parameters estimation and C.I.

Factors	OR	C.I. (95%)	
		Inf.	Sup.
Age	1.244	0.924	1.675
[Sex=M]	0.756	0.465	1.229
Spaciousness *	2.244	1.367	3.685
Toilets usability *	1.817	1.220	2.707
Cleanliness	1.180	0.715	1.947
Equipment availability *	1.733	1.113	2.699
Service cost *	2.918	1.926	4.420
Time to reach the gym	1.049	0.797	1.381
[Noice =No]	2.041	0.458	9.087
[Disorganization=No]	2.585	0.552	12.105
[Waiting time=No] *	3.387	1.344	8.534
[Temper. Supportability=No] *	2.698	1.326	5.489
[Crowding=No]	1.234	0.635	2.398

In brackets [ ] we reported the categorical variables; with * we indicated the significant parameters

In particular, if we focus our attention on the significant parameters (pointed by an asterisk), we can identify variables that determine a higher risk of dissatisfaction. In particular, based on descending values of OR, we can draw up the «importance ordering» of these variables: "waiting time" is the first variable that characterizes the satisfaction/dissatisfaction, followed by "service cost" and "temperature supportability". The significant variable that less influences the satisfaction/dissatisfaction level is, however, the equipment availability.

5. Final remarks.

Gyms examined in the statistical survey involving mostly individuals, aged between 20 and 29 years, mostly students; the main causes which give rise to interest in fitness practice is due to maintain physical fitness and stress disposal, the need to treat its appearance and the health care. Respondents demonstrate a frequent participation in the service, but this participation may, however, be discouraged by the existence of discomfort, particularly from overcrowding and the temperature in the fitness rooms. Furthermore, respondents expressed their preference related to the kind of payment and, consequently, to the service costs. In general, focusing our attention on the examined variables, we can affirm that the statistical analysis showed a significant link between customer satisfaction and toilets quality, spaciousness of rooms, equipment availability and service costs; it was not possible, however, appreciate a significant change in satisfaction according to assessments made on other indicators. The more perceived inconveniences are the waiting time and the temperature inside the fitness rooms; the absence of such discomforts involves the achievement of high standards of satisfaction

As is known, the most used test to verify the estimated model is the *Likelihood Ratio test*: it is distributed as a chi-square random variable: we accept the estimated model if LR is very high and its P-value is very small, considering the relative degrees of freedom.

Regarding the comparison between models for ordinal response variables, with different link function, all estimated models are significant; but the *probit* link function (followed by *logit*) provides the best results with regard to *Likelihood*, although the differences are minimal compared to other models.

In both models, the independent variables are presumed to affect the satisfaction/dissatisfaction level and represent a priori beliefs about the causal or associative elements important in the expressed ordinal opinion. In the case of ordinal scale variables, an ordered *logit* or *probit* model have the advantage of the additional information provided by the ordinal over the nominal scale. The choice between a *logit* or *probit* depends only on practical reasons because there aren't theoretical reasons for choice (Amemiya, 1981) and in different applications substantive differences between the two models are not highlighted.

References.

Agresti A., 1990. Categorical Data Analysis, Wiley.

Agresti A. 2002, Categorical data analysis (2nd edition). New York: Wiley.

Amemiya, T., 1981, Qualitative response models: a survey, Journal of Economic Literature 19, 1483-1536.

Lawson, C., Montgomery, C., 2006. Logistic Regression Analysis of Customer Satisfaction Data. Quality and Reliability Engineering International. 22, 971- 984.

Bogani G. 2001, La qualità del sistema dei processi realizzativi: i sistemi di gestione per la qualità, T. Conti, P. De Risi (a cura di), Manuale della qualità, Il Sole 24 ore, Milano.

Giarelli G. 2002, Oltre la customer satisfaction: il problema di cogliere la complessità di un punto di vista, a cura di C. Cipolla, G. Giarelli, L. Altieri , Valutare la qualità in sanità, Franco Angeli, Milano.

Muggeo V., Aiello F., (2008), Modelli di regressione per variabile risposta ordinale con funzioni link alternative: un'applicazione alla misura della qualità percepita di un servizio agli studenti, Atti del Convegno "La Statistica, la Valutazione e l'Università", 10 – 12 luglio 2008, Palermo.

RENDICONTI DEL CIRCOLO MATEMATICO DI PALERMO
Serie II, Suppl. 83 (2011), pp. 279-288

A STATISTICAL APPROACH TO COMPARE ANG-2 AND α-FP SERUM LEVELS INTO DETECTING HEPATOCELLULAR CARCINOMA[1]

AGATA ZIRILLI - ANGELA ALIBRANDI

1. Introduction.

Hepatocellular carcinoma (HCC) is one of the leading causes of death for patients with liver cirrhosis. Only an early diagnosis allows for a truly effective and decisive treatment of this disease, otherwise it would have a very rapid evolution. Currently, a monitoring program based on a determination of serum α-fetoprotein (α-FP) is produced (Chen et al., 2005; Nomura et al., 2006; Kailapuri et al, 2008; Chan et al., 2009). However, this protocol has limitations because the α-FP is diagnostic only for extremely high values. There is, therefore, the need to search for new markers (Glypican-3, IGF-II, IGF beta1, TGF beta1, Chromogranin A, etc) with greater sensitivity and specificity, but the results were almost always not very encouraging.

On the basis of histological data already acquired, which highlight the increased vascularity of HCC compared to cirrhotic liver tissue, it was demonstrated a high tissue expression of a vascular growth factor, called Angiopoietin-2 (Ang-2). In literature there are few references about a possible use of Ang-2 as a serological marker for detecting HCC (Tanaka et al., 1999).

In this paper we focused our statistical attention on ANG-2: in particular we want to compare ANG-2 and α-FP serum levels among

[1] This note, though it is the result of a close collaboration, was specifically elaborated as follows: paragraphs 1, 5, 6 and 7 by A. Zirilli and paragraphs 2, 3 and 4 by A. Alibrandi

three groups of patients (HCC patients, cirrhotic patients and healthy controls); moreover, through a sensitivity and specificity analysis, we aim to assess the ANG-2 diagnostic utility in hepatocellular carcinoma and to underline its utility as complementary tumour marker to α-FP.

2. The data.

The data were collected by an hepatology specialized team of Universitary Policlinic in Messina. In this context, we have to thank dott. Aldo Spadaro for his scientific support with regard to the medical competences.

Our dataset is composed by three groups of subjects. In particular, 59 patients (45 male and 14 female) were affected by hepatocellular carcinoma, 57 (37 male and 20 female) by cirrhosis alone and 40 healthy controls (24 male and 16 female); all subjects were aged between 21 and 84 years.

For each subject we collected information about gender, age, bilirubin, albumin, ascites (presence or absence), encephalopathy (presence or absence), ANG-2 and α-FP serum levels and, for only HCC patients, the nodules number and their maximum diameter. In table 1 we reported the descriptive statistics for the numerical variables, for each group of subjects.

Figure 1 and 2 show the boxplots for log(α-FP) (the "log" transformation was necessary to better visualize the α-FP distribution) and for ANG-2, respectively.

Figure 1: Boxplot for log (α-FP) in the three groups

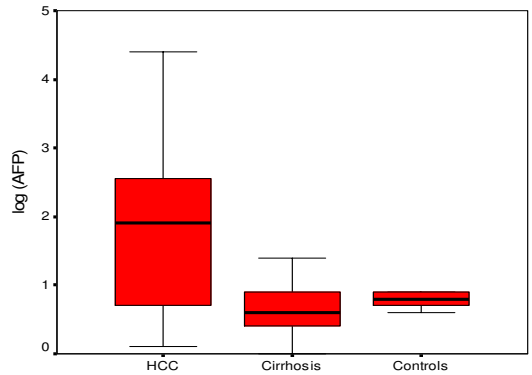

Figure 2: Boxplot for ANG-2 in the three groups

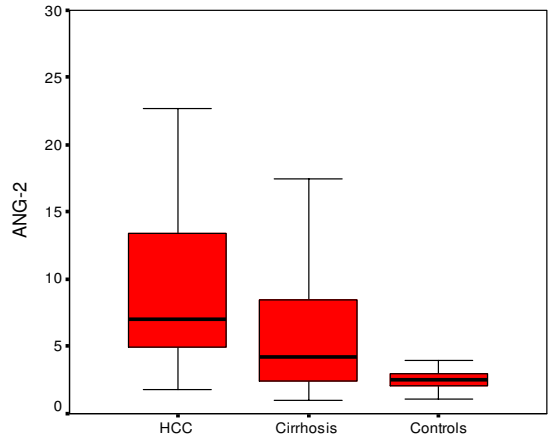

Table 1: Descriptive statistics for the numerical variables

	HCC			
VARIABLES	Mean	S.D.	Min	Max
Bilirubin	2.52	2.49	0.40	14.30
Albumin	3.30	0.62	2.10	5.10
α-FP	1416.27	4040.11	1.40	27039.00
ANG-2	9.75	6.62	1.79	26.57
Nod_number	1.78	1.16	1.00	6.00
Nod_diam	3.58	1.85	1.00	10.00
	CHIRROTICS			
Bilirubin	2.78	5.89	0.44	44.00
Albumin	3.56	0.64	2.00	4.80
α-FP	15.69	52.95	1.10	325.32
ANG-2	6.23	5.09	1.02	2.71
	CONTROLS			
Bilirubin	1.22	3.18	0.41	10.00
Albumin	2.65	0.60	2.00	4.80
α-FP	6.05	1.27	3.90	8.10
ANG-2	2.69	1.11	1.08	5.13

3. The NPC Methodology.

The low sampling number and the lack of normality in the distribution of the examined variables didn't guarantee valid asymptotic results. For this reason we have used a nonparametric approach. In order to assess the existence of possible significant differences between the three groups of subjects (HCC, Cirrhotics and Controls) in relationship to the different measured parameters, a non parametric inference based on permutation tests has been applied; in particular we referred to the Non Parametric Combination Test (NPC Test) (Pesarin, 2001).

Permutation tests represent an effective solution for problems concerning the verifying of multidimensional hypotheses, because they are difficult to face in parametric context. In comparison to the classical approach, NPC test is characterized by several advantages: it doesn't request normality and homoschedasticity assumption, it draws any type of variable, it assumes a good behaviour also in presence of lacking data, it is powerful in presence of low sampling size, it resolves multivariate problems without the necessity to specify the structure of dependence among variables, it allows stratified analyses and resolves problems in which observations number is smaller than variables number.

We supposed to notice K variables on N observations (dataset $N \times K$) and that an appropriate K-dimensional distribution P exists.

The null hypothesis postulates the equality in distribution of k-dimensional distribution among all C groups

$$H_0 = [P_1 = \ldots = P_C] = [X_1 \overset{d}{=} \ldots \overset{d}{=} X_C] \text{ i.e.}$$

$$H_0 = [\bigcap_{i=1}^{k} X_{1i} \overset{d}{=} \ldots \overset{d}{=} X_{Ci}] = [\bigcap_{i=1}^{k} H_{0i}]$$

against the alternative hypothesis

$$H_1 = \bigcup_{i=1}^{k} H_{1i} .$$

Let's assume that, without loss of generality, the partial tests assume real values and they are marginally correct, consistent and significant for great values; the NPC test procedure (based on

Conditional Monte Carlo resampling) develops into the following phases:

1. the value of the k-variated statistic is calculated on observations;
2. for every resampling conditioned to the observed data, we calculate the vector of the permuted statistics;
3. for each partial test and resampling, the transformation in rank is performed;
4. p-values related to the partial tests are calculated;
5. the combined resampling value is calculated using the combination Fisher function;
6. the observed value of the second order combined test and its p-value are calculated.
7. if p-value is minor than α, the H_0 hypothesis is rejected at fixed significance level.

In order to check the multiplicity effects, the Closed Testing procedure (Finos et al., 2003) has been applied for correcting the p-values of the two-by-two comparisons.

4. The NPC test results.

By means of the above-mentioned methodology, we have verified the following hypotheses system.

$$H_0 : \left\{ Bilirubin_1 \overset{d}{=} Bilirubin_2 \right\} \cap \ldots \cap \left\{ \alpha FP_1 \overset{d}{=} \alpha FP_2 \right\}$$

$$H_1 : \left\{ Bilirubin_1 \overset{d}{\neq} Bilirubin_2 \right\} \cup \ldots \cup \left\{ \alpha FP_1 \overset{d}{\neq} \alpha FP_2 \right\}$$

where 1 and 2 are the two compared groups. Partial and combined p-value for comparison between groups was reported in Table 2.

NPC test application and Closed Testing correction (Finos et al., 2003) have shown that, in patients affected by HCC, both ANG-2 and α-FP levels were significantly higher than in cirrhotic patients and in healthy controls, as we can see examining the results in Table 2. Any

significant differences exist between cirrhotics and controls for α-FP marker; ANG-2 serum levels were significantly higher in cirrhotic patients when compared to healthy controls.

Table 2: NPC test results for comparison between groups

VARIABLES	HCC vs CIRRHOTICS	HCC vs CONTROLS	CIRRHOTICS vs CONTROLS
Bilirubin	0,866	0,001	0,003
Albumin	**0,028**	0,004	0,005
Ascites	**0,011**	-	-
Encephalopathy	0,398	-	-
α-FP	**0,000**	**0,000**	0,306
ANG-2	**0,002**	**0,000**	**0,001**
	↓	↓	↓
Combined	0,015		

With reference to the compliances "ascites" and "encephalopathy", we can perform only the comparison between HCC and Cirrhotics patients, because such compliances weren't, obviously, observable in healthy control subjects.

5. Diagnostic tests: assumptions

Diagnostic tests (Zou et al., 2007) represent widely used indexes to evaluate the performance of a specific marker; they have the advantage to be independent on the prevalence of the examine pathology in the population. Let's consider the following table:

	Pathology		
Test	Presence	Absence	Total
Positive	TP	FP	N(T+)
Negative	FN	TN	N(T-)
Total	N(D+)	N(D-)	N

with:

- TP (True Positive) = patients with pathology and positive test;
- FP (False Positive) = patients without pathology and with positive test;
- TN (True Negative): patients without pathology and with negative test;
- FN (False Negative): patients with pathology and with negative test;
- N(D+): total number of patients with pathology;
- N(D-): total number of patients without pathology;
- N(T+): total number of patients with positive test;
- N(T-): total number of patients with negative test;
- N: total number of patients.
- The *sensibility* is the proportion of subjects with pathology that result positive at a particular test. Sensibility is estimable as:

$$\text{Sensibility} = TP/N(D+)$$

- The *specificity* is the proportion of subjects without pathology that result negative at the same test. Specificity is estimable as:

$$\text{Specificity} = TN/N(D-)$$

- The *Predictive value of a positive test* (PVP) is the probability of the pathology presence in case of positive test. It is estimable as:

$$TP/N(T+)$$

- The *Predictive value of a negative test* (PVN) is the probability of the pathology absence in case of negative test. It is estimable as:

$$TN/N(T-)$$

The area under curve (*AUC*) is an essential parameter for evaluating the performance of a test and represents a measure of accuracy. Since AUC is an estimate of the sample, it is almost always necessary to test the significance of the discriminating ability of the test, or if the area under the curve significantly exceeds its expected value of 0.5. This procedure allows to verify if the proportion of true positives is higher than that of false positives.

6. The sensitivity and specificity results.

The optimal cut off was individualized by means of ROC analysis (Bottarelli and Parodi, 2003); for the two examined markers we obtained the values:

- 200 ng/ml for α-FP with area under ROC curve of 64,7%;
- 6,3 ng/ml for ANG-2, with area under ROC curve of 62.9%

Sensitivity, specificity, positive and negative predictive value and diagnostic accuracy were calculated for α-FP and ANG-2, singly and jointly (Altman and Bland, 1994), into detecting HCC presence. Table 3 shows the results of the above-mentioned diagnostic tests.

Table 3: Diagnostic test for α–FP and ANG-2
(singly and jointly considered) into detecting HCC

Marker	Sensibility	Specificity	VP+	VP-	Accuracy
α-FP	33.9%	96.5%	90.9%	58.5%	64.7%
ANG-2	64.4%	61.4%	63.3%	62.5%	62.9%
α-FP and ANG-2	74.6%	61.4%	66.7%	70.0%	68.1

Comparing the two markers, we can notice that the ANG-2 shows a higher sensibility value than α-FP, but a lower specificity; the difference between the two markers is lower with reference to the accuracy, even if the α-FP guarantees a slightly higher value. Evaluating the sensibility and specificity of AFP and ANG-2 jointly used, we obtained a more elevated sensibility (in comparison to every marker singly used) even if the specificity is lower (exactly equal to the ANG-2 specificity). This underlines the informative and diagnostic utility of ANG-2, to be used jointly to the commonly used α-FP marker.

7. Final Remarks

Serum α-FP is among the most intensively studied tumor markers for HCC. The test, when used with the conventional cut-off point of 400 ng/ml, has a sensitivity of about 48-63% and a specificity of

100% in detecting the presence of HCC in patients with compensated cirrhosis. In recent years various other serological markers have been developed for the diagnosis of HCC. However, most of these markers have been shown to be unsatisfactory in diagnosing small HCC due to low sensitivity. For this reason, we focalized our interest toward ANG-2 as HCC marker. Such as α-FP, also ANG-2 levels in HCC were significantly higher than cirrhotic patients and than controls. The optimal cut-off values into diagnosing HCC, determined with ROC curve, was 200 ng/ml for α-FP and 6,30 ng/ml for ANG-2. The diagnostic utility of the joined action of α-FP and ANG-2 was assessed by the sensibility value, that is more elevated in comparison to every marker singly used.

So, this paper underlines the informative and diagnostic utility of ANG-2; it, if jointly used to the α-FP marker, can be an effective strategy into detecting hepatocellular carcinoma.

References.

Altman DG, Bland JM.(1994), Diagnostic tests: sensitivity and specificity. *BMJ* 1994;308:1552

Bottarelli E, Parodi S, (2003) Un approccio per la valutazione della validità dei test diagnostici: le curve R.O.C (Receiver Operating Characteristic). *Ann. Fac. Medic. Vet. di Parma,* Vol. XXIII, 49-68.

Chan SL, Mo FK, Johnson PJ (2009) New utility of an old marker: Serial alpha-fetoprotein measurement in predicting radiologic response and survival of patients with hepatocellular carcinoma undergoing systemic chemotherapy. *Journal of Clinical Oncology*, 27:446–452.

Chen LT, Liu TW, Chao Y.(2005) Alpha-fetoprotein response predicts survival benefits of thalidomide for advanced hepatocellular carcinom. *Alimentary Pharmacology & Therapeutics*, 22:217–226.

Finos L., Pesarin F., Salmaso L. (2003), Test combinati per il controllo della molteplicità mediante procedure di Closed Testing, *Statistica Applicata*, 15, 2, 301-329.

Kailapuri M.G., Mathewsb S., Jayanthic V., Shankara E.M., Harid R., Surendranc R., Vengatesanc A., Raghuramb K., Rajasambandamb P., Muralic A., Srinivasc Usha, Palaniswamye K.R., Pugazhendhib T., Panchatcharam Thyagarajand Sadras (2008), α-fetoprotein as a tumor marker in hepatocellular carcinoma: investigations in south Indian subjects with hepatotropic virus and aflatoxin etiologies, *International Journal of Infectious Diseases*, 12 (6), 71-76

Nomura, F., Ohnishi, K. and Tanabe, Y. (1989), Clinical features and prognosis of

hepatocellular carcinoma with reference to serum alpha-fetoprotein levels. Analysis of 606 patients. *Cancer*, 64, 1700–1707.

Pesarin F. (2001) *Multivariate permutation tests with applications in biostatistics*. Wiley, Chichester.

Tanaka S., Mori M., Sakamoto Y., Makuuchi M., Sugimachi K., Wands J.R. (1999), Biologic significance of angiopoietin-2 expression in human hepatocellular carcinoma, *Journal of Clinical Investigation*, 103(3): 341–345

Zou KH, O'Malley AJ, Mauri L (2007), Receiver-Operating Characteristic Analysis for Evaluating Diagnostic Tests and Predictive Models. *Circulation*;115:654-657.

Tipografia A.C.
Finito di stampare dalla
Tipografia A. C.
Via Filippo Marini, 15 - Palermo
Maggio 2011
E-mail: tipografiaac@alice.it